HEINRICH HEINE
UNIVERSITÄT DÜSSELDORF

Bioactive Secondary Metabolites from Marine-Derived Fungi and Exploration in Fungal-Bacterial Co-Cultivation

Inaugural dissertation

for the attainment of the title of doctor
in the Faculty of Mathematics and Natural Sciences
at the Heinrich Heine University Düsseldorf

presented by

Shuai Liu

from Hubei, P.R. China

Düsseldorf, 10. 2016

from the institute for Pharmaceutical Biology and Biothechnology
at the Heinrich Heine University Düsseldorf

Published by permission of the
Faculty of Mathematics and Natural Sciences at
Heinrich Heine University Düsseldorf

Supervisor: Prof. Dr. Peter Proksch
Co-supervisor: Prof. Dr. Rainer Kalscheuer

Date of the oral examination: 12/12/2016

Devoted to my parents

Zhengxi Liu and Chuntao Jian

and
my wife

Dr. Shuangshuang Zhang

CONTENTS

Abstract

From penicillin to phenylahistin, microbes (fungi and bacteria) have continued to provide important pharmaceuticals for humans to fight against bacterial or fungal infections, cancers, transplant rejections, parasitic worms and so on. For the last two decades, fungi from marine habitats (such as mangroves and sponges) have attracted increasing interest by producing novel natural products with various bioactivities. In this dissertation, the study of three marine-derived fungi: *Fusarium oxysporum*, *Pestalotiopsis microspora*, and *Aspergillus* sp. led to the isolation of three types of secondary metabolites. These included fusaric acid derivatives exhibiting phytotoxicity, 14-membered macrolides with cytotoxic activity, and phenolic bisabolanes with antibacterial activity, respectively. The absolute configurations of the new compounds were confirmed by chiral GC-MS, X-ray crystallographic analysis, Mosher's reaction or ECD calculation.

It has been proven that most fungal gene clusters remain silent during standard laboratory cultivation conditions. In order to trigger silent genes in fungi encoding for biosynthesis of new compounds, co-cultivation experiments of fungi (*P. microspora*, or *Aspergillus* sp.) with bacteria (*Streptomyces lividans*, or *Bacillus subtilis*) were conducted.

This dissertation contains the following published or submitted manuscripts:

New fusaric acid derivatives from the endophytic fungus F. oxysporum and their phytotoxicity to barley leaves

Chemical investigation of the endophytic fungus *F. oxysporum* isolated from fruits of the Mangrove plant *Drepanocarpus lunatus* afforded eight new fusaric acid derivatives, fusaricates A−G, **1**−**7**, and 10-hydroxy-11-chlorofusaric acid, **8**, along with four known compounds. Their structures were elucidated by one- and two-dimensional NMR as well as MS data and by comparison with the literature. The absolute configurations of fusaricates C−E, **3**−**5**, were determined using chiral GC-MS. Fusaricates A−G, **1**−**7**, represent the first examples of fusaric acid linked to a polyalcohol moiety via an ester bond. All isolated fusaric acid derivatives **1**−**8** showed significant phytotoxicity to leaves of barley.

Cytotoxic 14-membered macrolides from a mangrove-derived endophytic fungus, P. microspora

Seven new 14-membered macrolides, pestalotioprolides C (**2**), D−H (**4**−**8**), and

7-*O*-methylnigrosporolide (**3**), together with four known analogues, pestalotioprolide B (**1**), seiricuprolide (**9**), nigrosporolide (**10**), and 4,7- dihydroxy-13-tetradeca-2,5,8-trienolide (**11**), were isolated from the mangrove-derived endophytic fungus *P. microspora*. Their structures were elucidated by analysis of NMR and MS data and by comparison with literature data. Single-crystal X-ray diffraction analysis was used to confirm the absolute configurations of **1**, **2**, and **10**, while Mosher's method and the TDDFT-ECD approach were applied to determine the absolute configurations of **5** and **6**. Compounds **3**−**6** showed significant cytotoxicity against the murine lymphoma cell line L5178Y with IC_{50} values of 0.7, 5.6, 3.4, and 3.9 μM, respectively, while compound **5** showed potent activity against the human ovarian cancer cell line A2780 with an IC_{50} value of 1.2 μM. Co-culture of *P. microspora* with *S. lividans* caused a roughly 10-fold enhanced accumulation of compounds **5** and **6** compared to axenic fungal control.

Phenolic bisabolanes from the sponge-derived fungus Aspergillus sp.

Two new phenolic bisabolane sesquiterpenes, asperchondols A (**1**) and B (**2**), together with seven known analogues (**3**–**9**) and four known diphenyl ethers (**10**–**13**) were obtained from *Aspergillus* sp., that had been isolated from the marine sponge *Chondrilla nucula*. Their structures were elucidated through NMR and MS analysis, and by comparison with literature data. All isolated compounds were evaluated for their antibacterial activity against eight human pathogenic bacteria. Co-cultivation experiment of *Aspergillus* sp. with *B. subtilis* was also conducted.

Inducing new secondary metabolites through co-cultivation of the fungus P. microspora with the bacterium B. subtilis

Two new lactones pestalotioprolide J (**1**) and K (**2**), together with three known compounds (**3**-**5**) were isolated from the culture of the mangrove endophytic fungus *Pestalotiopsis microspora*. The co-cultivation of this fungus with *Bacillus subtilis* afforded two new sesquiterpenes pestabacillin A (**6**), B (**7**), and eight known compounds (**8**–**15**). The structures of the new compounds (**1**, **2**, **6**, and **7**) were determined from one- and two-dimensional NMR and HRESIMS spectra. As an unusual sesquiterpene, the structure of **6** was further confirmed by single crystal X-ray diffraction.

Zusammenfassung

Als Quelle für Arzneistoffe spielen Mikroorganismen (Pilze und Bakterien) seit Langem eine wichtige Rolle in der Therapie von bakteriellen oder pilzlichen Infektionen, Krebs, Transplantatabstoßungen und Wurmerkrankungen. In den letzten beiden Jahrzehnten ist das Interesse an marinen Pilzen aus z.B. Mangroven oder Schwämmen durch ihre Vielfalt an neuen chemischen Verbindungen mit verschiedensten Bioaktivitäten stetig gewachsen. Diese Dissertation umfasst Daten zu drei marinen Pilze: *Fusarium oxysporum*, *Pestalotiopsis microspora* und *Aspergillus* sp.. Aus den genannten Pilzen konnten insgesamt drei Typen von Sekundärmetaboliten isoliert werden: phytotoxische Fusarinsäurederivate, zytotoxische 14-gliedrige Makrolide und antibakterielle phenolische Bisabolane. Die absoluten Konfigurationen der neuen Substanzen wurden mittels chiraler GC-MS, Röntgenkristallographie, Mosher Reaktion oder ECD-Berechnungen erhalten.

Bei der standardisierten Kultivierung von Pilzen im Labor werden die meisten Biosynthesegencluster stillgelegt. Um die schlafenden Gene zur Biosynthese neuer Verbindungen zu aktivieren, wurde eine Co-Kultivierung zwischen jeweils einem Pilz (*P. microspora* oder *Aspergillus* sp.) und einem Bakterienstamm (*Streptomyces lividans* oder *Bacillus subtilis*) durchgeführt.

Diese Dissertation enthält die folgenden veröffentlichten oder eingereichten Publikationen:

New fusaric acid derivatives from the endophytic fungus F. oxysporum and their phytotoxicity to barley leaves

Die chemische Aufarbeitung des endophytischen Pilzes *F. oxysporum* ergab die acht neuen Fusarinsäurederivate Fusaricate A−G (**1-7)** und 10-Hydroxy-11-Chlorfusarinsäure (**8)**, zusammen mit vier bekannten Verbindungen. Der Pilz wurde aus den Früchten der Mangrovenpflanze *Drepanocarpus lunatus* isoliert. Die Strukturen der neuen Verbindungen wurden über ein- und zweidimensionale NMR-Spektroskopie, MS-Daten, sowie über den Vergleich mit der Literatur bestimmt. Die absolute Konfiguration der Fusaricate C-E (**3**-**5**) wurde per chiraler GC-MS festgestellt. Die Fusaricate A-G (**1**-**7**) stellen die ersten Beispiele für eine Esterbindung zwischen Fusarinsäure und einem Polyalkoholrest dar. Alle isolierten Fusarinsäurederivate zeigten signifikante Phytotoxizität gegen Gerstenblätter.

Cytotoxic 14-membered macrolides from a mangrove-derived endophytic fungus, P. microspora

Aus dem Mangrovenpilz *P. microspora* konnten sieben neue 14-gliedrige Makrolide, darunter die Pestalotioprolide C (**2**), D-H (**4**-**8**) und 7-O-Methylnigrosporolid (**3**), zusammen mit den vier bekannten Derivaten Pestalotioprolide B (**1**), Seiricuprolid (**9**), Nigrosporolid (**10**) und 4,7-Dihydroxy-13-Tetradeca-2,5,8-Trienolid (**11**) isoliert werden. Die Strukturen wurden per NMR- und MS-Analyse und über den Vergleich mit der Literatur aufgeklärt. Zur Bestimmung der absoluten Konfiguration von **1**, **2** und **10** diente Röntgenkristallographie, während auf **5** und **6** die Mosher-Methode und das TDDFT-ECD-Verfahren angewendet wurden. Die Verbindungen **3**-**6** zeigten signifikante Zytotoxizität gegen die murine Lymphom-Zelllinie L5178Y (IC_{50}-Werte: 0.7, 5.6, 3.4, und 3.9 μM). Verbindung **5** wies Aktivität gegen die humane Ovarial-Krebs-Zelllinie A2780 (IC_{50}-Wert 1.2 μM) auf. Die Co-Kultivierung von *P microspora* mit *S. lividans* bewirkte eine zehnfach erhöhte Akkumulation von Verbindung **5** und **6** im Vergleich zur axenischen Kontrolle des Pilzes.

Phenolic bisabolanes from the sponge-derived fungus Aspergillus sp.

Bei der Aufarbeitung von *Aspergillus sp.* wurden zwei neue phenolische Bisabolan-Sesquiterpene, Asperchondol A (**1**) und B (**2**), zusammen mit sieben bekannten Analoga (**3**-**9**) und vier bekannten Diphenylethern (**10**-**13**) erhalten. Der Pilz wurde aus dem marinen Schwamm *Chondrilla nucula* isoliert. Die Strukturen wurden per NMR- und MS-Analyse und über den Vergleich mit der Literatur aufgeklärt. Alle isolierten Verbindungen wurden hinsichtlich ihrer antibakteriellen Eigenschaften gegen acht humanpathogene Bakterien untersucht. Ein Co-Kultivierungsexperiment mit *B. subtilis* wurde ebenfalls durchgeführt.

Inducing new secondary metabolites through the co-cultivation of the fungus P. microspora with the bacterium B. subtilis

Aus der Kultur des Mangrovenpilzes *Pestalotiopsis microspora* konnten zwei neue Lactone, Pestalotioprolid J (**1**) und K (**2**), zusammen mit drei bekannten Verbindungen (**3**-**5**) gewonnen werden. Die Co-Kultivierung des Pilzes mit *Bacillus subtilis* ergab die zwei neuen Sesquiterpene Pestabacillin A (**6**) und B (**7**) und acht bekannte Verbindungen (**8**–**15**). Die Strukturen der neuen Verbindungen (**1**, **2**, **6** und **7**) wurden durch 1D- und 2D-NMR-Spektroskopie und HR-ESI-MS bestimmt. Des Weiteren wurde die Struktur des ungewöhnlichen Sesquiterpens **6** per Röntgenkristallographie bestätigt.

Chapter 1

General Introduction

观天之道，执天之行，尽已。

Explore how nature works, take things into nature's route, that's all!

- starting words of *Taigong Yinfu Jing*, an ancient Chinese book around 3000 years ago.

1.1 Food Fermentation in Ancient Time

Before Antonie Van Leeuwenhoek discovered microorganisms by microscopes improved by himself in 1675 (Payne and van Leeuwenhoek, 1970), people had already mastered the techniques of applying microbes to the fermentation of wine, beer, cheese, bread, vinegar, soy sauce, and kimchi for a long period. The chemical analyses of ancient organics in pottery jars from Jiahu in Henan province of China suggested that the earliest wine fermentation can be traced back 9,000 years (McGovern *et al*., 2004). New evidence by Peter Bogucki proved that early farmers in north Europe have been making cheese to preserve and get the best use of milk since 7,500 years ago (Salque *et al.*, 2013). Vinegar, the daily cooking ingredient fermented by acetic acid bacteria, can be dated back to 3,000 BC in Egyptian urns (Solieri and Giudici, 2009).

1.2 Drugs Discovered from Microbes

The era of microbial drug discovery started in 1928, when Alexander Fleming noticed that a petri dish of *Staphylococcus aureus* was polluted and killed by a blue-green mold (Fleming, 1929). The mold, later identified as *Penicillium notatum*, was able to produce a diffusible antibacterial substance, which Fleming termed penicillin (Tager, 1946). The significance of discovery of penicillin was not only rescuing numerous soldiers from fatal bacterial infections in World War II (Woodward, 2009), but also inspiring scientists to search for new drugs from the broth of microbes (Demain and Sanchez, 2009). Figure 1 shows the representative chemicals of drug classes discovered from fungi and bacteria between the year 1896 and the year1997 (Demain and Sanchez, 2009; Beekman and Barrow, 2014).

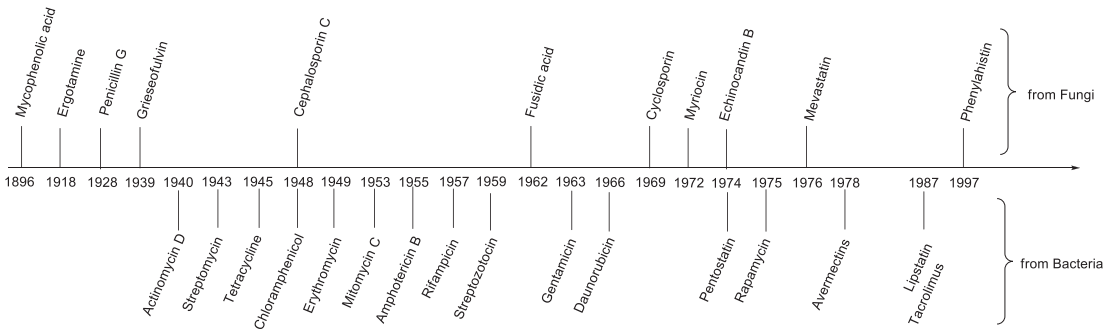

Figure 1. Time line of the original discovery of pharmaceuticals from fungi and bacteria (modified after Beekman and Barrow, 2014).

The World Health Organization's (WHO) List of Essential Medicines includes the most important pharmaceuticals, which are necessary for the basic health system and available for the majority of the population on earth (Organization, 2015). On the 19th edition of this list, 108 anti-infective medicines were selected, and among them, 50 pharmaceutical entities originated or were chemically derived from natural products from microbes, plants and sponges. The anti-infective medicines were divided into anthelminthics, antibacterial, antifungal, antiviral and antiprotozoal medicines. In the category of antibacterial medicines, 31 out of the 47 antibiotics, which included penicillins, cephalosporins, aminoglycosides, tetracyclines and macrolides were of microbial origin. In the antifungal category, 7 antifungal medicines were listed including 3 microbial original drugs: amphotericin B, griseofulvin and nystatin. Though only two immunosuppressive medicines were chosen for the essential medicines including azathioprine and cyclosporine, the latter one was first isolated from the fungus *Tolypocladium inflatum* in 1969. In total, 27 cytotoxic agents were listed for cancer chemotherapy, and 7 of them originated from microorganism, such as bleomycin and daunorubicin.

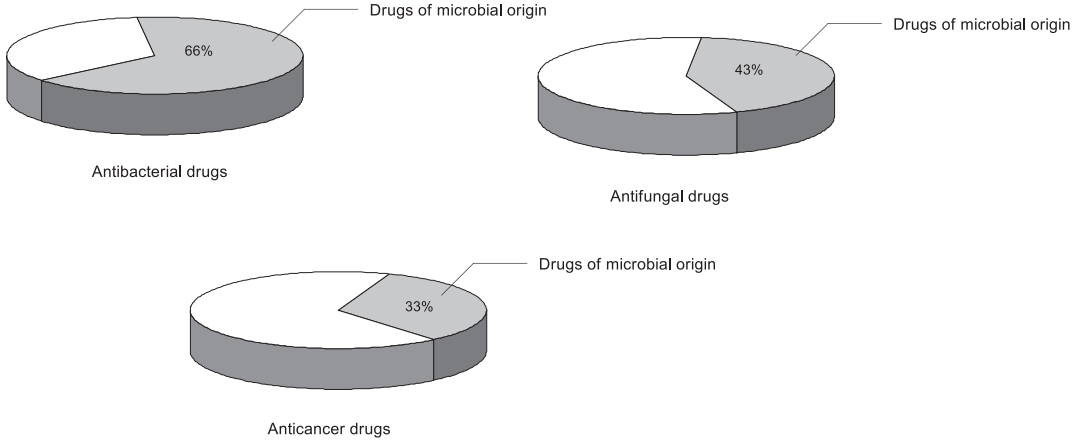

Figure 2. Antibacterial, antifungal and anticancer drugs of microbial origin on the 19th WHO

Model List of Essential Medicines in 2015.

1.2.1 Antibacterial Agents

In 1941, based on Fleming's work on penicillin, Australian scientist Howard Florey and his colleague Ernst Boris Chain first put penicillin to clinical use in Oxford (Florey, 1946), a short distance from Fleming's laboratory in St Mary's Hospital of London. Since then, penicillin's era in pharmaceutics started, and these three scientists shared the Nobel Prize in Physiology or Medicine in 1945 (Lindsten and Ringertz, 2001). Today, a number of penicillins with diverse antibacterial spectrum can be found on the market, and they all share the chemical core of 6-aminopenicillanic acid (6-APA) (Batchelor *et al*., 1959). The mechanism of penicillins' antibacterial activities is that they can bind and disable penicillin-binding proteins (PBP), which are essential for the formation of peptidoglycan cross-links in bacterial cell walls (Park and Stromistger, 1957). As a result, the weakened bacterial cell wall can not hold the osmotic pressure of cytoplasm inside and the bacteria end up with cytolysis (Hobby *et al*., 1942). Depending on their antibacterial activity and time of development, penicillins are divided into four generations. As a representative of the first generation, penicillin G is a naturally occurring penicillin, which can only be given by injection due to its low acid tolerability to acidic environment in stomach (McCarthy *et al*., 1960). In the industry, penicillin G, produced by the fermentation of an improved strain *P. chrysogenum*, is a very important raw material for other semi-synthetic penicillins and cephalosporins (Elander, 2003). Unlike the first generation penicillins, the second generation like cloxacillin, dicloxacillin and methicillin can still be active when exposed to some penicillin-resistant bacteria, which can produce *β*-lactamase to break the *β*-lactam ring (McDougal and Thornsberry, 1986). The first and second generations are applied to Gram-positive bacteria and they possess narrow antibacterial spectrum. As a member of the third generation, amoxicillin can be taken orally due to its high oral bioavailability and stability to stomach acidity (Welling *et al*., 1977) and it possesses broad antibacterial spectrum (Neu, 1979). The fourth generation of penicillins, like carbenicillin and piperacillin, they have extended antibacterial spectra, especially towards Gram-negative bacteria (Knudsen *et al*., 1967; Winston *et al*., 1980).

Cephalosporins are another group of *β*-lactam antibiotics, which share the same chemical core: 7-aminocephalosporanic acid (7-ACA) (Morin *et al*., 1962). It was Giuseppe Brotzu, an Italian scientist, who first investigated the cephalosporin-producing fungus *Cephalosporium*

acremonium (now known as *Acremonium chysogenum*) and discovered that the extracts of the fungus exhibited activities against Gram-negative bacteria in 1945 (Paracchini, 1992). Cephalosporins have the same mode of action as penicillins (Ghuysen *et al*., 1979). However, compared with penicillins, cephalosporins exhibit better antibacterial activity against *β*-lactamase-producing bacteria (Sykes and Matthew, 1976). Cephalosporin C was the first natural product of this group isolated by Guy Newton and Edward Abraham in 1953 (Newton and Abraham, 1954). Although cephalosporin C itself is not used as a drug because of the low activity, its mass production can be accomplished from the large-scale fermentation and it is a very important raw material for 7-ACA, which is the essential intermediate for other semi-synthetic cephalosporins (Elander, 2003).

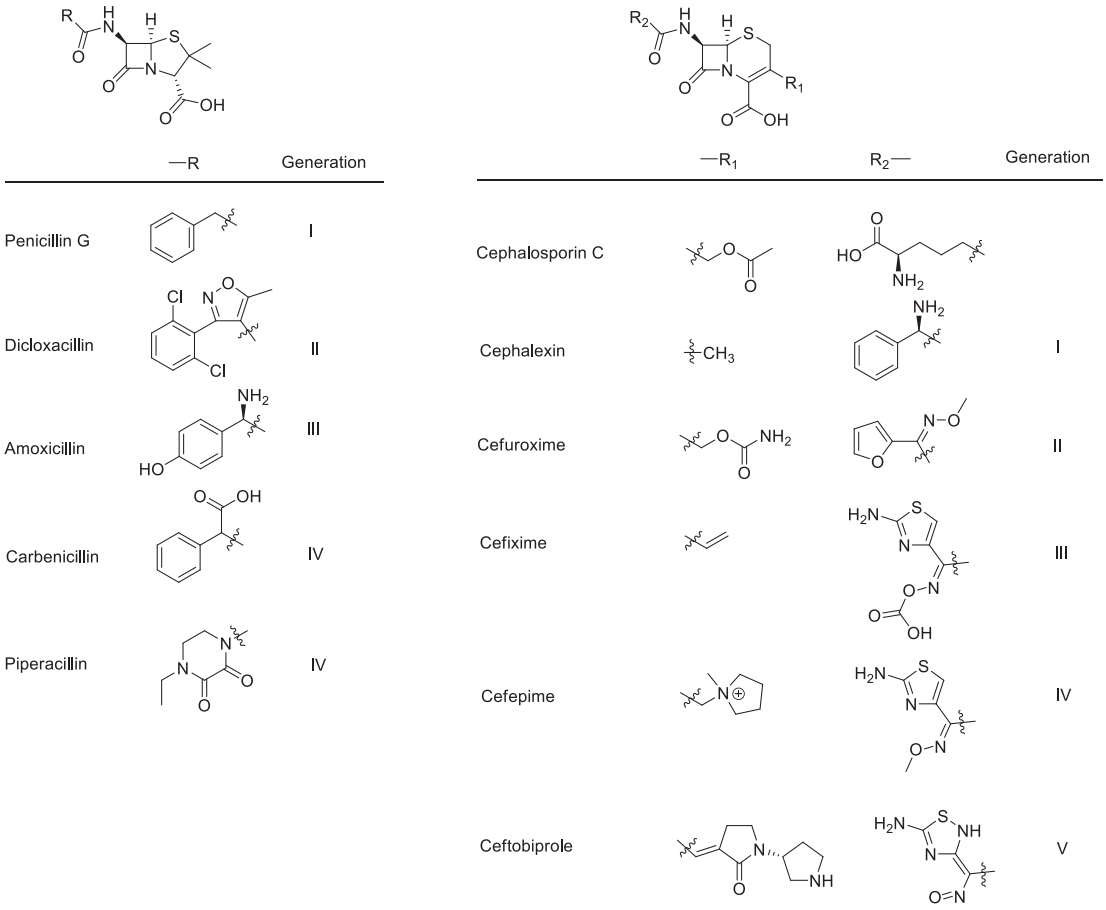

Figure 3. Representative drugs of different generations of *β*-lactam antibiotics.

Presently, five generations of cephalosporins are recognized. The first-generation cephalosporins such as cefalexin are predominantly active against Gram-positive, but it is not effective against infections caused by methicillin-resistant *Staphylococcus aureus* (MRSA) (Enright *et al*., 2002). Cefuroxime is a second-generation cephalosporin antibiotic, which can be

taken through oral administration due to its chemical stability in acidic environment (Glaxo, 2010). It has a broader antibacterial spectrum than the first generation, and it can cross the blood-brain barrier (Lebel *et al*., 1989). As one of the third-generation cephalosporins, cefixime has a broad antibacterial spectrum, which is often prescribed to cure infections of the ear, the urinary tract and upper respiratory tract (Girgis *et al*., 1993). Cefepime, a fourth generation cephalosporin, possesses a well-designed molecular structure and more extensive antibacterial activities than the last generation catalogues (Barradell, *et al*., 1994). As a member of the fifth generation, ceftobiprole can kill MRSA due to its high affinity for PBP2a (Syed, 2014).

Streptomycin was first isolated from *Streptomyces griseus* by Albert Schatz in1943 (Schatz *et al*., 1944). It was the first chemical of aminoglycoside antibiotics and also the first drug applied to cure tuberculosis (Lawn and Zumla, 2011). Streptomycin can be effective on infections caused by both Gram-positive and Gram-negative bacteria, and it also possesses inhibitory effects on the growth of some plant pathogens in agriculture (Stockwell, 2012). The action mechanism of streptomycin, like other aminoglycosides (gentamicin, neomycin), is binding to 30S subunit in bacterial ribosomes, as a result to inhibit the protein synthesis (Sharma *et al*., 2007). Since the ribosome structures in humans differ from those of bacteria, streptomycin is safe for the human bodies.

Erythromycin was first isolated from the soil derived bacterium *Streptomyces erythreus* by Eli Lilly's research group in 1949 (McGuire *et al*., 1952). Erythromycin belongs to the family of macrolide antibiotics, and is used for treatment of a number of bacterial infections caused by *Haemophilus influenzae*, *Streptococcus pyogenes*, *Entamoeba histolytica*, *Chlamydia trachomatis* and *Corynebacterium diphtheria* (Abbott, 2002). It is generally safe for pregnant women and an effective alternative for patients who are allergic to penicillin (Oradell, 1994). One of the targets of erythromycin is the 50S subunit of bacterial ribosome, which is very important for the protein synthesis and replication of bacteria (Champney and Burdine, 1996).

Rifampicin was first isolated by Piero Sensi and Maria Teresa Timbal in 1959 from *Amycolatopsis rifamycinica*, which was derived from a soil sample collected in a pine forest (Sensi *et al*. 1959). Rifampicin is the first-line drug to cure tuberculosis, usually prescribed together with isoniazid, pyrazinamide and ethambutol (Lawn and Zumla, 2011). Rifampicin can be also applied to treat MRSA infections when combined with fusidic acid (Aboltins *et al*., 2007).

Because rifampicin only targets the RNA polymerase to inhibit bacterial DNA-dependent RNA synthesis, the resistance to rifampicin develops quickly during the treatment (Levin and Hatfull, 1993). Due to this resistance, rifampicin is always used in combination with other antibiotics. Except for its antibacterial activities, rifampicin also possesses antiviral activity against vaccinia virus (Charity *et al*., 2007).

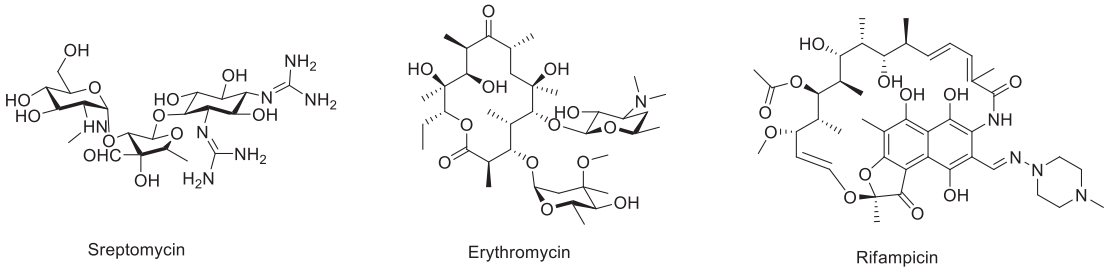

Figure 4. Structures of streptomycin, erythromycin and rifampicin.

1.2.2 Antifungal Agents

Compared with other infections, most fungal infections (or mycosis) generally result in no fatal illness. However, it is the 4th most common disease in 2010 affecting 984 million people (Hay *et al*., 2014).

Griseofulvin was first isolated from *Penicillium griseofulvum* by Harold Raistrick and his coworkers in 1939 (Oxford *et al*., 1939). Later in 1952 and in 1959, the structure and stereochemistry of griseofulvin were determined respectively by MacMillan (Grove *et al*., 1952; MacMillan, 1959). Griseofulvin has been approved for the treatment of skin and nail infections caused by *Trichophyton*, *Microsporum*, or *Epidermophyton floccosum* since 1959 (Ortho, 2002). Griseofulvin acts by binding to tubulin proteins in fungi to inhibit fungal mitosis (Bent and Moore, 1966).

Amphotericin B was originally isolated from the soil-derived bacterium *Streptomyces nodosus* in 1955 (Dutcher, 1968). The complexity of its macrocyclic ring delayed the determination of its absolute stereochemistry until 1970 by X-ray crystallographic analysis of the N-iodoacetyl derivative (Ganis *et al*., 1971). Amphotericin B binds to ergosterol, which is a component of fungal cell membranes, resulting the leakage of monovalent ions (K^+, H^+, Na^+, Cl^-) and subsequent cell death of fungi (Mesa-Arango *et al*., 2012).

Echinocandin B was the first natural original echinocandins isolated from the fungus *Aspergillus nidulans* in 1974 (Nyfeler and Keller-Schierlein, 1974). Echinocandins are antifungal

lipopeptides, which are structurally comprised of a cyclic peptide ring and a long fatty acid chain. Though echinocandin B was not approved for clinical use because of the high risk of hemolysis (Morris and Villmann, 2006), its semi-synthetic derivatives caspofungin, micafungin and anidulafungin are used clinically through intravenous injection to cure fungal infections caused by *Candida* spp. (Gordee *et al*., 1984). Like penicillins acting at the bacterial cell wall, echinocandins inhibit 1,3-*β*-glucan synthase, which is an essential enzyme for the synthesis of glucan in the fungal cell wall (Morris and Villmann, 2006).

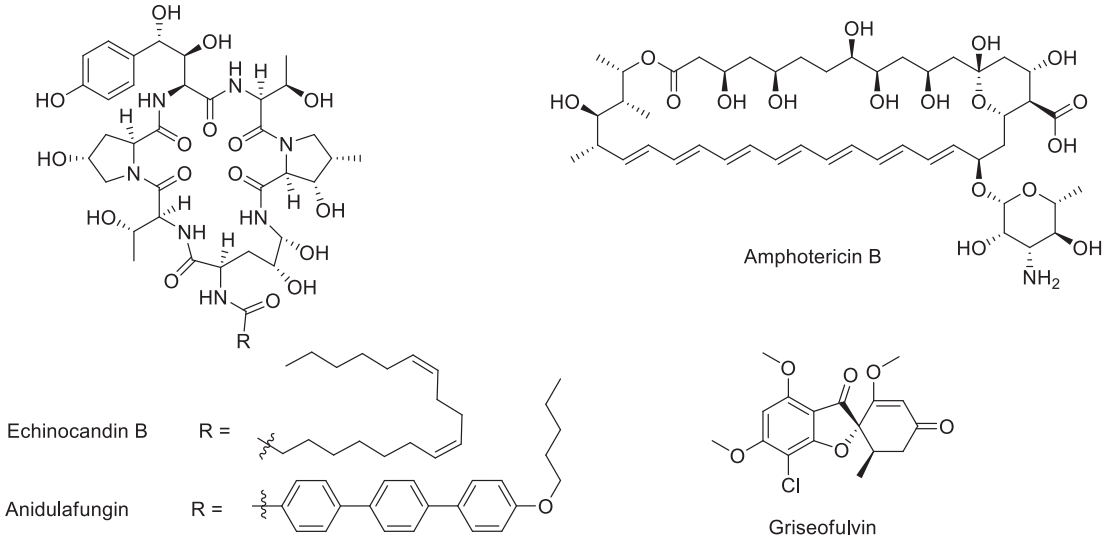

Figure 5. Structures of antifungal drugs from microbial source.

1.2.3 Anticancer Agent

In 2012, over 14 million people were diagnosed as cancer worldwide and over 8 million deaths (accounting 14.6 % of human deaths) were caused by cancer (Bernard and Christopher, 2014). For women, the most common cancer types were breast cancer, colorectal cancer (CRC), lung carcinoma and cervical cancer, while lung cancer, prostate cancer, colorectal cancer and stomach cancer were the most prevalent amongst males (Bernard and Christopher, 2014).

Actinomycin D is a polypeptide isolated from the soil derived bacterium *Streptomyces antibioticus* in 1940 (Waksman *et al*., 1940). It is the first microbial metabolite used to treat a variety of cancers including Wilm's tumor, rhabdomyosarcoma, and Ewing's sarcoma by intravenous administration (Merk, 2005). Actinomycin D inhibits transcription by binding to DNA and preventing RNA polymerase to elongate the RNA chain (Sobell, 1985).

Daunorubicin, combining Italian word *Dauni* with French word *ruby*, is an anthracycline

isolated from *Streptomyces peucetius* by two groups in Italy and France independently nearly at the same time in 1966 (Weiss, 1992). It has been clinically used to teat acute lymphocytic leukemia, acute myeloid leukemia, and chronic myelogenous leukemia (Anon, 2003). Daunorubicin also serves as the starting material for other semi-synthetic anthracyclines like doxorubicin, epirubicin and idarubicin. The mechanism of action of daunorubicin includes interacting with DNA by intercalation and inhibiting topoisomerase II, and result in the blocking of DNA transcription and replication (Momparler *et al*., 1976; Fornari *et al*., 1994).

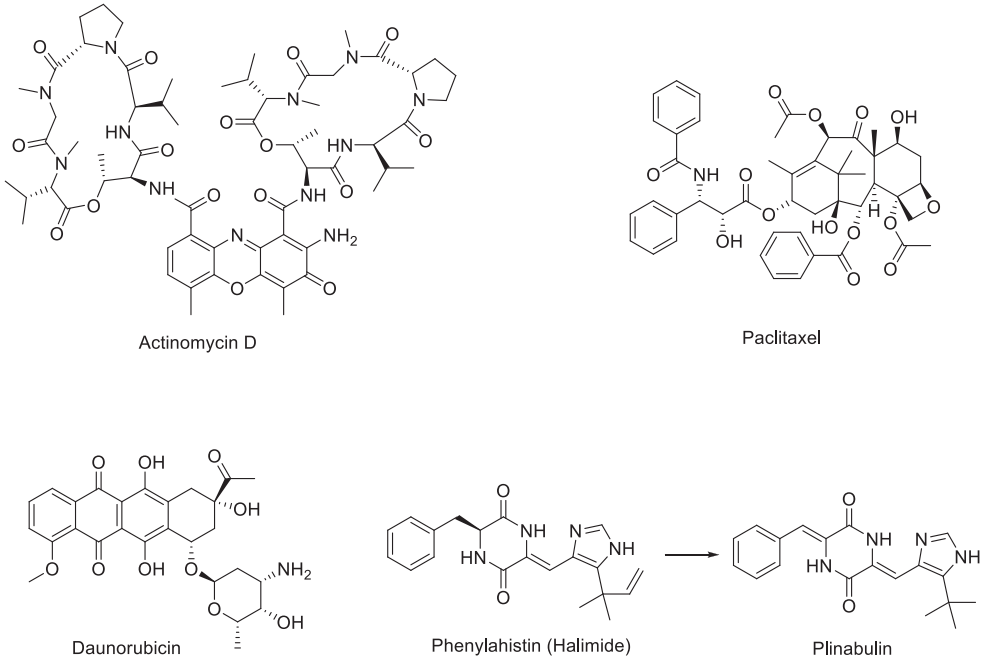

Figure 6. Structures of anticancer drugs from microbes.

Paclitaxel (taxol) was first isolated from the plant *Taxus brevifolia* as a plant secondary metabolite in 1967 (Wall and Wani, 1995), but was also reported as a fungal natural product from *Taxomyces andreanae* in 1993 (Stierle *et al*., 1993) and *Nodulisporium sylviforme* in 2004 (Zhao *et al*., 2004). Paclitaxel has been approved for the treatment of ovarian, breast, and lung cancers as well as other types of solid tumor cancers (Guchelaar *et al*., 1994). Paclitaxel production is presently conducted by two ways: semi-synthetic method on the precursor extracted from the plant *Taxus baccata* (Patel, 1998), and *Taxus* cell fermentation with the fungus *Penicillium raistrickii* (Tabata, 2004). Apart from the conventional paclitaxel dosage form, albumin-bound paclitaxel is an alternative formation, which is administered by IV infusion (Celgene, 2013). Paclitaxel binds the *β*-subunit of tubulin in cancer cells, resulting in tubulin polymerization and no breakdown of microtubules during cell division (Kumar, 1981).

Phenylahistin (or halimide) was first isolated from a marine fungus *Asperigillus ustus* in1997 (Kanoh *et al*., 1997). Its brilliant cytotoxicity against 38 different carcinoma cell lines motivated the synthesis of several phenylahistin analogs and culminated in plinabulin (Yamazaki *et al*., 2010), which is now under phase III clinical trial for non-small cell lung cancer. Plinabulin acts as a potent microtubule-disrupting agent like colchicine, and also disrupts tumor's vascular endothelial cells resulting in tumor necrosis (Singh *et al*., 2011).

1.2.4 Immunosuppressants

Immunosuppressants or immunosuppressive drugs can inhibit the immune system and they are clinically used for organ transplantation and autoimmune diseases like rheumatoid arthritis, and multiple sclerosis (Allison, 2000).

Mycophenolic acid was first discovered as a fungal secondary metabolite from *Penicillium* sp. in 1896, even earlier than the discovery of penicillin (Gosio, 1896). However, until 1940s, mycophenolic acid was proved to have multiple activities including antiviral, antifungal, anticancer and immunosuppressive activities (Kitchin *et al*., 1997). In 1995, mycophenolic acid was approved by US Food and Drug Administration (FDA) for use in kidney transplantations (Food, 2010). Mycophenolic acid can block the activation of T- and B-lymphocytes by inhibiting the enzyme IMPDH (Allison and Eugui, 2000).

Cyclosporin (cyclosporine or cyclosporin A) was first isolated from the soil-derived fungus *Tolypocladium inflatum* in1969 (Svarstad *et al.*, 2000). It is a cyclic nonribosomal peptide of 11 amino acids, containing a rare D-alanine. The absolute structure of cyclosporine was confirmed by X-ray crystallography analysis of its iodinated derivative in 1976 (Petcher *et al*., 1976). Cyclosporin has been used clinically to prevent allograft rejection in kidney, liver, heart or bone marrow transplant patients, and also been used for patients with rheumatoid arthritis or psoriasis (Canafax, 1983). Cyclosporin binds to cyclophylin, forming a complex. The complex binds and blocks the function of the enzyme calcineurin, which is very important for the activation of T-cells (Matsuda, 2000).

Tacrolimus was a 23-membered macrolide originally isolated from a soil bacterium *Streptomyces tsukubaensis* in 1987 (Kino *et al*., 1987). It has been approved for patients with allograft rejection after liver or kidney transplantation (Hooks, 1994). As an ointment, tacrolimus is also used in the treatment of atopic dermatitis, which is a type of inflammation of the skin

caused by immune system dysfunction (Hanifin *et al*., 2001). Similar to cyclosporin, tacrolimus acts as calcineurin inhibitor by binding to immunophilin FKBP12, lead to the failure of T- cells activation (Thomson *et al*., 1995).

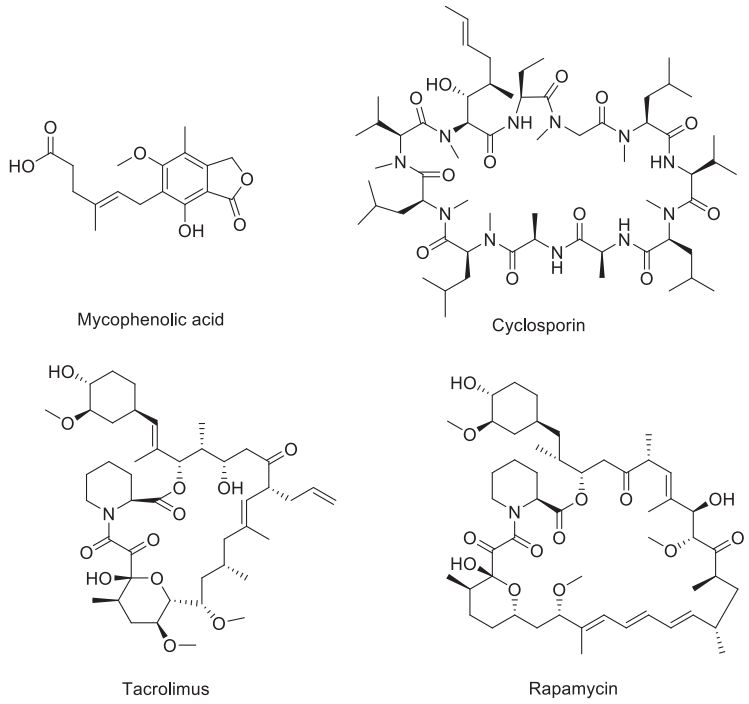

Figure 7. Structures of immunosuppressive agents from microbes.

Rapamycin (Sirolimus) is another macrolide used as immunosuppressive drug, which was first isolated from *Streptomyces hygroscopicus* in 1972 (Vezina *et al*., 1975). Rapamycin was originally introduced as an antifungal compound, but it was rather approved by FDA for its potent immunosuppressive activity in 1999. It has been used for the prevention of rejection in liver, kidney, or lung transplant patients (Wyeth, 2010). Like tacrolimus, rapamycin also binds to FKBP12, but the complex inhibits the mechanistic target of rapamycin (mTOR), rather than calcineurin, to block the activation of T and B cells (Dumont and Su, 1995). In 2015, the FDA approved rapamycin for the treatment of lymphangioleiomyomatosis (LAM), a rare, progressive lung disease (Pahon, 2015).

1.2.5 Cholesterol-lowering and Anti-obesity Agents

Statins are a group of cholesterol-lowering drugs, which competitively inhibit HMG-CoA reductase, a starting enzyme of mevalonate pathway (Endo, 1992). Mevastatin was the first compound of this group isolated from the fungi *Penicillium citrinum* (Endo *et al*., 1976) and *Penicillium brevicompactum* (Brown *et al*., 1976) in 1976. In 1979, another natural product

lovastatin was isolated from the fungus *Monascus rubber*, and turned out to be a widely prescribed drug (Endo, 1979). In 1986, two semi-synthetic statins: simvastatin (Willard and Smith, 1982) and pravastatin (Tsujita *et al*., 1986) with stronger activity were derived from lovastatin and mevastatin, respectively. Based on the structure and activity relationship (SAR) of the natural statins and semi-synthetic statins, it was found that the chiral lactone-derived moiety was necessary for cholesterol-lowering activity, but the bicyclic moiety was not the active center (Endo and Hasumi, 1993). This discovery led to the development of synthetic statins such as fluvastatin, atorvastatin, and rosuvastatin between the late 1980s and early 1990s. Among them, atorvastatin was one of the best-selling drugs in the US from 2007 to 2012 (McGrath *et al*., 2010).

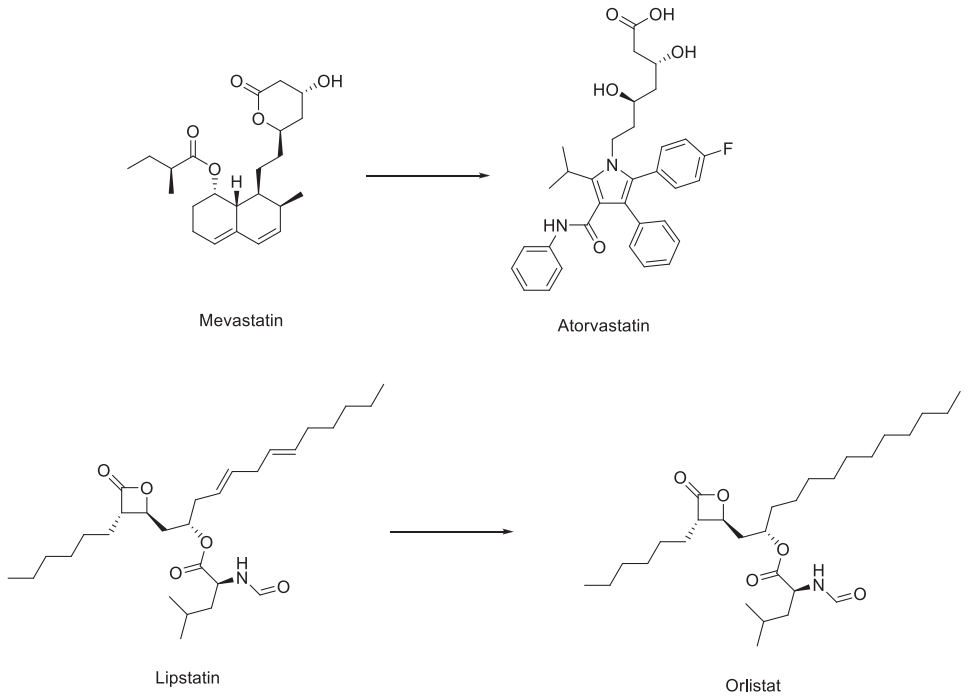

Figure 8. Structures of cholesterol-lowering and anti-obesity agents derived from microbes.

Lipstatin is a natural product, which was first isolated from the bacterium *Streptomyces toxytricini* in 1987 (Weibel *et al*., 1987). It is a potent, irreversible inhibitor of pancreatic lipase, which is an enzyme used for breaking down triglycerides in the intestine (Al-Suwailem *et al*., 2006). When the lipase activity is blocked, absorbable fatty acids can not be produced from the diet. In this way, orlistat, a semi-synthetic derivative from lipstatin, serves as an anti-obesity drug (Hauptman *et al*., 1992). In 2009, the European Medicines Agency (EMA) approved orlistat to be sold without a prescription (Glaxo, 2009).

1.2.6 Antiparasitic Agents

Half of the 2015 Nobel Prize in Physiology or Medicine was awarded to Youyou Tu for the discovery of artemisinin, and the other half was awarded to William C. Campbell and Satoshi Ōmura for discovering avermectins (Campbell *et al*., 2015). Artemisinin (*qinghaosu* in Chinese) was first isolated from the plant *Artemisia annua* in1972 (Miller and Su, 2011). Artemisinin and its semi-synthetic derivatives are the most effective drugs against *Plasmodium falciparum* malaria (White, 1997). Avermectins are a group of 16-membered macrolides, which were first isolated as four pairs of homologues compounds from the soil actinomycete *Streptomyces avermitilis* in 1978 (Burg *et al*., 1979). Avermectins and their semi-synthetic analogues ivermectin, selamectin, doramectin and abamectin, have been widely used against parasites (nematode and arthropod) in humans and animals (Pitterna *et al*., 2009). Avermectins act at the invertebrate nerve by blocking the transmission of electrical activity, resulting in the paralysis of invertebrate neuromuscular systems (Cully *et al*., 1994).

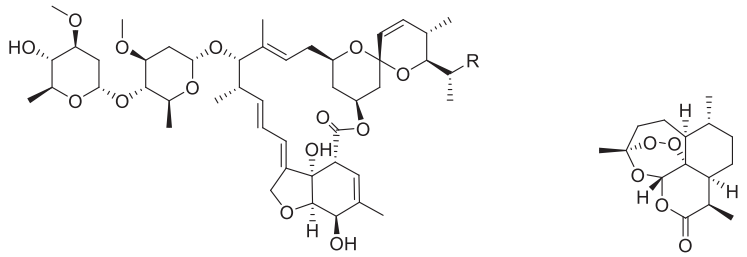

Figure 9. Structures of avermectins from microbes and artemisinin from plants.

1.2.7 Insecticides and Herbicides

In addition to their use in medicine, some microbial secondary metabolites have also been applied to agriculture. Compared with other insecticides and herbicides, microbial natural products are safer and more environmentally friendly, because they are highly targeted and easily degraded (Cutler, 1988).

Spinosyns are compounds containing four-cyclic rings and two deoxysugars, which were first discovered from *Saccharopolyspora spinosa* in1989 (Mertz and Yao, 1990). They possess insecticidal activities against plant pests like dipterans and lepidopterans, with no antimicrobial activity and low mammalian toxicity (Kirst *et al*., 2002). Spinosad, which contains 85% spinosyn A and 15% spinosyn D has been introduced to the market for pest control in organic crops and animal health (Kirst, 2010). By binding to two receptors of neural transmitters, spinosyns act on

the nervous system of insects (Salgado, 1998).

Bialaphos is a natural herbicide, which was discovered from two species of *Streptomyces* bacteria in Germany and Japan independently between the late 1960s and early 1970s (Donn and Köcher, 2012). In plants, bialaphos can be transferred to the active molecular glufosinate, which decreases the activity of glutamine synthetase, which causes the plant death with metabolic disorders (Duke and Dayan, 2011). As bialaphos exhibits no influence on soil microorganisms and has only 2-hour half life, it enjoys great interest from environmentalists (Duke and Lydon, 1987).

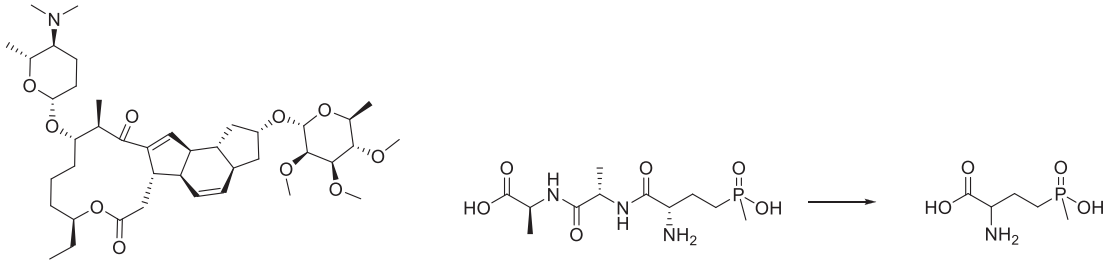

Figure 10. Structures of insecticides and herbicides from microbes.

1.3 Today's Natural Product Discovery

From "the Golden Age" (1940s-1970s) to present, the natural product discovery has continued to be attractive and active in the scientific world (Kaltz and Baltz, 2016). Scientists in natural product chemistry are fascinated by the endless novel chemical structures and diverse bioactivities. Scientists in organic chemistry are attracted to develop synthetic routes to achieve the same stereo-complexity of secondary metabolites. The microbiologists are pleased to discover a productive strain to produce novel bioactive molecules. The organic chemists and pharmaceutical companies are attracted to the development of semi-synthetic derivatives (Kaltz and Baltz, 2016). Until the year of 2013, 1,453 chemical structures had been approved by the FDA, and among them, around 40% are natural products or their inspired derivatives (Kinch et al., 2014). With new strategies and technologies, more than 10,000 new natural products per year are discovered nowadays, and 25% of them are biologically active (Kinch et al., 2014). From the beginning of 1990s to today, sharply increasing new compounds have been published from marine fungi, since this source is far underexplored.

1.3.1 Marine Fungi

Marine fungi are defined from their ecological habitats, but not their physiological or

taxonomical properties (Hyde *et al*., 1998). From the deep ocean to the surface of seawater, and even to the coast line with mangrove swamps, marine fungi can be found nearly everywhere in marine habitats, like non-living material (soil, sediments, driftwood, ship bases, artificial materials), marine plants (most notably mangrove plants, algae, lichens, sea grasses), marine invertebrates (especially sponges, ascidians, holothurians, crustaceans, corals, bivalves) and vertebrates (whales, dolphins, seals, fishes) (Rateb and Ebel, 2011; Demain, 2014). Under the specific evolutionary stress, diverse fungal communities have been developing in different niches.

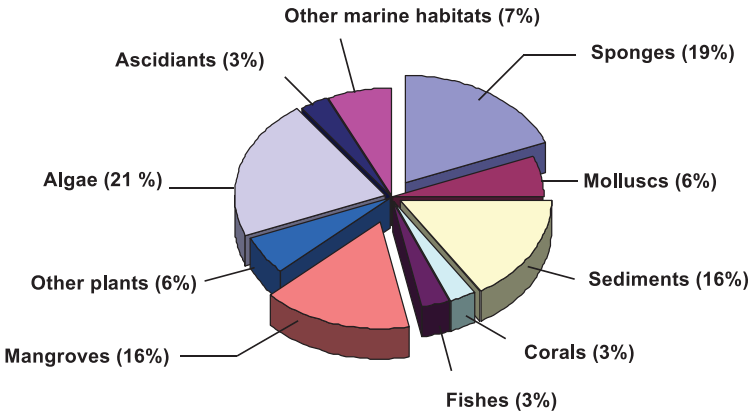

Figure 11. New natural products from marine fungi until mid-2010, categorized by habitats of fungal strains (modified after Rateb and Ebel, 2011).

Figure 11 shows an overview of the new compounds isolated from marine-derived fungi from different marine habitats until mid-2010 (Rateb and Ebel, 2011). It indicates that most of the published new compounds produced by marine fungi were derived from four main original habitats, including algae (21%), sponges (19%), mangroves (16%), and sediments (16%). Interestingly, except sediments and artificial substrates, the frequent studied original habitats for marine fungi like algae, mangroves, sponges and fishes are all living organisms. The possible reason is that the symbiotic fungi have been well evolved during the long period of interactions with their hosts.

1.3.1.1 Mangrove Endophytes

Mangroves are a group of trees that live in coastal lines in tropical or subtropical areas (Twilley and Day 2012). In the high-salinity (17.0 – 36.4%) environment, mangrove plants (also called halophytes) have evolved their special organs (like salt-excreting glands on leaves) and mechanisms to survive (Walsh, 1974). The long aerial roots have enabled mangroves to absorb

oxygen from the air to adapt to low oxygen environments (Tomlinson, 1994). However, the niches of mangroves are more complex with various factors, including a wide temperature range (10 – 40 °C), over-lighted exposure, limited nutrient, droughts and floods caused by the tides, and plant pathogens (Feller *et al*., 2010). Numerous scientists assumed that the interactions between the endophytes and mangroves evolutionally facilitated the ecological success of mangroves (Arnold *et al*., 2003; Reinhold-Hurek and Hurek, 2011; Aly *et al*., 2011).

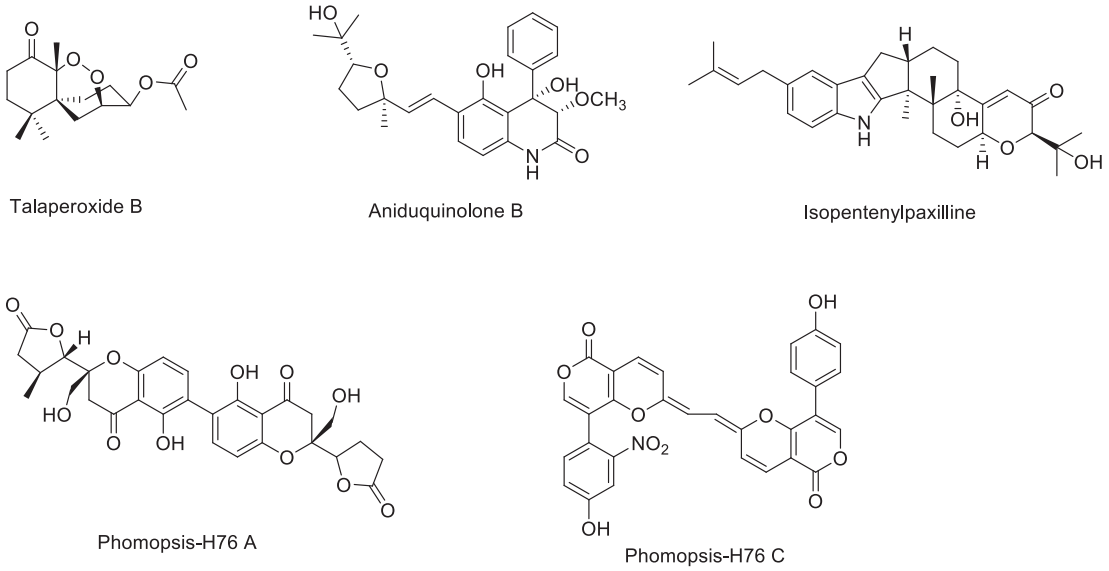

Figure 12. Novel structures from mangrove endophytic fungi.

In recent decades, the mangroves have attracted an increasing number of natural product chemists to study the secondary metabolites produced by their endophytes. Inspiringly, many interesting compounds with novel structures and diverse activities were discovered. Example like talaperoxide B from the mangrove endophyte *Talaromyces flavus* showed potent cytotoxicity with IC_{50} values ranging from 0.89 to 2.78 μg/mL against five different carcinoma cell lines (Li *et al*., 2011). Aniduquinolone B, isolated from the mangrove endopyhte *Aspergillus nidulans*, was toxic against brine shrimp larvae with LD_{50} value of 7.1 μM (An *et al*., 2013). Antiviral compound, isopentenylpaxilline, was first isolated from the fungus *Eupenicillium shearii* (Belofsky *et al*., 1995), and rediscovered from *Penicillium camemberti*, a fungus isolated from the sediment around the mangrove roots (Fan *et al*., 2013). Phomosis-H76 A and C were discovered in the mangrove endophytic fungus *Phomopsis* sp. Interestingly, these two compounds showed absolute totally different effects on the growth of subintestinal vessel plexus (Yang *et al*., 2010).

1.3.1.2 Sponge-Associated Fungi

Sponges are jelly-like multicellular organisms that feed and breathe by constantly pumping sea water (Krautter, 1998). Even though there are debates on whether fungi live inside sponges as endosymbionts, sponges have been generally accepted to be an important source to provide productive fungi, which possess special gene clusters for secondary metabolites with novel structures (Proksch *et al*., 2008). Marilone A and B were discovered through chemical investigation on the sponge-associated fungus *Stachylidium* sp. Marilone A inhibited the growth of malaria parasite *Plasmodium berghei* with an IC_{50} value of 12.1 μM. However, marilone B, without a geranyl side chain, showed selective antagonistic activity to serotonin receptor 2B with 7.7 μM K_i value (Almeida *et al*., 2011). Fumiquinazoline K, a novel alkaloid with an unusual cyclopropane ring was produced by *Aspergillus* sp., which was derived from the sponge *Tethya aurantium* (Zhou *et al*., 2013). Insuetolide A, a novel antifungal meroterpenoid, was obtained from the chemical investigation on *Aspergillus insuetus*, which was a sponge-associated fungus (Cohen *et al*., 2011).

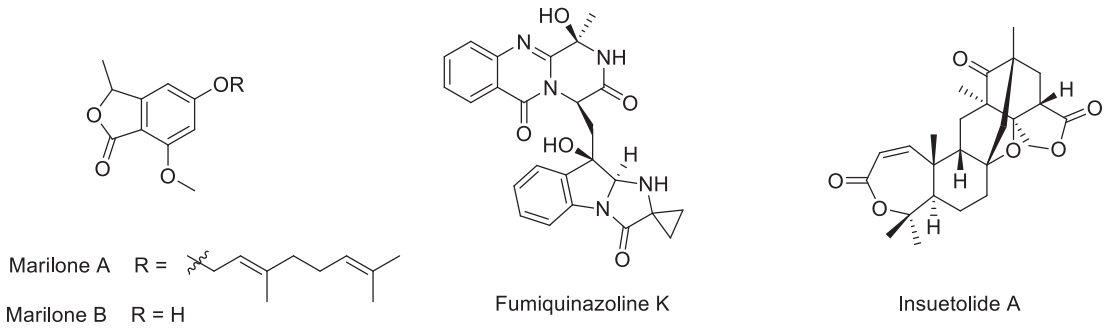

Figure 13. Novel structures from sponge associated fungi.

1.3.2 Activation of Silent Gene Clusters for New Fungal Secondary Metabolites

In the past decade, the whole genome sequence analyses of two *Streptomyces* reached a surprising finding that only a small part of gene clusters in the microbial genome were expressed for the biosynthesis of secondary metabolites (Bentley *et al*., 2002; Ikeda *et al*., 2003; Challis, 2014). Fungal genes for secondary metabolites were also discovered as clusters (Smith *et al*., 1990). More and more studies of fungal genome sequences revealed that the potential for diverse chemical structures in fungi is far underestimated, since most gene clusters keep silent during cultivation at standard laboratory conditions (Bergmann *et al*., 2007; Chiang *et al*., 2008). Therefore, one of the new tasks of today's natural product chemistry is to trigger the silent biosynthetic gene clusters in fungi for new compounds. A number of strategies for triggering silent

gene clusters were reported recently (Marmann *et al*., 2014; Reen *et al*., 2015; Deepika *et al*., 2016). Most of them appeared empirically at chemical level, including OSMAC (one strain many compounds), epigenetic modulation, and co-cultivation.

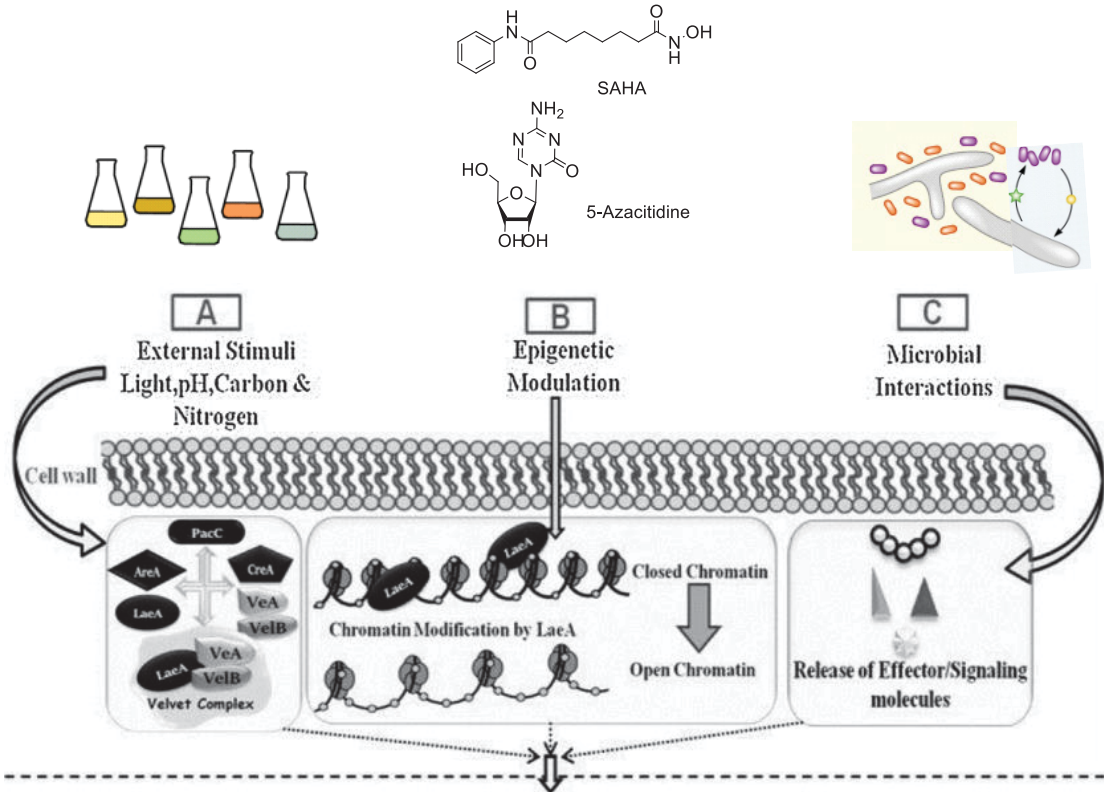

Figure 14. Strategies to activate the silent gene clusters for new secondary metabolites in fungi (modified after Deepika *et al*., 2016).

OSMAC is an approach that involves the induction of diverse secondary metabolites from one fungus by changing cultivation factors, like culture media (pH, carbon source, nitrogen source, halogens et al.), temperature, aeration, or flasks' shape (Bode *et al*., 2000; Bode *et al*., 2002; Grond *et al*., 2002). For example, the endolichenic fungus *Ulocladium* sp. cultured on rice medium was reported by Lixin Zhang's group to have produced thirteen phenolic compounds (Wang *et al*., 2012). However, when the same fungus was cultured on Czapek's liquid medium, thirteen completely different terpenoids, which can not be detected previously, were isolated by the same group (Wang *et al*., 2013).

Histone deacetylase (HDAC) is an enzyme that removes the acetyl groups from lysine residues on histone, forming a condensed chromatin, which can not be transcribed (Choudhary *et al*., 2009). Hence, adding HDAC inhibitors (suberanilohydroxamic acid (SAHA), suberoyl

bis-hydroxamic acid (SBHA)) to the medium is one way to open the chromatin and help the expression of silent secondary metabolite genes in fungi. Recent publication reported that 1 mM SBHA in liquid medium, successfully induced an entomophatogenic fungus *Torrubiella luteorostrata* to produce three new compounds luteorides A-C (Asai *et al*., 2011).

1.3.2.1 Co-Cultivation

The co-cultivation approach of fungi vs. bacteria is a new method that triggers the expression of silent gene clusters, which were only described in of recent publications (Angell *et al*., 2006; Oh *et al*., 2007; Scherlach *et al*., 2009). In most natural environments, fungi and bacteria have lived together and interacted with each other since nearly the start of their lives. The biofilms on the surfaces of submerged objects contain both fungi and bacteria, and the fungi may support the growth of bacteria as skeleton (Donlan and Costerton, 2002). With the long evolutionary process, fungi and bacteria interact with each other in many different ways: antibiosis (penicillin, surfactin), growth promoting signals (auxofuran), altering the physiochemical environment (pH), cellular contacts, nutritional competition, and cooperative metabolism (Frey-Klett *et al*., 2011). Several successful experiments of fungal-bacterial co-cultivation conducted in our group have proved that it is a very effective way to trigger new secondary metabolites or enhance the production of low-amount compounds from fungi. For instance, co-cultivation of endophytic fungus *Fusarium tricinctum* and the bacterium *Bacillus subtilis* triggered the biosynthesis of three new natural products, which were not detected in fungal axenic culture (Ola *et al*., 2013). When the endophytic fungus *Aspergillus austroafricanus* was cultured with bacteria *Streptomyces lividans* or *Bacillus subtilis*, the production of four diphenyl ethers increased up to 29-fold (Ebrahim *et al*., 2016). When the soil-dwelling fungus *Aspergillus terreus* was co-cultured with two *Bacillus* species, four butyrolactones including two new ones were induced (Chen *et al*., 2015).

1.4 Aims and significance of the study

As a promising source of natural products, marine fungi have continued to provide numerous compounds with novel structures and interesting activities. This study covers the chemical investigation of three marine fungi, including two mangrove endophytes (chapter 2, 3, 5) and one sponge associated fungus (chapter 4). The three marine fungi were chosen, based on their interesting UV spectra from HPLC-UV analysis or significant activities of the crude extracts (cytotoxic or antibacterial) from small scale culture. Three different types of secondary

metabolites: fusaric acid derivatives (chapter 2), 14-membered macrolides (chapter 3), and phenolic bisabolanes (chapter 4) were purified from the rice culture of these three fungi. Moreover, various methods were applied to confirm the new compounds' absolute configurations: GC-MS (chapter 2), X-ray crystallographic analysis (chapter 3, 5), Mosher's reaction (chapter 3), and ECD calculation (chapter 3).

In order to trigger the silent genes in fungi for biosynthesis of new compounds, co-cultivations of the fungus (*Pestalotiopsis microspora*, or *Aspergillus* sp.) with the bacterium (*Streptomyces lividans*, or *Bacillus subtilis*) were conducted. As a result, it was found that the high density (0.2 g/flask) of *S. lividans* can induce the fungus *P. microspora* to produce new macrolides and also increase the accumulation of known compounds, but the low concentration (0.05 g/flask) of this bacterium didn't show any influence compared to axenic culture (chapter 3). The long term co-cultivation of *P. micropsora* with *B. subtilis* resulted in the production of two new secondary metabolites, which were cryptic in axenic controls (chapter 5).

The isolated products were submitted to various bioassays: phytotoxicity on barley leaves (chapter 2), cytotoxicity against mouse or human carcinoma cell lines (chapter 3), or antibacterial activities against *Mycobacterium tuberculosis* and seven other human pathogenic bacteria (chapter 4). The results of these studies are described in this dissertation.

Chapter 2

New Fusaric Acid Derivatives from the Endophytic Fungus *Fusarium oxysporum* and Their Phytotoxicity to Barly Leaves

Published in “Journal of Agricultural and Food Chemistry”.

Impact Factor: 2.857.

JOURNAL OF AGRICULTURAL AND FOOD CHEMISTRY

Article

pubs.acs.org/JAFC

New Fusaric Acid Derivatives from the Endophytic Fungus *Fusarium oxysporum* and Their Phytotoxicity to Barley Leaves

Shuai Liu,[†] Haofu Dai,[§] Raha S. Orfali,[#] Wenhan Lin,[⊗] Zhen Liu,[*,†] and Peter Proksch[*,†]

[†]Institute of Pharmaceutical Biology and Biotechnology, Heinrich-Heine-Universität Düsseldorf, Universitätsstrasse 1, 40225 Düsseldorf, Germany

[§]Key Laboratory of Biology and Genetic Resources of Tropical Crops, Ministry of Agriculture, Institute of Tropical Bioscience and Biotechnology, Chinese Academy of Tropical Agricultural Sciences, Haikou 571101, China

[#]Department of Pharmacognosy, Faculty of Pharmacy, King Saud University, Riyadh, Saudi Arabia

[⊗]State Key Laboratory of Natural and Biomimetic Drugs, Peking University, Beijing 100191, China

Supporting Information

ABSTRACT: Chemical investigation of the endophytic fungus *Fusarium oxysporum* isolated from fruits of *Drepanocarpus lunatus* afforded eight new fusaric acid derivatives, fusaricates A−G, **1**−**7**, and 10-hydroxy-11-chlorofusaric acid, **8**, along with four known compounds. Their structures were elucidated by one- and two-dimensional NMR as well as MS data and by comparison with the literature. The absolute configurations of fusaricates C−E, **3**−**5**, were determined using chiral GC-MS. Fusaricates A−G, **1**−**7**, represent the first examples of fusaric acid linked to a polyalcohol moiety via an ester bond. All isolated fusaric acid derivatives **1**−**8** showed significant phytotoxicity to leaves of barley.

KEYWORDS: *Fusarium oxysporum, fusaricates A−G, structural elucidation, phytotoxicity*

INTRODUCTION

Endophytes are defined as microorganisms, including bacteria and fungi, that live within plant tissues for all or part of their life cycle without causing any visible symptoms of their presence such as diseases.[1,2] The relationships between plants and their endophytes are complex and not well understood in all aspects. It is assumed that plants survive and flourish in stressed ecosystems due to their endophytes, which have coevolved and are essential for their adaptation to changing environments.[3] It has also been shown that endophytes influence the growth of their host plants by manipulating phytohormones such as indole-3-acetic acid.[4] As an important source of natural products, endophytic fungi provide a wide range of bioactive compounds with anticancer, antibacterial, antiviral, and immunosuppressive activities.[5]

Fusarium is a genus of filamentous fungi that produce diverse bioactive secondary metabolites, including beauvericin, which possesses antibacterial and insecticidal activities; trichothecenes, which are strongly associated with chronic and fatal toxic effects in animals or humans; and gibberellins, which are plant hormones.[6] Fusaric acid (5-butylpyridinecarboxylic acid) is a typical secondary metabolite of members of this genus showing various bioactivities such as inhibition of dopamine-β-hydroxylase in vitro at 10^{-8} M.[7,8] A recent evaluation of the phytotoxicity of fusaric acid analogues underscored their potential as bioherbicides for organic farming.[9,10]

As part of our ongoing studies on bioactive natural products from endophytic fungi,[11−14] *Fusarium oxysporum*, which was isolated from fresh and healthy fruits of the mangrove plant *Drepanocarpus lunatus* (Fabaceae) growing in Cameroon, was investigated. Eight new fusaric acid derivatives and four known compounds were isolated. Herein, we report the isolation and structural elucidation of the new compounds, as well as their phytotoxic and cytotoxic activities.

MATERIALS AND METHODS

General Method. Optical rotation values were measured by a P-1020 polarimeter (JASCO, Tokyo, Japan). NMR spectra were recorded on a Bruker Avance III 600 spectrometer (Bruker, Karlsruhe, Germany). HRESIMS data were obtained from a UHR-QTOF maxis 4G mass spectrometer (Bruker Daltonics, Bremen, Germany). HPLC analysis was conducted by a Dionex P580 system (Dionex Softron, Germering, Germany) with a 125 mm × 4 mm i.d., 5 μm, Eurospher C_{18} (Knauer, Berlin, Germany) column. Silica gel 60 F_{254} precoated aluminum plates (Merck, Darmstadt, Germany) were used for thin layer chromatography under detection at 254 and 365 nm. Silica 60 M (Macherey-Nagel, Dueren, Germany) was applied to column chromatography. The final purification of compounds was performed on a Merck-Hitachi Lachrom semipreparative RP-HPLC system (Merck) with a 300 mm × 8 mm i.d., 10 μm, Eurospher C_{18} column (Knauer). The analyses of chiral polyalcohols were carried out on a GC-MS QP-2010 Plus instrument (Shimadzu, Tokyo, Japan), equipped with a 50 m × 0.25 mm i.d., 0.25 μm, FS-CYCLODEX beta-I/P column (Chromatographie Service GmbH, Langerwehe, Germany). The chiral polyalcohol standards were acquired as follows: erythritol and xylitol (Alfa Aesar GmbH, Karlsruhe, Germany), L-threitol (TCI GmbH, Eschborn, Germany), adonitol and D-threitol (Sigma-Aldrich Chemie GmbH, Steinheim, Germany), D- and L-arabitol (Acros Organics, Geel, Belgium).

Fungal Material and Identification. This fungus was isolated from fresh fruits of *D. lunatus* (Fabaceae) collected in August 2013 from Douala in Cameroon. Isolation of the fungal strain was achieved

Received: January 15, 2016
Revised: April 5, 2016
Accepted: April 6, 2016
Published: April 6, 2016

DOI: 10.1021/acs.jafc.6b00219
J. Agric. Food Chem. 2016, 64, 3127−3132

according to a standard procedure as described before.[15] On the basis of DNA amplification and sequencing of the ITS region,[16] the fungus was identified as *F. oxysporum* (GenBank accession no. KT373853). A voucher strain (code DL-F-3-1) was deposited in one of the authors' laboratory (P.P.).

Fermentation, Extraction, and Isolation. The fermentation was performed in Erlenmeyer flasks (2 × 1 L) on solid rice medium containing 100 g of rice, 3.5 g of sea salt, and 110 mL of demineralized water. After autoclaving at 121 °C for 20 min and then cooling to room temperature, each flask was inoculated and then incubated at 20 °C under static conditions. After 30 days, the fermentation was stopped by adding 500 mL of EtOAc to each flask. The extraction was completed after the flasks had been shaken on a laboratory shaker at 150 rpm for 8 h.

Evaporation of the EtOAc solution gave a brown extract (1.5 g), which was subjected to vacuum liquid chromatography upon a 15 cm × 8 cm i.d. silica gel column using gradient solvent system (*n*-hexane/EtOAc, 10:0, 9:1, 7:3, 1:1, 3:7; CH_2Cl_2/MeOH, 9:1, 7:3, 1:1, 0:10; 500 mL each gradient) to obtain nine fractions (fractions A–I). Fraction D (82.5 mg) was subjected to a Sephadex LH-20 column using 100% MeOH as mobile phase to remove pigments and further purified by semipreparative HPLC with MeOH/H_2O as eluting system (0–5 min, 55% MeOH; 5–15 min, from 55 to 64% MeOH; 15–18 min, 100% MeOH) to yield pestalotiollide A (1.6 mg), pestalotiollide B (8.8 mg), and dehydroisopenicillide (1.4 mg). Following a similar purification process, fraction E (116.1 mg) yielded beauvericin (53.5 mg) (HPLC sequence: 0–3 min, 80% MeOH; 3–11 min, from 80 to 95% MeOH; 11–13 min, 100% MeOH), and fraction F (197.0 mg) afforded **1** (3.9 mg), **3** (2.0 mg), a mixture of **4** and **5** (12.4 mg), and a mixture of **6** and **7** (5.4 mg) (HPLC sequence: 0–5 min, 40% MeOH; 5–18 min, from 40 to 57% MeOH; 18–22 min, 100% MeOH), whereas fraction G (152.9 mg) gave **2** (1.9 mg) and **8** (3.2 mg) (HPLC sequence: 0–3 min, 20% MeOH; 3–17 min, from 20 to 60% MeOH; 17–21 min, 100% MeOH) (see Figure 1 for compound structures).

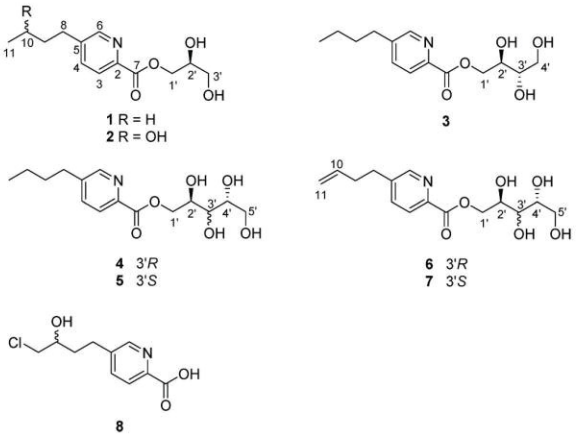

Figure 1. Structures of new fusaric acid derivatives isolated from *F. oxysporum*.

Determination of the Absolute Configuration of Polyalcohols in 3–5. An amount of 0.7 mg of each sample was hydrolyzed with 2 N HCl (1.0 mL) at 90 °C for 2 h. After evaporation in a freeze-dryer overnight, the hydrolysis products were treated with trifluoroacetic anhydride (200 μL) and DMAP (0.1 mg) in dichloromethane (200 μL). Trifluoroacetylation of polyalcohols was performed by heating the mixture at 80 °C for 10 min, and the product was subsequently analyzed by gas chromatography under the following conditions. The column temperature was set at 80 °C and ramped to 200 °C at a rate of 2 °C/min. In cochromatography experiments with D- or L-arabitol, the column temperature was set at 80 °C and ramped to 120 °C at a rate of 2 °C/min and then to 200 °C at a rate of 1 °C/min. The temperatures of the injector and detector were set at 200 °C. Helium was used as carrier gas with a flow rate of 30 cm/min.

Fusaricate A, 1: white amorphous powder; $[\alpha]^{20}_D$ +7.0 (*c* 0.55, EtOH); UV (MeOH) λ_{max} (log ε) 233 (4.11), 270 (3.83) nm; ^{1}H and ^{13}C NMR data, see Table 1; HRESIMS *m*/*z* 254.1384 $[M + H]^+$ (calcd for $C_{13}H_{20}NO_4$, 254.1387).

Fusaricate B, 2: light yellow solid; $[\alpha]^{20}_D$ +7.1 (*c* 0.48, MeOH); UV (MeOH) λ_{max} (log ε) 233 (4.13), 270 (3.86) nm; ^{1}H and ^{13}C NMR data, see Table 1; HRESIMS *m*/*z* 270.1335 $[M + H]^+$ (calcd for $C_{13}H_{20}NO_5$, 270.1336).

Fusaricate C, 3: white amorphous powder; $[\alpha]^{20}_D$ −26.9 (*c* 0.10, acetone); UV (MeOH) λ_{max} (log ε) 233 (4.15), 270 (3.87) nm; ^{1}H and ^{13}C NMR data, see Table 1; HRESIMS *m*/*z* 284.1493 $[M + H]^+$ (calcd for $C_{14}H_{22}NO_5$, 284.1492).

Mixture of Fusaricate D, 4, and Fusaricate E, 5: white amorphous powder; UV (MeOH) λ_{max} (log ε) 233 (4.20), 271 (3.92) nm; ^{1}H and ^{13}C NMR data, see Table 2; HRESIMS *m*/*z* 314.1597 $[M + H]^+$ (calcd for $C_{15}H_{24}NO_6$, 314.1598).

Mixture of Fusaricate F, 6, and Fusaricate G, 7: light yellow solid; UV (MeOH) λ_{max} (log ε) 232 (4.21), 271 (3.92) nm; ^{1}H and ^{13}C NMR data, see Table 2; HRESIMS *m*/*z* 312.1443 $[M + H]^+$ (calcd for $C_{15}H_{22}NO_6$, 312.1442).

10-Hydroxy-11-chlorofusaric acid, 8: white amorphous powder; $[\alpha]^{20}_D$ + 30.7 (*c* 0.80, MeOH); UV (MeOH) λ_{max} (log ε) 222 (3.78), 272 (3.88) nm; ^{1}H and ^{13}C NMR data, see Table 3; HRESIMS *m*/*z* 230.0577 $[M + H]^+$ (calcd for $C_{10}H_{13}ClNO_3$, 230.0578).

Phytotoxicity Assay. Phytotoxicity was investigated according to the cotton cotyledonary leaf bioassay described by Stipanovic et al.[9] Barley plants ('Bonus', a Swedish cultivar) were inoculated 15 days after planting and scored 48 h after inoculation. A pipet tip was used to scratch the surface of barley leaf, and then the test solution (20 μL) was placed at three locations on each leaf. Different concentrations (0.5–8.0 mM) of test compounds were prepared by dissolving the compounds with distilled water. Commercial fusaric acid and distilled water were used as positive and negative control, respectively.

Cell Proliferation Assay. MTT method was performed to test cytotoxicity against L5178Y mouse lymphoma cell line.[17] Experiments were carried out three times with Kahalalide F as positive control and media with 0.1% EGMME–DMSO as negative control.

■ RESULTS AND DISCUSSION

Compound **1** was obtained as a white amorphous powder. Its molecular formula was established as $C_{13}H_{19}NO_4$ by HRESIMS, indicating five degrees of unsaturation. Its UV spectrum showed characteristic peaks of fusaric acid analogues at λ_{max} 233 and 270 nm.[18] The ^{1}H NMR spectrum (Table 1) exhibited three aromatic protons typical for an ABX coupling system at δ_H 8.54 (H-6, d, *J* = 2.2 Hz), δ_H 8.13 (H-3, d, *J* = 8.0 Hz), and δ_H 7.86 (H-4, dd, *J* = 8.0, 2.2 Hz), suggesting the presence of a 2,5-substituted pyridine ring, which was confirmed by the HMBC correlations from H-3 to C-5 (δ_C 144.6), from H-4 to C-2 (δ_C 146.3) and C-6 (δ_C 150.7), and from H-6 to C-2 and C-4 (δ_C 138.9). A butyl group at C-5 was deduced from the COSY correlations between H_2-8 (δ_H 2.76, t)/H_2-9 (δ_H 1.66, qui), H_2-9/H_2-10 (δ_H 1.40, sext), and H_2-10/H_3-11 (δ_H 0.97, t), together with the HMBC correlations from H_2-8 to C-4, C-5, and C-6. According to the HSQC spectrum, five proton signals at δ_H 4.46 (H_a-1′, dd, *J* = 11.3, 3.8 Hz), 4.33 (H_b-1′, dd, *J* = 11.3, 6.6 Hz), 3.99 (H-2′, ddt, *J* = 6.6, 3.8, 5.7 Hz), and 3.65 (2H, H_2-3′, d, *J* = 5.7 Hz) were assigned to three oxygenated carbons at δ_C 68.1 (C-1′), 71.1 (C-2′), and 63.9 (C-3′), which were attributed to a glycerol unit, as further supported by the COSY correlations between H_a-1′/H-2′, H_b-1′/H-2′, and H-2′/H_2-3′. An ester linkage between C-2 of the pyridine ring and C-1′ of the glycerol unit was confirmed by

DOI: 10.1021/acs.jafc.6b00219
J. Agric. Food Chem. 2016, 64, 3127–3132

Table 1. ^{1}H (600 MHz) and ^{13}C (150 MHz) NMR Data of Fusaricates A–C, 1–3 (CD_3OD)

	1		2		3	
position	δ_H (J in Hz)	δ_C	δ_H (J in Hz)	δ_C	δ_H (J in Hz)	δ_C
2		146.3, C		146.4, C		146.4, C
3	8.13, d (8.0)	126.4, CH	8.14, d (8.1)	126.5, CH	8.15, d (8.0)	126.5, CH
4	7.86, dd (8.0, 2.2)	138.9, CH	7.88, dd (8.1, 2.2)	138.9, CH	7.87, dd (8.0, 2.2)	138.9, CH
5		144.6, C		144.4, C		144.6, C
6	8.54, d (2.2)	150.7, CH	8.57, d (2.2)	150.8, CH	8.54, d (2.2)	150.7, CH
7		166.0, C		166.0, C		166.0, C
8	2.76, t (7.5)	33.5, CH_2	2.89, ddd (13.9, 9.1, 6.4) 2.80, ddd (13.9, 9.1, 7.4)	30.2, CH_2	2.76, t (7.5)	33.5, CH_2
9	1.66, tt (7.5, 7.5)	34.2, CH_2	1.77, m	41.2, CH_2	1.67, tt (7.5, 7.5)	34.2, CH_2
10	1.40, tq (7.5, 7.5)	23.3, CH_2	3.75, tq (6.2, 6.2)	67.6, CH	1.40, tq (7.5, 7.5)	23.3, CH_2
11	0.97, t (7.5)	14.1, CH_3	1.21, d (6.2)	23.6, CH_3	0.97, t (7.5)	14.1, CH_3
1′	4.46, dd (11.3, 3.8) 4.33, dd (11.3, 6.6)	68.1, CH_2	4.46, dd (11.3, 3.8) 4.34, dd (11.3, 6.6)	68.2, CH_2	4.60, dd (11.4, 2.8) 4.41, dd (11.4, 6.6)	68.9, CH_2
2′	3.99, ddt (6.6, 3.8, 5.7)	71.1, CH	3.99, ddt (6.6, 3.8, 5.6)	71.2, CH	3.90, ddd (7.5, 6.6, 2.8)	71.5, CH
3′	3.65, d (5.7)	63.9, CH_2	3.65, d (5.6)	63.9, CH_2	3.67, m	73.5, CH
4′					3.81, m 3.66, m	63.9, CH_2

Table 2. ^{1}H (600 MHz) and ^{13}C (150 MHz) NMR Data of Fusaricates D–G, 4–7 (CD_3OD)

	4		5		6		7	
position	δ_H (J in Hz)	δ_C	δ_H (J in Hz)	δ_C	δ_H (J in Hz)	δ_C	δ_H (J in Hz)	δ_C
2		146.3, C		146.4, C		146.5, C		146.5, C
3	8.13, br d (8.1)	126.4, CH	8.15, br d (8.1)	126.5, CH	8.13, br d (8.1)	126.4, CH	8.15, br d (8.1)	126.4, CH
4	7.85, br d (8.1)	138.8, CH	7.86, br d (8.1)	138.9, CH	7.86, br d (8.1)	139.1, CH	7.87, br d (8.1)	139.1, CH
5		144.5, C		144.6, C		143.6, C		143.6, C
6	8.53, br s	150.6, CH	8.53, br s	150.7, CH	8.54, br s	150.8,CH	8.54, br s	150.8, CH
7		166.0, C		166.1, C		166.0, C		166.1, C
8	2.76, t (7.5)	33.5, CH_2	2.76, t (7.5)	33.5, CH_2	2.86, m	33.2, CH_2	2.86, m	33.2, CH_2
9	1.66, tt (7.5, 7.5)	34.2, CH_2	1.66, tt (7.5, 7.5)	34.2, CH_2	2.44, m	35.8, CH_2	2.44, m	35.8, CH_2
10	1.39, tq (7.5, 7.5)	23.3, CH_2	1.39, tq (7.5, 7.5)	23.3, CH_2	5.85, m	138.1, CH	5.85, m	138.1, CH
11	0.96, t (7.5)	14.1, CH_3	0.96, t (7.5)	14.1, CH_3	5.01, d (17.1) 4.99, d (9.8)	116.5, CH_3	5.01, d (17.1) 4.99, d (9.8)	116.5, CH_3
1′	4.45, m	68.6, CH_2	4.64, dd (11.3, 2.5) 4.45, dd (11.3, 6.2)	69.1, CH_2	4.45, m	68.6, CH_2	4.64, dd (11.3, 2.5) 4.45, m	69.1, CH_2
2′	4.27, ddd (7.3, 5.4, 1.7)	69.2, CH	4.04, ddd (8.6, 6.2, 2.5)	70.4, CH	4.27, ddd (7.3, 5.4, 1.7)	69.2, CH	4.03, ddd (8.6, 6.2, 2.5)	70.4, CH
3′	3.59, dd (8.5, 1.7)	72.2, CH	3.64, dd (8.6, 1.5)	71.8, CH	3.59, dd (8.5, 1.7)	72.2, CH	3.65, m	71.8, CH
4′	3.76, ddd (8.5, 5.5, 3.4)	72.7, CH	3.96, ddd (6.3, 6.3, 1.5)	71.5, CH	3.76, ddd (8.5, 5.5, 3.4)	72.7, CH	3.96, ddd (6.3, 6.3, 1.5)	71.5, CH
5′	3.83, dd (11.3, 3.4) 3.66, dd (11.3, 5.5)	65.0, CH_2	3.65, m	64.8, CH_2	3.82, dd (11.3, 3.4) 3.66, dd (11.3, 5.5)	65.0, CH_2	3.66, m	64.8, CH_2

key HMBC correlations from H-3 and H_2-1′ to C-7 (δ_C 166.0). Thus, the structure of **1** was identified as a new fusaric acid derivative named fusaricate A (Figure 2). By comparing its optical rotation value {$[\alpha]^{20}_D$ +7.0, (c 0.55, EtOH)} with those of similar known compounds such as (*R*)-1-benzoyloxypropane-2,3-diol {$[\alpha]^{20}_D$ −15.9, (c 1, EtOH)} and (*S*)-1-benzoyloxypropane-2,3-diol {$[\alpha]^{20}_D$ +15.8, (c 1, EtOH)},[19] the absolute configuration of fusaricate A was proposed to be *S*.

The HRESIMS spectrum of fusaricate B, **2**, indicated the molecular formula $C_{13}H_{19}NO_5$, which contains an additional oxygen atom compared to **1**. The NMR data (Table 1) of **2** were closely related to those of **1**, except for the presence of signals of a hydroxymethine group (δ_C 67.6, δ_H 3.75) in **2**. The proton of this hydroxymethine exhibited correlations with H_2-9 (δ_H 1.77, m) and H_3-11 (δ_H 1.21, d) in the COSY spectrum, indicating fusaricate B, **2**, to be a 10-hydroxy derivative of fusaricate A, **1**. Attempts to determine the absolute configuration of C-10 were unsuccessful due to the insufficient amount of this sample.

Fusaricate C, **3**, was obtained as a white amorphous powder, and its UV spectrum was almost identical to that of fusaricate A (**1**). The molecular formula of **3** was determined to be $C_{14}H_{21}NO_5$ by HRESIMS, implying an additional 30 Da compared to **1**. Comparison of the NMR data (Table 1) indicated the gross structure of **3** to be similar to that of **1**, except for the replacement of the glycerol unit of **1** by a tetritol unit. This was confirmed by the COSY correlations between H_2-1′ (δ_H 4.60, dd; 4.41, dd)/H-2′ (δ_H 3.90, ddd), H-2′/H_2-3′ (δ_H 3.67, m), and H-3′/H_2-4′ (δ_H 3.81, m; 3.66, m), as well as by the HMBC correlations from H_2-1′ to C-7 (δ_C 166.0). Moreover, the tetritol unit was determined to be erythritol using chiral GC-MS after hydrolysis of the compound.[20] By

DOI: 10.1021/acs.jafc.6b00219
J. Agric. Food Chem. 2016, 64, 3127−3132

Table 3. ^{1}H (600 MHz) and ^{13}C (150 MHz) NMR Data of 8 (CD_3OD)

	8	
position	δ_H (J in Hz)	δ_C
2		145.8 C
3	8.03, d (7.7)	125.7 CH
4	7.84, d (7.7)	139.6 CH
5		142.7 C
6	8.59, s	149.9 CH
7		not detected
8	2.88, m	29.7 CH_2
	2.77, m	
9	1.89, m	36.2 CH_2
	1.77, m	
10	3.68, m	71.3 CH
11	3.55, dd (11.2, 4.6)	50.0 CH_2
	3.50, dd (11.2, 5.8)	

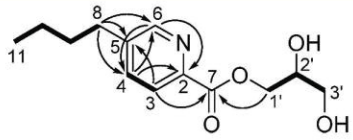

Figure 2. COSY (—) and key HMBC (→) correlations of 1.

comparing the optical rotation of 3 {$[\alpha]^{20}_D$ −26.9, (c 0.10, acetone)} with those of the two related known compounds (2R,3S)-montagnetol {$[\alpha]^{20}_D$ +11, (c 0.4, acetone)}[21] and (2S,3R)-montagnetol {$[\alpha]^{20}_D$ −10.1, (c 0.5, acetone)},[22] the absolute configuration of 3 is suggested to be 2′S,3′R.

Fusaricates D and E, 4 and 5, were obtained as a pair of inseparable diastereomers with a ratio of 1:1 as deduced by ^{1}H NMR. Both compounds shared the molecular formula $C_{15}H_{23}NO_6$ as determined by HRESIMS data. By comparing their ^{1}H and ^{13}C NMR data (Table 2) with those of 1 and 3, the fusaric acid partial structure of N-1 to C-11 could be easily identified. The additional 14 proton signals detected between δ_H 4.70 and 3.50 were assigned to 10 oxygenated carbons between δ_C 73.0 and 64.0 according to the HSQC spectrum. A close inspection of the COSY and HMBC spectra revealed the presence of two pentitol units and their attachments to C-7 through ester linkages. The chiral GC-MS method[20] was used to determine the absolute configurations of pentitol following hydrolysis of 4 and 5. Both 4 and 5 contained D-arabitol, which is also found in the fungi *Gilocladium roseum*,[20] *Gliocladium catenulatum*,[23] and *Clonostachys candelabrum*.[24] The coupling constants of 4 and 5 were 1.7 and 8.6 Hz between H-2′ and H-3′ and 8.5 and 1.5 Hz between H-3′ and H_2-4′, respectively. Thus, fusaricates D and E, 4 and 5, were determined to have the absolute configurations 2′R,3′R,4′R and 2′R,3′S,4′R, respectively. It could be assumed that esterification of the fusaric acid moiety with the different terminal hydroxy group of D-arabitol during biosynthesis led to 3′-epimers 4 and 5.

Fusaricates F and G, 6 and 7, were isolated as a mixture of stereoisomers with a ratio of 1:1. Attempts to separate both compounds were unsuccessful. The HRESIMS spectrum of 6 and 7 showed the pseudomolecular ion peak indicating the molecular formula $C_{15}H_{21}NO_6$. The ^{1}H NMR data were very similar to those of 4 and 5. The disappearance of the signals for a methyl and a methylene group, together with the detection of three additional olefinic protons at δ_H 5.85 (H-10, m), 5.01 (H_a-11, d, J = 17.1 Hz), and 4.99 (H_b-11, d, J = 9.8 Hz) in the ^{1}H NMR spectrum of 6 and 7 suggested the presence of a double bond at C-10/C-11 in the latter two compounds. This was confirmed by the COSY correlations between H_2-11 and H-10, between H-10 and H_2-9 (δ_H 2.44, m), and between H_2-9 and H_2-8 (δ_H 2.86, m). Except for the presence of a double bond, the structures of 6 and 7 including the pyridine ring, a D-arabitol unit, and an ester linkage were identical to those of 4 and 5 as evident from detailed examination of 1D and 2D NMR. Combined with analysis of the coupling constants, the structures of 6 and 7 were elucidated as shown.

The molecular formula of 8 was established as $C_{10}H_{12}ClNO_3$ by HRESIMS. Its ^{1}H and ^{13}C NMR data (Table 3) resembled those of 10,11-dihydroxyfusaric acid.[25] The obvious difference between both compounds was that C-11 (δ_C 50.0, CH_2) of 8 was shifted upfield by approximately 17 ppm compared to 10,11-dihydroxyfusaric acid. These findings indicated the attachment of the chlorine atom to C-11 in 8 instead of a hydroxy group as present in 10,11-dihydroxyfusaric acid. Thus, compound 8 was elucidated as 10-hydroxy-11-chlorofusaric acid. Attempts to determine its absolute stereochemistry using Mosher's method were unsuccessful because it was unstable under Mosher's reaction condition. It should be noted that compound 8 could not be detected in HPLC-MS analysis of the crude extract when growth medium without sea salt was used for fermentation. Therefore, sea salt added in the growth medium may be the source of chlorine in 8.

The known compounds were identified as pestalotiollides A and B,[26] dehydroisopenicillide,[27] and beauvericin[28] by comparison of their spectroscopic data with those in the literature.

The cytotoxicity of compounds 1−8 against L5178Y mouse lymphoma cells was evaluated using the MTT assay. However, only 2 showed weak cytotoxicity with an IC_{50} value of 37.7 μM. Compounds 1−8 were further evaluated for their phytotoxicity against barley leaves ('Bonus', a Swedish cultivar) (Table 4).

Table 4. Relative Phytotoxicity [0−5 (±SD)] of Fusaric Acid Derivatives 1−8[a]

	concentration				
compound	0.5 mM	1.0 mM	2.0 mM	4.0 mM	8.0 mM
1	1.3 (0.6)	1.3 (0.6)	1.7 (0.6)	2.3 (0.6)	5.0 (0.0)
2	0.3 (0.6)	0.0 (0.0)	1.0 (0.0)	1.7 (0.6)	2.7 (0.6)
3	1.3 (0.6)	0.7 (0.6)	1.3 (0.6)	1.7 (0.6)	2.7 (0.6)
4 and 5[b]	1.3 (0.6)	1.3 (0.6)	2.7 (0.6)	3.0 (0.6)	3.7 (0.6)
6 and 7[b]	1.0 (0.0)	0.7 (0.6)	1.7 (0.6)	1.7 (0.6)	3.0 (1.0)
8	1.3 (0.6)	1.3 (0.6)	2.0 (0.0)	3.0 (0.0)	3.7 (0.6)
fusaric acid	1.7 (0.6)	1.7 (0.6)	3.0 (0.0)	3.0 (0.0)	4.0 (0.0)

[a]Visual rating: 0 = no necrosis; 5 = severe necrosis; fusaric acid was used as positive control. [b]4 and 5, 6, and 7 were tested as mixtures.

The phytotoxicity of compounds 1, 4, 5, and 8 was found to be almost equal to that of commercial fusaric acid, suggesting their promising potential in organic farming. Comparison of the phytotoxicity of fusaricate A, 1, versus B, 2, suggested that the presence of the hydroxyl group at C-10 led to decreased phytotoxicity. The presence of a double bond between C-10 and C-11 also decreased phytotoxicity as evident from comparison of 4 and 5 versus 6 and 7.

The phytotoxicity of fusaric acid derivatives is nonspecific and harmful to both crops and weeds.[29] Their potential use as herbicides and application in agriculture have been discussed.[10] We described this strain *F. oxysporum* as a symptomless

DOI: 10.1021/acs.jafc.6b00219
J. Agric. Food Chem. 2016, 64, 3127−3132

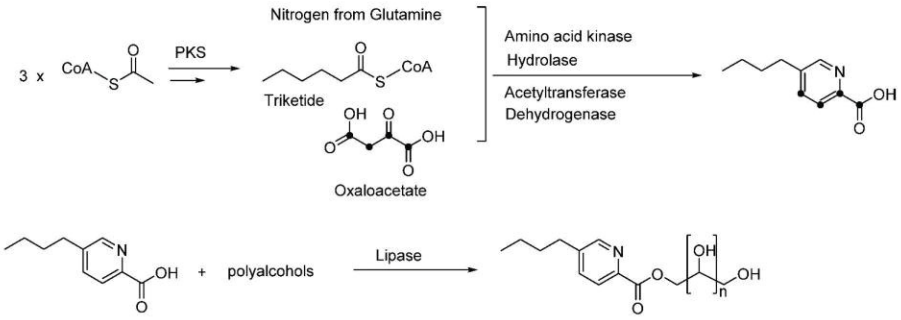

Figure 3. Proposed biosynthetic pathway of fusaric acid derivatives.

endophyte because it did not cause any visible symptoms to the host plant, which is similar to the relationship between *F. verticillioides* and maize.[30,31] The ecological role of fusaric acid derivatives could lie in the maintainance of an equilibrium between host and endophyte. For the host plant, the production of fusaric acid derivatives by endophyte is probably harmful, whereas the major fungal component beauvericin (around 3.6% of the EtOAc extract) may be beneficial due to its insecticidal activity.[32] The true nature of interaction between this endophytic fungus and its host plant remains to be elucidated.

^{13}C and ^{14}C isotopic tracer studies revealed that C-5, C-6, C-8, C-9, C-10, and C-11 of fusaric acid were derived from 3 units of acetate, whereas C-2, C-3, C-4, and C-7 were derived from oxaloacetate.[33,34] It has been proved that the nitrogen atom present in the pyridine ring originates mainly from glutamine.[35] According to a recent study, a 12-gene biosynthetic gene cluster was involved in the biosynthesis of fusaric acid.[36] The esterification of fusaric acid and the polyalcohols could be catalyzed by lipases similar to Novozyme 435 from *Candida antarctica*.[37]

In summary, a proposed biosynthetic pathway for the fusaric acid derivatives as found in this study is presented in Figure 3. Fusaricates A–G, **1**–**7**, represent the first examples of fusaric acid linked to a polyalcohol moiety via an ester bond.

■ ASSOCIATED CONTENT

Supporting Information

The Supporting Information is available free of charge at the ACS Publications website at DOI: 10.1021/acs.jafc.6b00219.

GC-MS analyses of polyalcohol standards and degraded samples from compounds **3**–**5**, UV, HRESIMS, and NMR spectra of compounds **1**–**8**, and phytotoxicity assay results (PDF)

■ AUTHOR INFORMATION

Corresponding Authors

*(Z.L.) Phone: +49 211 81 15979. Fax: +49 211 81 11923. E-mail: zhenfeizi0@sina.com.

*(P.P.) Phone: +49 211 81 14163. Fax: +49 211 81 11923. E-mail: proksch@uni-duesseldorf.de.

Funding

Financial support by the China Scholarship Council to S.L. is gratefully acknowledged. P.P. thanks the Manchot Foundation for support.

Notes

The authors declare no competing financial interest.

■ ACKNOWLEDGMENTS

We acknowledge the assistance and collaboration of Ansgar Rühlmann (Institute of Biochemistry, Heinrich-Heine-Universität Düsseldorf, Germany) for carrying out GC-MS experiments. We furthermore thank Sergi Herve Akone (Heinrich-Heine-Universität Düsseldorf, Germany) for collection of the plant material.

■ REFERENCES

(1) Faeth, S. H. Are endohpytic fungi defensive plant mutualists? *Oikos* **2002**, *98*, 25–36.

(2) Wilson, D. Endophyte: the evolution of a term, and clarification of its use and definition. *Oikos* **1995**, *73*, 274–276.

(3) Chadha, N.; Mishra, M.; Rajpal, K.; Bajaj, R.; Choudhary, D. K.; Varma, A. An ecological role of fungal endophytes to ameliorate plants under biotic stress. *Arch. Microbiol.* **2015**, *197*, 869–881.

(4) Ludwig-Müller, J. Bacteria and fungi controlling plant growth by manipulating auxin: balance between development and defense. *J. Plant Physiol.* **2015**, *172*, 4–12.

(5) Mishra, Y.; Singh, A.; Batra, A.; Sharma, M. M. Understanding the biodiversity and biological application of endophytic fungi: a review. *J. Microb. Biochem. Technol.* **2014**, *s8*, S8-004.

(6) Ma, L. J.; Geiser, D. M.; Proctor, R. H.; Rooney, A. P.; O'Donnell, K.; Trail, F.; Gardiner, D. M.; Manners, J. M.; Kazan, K. *Fusarium* pathogenomics. *Annu. Rev. Microbiol.* **2013**, *67*, 399–416.

(7) Smith, T. K.; Sousadias, M. G. Fusaric acid content of swine feedstuffs. *J. Agric. Food Chem.* **1993**, *41*, 2296–2298.

(8) Goodwin, F. K.; Sack, R. L. Behavioral effects of a new dopamine-β-hydroxylase inhibitor (fusaric acid) in man. *J. Psychiatr. Res.* **1974**, *11*, 211–217.

(9) Stipanovic, R. D.; Puckhaber, L. S.; Liu, J.; Bell, A. A. Phytotoxicity of fusaric acid and analogs to cotton. *Toxicon* **2011**, *57*, 176–178.

(10) Capasso, R.; Evidente, A.; Cutignano, A.; Vurro, M.; Zonno, M. C.; Bottalico, A. Fusaric and 9,10-dehydrofusaric acids and their methyl esters from *Fusarium nigamai*. *Phytochemistry* **1996**, *41*, 1035–1039.

(11) El Amrani, M.; Lai, D.; Debbab, A.; Aly, A. H.; Siems, K.; Seidel, C.; Schnekenburger, M.; Gaigneaux, A.; Diederich, M.; Feger, D.; Lin, W.; Proksch, P. Protein kinase and HDAC inhibitors from the endophytic fungus. *J. Nat. Prod.* **2014**, *77*, 49–56.

(12) Liu, Y.; Wray, V.; Abdel-Aziz, M. S.; Wang, C. Y.; Lai, D.; Proksch, P. Trimeric anthracenes from the endophytic fungus *Stemphylium globuliferum*. *J. Nat. Prod.* **2014**, *77*, 1734–1738.

(13) Liu, Y.; Marmann, A.; Abdel-Aziz, M. S.; Wang, C. Y.; Müller, W. E. G.; Lin, W. H.; Mándi, A.; Kurtán, T.; Daletos, G.; Proksch, P. Tetrahydroanthraquinone derivatives from endophytic fungus *Stemphylium globuliferum*. *Eur. J. Org. Chem.* **2015**, *2015*, 2646–2653.

(14) Uzor, P. F.; Ebrahim, W.; Osadebe, P. O.; Nwodo, J. N.; Okoye, F. B.; Müller, W. E. G.; Lin, W.; Liu, Z.; Proksch, P. Metabolites from *Combretum dolichopetalum* and its associated endophytic fungus

DOI: 10.1021/acs.jafc.6b00219
J. Agric. Food Chem. 2016, 64, 3127–3132

Nigrospora oryzae – evidence for a metabolic partnership. *Fitoterapia* **2015**, *105*, 147–150.
(15) Debbab, A.; Aly, A. H.; Edrada-Ebel, R.; Wray, V.; Müller, W. E. G.; Totzke, F.; Zirrgiebel, U.; Schächtele, C.; Kubbutat, M. H. G.; Lin, W. H.; Mosaddak, M.; Hakiki, A.; Proksch, P.; Ebel, R. Bioactive metabolites from the endophytic fungus *Stemphylium globuliferum* isolated from *Mentha pulegium*. *J. Nat. Prod.* **2009**, *72*, 626–631.
(16) Kjer, J.; Debbab, A.; Aly, A. H.; Proksch, P. Methods for isolation of marine-derived endophytic fungi and their bioactive secondary products. *Nat. Protoc.* **2010**, *5*, 479–490.
(17) Ashour, M.; Edrada, R.; Ebel, R.; Wray, V.; Wätjen, W.; Padmakumar, K.; Müller, W. E. G.; Lin, W. H.; Proksch, P. Kahalalide derivatives from the Indian sacoglossan mollusk *Elysia grandifolia*. *J. Nat. Prod.* **2006**, *69*, 1547–1553.
(18) Nielsen, K. F.; Smedsgaard, J. Fungal metabolite screening: database of 474 mycotoxins and fungal metabolites for dereplication by standardised liquid chromatography-UV-mass spectrometry methodology. *J. Chromatogr. A* **2003**, *1002*, 111–136.
(19) Casati, S.; Ciuffreda, P.; Santaniello, E. Synthesis of enantiomerically pure (*R*)- and (*S*)-1-benzoyloxypropane-2,3-diol and revision of the stereochemical outcome of the *Candida antarctica* lipase-catalyzed benzoylation of glycerol. *Tetrahedron: Asymmetry* **2011**, *22*, 658–661.
(20) Tabata, N.; Ohyama, Y.; Tomoda, H.; Abe, T.; Namikoshi, M.; Omura, S. Structure elucidation of roselipins, inhibitors of diacylglycerol acyltransferase produced by *Gliocladium roseum* KF-1040. *J. Antibiot.* **1999**, *52*, 815–826.
(21) Basset, J. F.; Leslie, C.; Hamprecht, D.; White, A. J. P.; Barrett, A. G. M. Studies on the resorcylates: biomimetic total syntheses of (+)-montagnetol and (+)-erythrin. *Tetrahedron Lett.* **2010**, *51*, 783–785.
(22) Kumbaraci, V.; Gunduz, H.; Karadeniz, M. Facile syntheses of (−)-montagnetol and (−)-erythrin. *Tetrahedron Lett.* **2013**, *54*, 6328–6330.
(23) Kohno, J.; Nishio, M.; Sakurai, M.; Kawano, K.; Hiramatsu, H.; Kameda, N.; Kishi, N.; Yamashita, T.; Okuda, T.; Komatsubara, S. Isolation and structure determination of TMC-151s: novel polyketide antibiotics from *Gliocladium catenulatum* Gilman & Abbott TC 1280. *Tetrahedron* **1999**, *55*, 7771–7786.
(24) Ayers, S.; Zink, D.; Mohn, K.; Powell, J. S.; Brown, C. M.; Bills, G.; Grund, A.; Thompson, D.; Singh, S. B. Anthelmintic constituents of *Chonostachys candelabrum*. *J. Antibiot.* **2010**, *63*, 119–122.
(25) Burmeister, H. R.; Grove, M. D.; Peterson, R. E.; Weisleder, D.; Plattner, R. D. Isolation and characterization of two new fusaric acid analogs from *Fusarium moniliforme* NRRL 13,163. *Appl. Environ. Microbiol.* **1985**, *50*, 311–314.
(26) Xu, J.; Aly, A. H.; Wray, V.; Proksch, P. Polyketide derivatives of endophytic fungus *Pestalotiopsis* sp. isolated from the Chinese mangrove plant *Rhizophora mucronata*. *Tetrahedron Lett.* **2011**, *52*, 21–25.
(27) Kawamura, H.; Kaneko, T.; Koshino, H.; Esumi, Y.; Uzawa, J.; Sugawara, F. Penicillides from *Penicillium* sp. isolated from *Taxus cuspidata*. *Nat. Prod. Lett.* **2000**, *14*, 477–484.
(28) Zhan, J.; Burns, A. M.; Liu, M. X.; Faeth, S. H.; Gunatilaka, A. A. L. Search for cell motility and angiogenesis inhibitors with potential anticancer activity: beauvericin and other constituents of two endophytic strains of *Fusarium oxysporum*. *J. Nat. Prod.* **2007**, *70*, 227–232.
(29) Bani, M.; Rispail, N.; Evidente, A.; Rubiales, D.; Cimmino, A. Identification of the main toxins isoltated from *Fusarium oxysporum* f. sp. *pisi* race 2 and their relation with isolates' pathogenicity. *J. Agric. Food Chem.* **2014**, *62*, 2574–2580.
(30) Snook, M. E.; Mitchell, T.; Hinton, D. M.; Bacon, C. W. Isolation and characterization of Leu^7-surfactin from the endophytic bacterium *Bacillus mojavensis* RRC 101, a biocontrol agent for *Fusarium verticillioides*. *J. Agric. Food Chem.* **2009**, *57*, 4287–4292.
(31) Bacon, C. W.; Hinton, D. M. Symptomless endophytic colonization of maize by *Fusarium moniliforme*. *Can. J. Bot.* **1996**, *74*, 1195–1202.
(32) Gupta, S.; Krasnoff, S. B.; Underwood, N. L.; Renwick, J. A. A.; Roberts, D. W. Isolation of beauvericin as an insect toxin from *Fusarium semitectum* and *Fusarium moniliforme* var. *Mycopathologia* **1991**, *115*, 185–189.
(33) Desaty, D.; McInnes, A. G.; Smith, D. G.; Vining, L. C. Use of ^{13}C in biosynthetic studies. Incorporation of isotopically labeled acetate and aspartate into fusaric acid. *Can. J. Biochem.* **1968**, *46*, 1293–1297.
(34) Dobson, T. A.; Desaty, D.; Brewer, D.; Vining, L. C. Biosynthesis of fusaric acid in cultures of *Fusarium oxysporum* Schlecht. *Can. J. Biochem.* **1967**, *45*, 809–813.
(35) Stipanovic, R. D.; Wheeler, M. H.; Puckhaber, L. S.; Liu, J.; Bell, A. A.; Williams, H. J. Nuclear magnetic resonance (NMR) studies on the biosynthesis of fusaric acid from *Fusarium oxysporum* f. sp. *vasinfectum*. *J. Agric. Food Chem.* **2011**, *59*, 5351–5356.
(36) Brown, D. W.; Lee, S. H.; Kim, L. H.; Ryu, J. G.; Lee, S.; Seo, Y.; Kim, Y. H.; Busman, M.; Yun, S. H.; Proctor, R. H.; Lee, T. Identification of a 12-gene fusaric acid biosynthetic gene cluster in *Fusarium* species throung comparative and functional genomics. *Mol. Plant-Microbe Interact.* **2015**, *28*, 319–332.
(37) Croitoru, R.; Fiţigău, F.; van den Broek, L. A. M.; Frissen, A. E.; Davidescu, C. M.; Boeriu, C. G.; Peter, F. Biocatalytic acylation of sugar alcohols by 3-(4-hydroxyphenyl)propionic acid. *Process Biochem.* **2012**, *47*, 1894–1902.

DOI: 10.1021/acs.jafc.6b00219
J. Agric. Food Chem. 2016, 64, 3127–3132

Supporting Information

New Fusaric Acid Derivatives from the Endophytic Fungus *Fusarium oxysporum* and Their Phytotoxic Effect on Barley Leaves.

Shuai Liu,[†] Haofu Dai,[‡] Raha S. Orfali,[§] Wenhan Lin,[τ] Zhen Liu,[*,†] Peter Proksch[*,†]

[†]Institute of Pharmaceutical Biology and Biotechnology, Heinrich-Heine-Universität Düsseldorf, Universitätsstrasse 1, 40225 Düsseldorf, Germany

[‡]Key Laboratory of Biology and Genetic Resources of Tropical Crops, Ministry of Agriculture, Institute of Tropical Bioscience and Biotechnology, Chinese Academy of Tropical Agricultural Sciences, Haikou 571101, China

[§]Department of Pharmacognosy, Faculty of Pharmacy, King Saud University, Riyadh, Saudi Arabia

[τ]State Key Laboratory of Natural and Biomimetic Drugs, Peking University, Beijing 100191, China

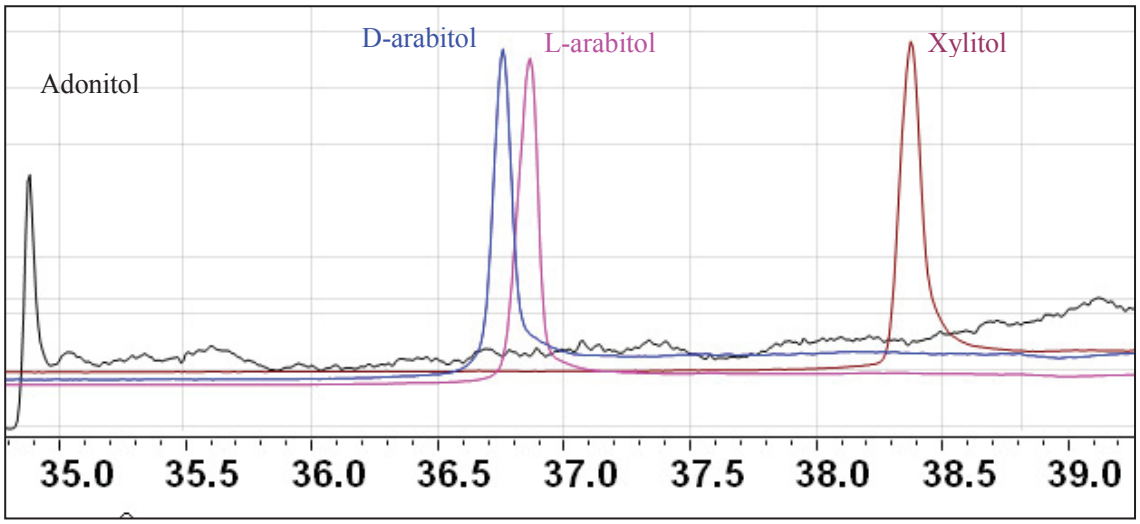

S1-A. Analysis of trifluoroacetyl pentitol standards by gas chromatography.

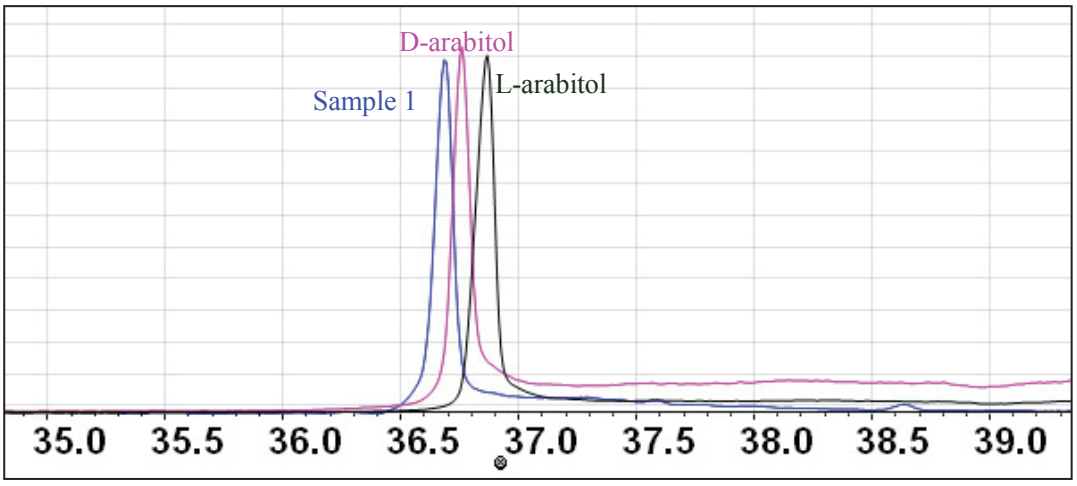

S1-B. Analysis of trifluoroacetyl sample 1 (degraded from mixture of compounds **4** and **5**) by gas chromatography.

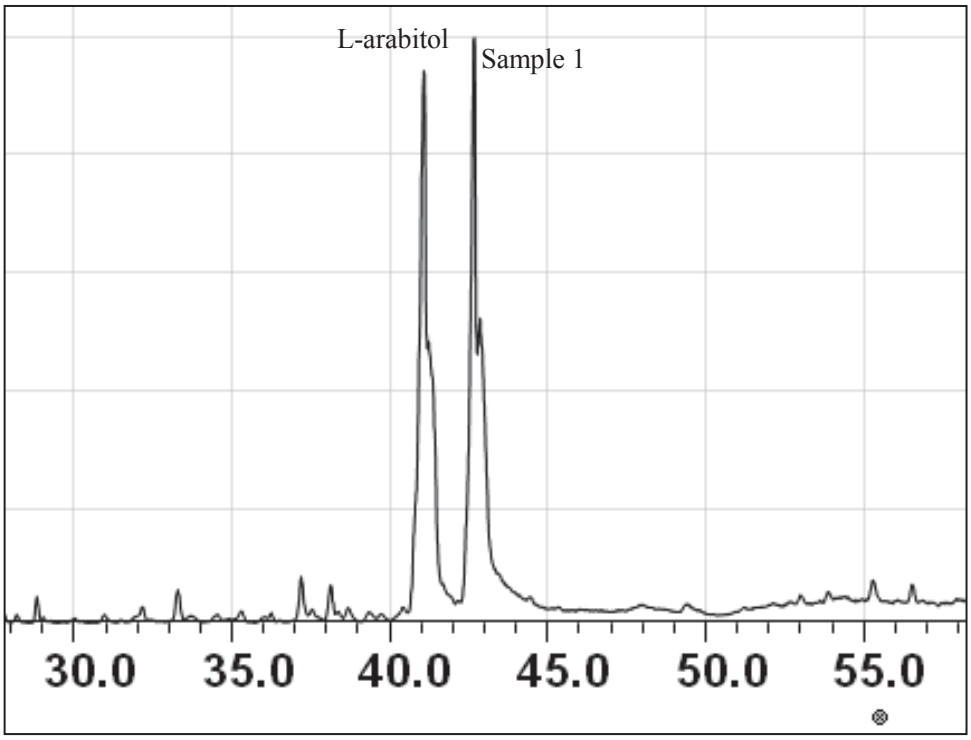

Retention time (minute)

S1-C. Analysis of trifluoroacetyl sample 1 (degraded from mixture of compounds **4** and **5**) and L-arabitol in one injection by gas chromatography.

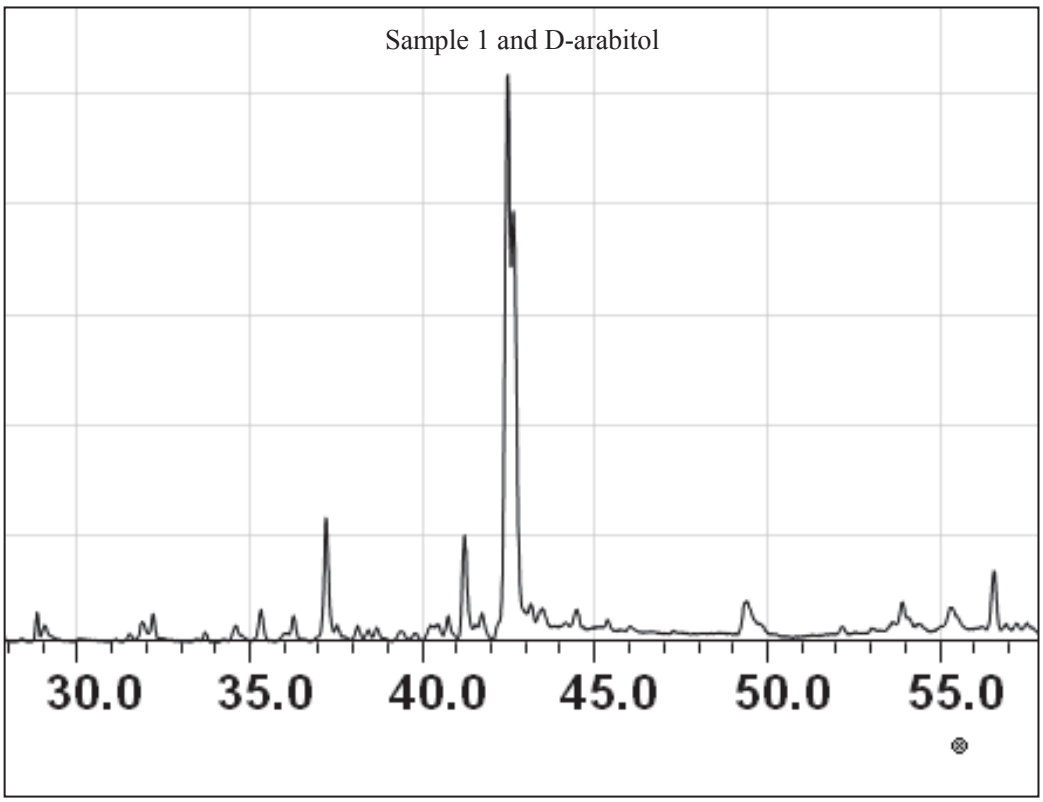

Retention time (minute)

S1-D. Analysis of trifluoroacetyl sample 1 (degraded from mixture of compounds **4** and **5**) and D-arabitol in one injection by gas chromatography.

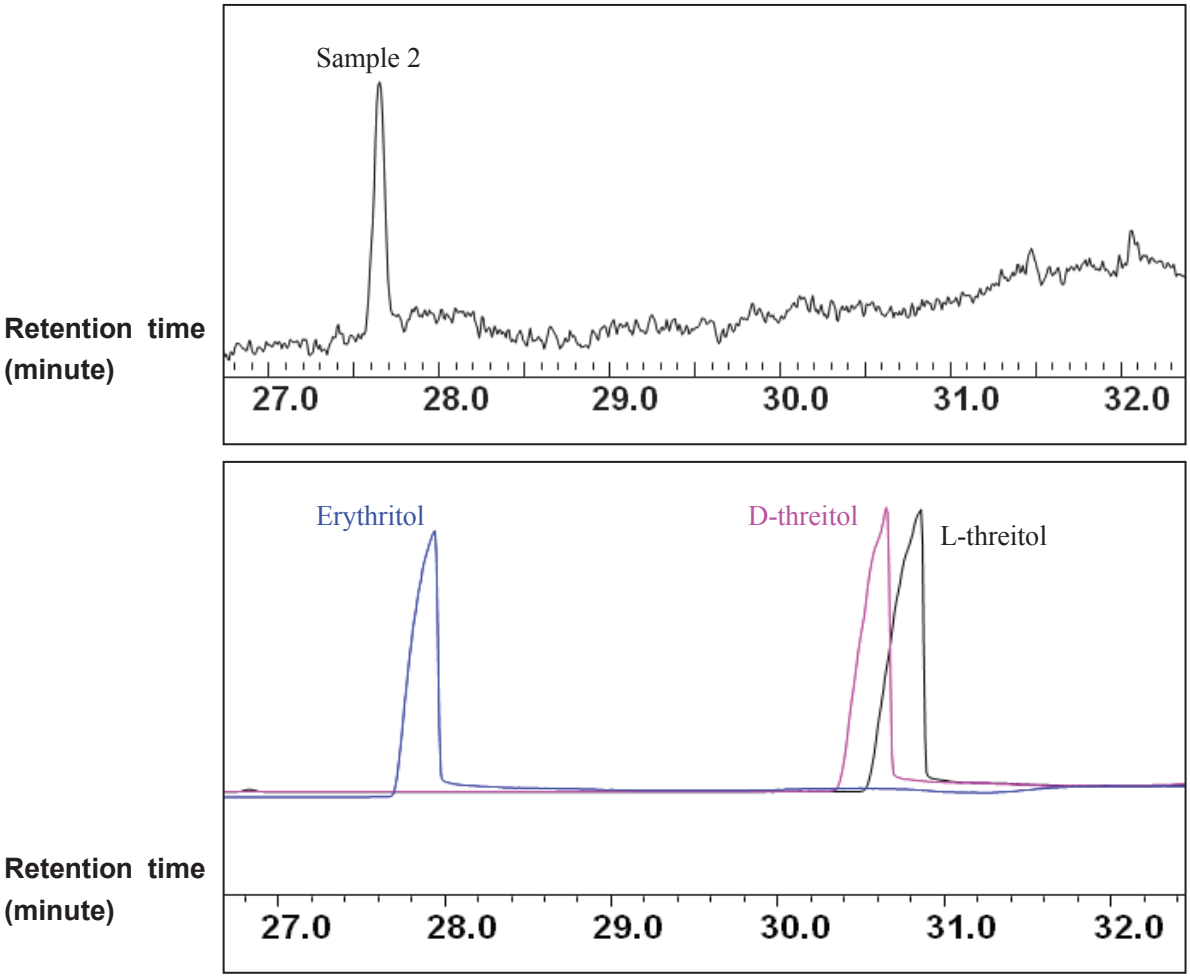

S1-E. Analysis of trifluoroacetyl sample 2 (degraded from compound **3**) (uper) and trifluoroacetyl tetritol standards (down) by gas chromatography.

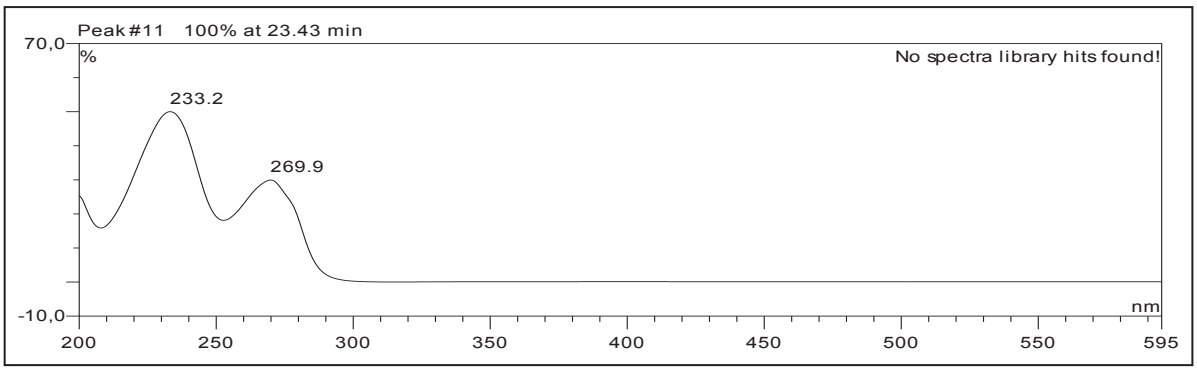

S2. UV spectrum of compound **1**.

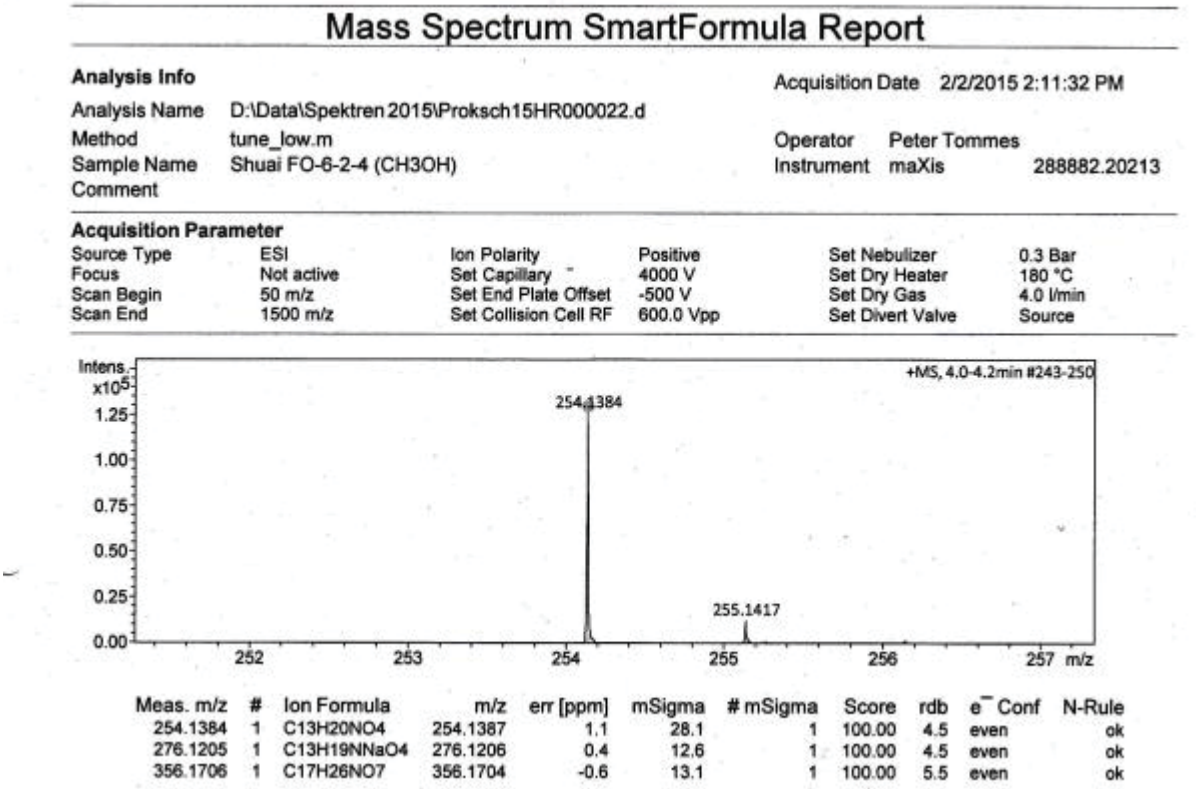

Mass Spectrum SmartFormula Report

Analysis Info

Analysis Name	D:\Data\Spektren 2015\Proksch15HR000022.d	Acquisition Date	2/2/2015 2:11:32 PM
Method	tune_low.m	Operator	Peter Tommes
Sample Name	Shuai FO-6-2-4 (CH3OH)	Instrument	maXis 288882.20213
Comment			

Acquisition Parameter

Source Type	ESI	Ion Polarity	Positive	Set Nebulizer	0.3 Bar
Focus	Not active	Set Capillary	4000 V	Set Dry Heater	180 °C
Scan Begin	50 m/z	Set End Plate Offset	-500 V	Set Dry Gas	4.0 l/min
Scan End	1500 m/z	Set Collision Cell RF	600.0 Vpp	Set Divert Valve	Source

Meas. m/z	#	Ion Formula	m/z	err [ppm]	mSigma	# mSigma	Score	rdb	e⁻ Conf	N-Rule
254.1384	1	C13H20NO4	254.1387	1.1	28.1	1	100.00	4.5	even	ok
276.1205	1	C13H19NNaO4	276.1206	0.4	12.6	1	100.00	4.5	even	ok
356.1706	1	C17H26NO7	356.1704	-0.6	13.1	1	100.00	5.5	even	ok

S3. HRESIMS spectrum of compound **1.**

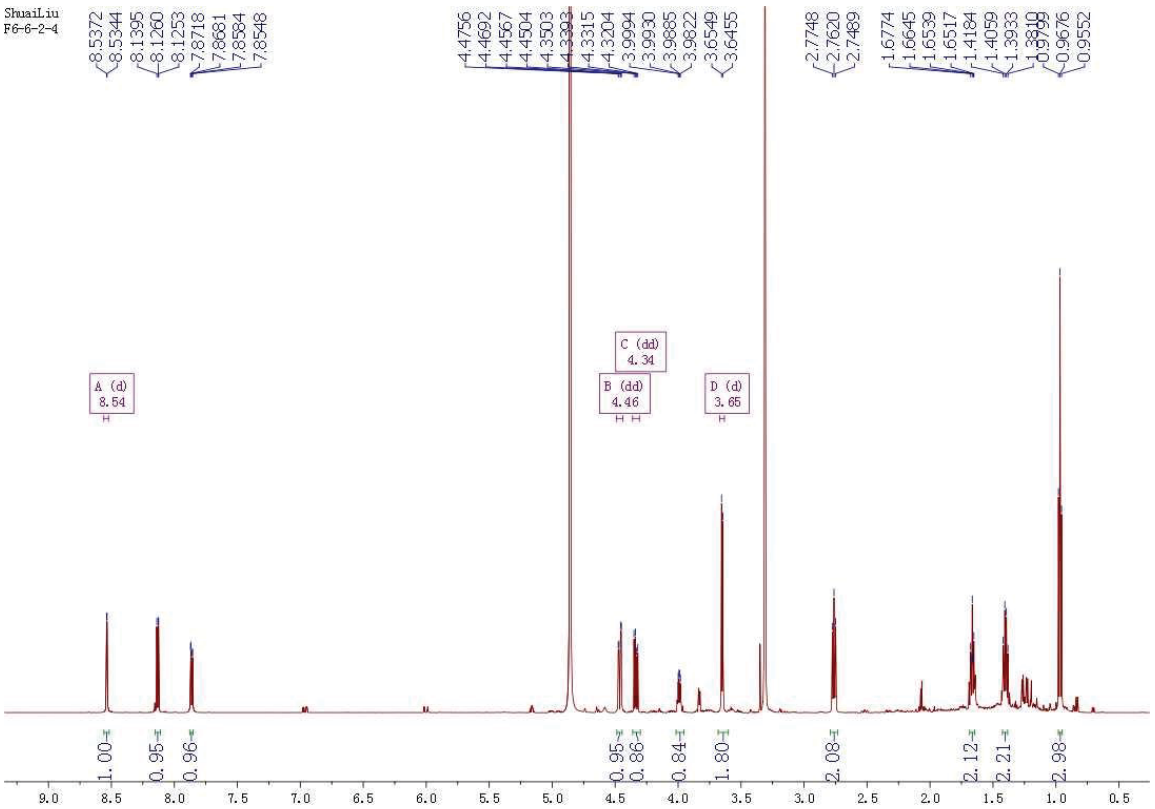

S4. ^{1}H NMR (600 MHz, CD_3OD) spectrum of compound **1**.

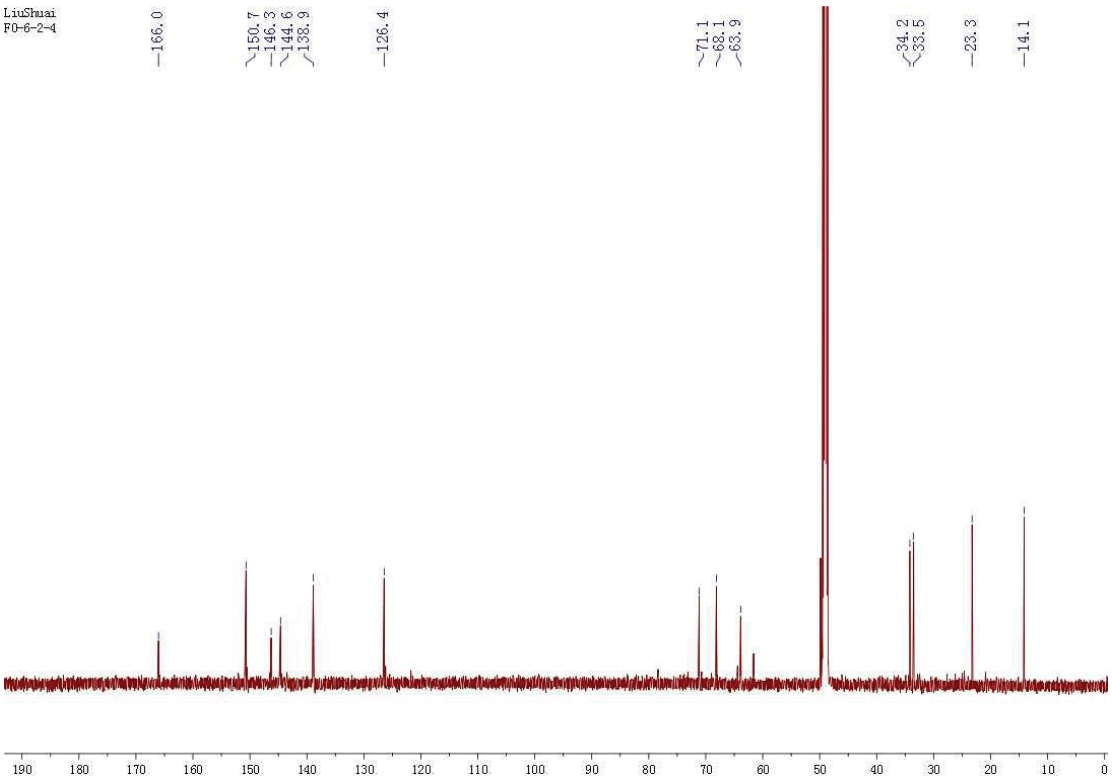

S5. ^{13}C NMR (150 MHz, CD_3OD) spectrum of compound **1**.

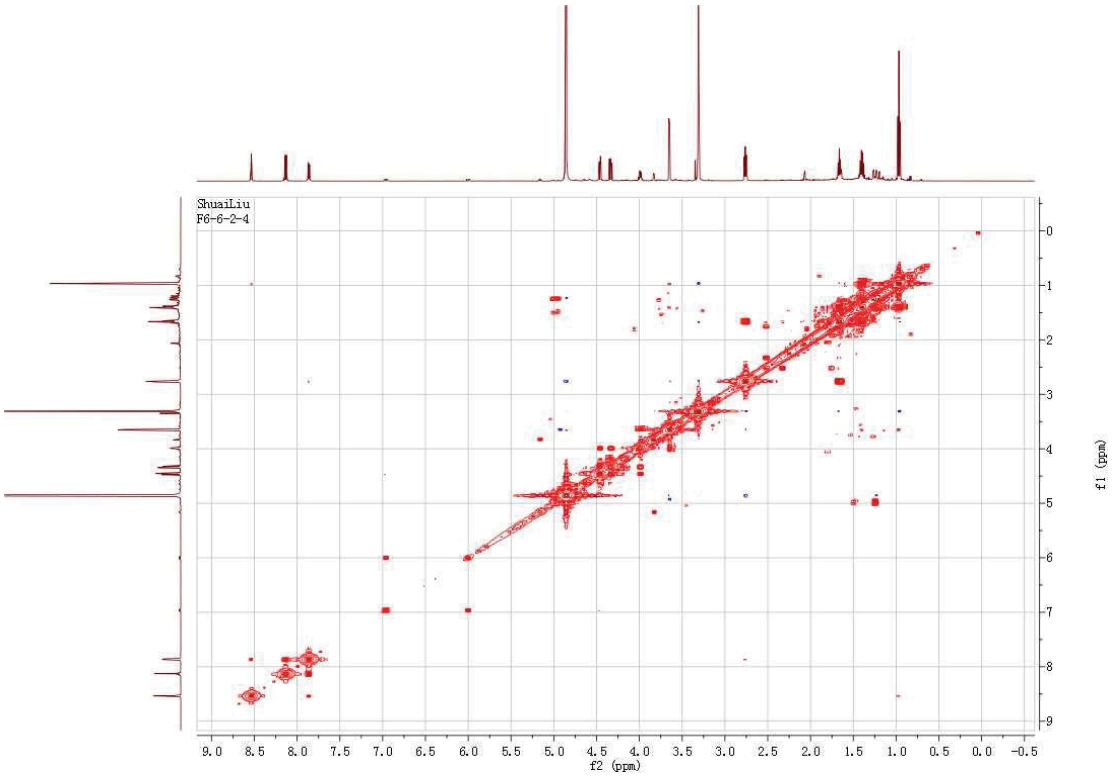

S6. ^{1}H-^{1}H COSY (600 MHz, CD_3OD) spectrum of compound **1**.

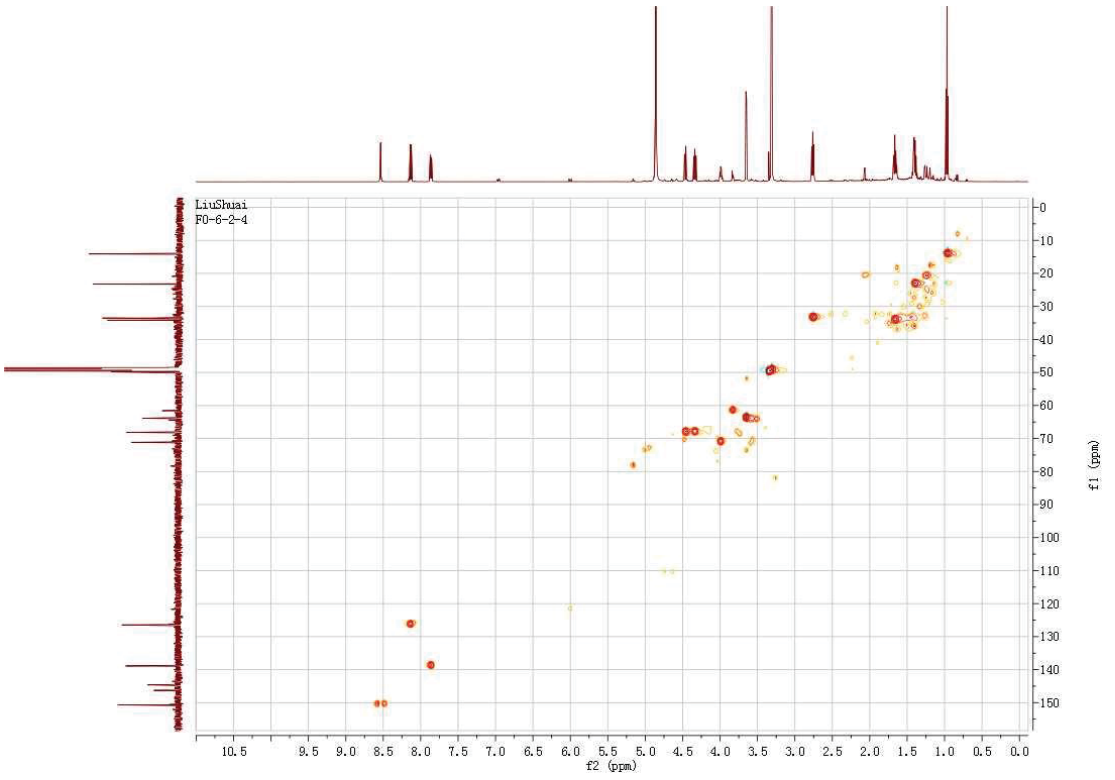

S7. HSQC (600 and 150 MHz, CD_3OD) spectrum of compound **1**.

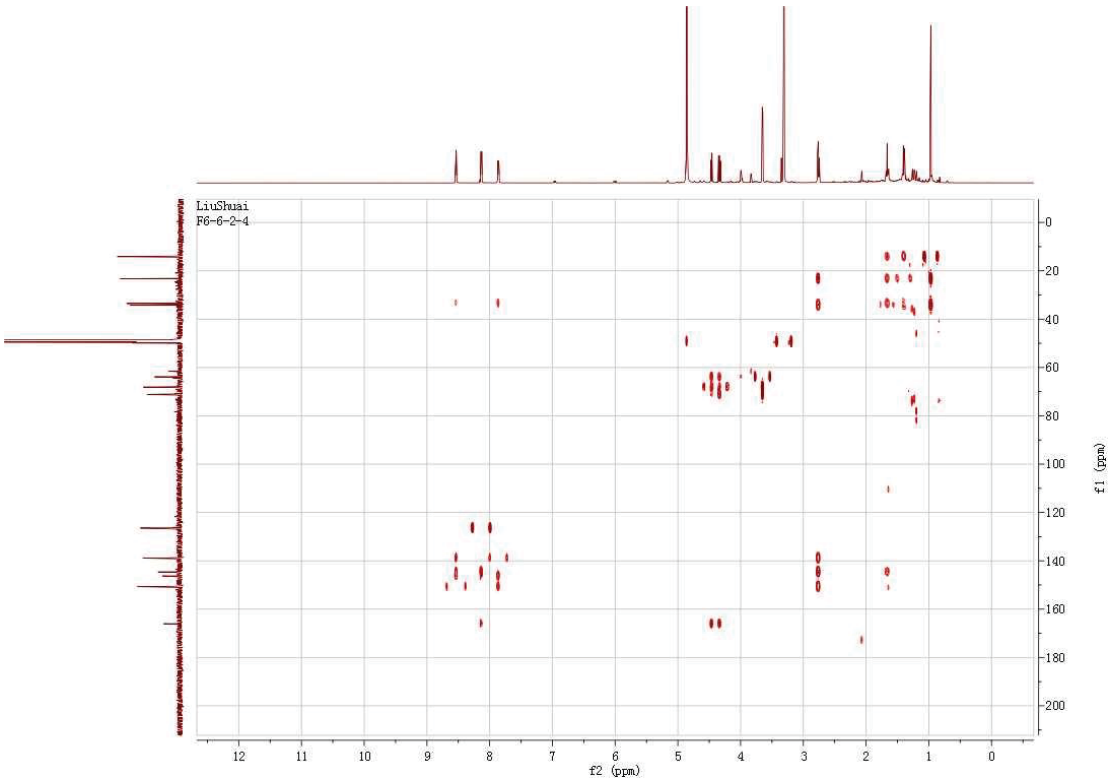

S8. HMBC (600 and 150 MHz, CD_3OD) spectrum of compound **1**.

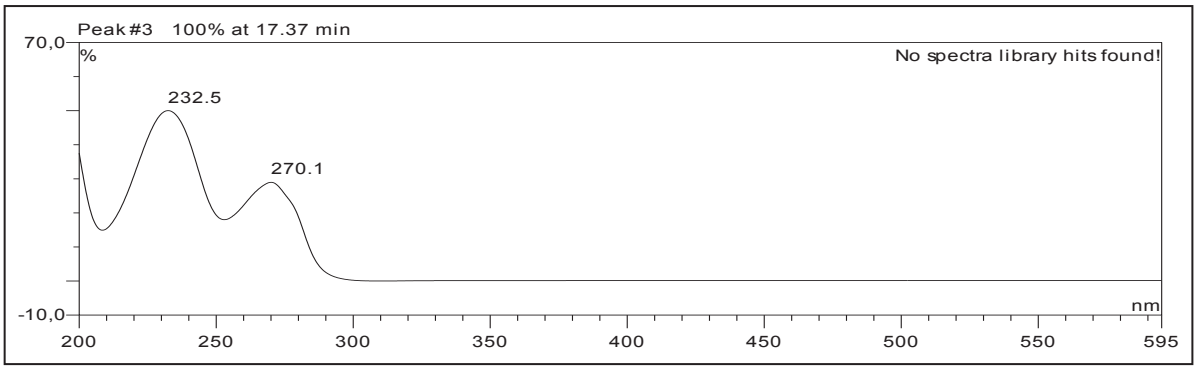

S9. UV spectrum of compound **2**.

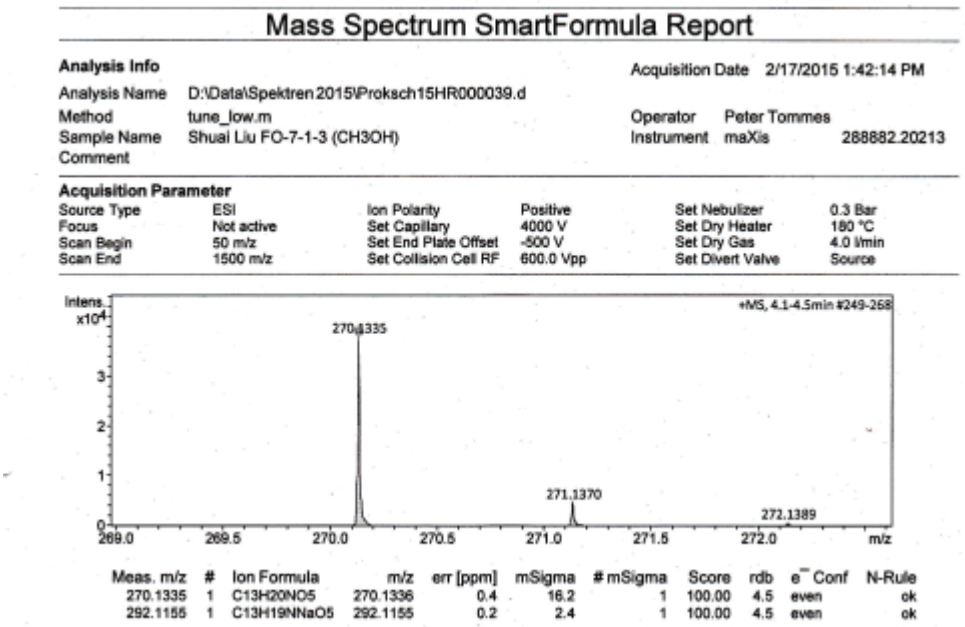

Mass Spectrum SmartFormula Report

Analysis Info

Analysis Name	D:\Data\Spektren 2015\Proksch15HR000039.d	Acquisition Date	2/17/2015 1:42:14 PM
Method	tune_low.m	Operator	Peter Tommes
Sample Name	Shuai Liu FO-7-1-3 (CH3OH)	Instrument	maXis 288882.20213
Comment			

Acquisition Parameter

Source Type	ESI	Ion Polarity	Positive	Set Nebulizer	0.3 Bar
Focus	Not active	Set Capillary	4000 V	Set Dry Heater	180 °C
Scan Begin	50 m/z	Set End Plate Offset	-500 V	Set Dry Gas	4.0 l/min
Scan End	1500 m/z	Set Collision Cell RF	600.0 Vpp	Set Divert Valve	Source

Meas. m/z	#	Ion Formula	m/z	err [ppm]	mSigma	# mSigma	Score	rdb	e⁻ Conf	N-Rule
270.1335	1	C13H20NO5	270.1336	0.4	16.2	1	100.00	4.5	even	ok
292.1155	1	C13H19NNaO5	292.1155	0.2	2.4	1	100.00	4.5	even	ok

S10. HRESIMS spectrum of compound **2.**

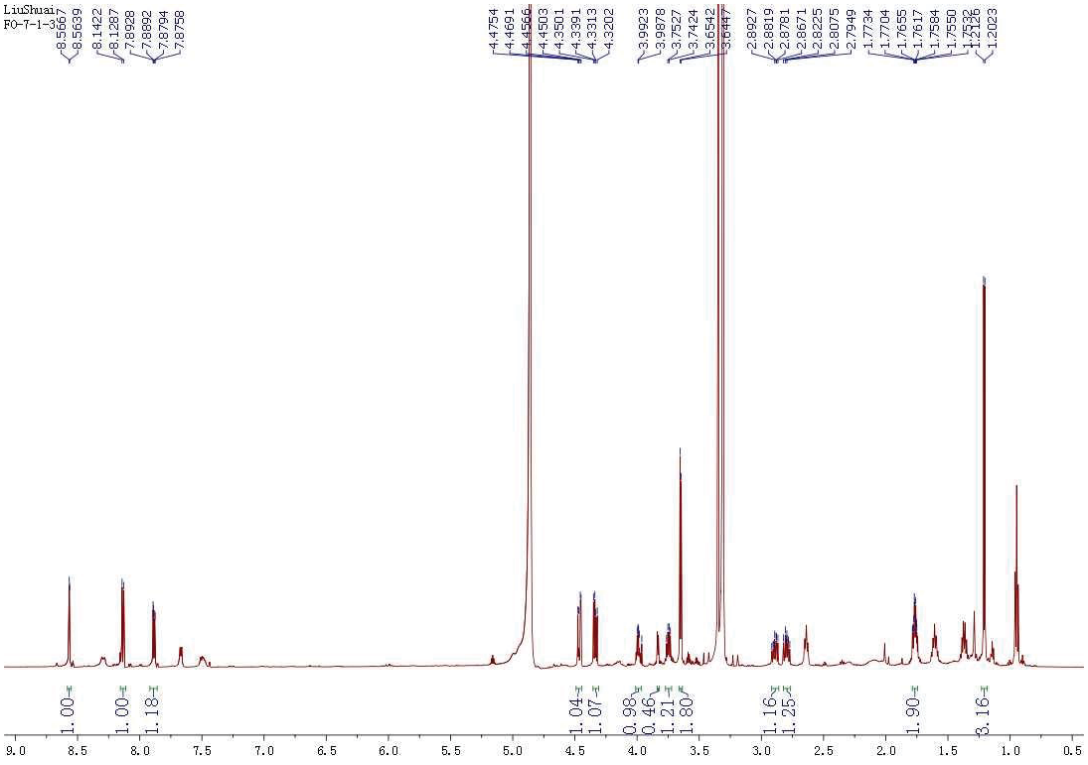

S11. ^{1}H NMR (600 MHz, CD_3OD) spectrum of compound **2**.

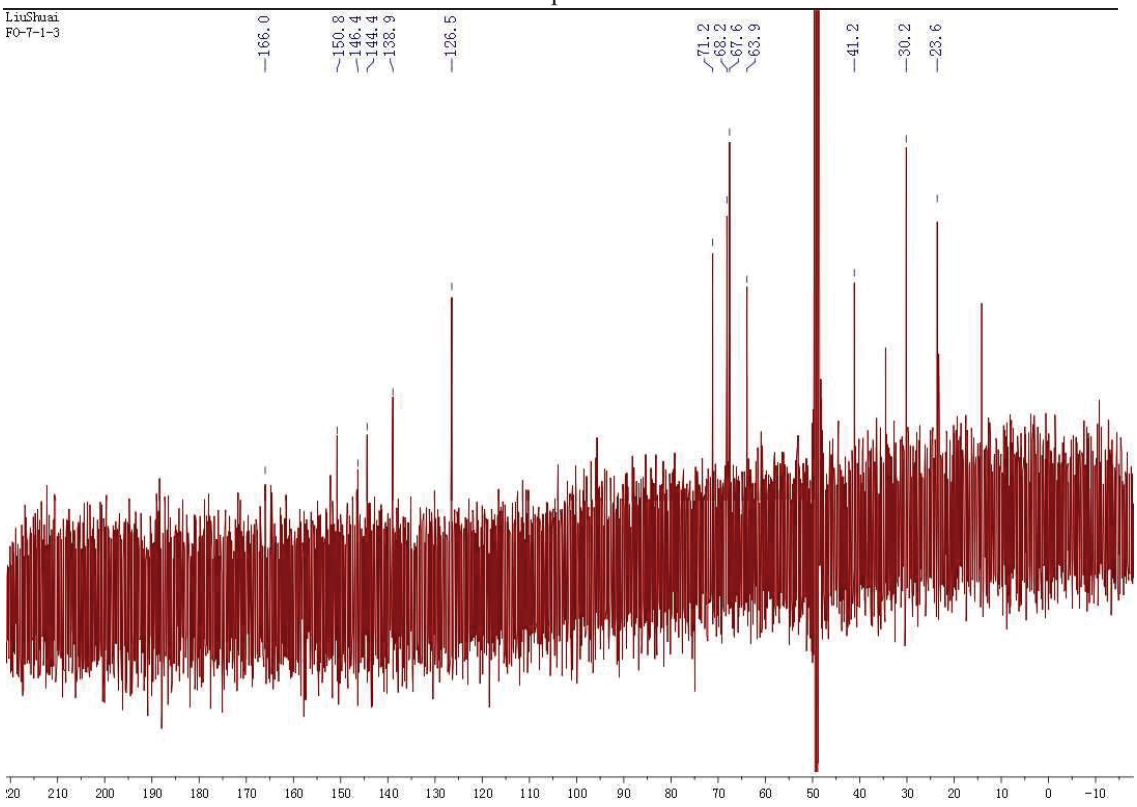

S12. ^{13}C NMR (150 MHz, CD_3OD) spectrum of compound **2**.

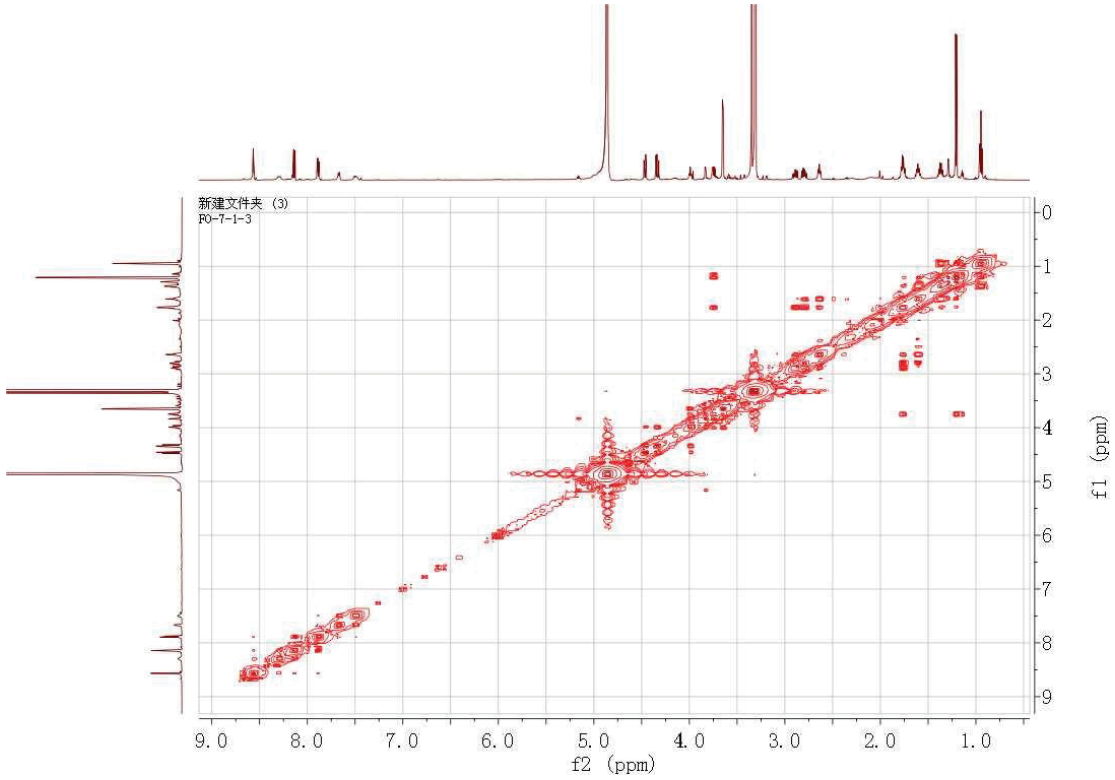

S13. ^{1}H-^{1}H COSY (600 MHz, CD_3OD) spectrum of compound **2**.

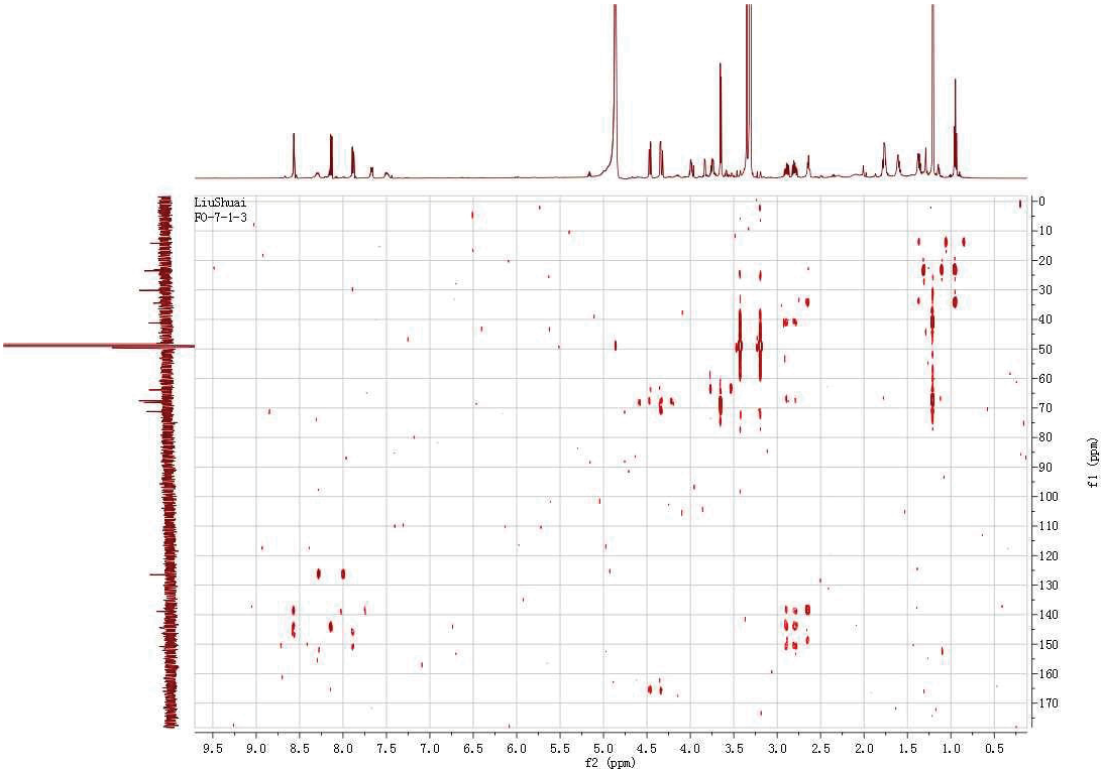

S14. HMBC (600 and 150 MHz, CD_3OD) spectrum of compound **2**.

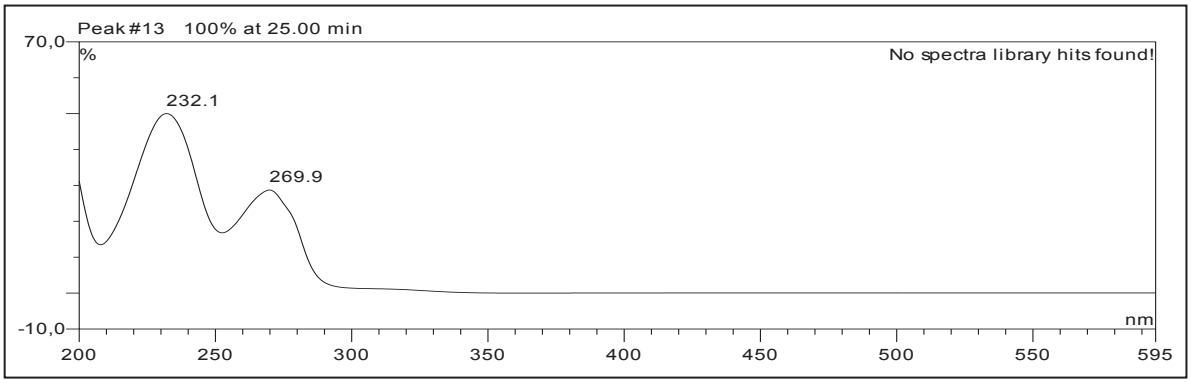

S15. UV spectrum of compound **3**.

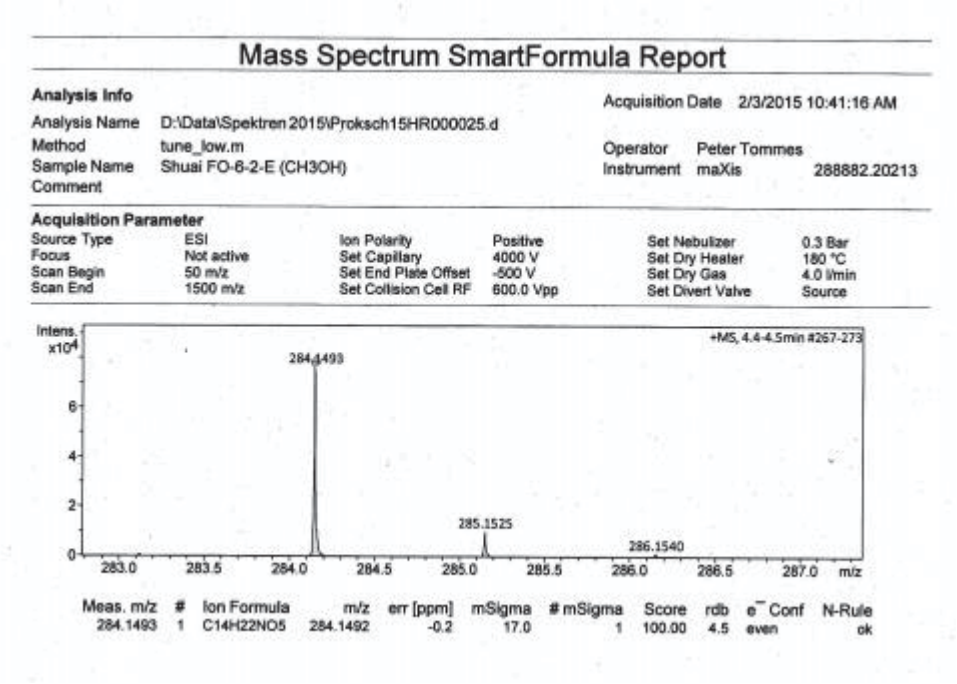

S16. HRESIMS spectrum of compound **3.**

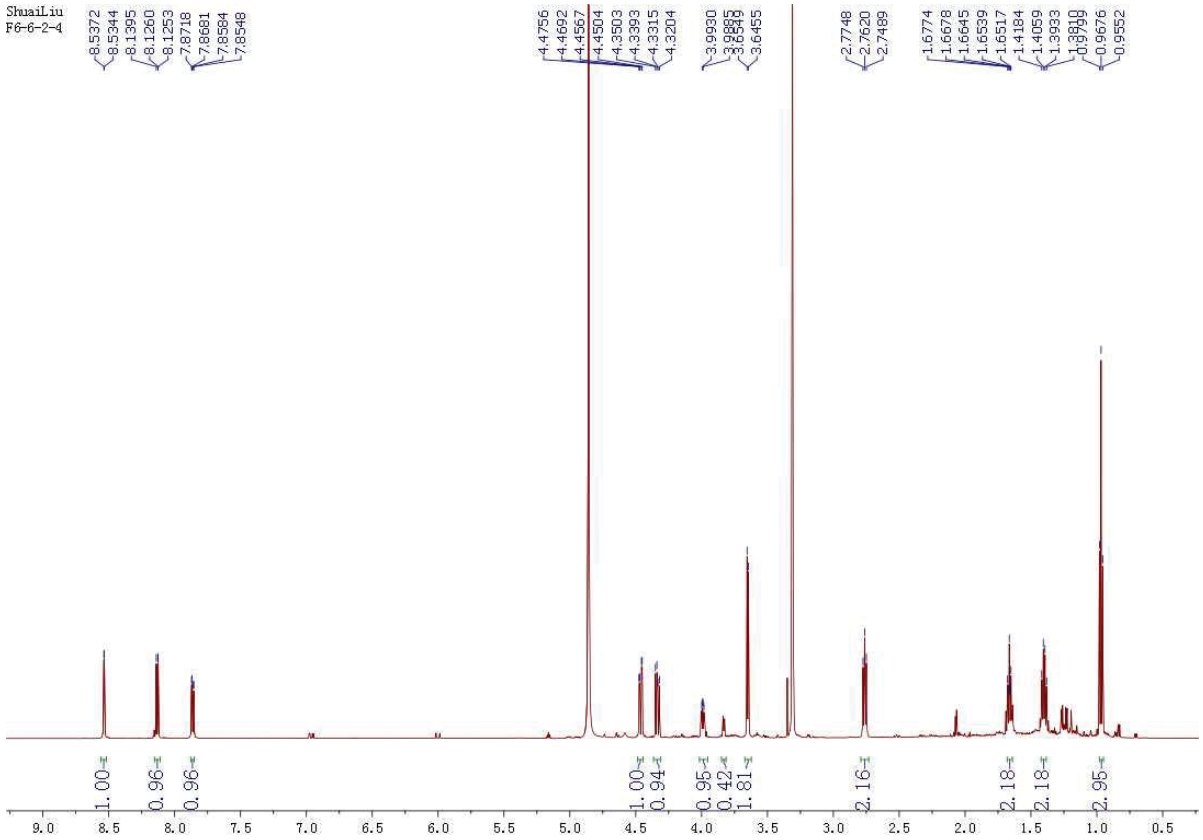

S17. ^{1}H NMR (600 MHz, CD_3OD) spectrum of compound **3**.

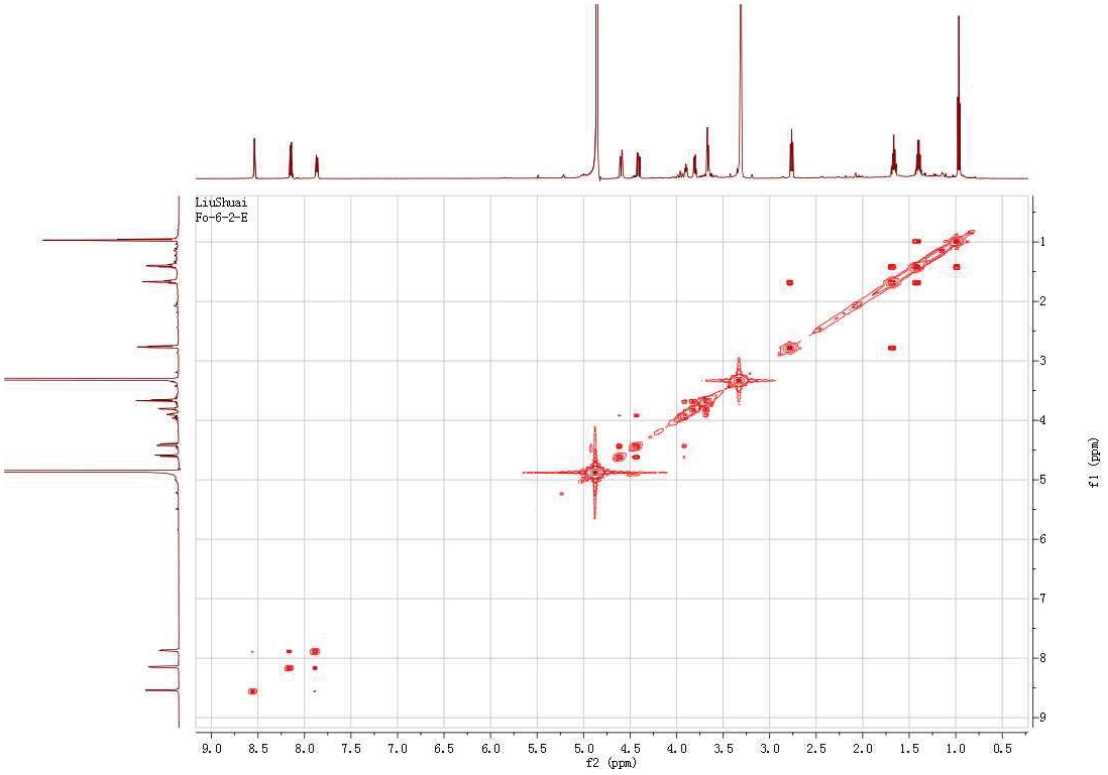

S18. ^{1}H-^{1}H COSY (600 MHz, CD_3OD) spectrum of compound **3**.

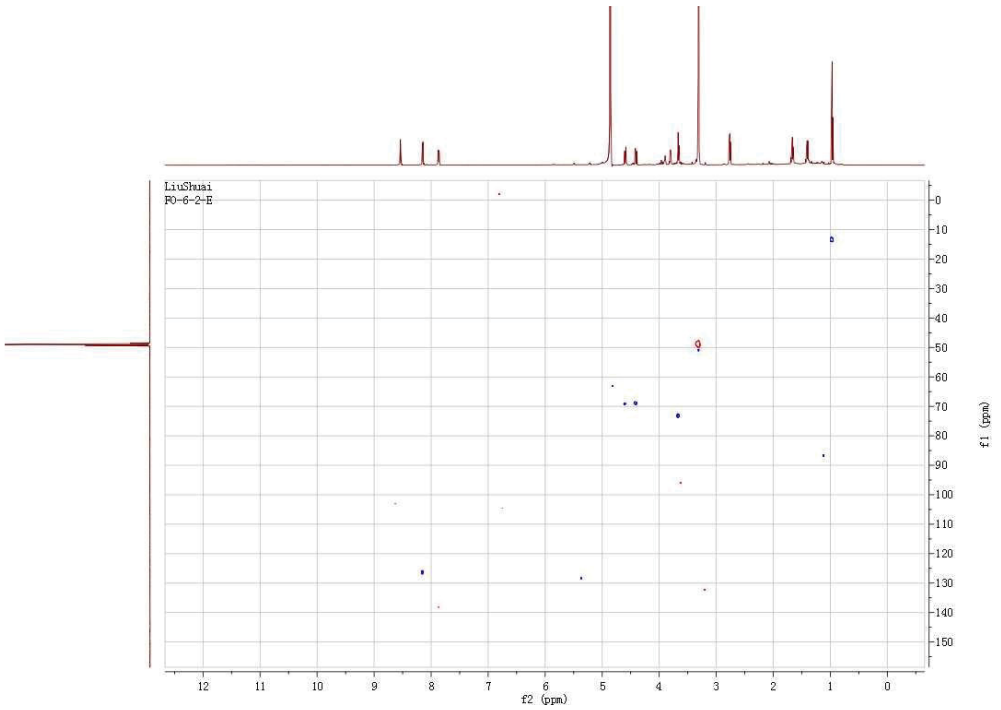

S19. HSQC (600 and 150 MHz, CD_3OD) spectrum of compound **3**.

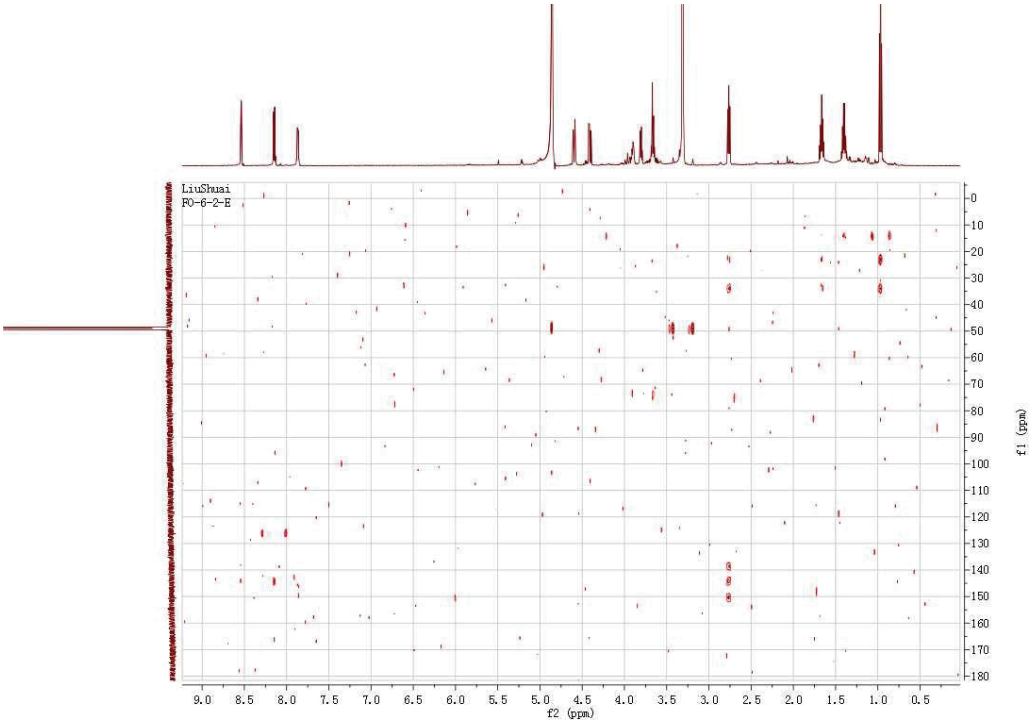

S20. HMBC (600 and 150 MHz, CD_3OD) spectrum of compound **3**.

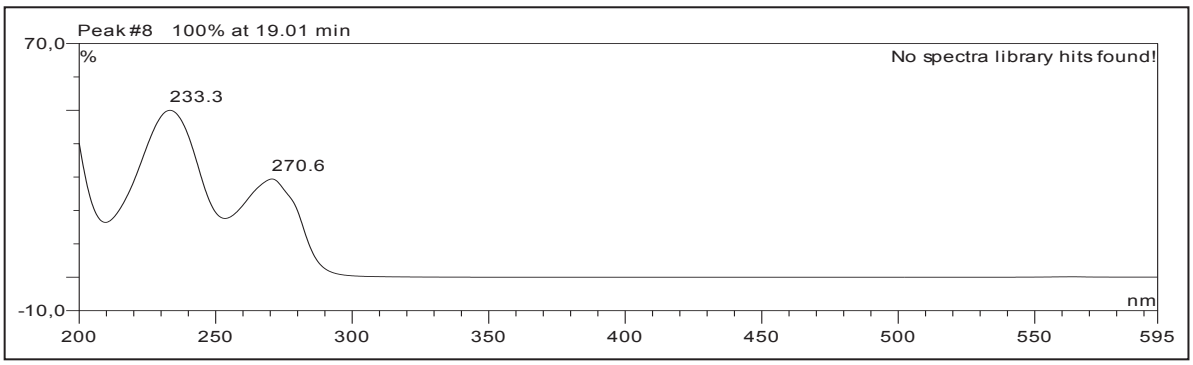

S21. UV spectrum of mixture of **4** and **5**.

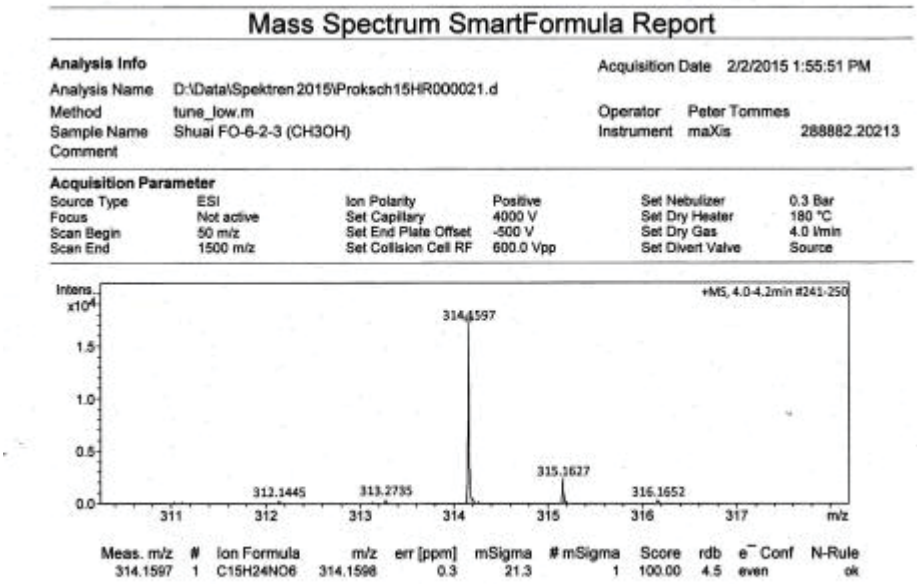

S22. HRESIMS spectrum of mixture of **4** and **5.**

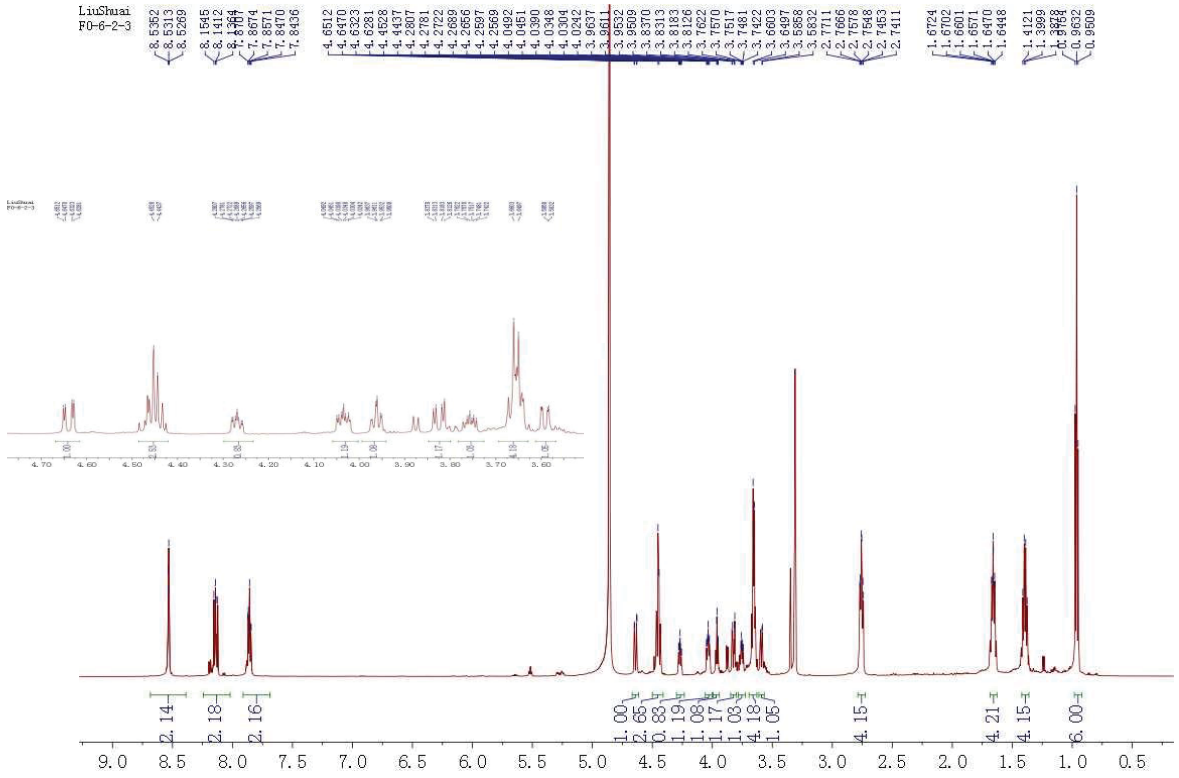

S23. ^{1}H NMR (600 MHz, CD_3OD) spectrum of mixture of **4** and **5.**

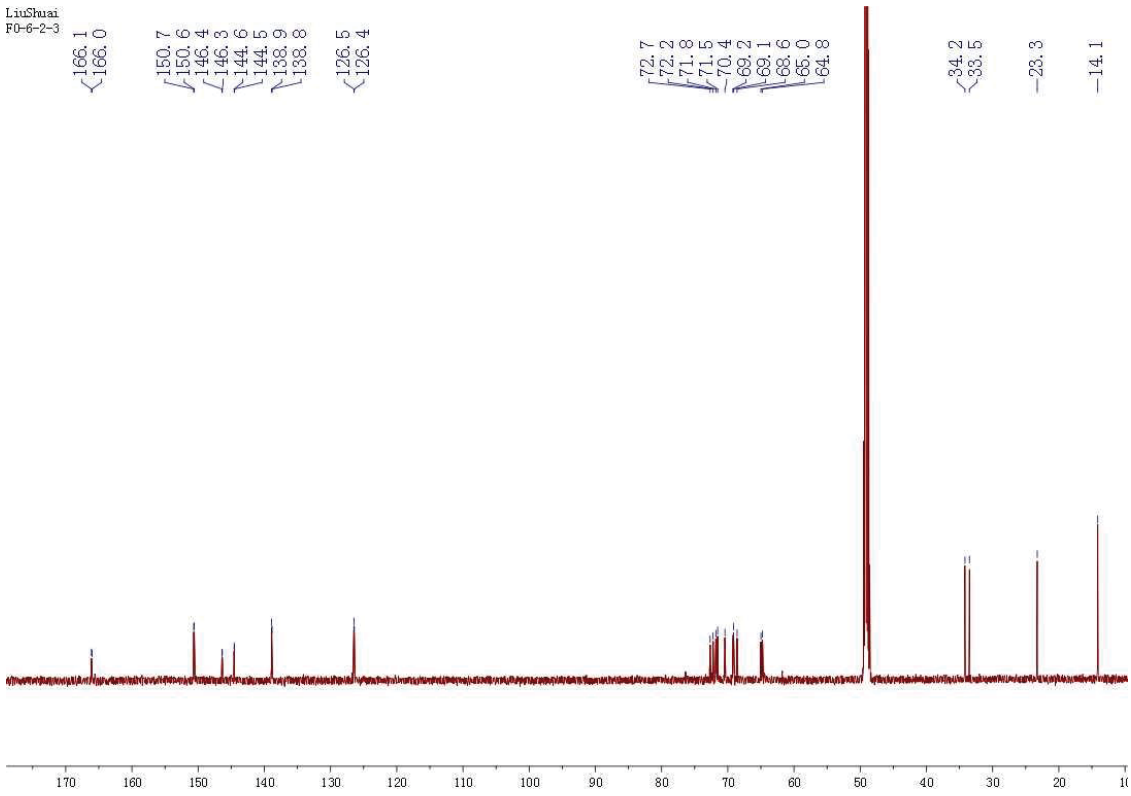

S24. ^{13}C NMR (150 MHz, CD_3OD) spectrum of mixture of **4** and **5.**

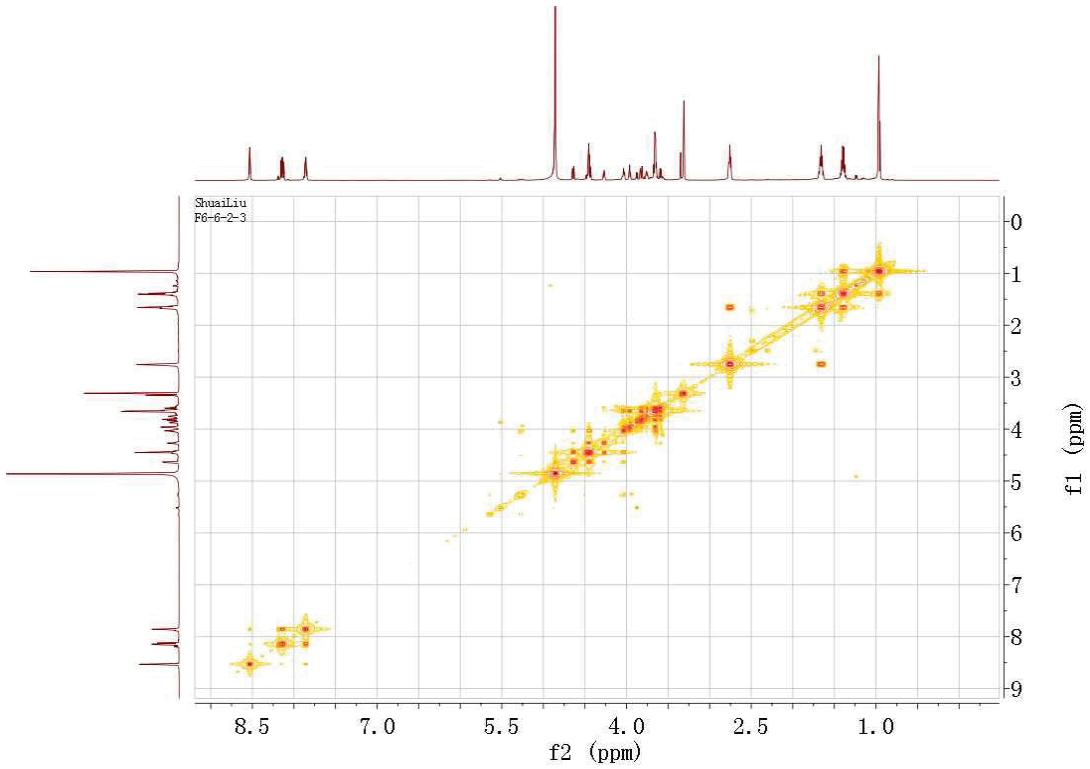

S25. ^{1}H-^{1}H COSY (600 MHz, CD_3OD) spectrum of mixture of **4** and **5.**

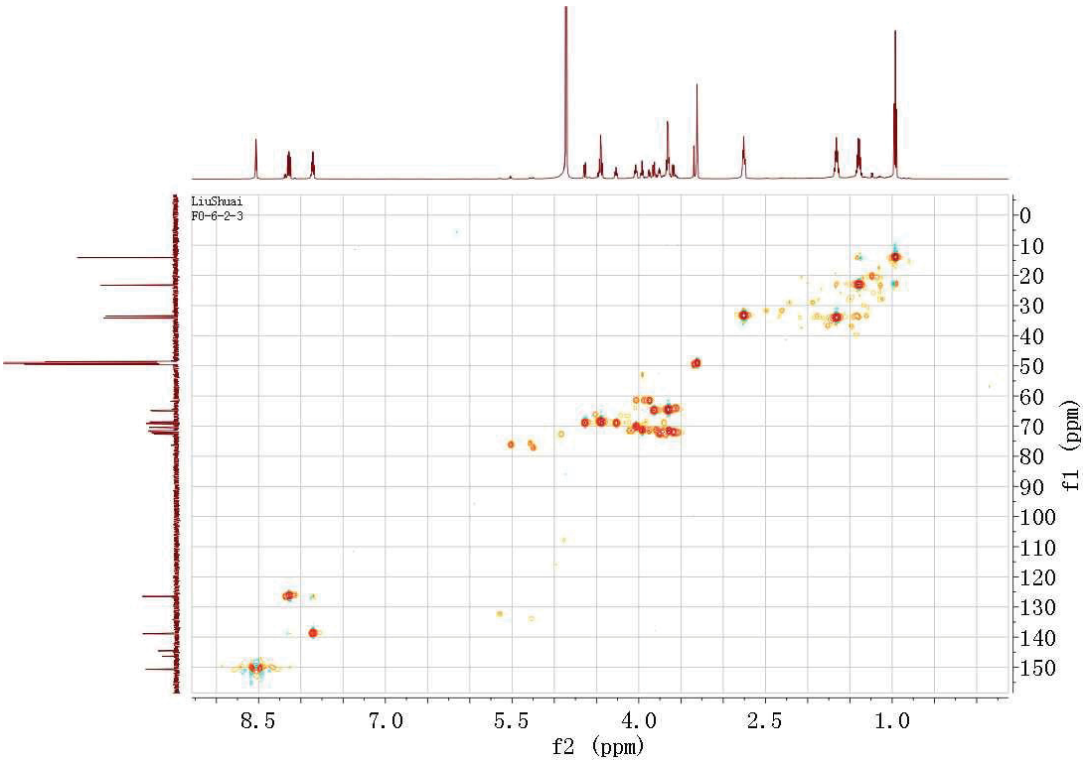

S26. HSQC (600 and 150 MHz, CD_3OD) spectrum of mixture of **4** and **5.**

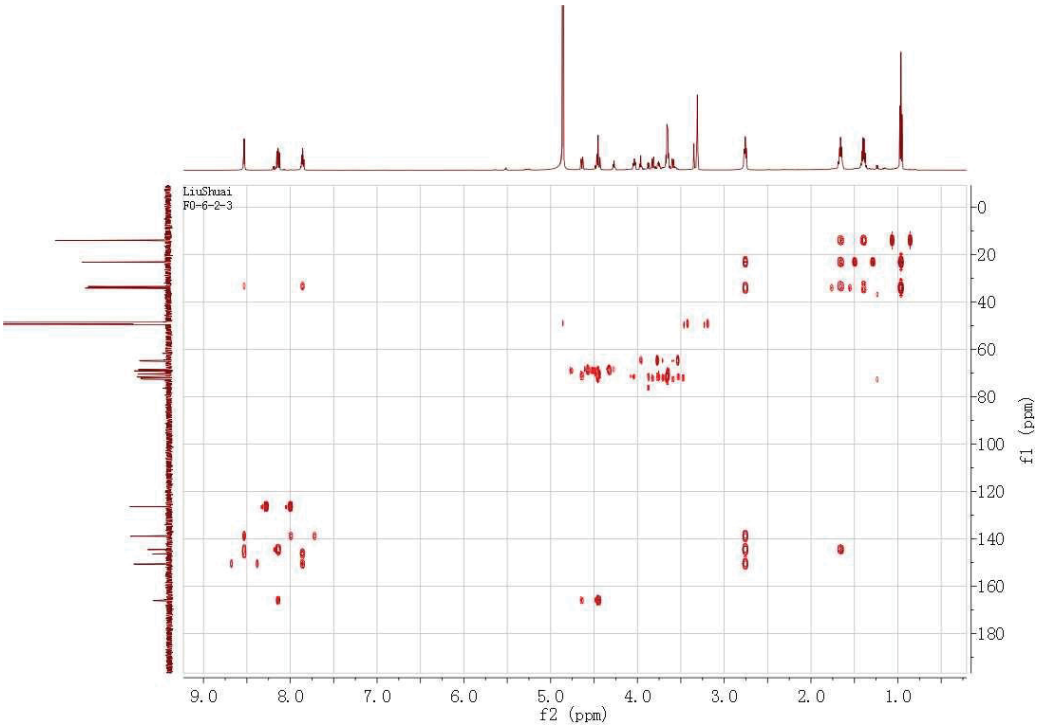

S27. HMBC (600 and 150 MHz, CD_3OD) spectrum of mixture of **4** and **5.**

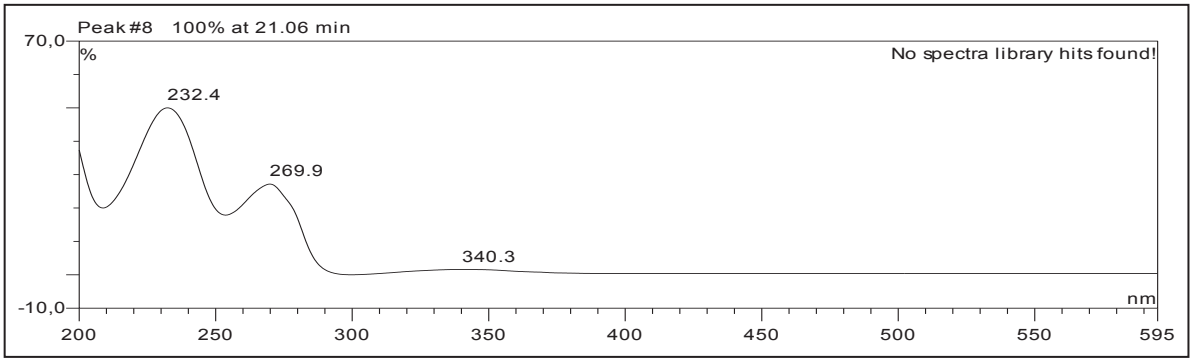

S28. UV spectrum of mixture of **6** and **7**.

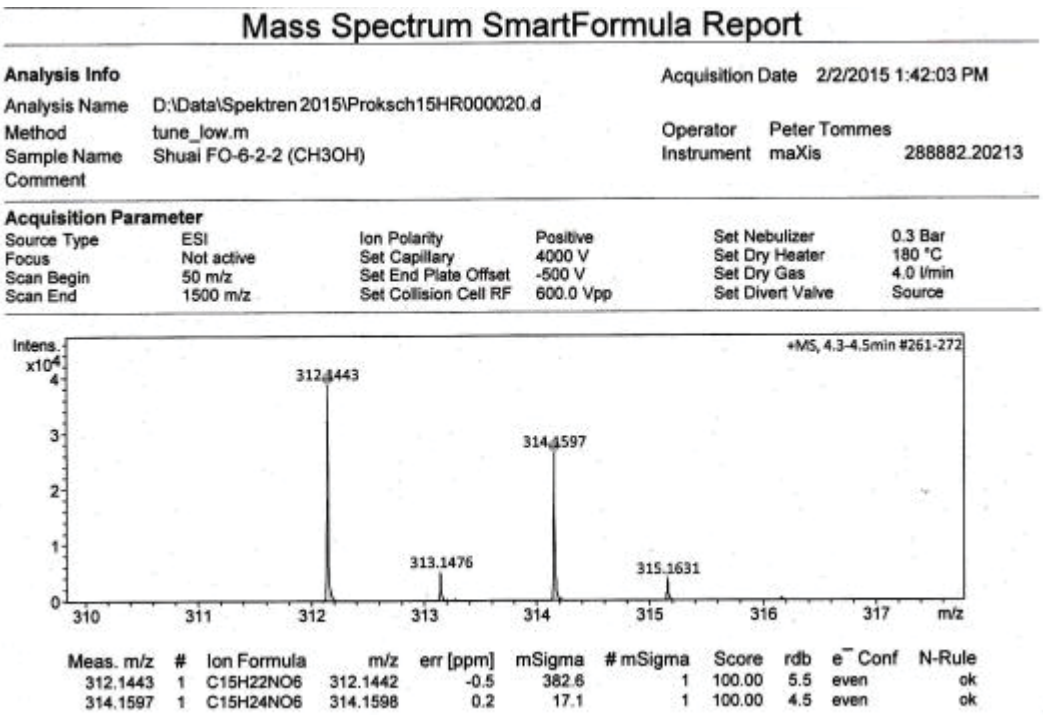

S29. HRESIMS spectrum of mixture of **6** and **7.**

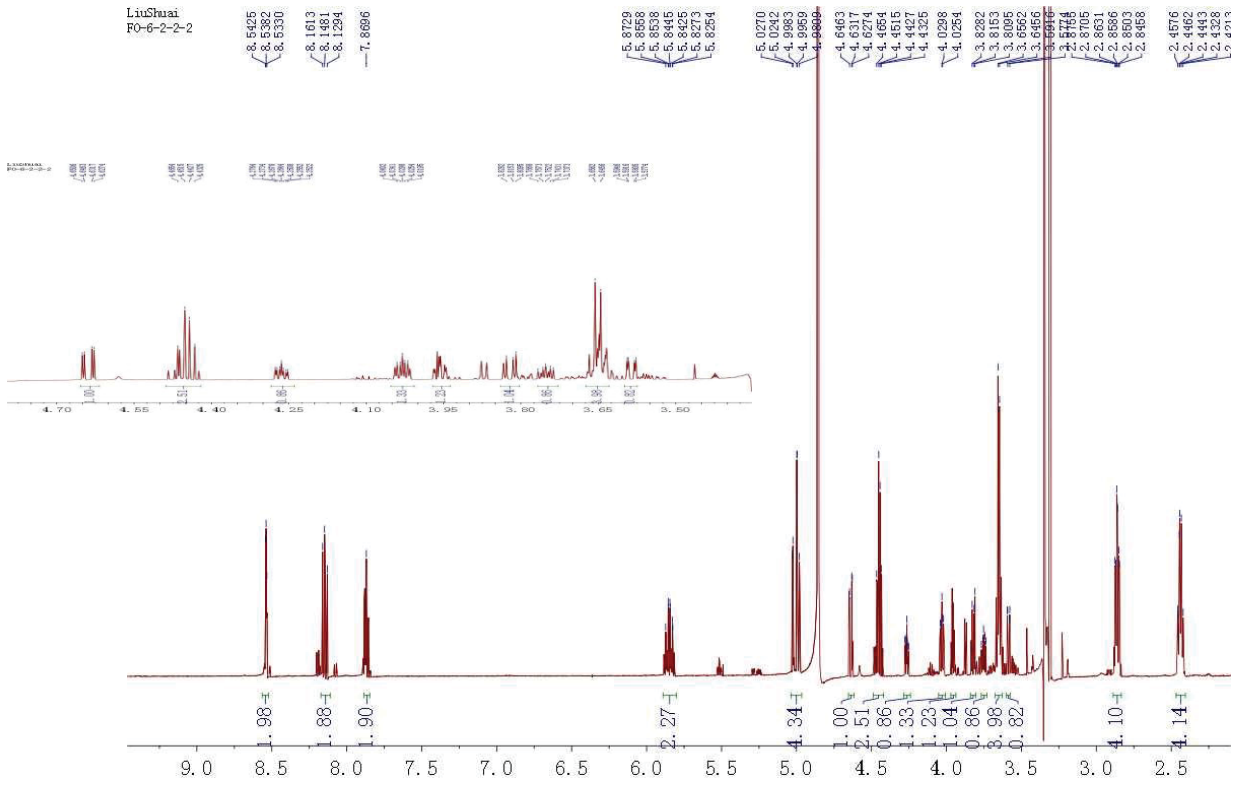

S30. ^{1}H NMR (600 MHz, CD_3OD) spectrum of mixture of **6** and **7.**

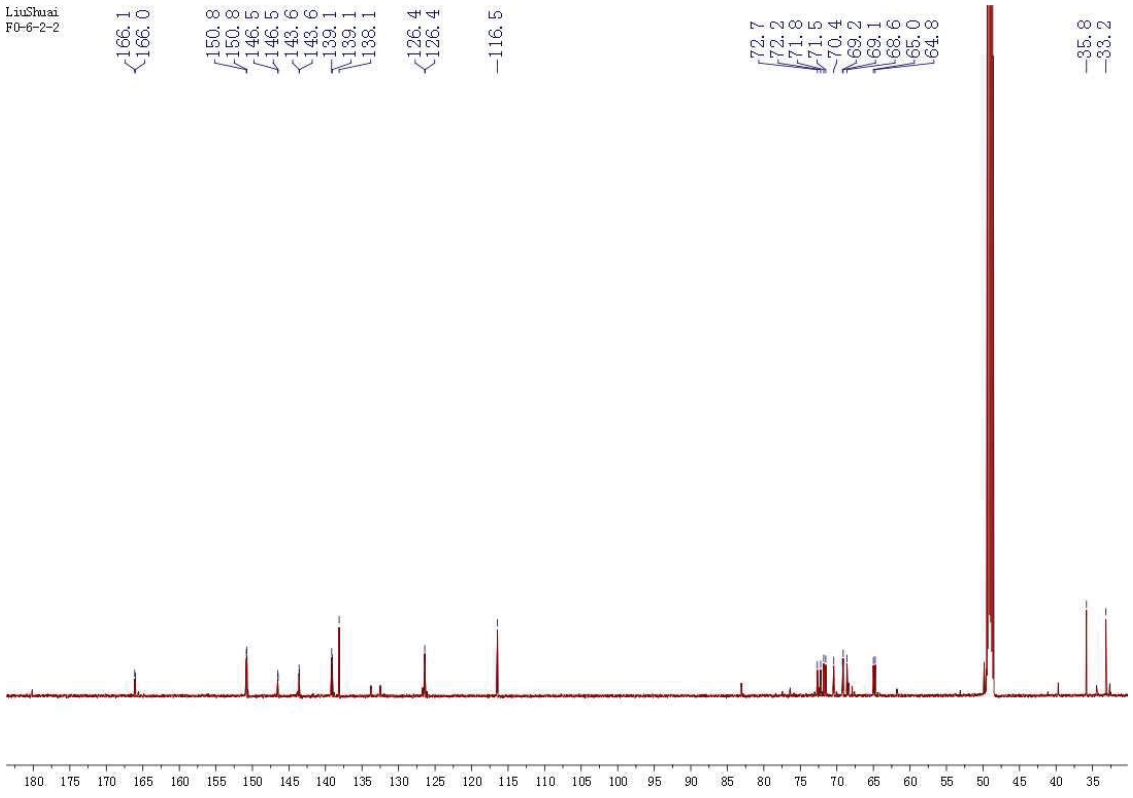

S31. ^{13}C NMR (150 MHz, CD_3OD) spectrum of mixture of **6** and **7.**.

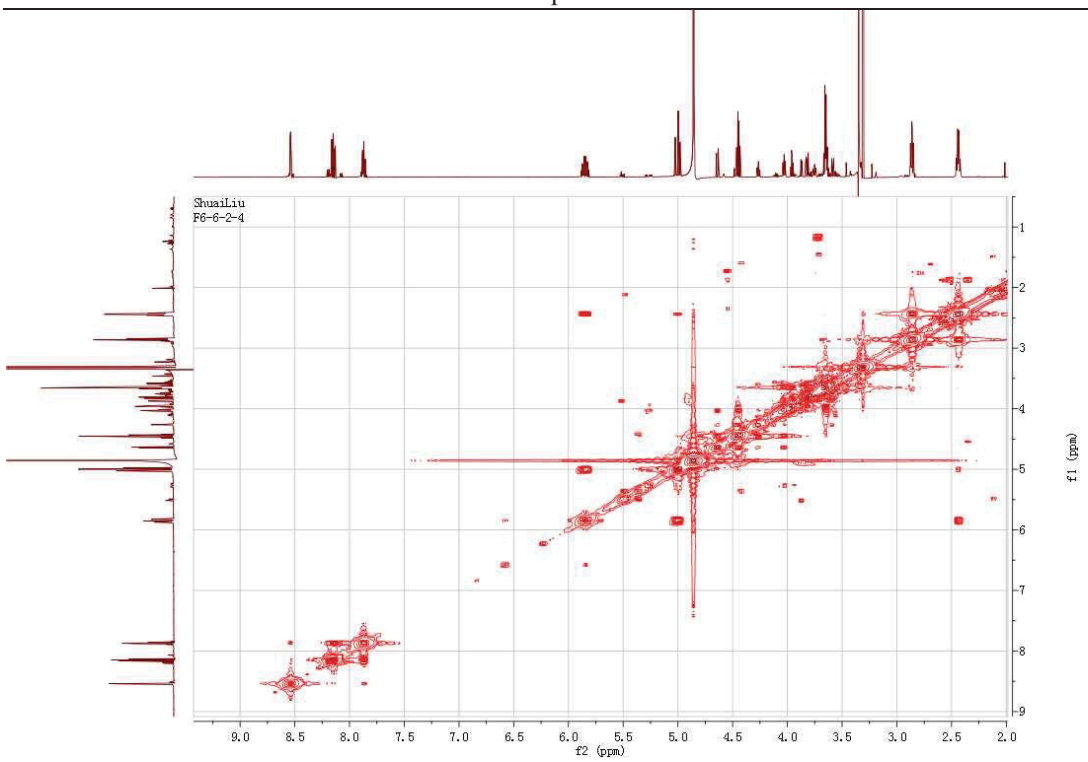

S32. ^{1}H-^{1}H COSY (600 MHz, CD_3OD) spectrum of mixture of **6** and **7.**

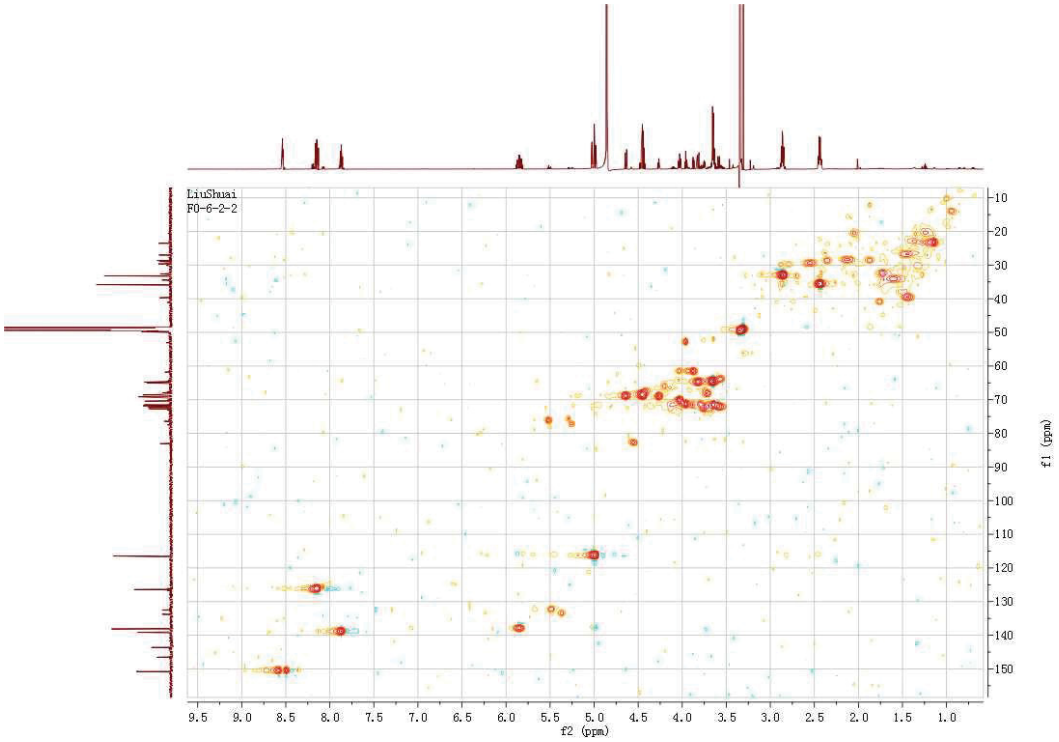

S33. HSQC (600 and 150 MHz, CD_3OD) spectrum of mixture of **6** and **7.**

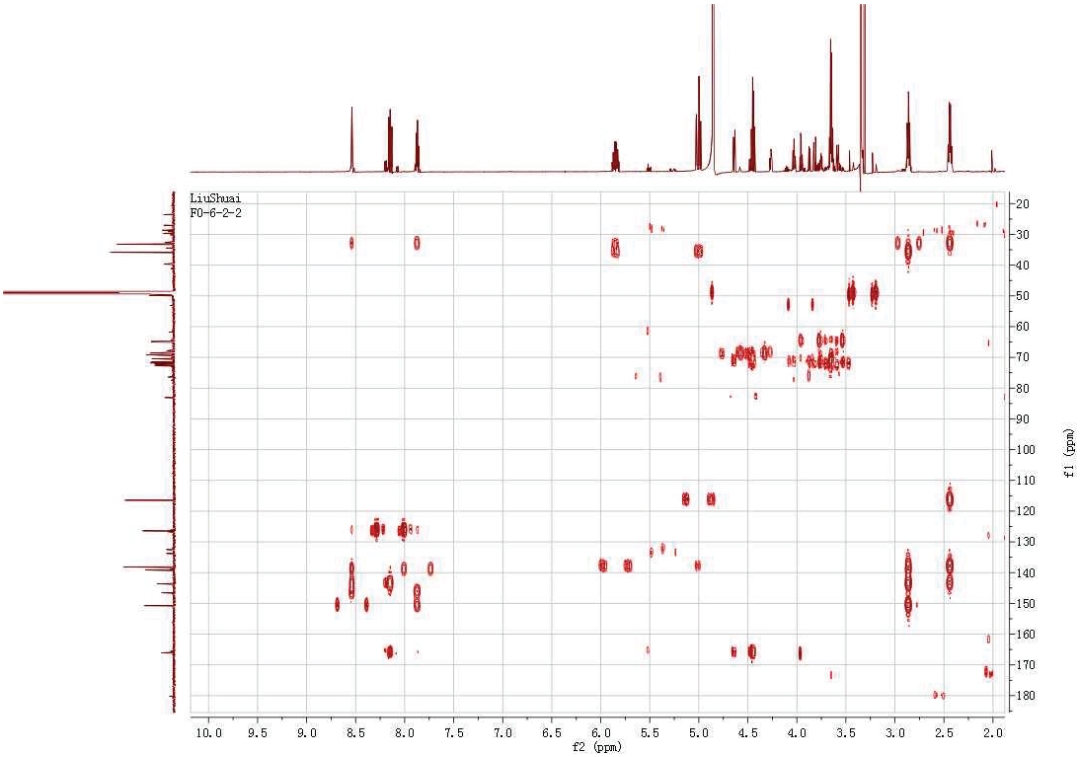

S34. HMBC (600 and 150 MHz, CD_3OD) spectrum of mixture of **6** and **7.**

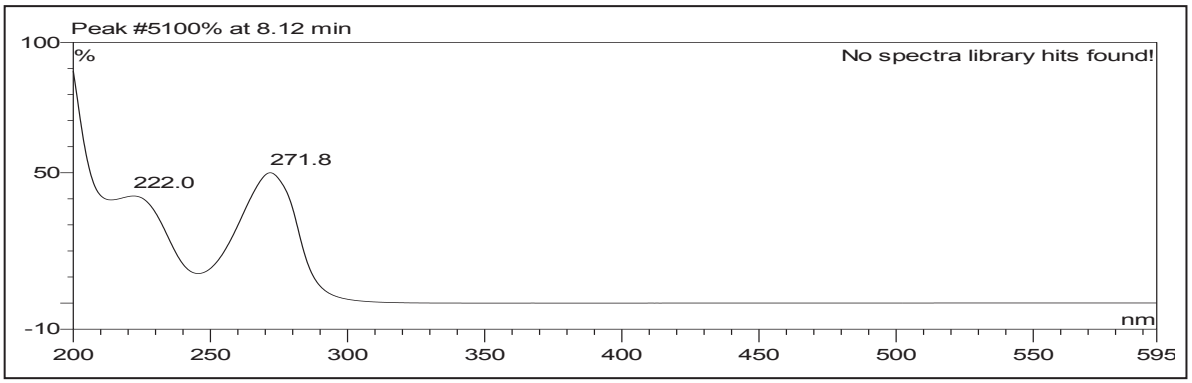

S35. UV spectrum of compound **8**.

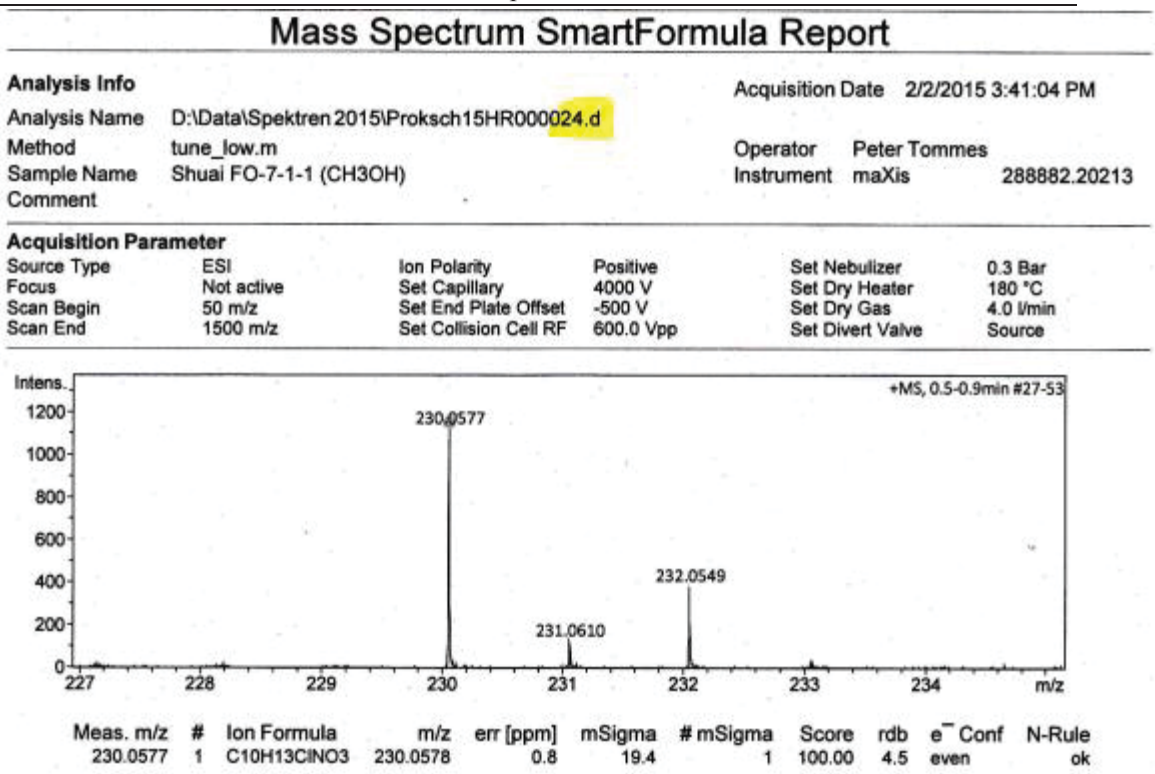

Mass Spectrum SmartFormula Report

Analysis Info

Analysis Name	D:\Data\Spektren 2015\Proksch15HR000024.d	Acquisition Date	2/2/2015 3:41:04 PM
Method	tune_low.m	Operator	Peter Tommes
Sample Name	Shuai FO-7-1-1 (CH3OH)	Instrument	maXis 288882.20213
Comment			

Acquisition Parameter

Source Type	ESI	Ion Polarity	Positive	Set Nebulizer	0.3 Bar
Focus	Not active	Set Capillary	4000 V	Set Dry Heater	180 °C
Scan Begin	50 m/z	Set End Plate Offset	-500 V	Set Dry Gas	4.0 l/min
Scan End	1500 m/z	Set Collision Cell RF	600.0 Vpp	Set Divert Valve	Source

Meas. m/z	#	Ion Formula	m/z	err [ppm]	mSigma	# mSigma	Score	rdb	e⁻ Conf	N-Rule
230.0577	1	C10H13ClNO3	230.0578	0.8	19.4	1	100.00	4.5	even	ok

S36. HRESIMS spectrum of compound **8.**

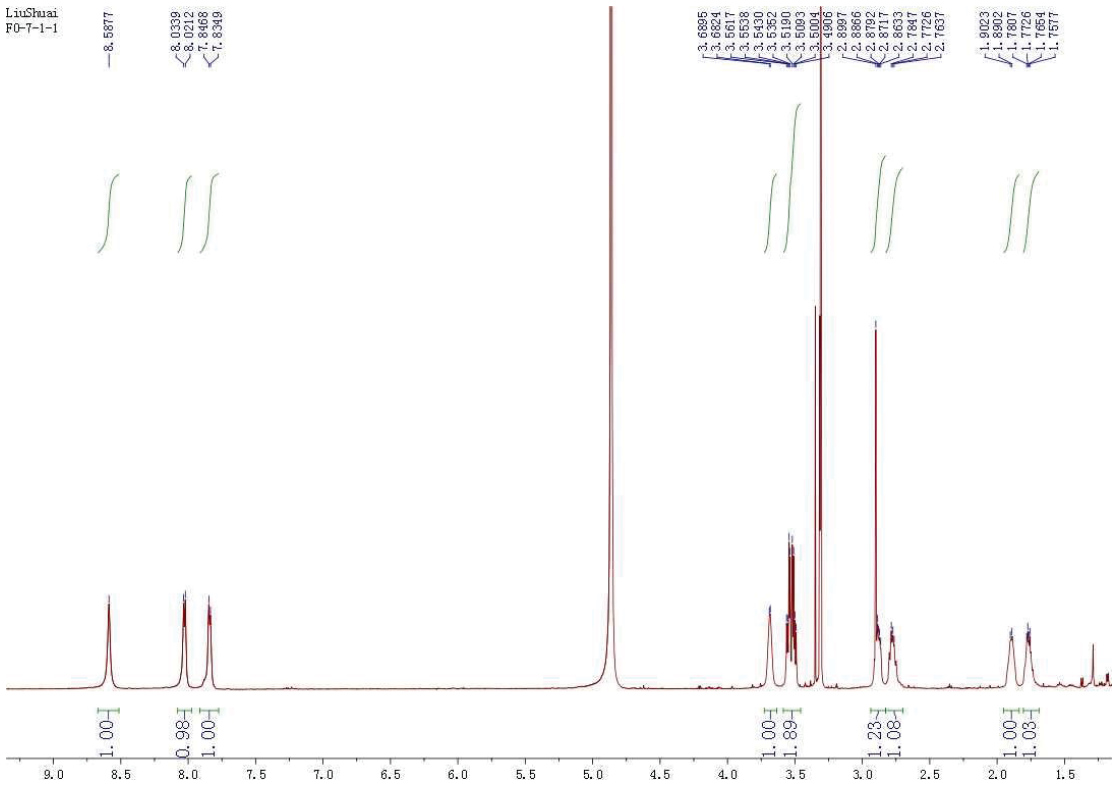

S37. ^{1}H NMR (600 MHz, CD_3OD) spectrum of compound **8**.

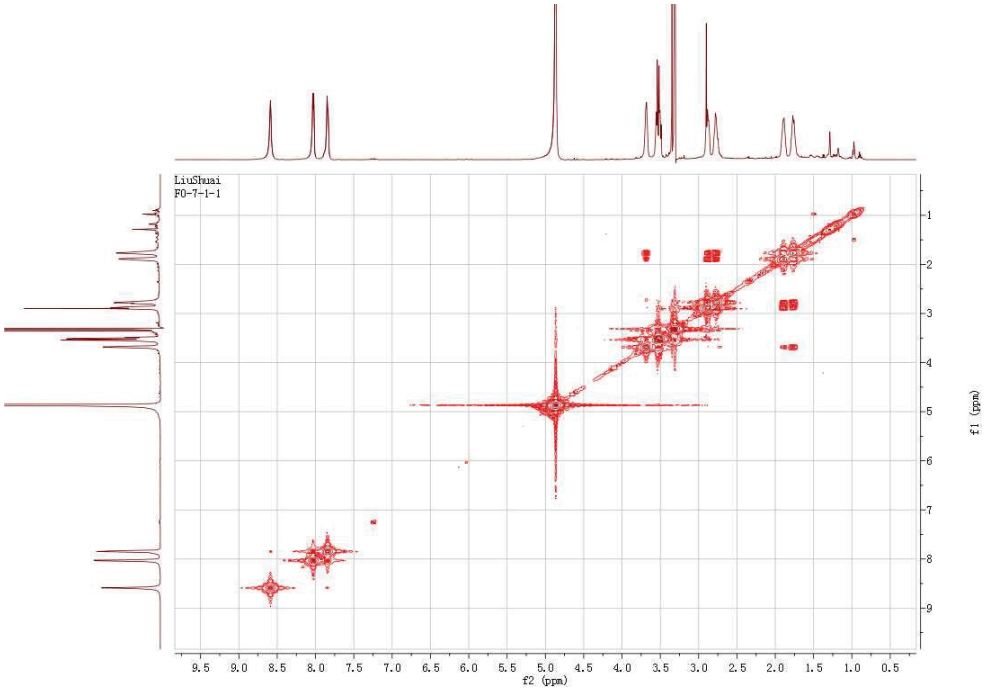

S38. ^{1}H-^{1}H COSY (600 MHz, CD_3OD) spectrum of compound **8**.

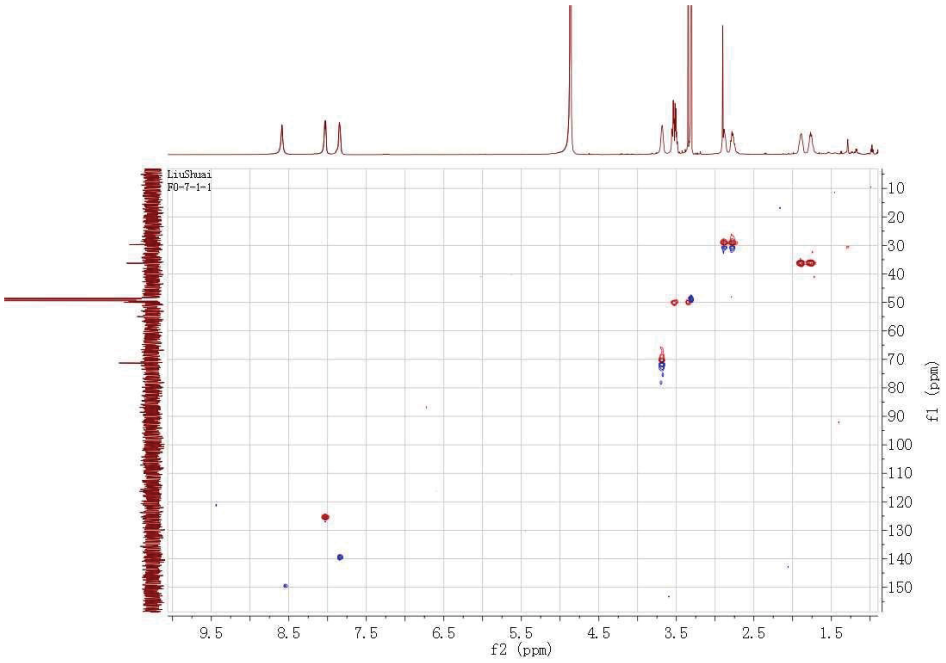

S39. HSQC (600 and 150 MHz, CD_3OD) spectrum of compound **8**.

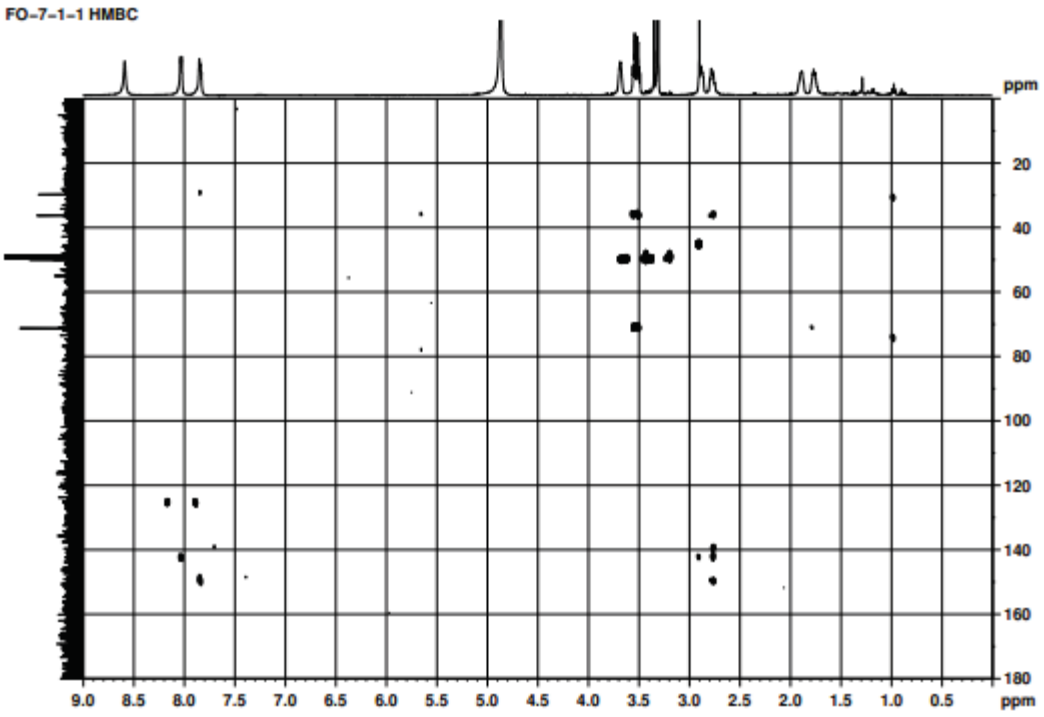

S40. HMBC (600 and 150 MHz, CD_3OD) spectrum of compound **8**.

S41. Phytotoxic bioassay for fusaric acid derivatives (20 μL at three locations on barley leaf).

Barley plants (Bonus, Swedish cultivar)[2] were inoculated 15 days after planting and scored 48 hours after inoculation. The test solution (20 μL) was placed at three locations on each barley leaf, and a pipette tip was used to scratch the surface of the leaf for the standing of the test solutions on the leaf. Different concentrations (0.5 mM, 1.0 mM, 2.0 mM, 4.0 mM and 8.0 mM) were prepared by dissolving the compounds with distilled water. The negative control leaves were inoculated by distilled water (20 μL per location) and the positive control leaves were inoculated by fusaric acid with different concentrations (20 μL per location)[3].

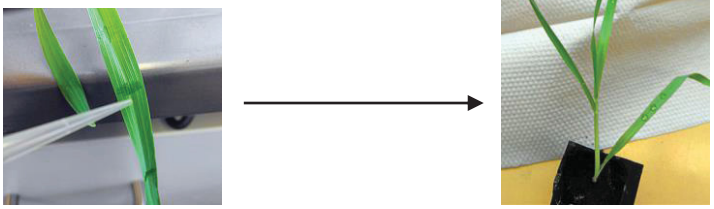

scratch the surface of the leaf add the test solution

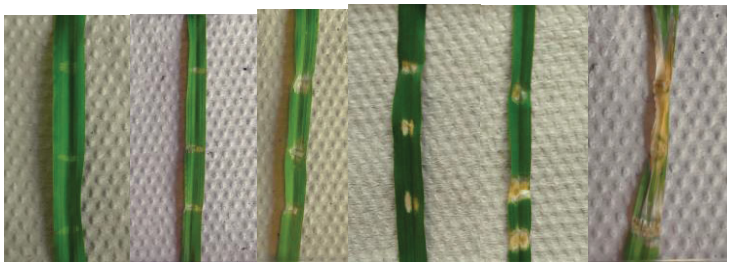

Score 0 1 2 3 4 5

Visual rating: 0 = no necrosis (negative control); 5 = severe necrosis.

Positive control

Score	0	2	2	3	3	4
Fusaric acid	0	0.5 mM	1.0 mM	2.0 mM	4.0 mM	8.0 mM

Compound **1**

0 0.5 mM 1.0 mM 2.0 mM 4.0 mM 8.0 mM

Compound **2**

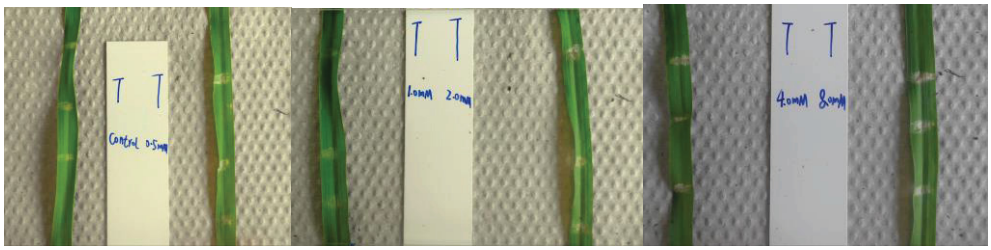

0 0.5 mM 1.0 mM 2.0 mM 4.0 mM 8.0 mM

Compound **3**

0 0.5 mM 1.0 mM 2.0 mM 4.0 mM 8.0 mM

Mixture of compounds **4** and **5**

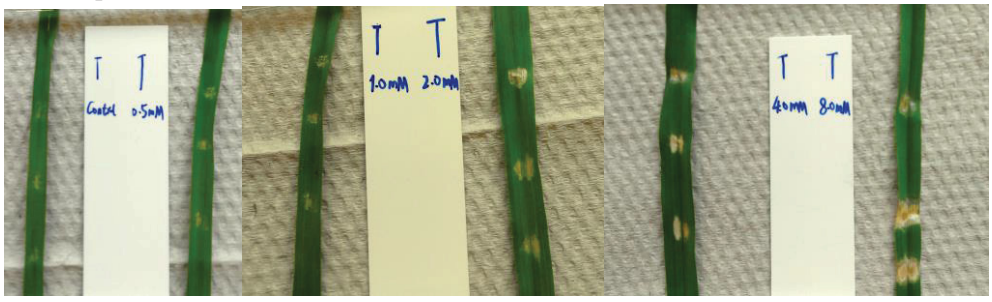

0 0.5 mM 1.0 mM 2.0 mM 4.0 mM 8.0 mM

Mixture of compounds **6** and **7**

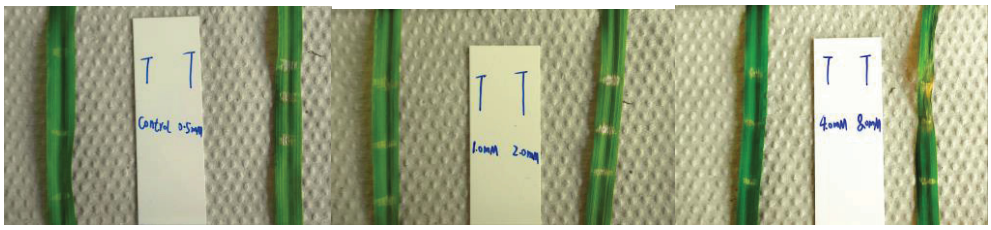

0 0.5 mM 1.0 mM 2.0 mM 4.0 mM 8.0 mM

Compound **8**

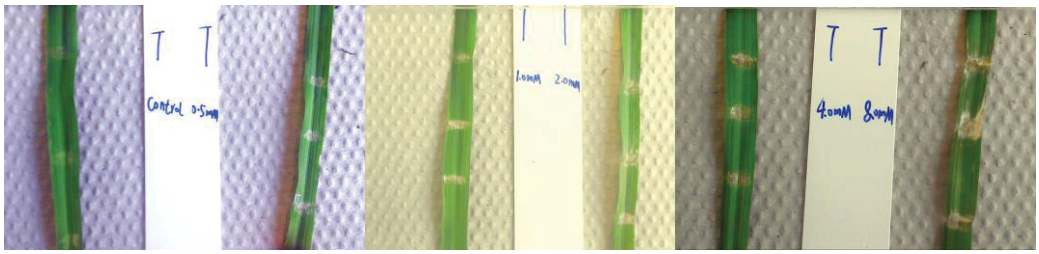

0 0.5 mM 1.0 mM 2.0 mM 4.0 mM 8.0 mM

References: (1). Stipanovic R. D.; Puckhaber L. S.; Liu J.; Bell A. A. Phytotoxicity of fusaric acid and analogs to cotton. *Toxicon* **2011**, *57*, 176−178.

(2). Gustafsson Å.; Hagberg A.; Lundqvist U. The induction of early mutants in Bonus barley. *Hereditas* **1960**, *57*, 675−699.

Chapter 3

Cytotoxic 14-Membered Macrolides from a Mangrove-Derived Endophytic Fungus, *Pestalotiopsis microspora*

Published in “Journal of Natural Products”.

Impact Factor: 3.662.

JOURNAL OF NATURAL PRODUCTS

Article

pubs.acs.org/jnp

Cytotoxic 14-Membered Macrolides from a Mangrove-Derived Endophytic Fungus, *Pestalotiopsis microspora*

Shuai Liu,[†] Haofu Dai,[‡] Gamall Makhloufi,[§] Christian Heering,[§] Christoph Janiak,[§] Rudolf Hartmann,[⊥] Attila Mándi,[#] Tibor Kurtán,[#] Werner E. G. Müller,[∥] Matthias U. Kassack,[○] Wenhan Lin,[¶] Zhen Liu,*[,†] and Peter Proksch*[,†]

[†]Institute of Pharmaceutical Biology and Biotechnology, [§]Institute of Inorganic and Structural Chemistry, and [○]Institute of Pharmaceutical and Medicinal Chemistry, Heinrich-Heine-Universität Düsseldorf, Universitätsstrasse 1, 40225 Düsseldorf, Germany

[‡]Key Laboratory of Biology and Genetic Resources of Tropical Crops, Ministry of Agriculture, Institute of Tropical Bioscience and Biotechnology, Chinese Academy of Tropical Agricultural Sciences, Haikou 571101, China

[⊥]Institute of Complex Systems: Strukturbiochemie, Forschungszentrum Juelich, Wilhelm-Johnen-Straße, 52428 Juelich, Germany

[#]Department of Organic Chemistry, University of Debrecen, P.O. Box 400, H-4002 Debrecen, Hungary

[∥]Institute of Physiological Chemistry, Universitätsmedizin der Johannes Gutenberg-Universität Mainz, Duesbergweg 6, 55128 Mainz, Germany

[¶]State Key Laboratory of Natural and Biomimetic Drugs, Peking University, Beijing 100191, China

Supporting Information

ABSTRACT: Seven new 14-membered macrolides, pestalotioprolides C (**2**), D−H (**4**−**8**), and 7-*O*-methylnigrosporolide (**3**), together with four known analogues, pestalotioprolide B (**1**), seiricuprolide (**9**), nigrosporolide (**10**), and 4,7-dihydroxy-13-tetradeca-2,5,8-trienolide (**11**), were isolated from the mangrove-derived endophytic fungus *Pestalotiopsis microspora*. Their structures were elucidated by analysis of NMR and MS data and by comparison with literature data. Single-crystal X-ray diffraction analysis was used to confirm the absolute configurations of **1**, **2**, and **10**, while Mosher's method and the TDDFT-ECD approach were applied to determine the absolute configurations of **5** and **6**. Compounds **3**−**6** showed significant cytotoxicity against the murine lymphoma cell line L5178Y with IC_{50} values of 0.7, 5.6, 3.4, and 3.9 μM, respectively, while compound **5** showed potent activity against the human ovarian cancer cell line A2780 with an IC_{50} value of 1.2 μM. Structure−activity relationships are discussed. Coculture of *P. microspora* with *Streptomyces lividans* caused a roughly 10-fold enhanced accumulation of compounds **5** and **6** compared to axenic fungal control.

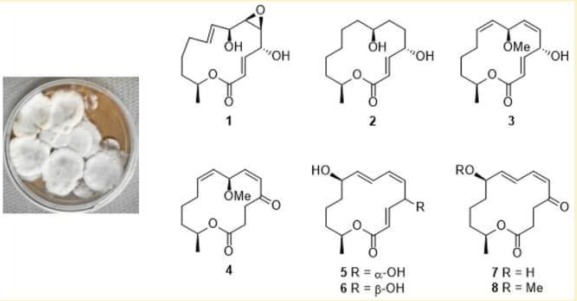

Since the discovery of the well-known antibiotic erythromycin in 1952, naturally occurring macrolides have attracted considerable attention due to their diverse structures and promising biological properties such as antibacterial, antitumoral, and anti-inflammatory effects.[1] They are biogenetically derived through the polyketide synthase pathways in bacteria and in fungi.[2] Previously, several 14-membered macrolides exhibiting different bioactivities were isolated from fungi, including the phytotoxic compound seiricurprolide obtained from *Seiridium cupressi*[3] and the mycotoxin zearalenone, a resorcinonic 14-membered macrolide, which is derived from fungi of the genus *Fusarium* and possesses estrogenic activity in pigs, cattle, and sheep.[4] Further examples include aspergillides A−C, isolated from the marine-derived fungus *Aspergillus ostianus*, which exhibit cytotoxicity against L1210 mouse lymphocytic leukemia cells.[5] In the course of our ongoing studies on new bioactive natural products from endophytic fungi,[6−9] *Pestalotiopsis microspora* was isolated from fresh fruits of the mangrove plant *Drepanocarpus lunatus* (Fabaceae) collected in Cameroon, which resulted in the isolation of 11 14-membered macrolides (**1**−**11**) including seven new compounds, pestalotioprolides C (**2**) and D−H (**4**−**8**) and 7-*O*-methylnigrosporolide (**3**). On the basis of our previous studies on cocultivation of fungi with bacteria,[10,11] coculture experiments of *P. microspora* with *Streptomyces lividans* were carried out. Compared to the axenically grown fungus, cocultivation of *P. microspora* with *S. lividans* resulted in a strong increase in the production of **5** and **6**. In this paper we report the isolation, structure elucidation, and cytotoxic activities of the macrolides, as well as the cocultivation results.

Received: May 24, 2016
Published: August 24, 2016

DOI: 10.1021/acs.jnatprod.6b00473
J. Nat. Prod. 2016, 79, 2332−2340

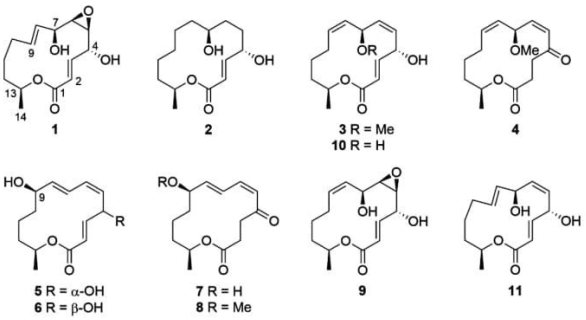

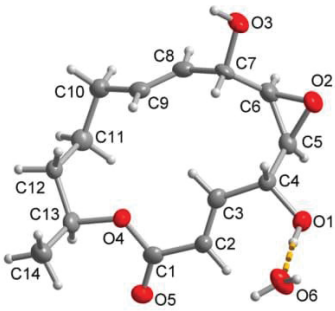

Figure 1. Molecular structure of **1** from single-crystal X-ray diffractometry.

RESULTS AND DISCUSSION

Compound **1** was obtained as colorless crystals. Its molecular formula $C_{14}H_{20}O_5$ was established by HRESIMS. The ^{13}C and ^1H NMR data of **1** (Table 1) were similar to those of seiricuprolide (**9**).[3] Detailed analysis of the 2D NMR spectra of **1** revealed that it was the known compound pestalotioprolide B, which was previously isolated as a diacetate derivative by Rukachaisirikul et al. because it was difficult to separate it from seiricuprolide (**9**).[12] However, the use of a chiral-phase HPLC column in our study overcame this problem. The absolute configuration of **1** was determined as 4*R*, 5*S*, 6*R*, 7*S*, and 13*S* by X-ray single-crystal diffraction (Figure 1).

The molecular formula of pestalotioprolide C (**2**) was determined as $C_{14}H_{24}O_4$ by HRESIMS, lacking two degrees of unsaturation compared to **1**. As expected, the NMR spectra of **2** showed one ester carbonyl carbon at δ_C 167.8 (C-1), signals of an α,β-unsaturated double bond at δ_C 152.0 (C-3), 121.8 (C-2) and at δ_H 6.96 (dd, H-3), 6.00 (dd, H-2), three oxygenated methine groups at δ_C 73.7 (C-13), 70.7 (C-4), and 70.7 (C-7) and at δ_H 5.01 (m, H-13), 4.48 (m, H-4), and 3.57 (m, H-7), and one methyl group at δ_C 21.0 (C-14) and δ_H 1.27 (d, H_3-14). However, the signals for the C-5/C-6 epoxy unit and the C-8/C-9 double bond of **1** were missing. Instead, seven

Table 1. ^1H and ^{13}C NMR Data for Compounds 1−4

	1[a]		**2**[b]		**3**[c]		**4**[b]	
position	δ_C, type	δ_H (J in Hz)	δ_C, type	δ_H (J in Hz)	δ_C, type	δ_H (J in Hz)	δ_C, type	δ_H (J in Hz)
1	166.1, C		167.8, C		168.4, C		174.7, C	
2	120.9, CH	5.99, dd (15.5, 2.0)	121.8, CH	6.00, dd (15.7, 1.8)	121.5, CH	6.09, dd (15.5, 1.3)	30.0, CH_2	2.80, ddd (15.0, 10.9, 2.8)
								2.41, ddd (15.0, 6.7, 2.9)
3	148.2, CH	7.11, dd (15.5, 4.0)	152.0, CH	6.96, dd (15.7, 4.2)	150.0, CH	6.93, dd (15.5, 6.9)	41.0, CH_2	2.96, ddd (17.8, 10.9, 2.9)
								2.74, ddd (17.8, 6.7, 2.8)
4	71.4, CH	4.32, m	70.7, CH	4.48, m	69.7, CH	5.17, m	201.5, C	
5	61.8, CH	2.92, dd (5.6, 4.6)	32.6, CH_2	1.92, m	136.3, CH	5.65, dd (11.4, 4.4)	127.4, CH	6.32, dd (11.5, 0.9)
				1.74, m				
6	59.3, CH	2.94, dd (8.9, 4.6)	30.4, CH_2	1.56, m	130.4, CH	5.27, ddd (11.4, 10.1, 2.3)	145.5, CH	5.90, dd (11.5, 9.6)
				1.34, m				
7	71.7, CH	3.94, ddd (8.9, 7.7, 3.9)	70.7, CH	3.57, m	73.4, CH	4.70, dd (10.1, 9.5)	73.0, CH	5.79, m
8	130.9, CH	5.55, dd (15.6, 7.7)	36.2, CH_2	1.42, m	128.6, CH	5.14, m	129.8, CH	5.23, m
9	135.2, CH	5.96, m	25.0, CH_2	1.42, m	135.2, CH	5.49, ddd (11.0, 11.0, 3.4)	135.0, CH	5.67, m
				1.25, m				
10	33.7, CH_2	2.12, m	29.6, CH_2	1.46, m	30.8, CH_2	2.55, m	30.0, CH_2	2.12, m
		2.01, m		1.24, m		1.98, m		1.85, m
11	25.4, CH_2	1.86, m	26.2, CH_2	1.47, m	26.9, CH_2	1.75, m	28.3, CH_2	1.31, m
		1.13, m		1.18, m		1.09, m		0.92, m
12	35.1, CH_2	1.80, m	35.8, CH_2	1.74, m	35.6, CH_2	1.90, m	37.4, CH_2	1.64, m
		1.56, m		1.51, m		1.47, m		1.54, m
13	72.3, CH	4.66, m	73.7, CH	5.01, m	74.3, CH	4.96, m	73.1, CH	4.90, m
14	20.3, CH_3	1.22, d (6.2)	21.0, CH_3	1.27, d (6.4)	20.7, CH_3	1.28, d (6.2)	20.4, CH_3	1.24, d (6.4)
4-OH		4.99, d (4.4)						
7-OH		4.17, d (3.9)						
7-OMe					55.4, CH_3	3.28, s	56.1, CH_3	3.30, s

[a]Recorded at 600 MHz (^1H) and 150 MHz (^{13}C) in CD_3COCD_3. [b]Recorded at 600 MHz (^1H) and 150 MHz (^{13}C) in CD_3OD. [c]Recorded at 700 MHz (^1H) and 175 MHz (^{13}C) in CD_3OD.

DOI: 10.1021/acs.jnatprod.6b00473
J. Nat. Prod. 2016, 79, 2332−2340

aliphatic methylene groups were observed in **2** at δ_C 36.2 (C-8), 35.8 (C-12), 32.6 (C-5), 30.4 (C-6), 29.6 (C-10), 26.2 (C-11), and 25.0 (C-9), suggesting the replacement of the C-5/C-6 epoxy ring and the C-8/C-9 double bond by four aliphatic methylene groups in **2**. This was further confirmed by the COSY correlations between H-4/H_2-5, H_2-5/H_2-6, H_2-6/H-7, H-7/H_2-8, and H_2-8/H_2-9 and by the HMBC correlations from H-3 to C-5, from H-4 to C-5 and C-6, and from H-7 to C-5 and C-9. Thus, pestalotioprolide C (**2**) was identified as shown, and its absolute configuration was determined as 4*S*, 7*S*, 13*S* by X-ray single-crystal diffraction analysis (Figure 2).

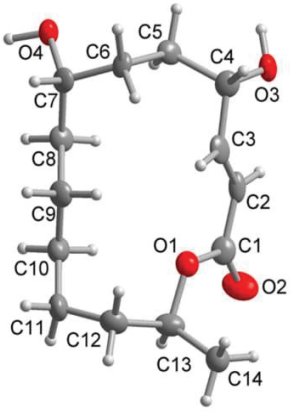

Figure 2. Molecular structure of **2** from single-crystal X-ray diffractometry.

Compound **3** was isolated as a colorless oil. Its molecular formula was established as $C_{15}H_{22}O_4$ by HRESIMS, containing an additional methyl substituent in comparison with nigrosporolide (**10**).[13] The NMR spectra of **3** were closely related to those of **10** except for the appearance of an additional methoxy group at δ_C 55.4 and δ_H 3.28. The location of this methoxy group at C-7 in **3** was confirmed by the HMBC correlation from its protons to C-7 (δ_C 73.4) and in turn from H-7 (δ_H 4.70, dd) to the carbon of the methoxy group. Thus, compound **3** was elucidated as 7-*O*-methylnigrosporolide. The relative configuration of nigrosporolide (**10**) was not disclosed in the previous report by Harwooda et al.[13] However, in our present study, we crystallized **10** and, by use of X-ray analysis, determined its absolute configuration as 4*S*, 7*S*, 13*S* (Figure 3). Considering the similarity of coupling constants and NOE correlations in **3** and **10**, as well as their close biogenetic relationship, the absolute configuration of **3** is proposed to be identical to **10**.

Pestalotioprolide D (**4**) shared the same molecular formula as **3** as deduced by HRESIMS. Comparison of the ^1H and ^{13}C NMR data of **4** with those of **3** revealed the presence of one additional ketone carbonyl (δ_C 201.5, C-4) and two additional methylene groups (δ_C 41.0, δ_H 2.96 and 2.74, CH_2-3; δ_C 30.0, δ_H 2.80 and 2.41, CH_2-2), as well as the disappearance of one double bond and one oxygenated methine in **4** compared to **3**. In the HMBC spectrum of **4**, both H-2ab and H-3ab exhibited correlations to C-1 (δ_C 174.7) and C-4, while H-5 (δ_H 6.32) showed a correlation to C-4, indicating the CO(1)−CH_2(2)−CH_2(3)−CO(4) fragment. The remaining substructure of **4** was found to be identical to that of **3**, as confirmed by detailed interpretation of the 2D NMR data. The similar *J* values and ROESY relationships between **3** and **4** suggested that both

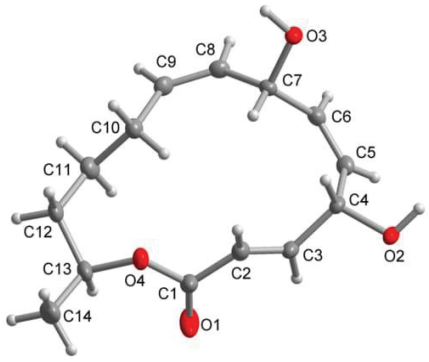

Figure 3. Molecular structure of **10** from single-crystal X-ray diffractometry.

compounds had the same configuration at the stereogenic centers C-7 and C-13 as 7*S* and 13*S*.

On the basis of the HRESIMS data, the molecular formula of pestalotioprolide E (**5**) was established to be the same as that of the known nigrosporolide (**10**).[13] Six olefinic methine protons at δ_H 7.27 (dd, H-3), 6.44 (dd, H-7), 6.14 (dd, H-6), 6.06 (dd, H-2), 5.71 (dd, H-5), and 5.51 (dd, H-8) and three oxygenated methine protons at δ_H 5.15 (m, H-13), 4.90 (ddd, H-4), and 4.04 (m, H-7) were observed in the ^1H NMR spectrum of **5** (Table 2). However, the observed COSY correlations between H-4/H-5, H-5/H-6, H-6/H-7, H-7/H-8, and H-8/H-9 indicated the conjugated double bonds of **5** to be located at C-5/C-6 and C-7/C-8, whereas a hydroxy group was present at C-9. Detailed analysis of 1D and 2D NMR spectra of **5** revealed the remaining structure of **5** to be identical to that of **10**. The configurations of the three double bonds in **5** were elucidated as 2*E*, 5*Z*, and 7*E*, respectively, on the basis of the coupling constants ($^2J_{2,3}$ = 15.8 Hz, $^2J_{5,6}$ = 11.3 Hz, $^2J_{7,8}$ = 15.6 Hz). The configuration of C-13 in **5** was assumed to be the same as that of the other pestalotioprolides due to biogenetic considerations. Mosher's method was applied to determine the absolute configuration of C-4 and C-9. Treatment of **5** with 2 equiv of (*R*)- or (*S*)-MTPACl yielded ester **5a** or **5b**, respectively (Figure 4). However, a double-bond rearrangement occurred from C-2 to C-3 during the acylation reaction, which was previously also described by Jiao et al.[14] This rearrangement prevented assignment of the C-4 absolute configuration. Analysis of the chemical shift differences $\Delta\delta^{SR}$ ($\delta_S - \delta_R$) between **5a** and **5b** indicated the 9*R* configuration.

Pestalotioprolide F (**6**) possessed the same molecular formula as **5** as determined by HRESIMS data. Detailed analysis of the COSY and HMBC spectra indicated that both compounds also had the same planar structure. The coupling constants ($^2J_{2,3}$ = 15.7 Hz, $^2J_{5,6}$ = 11.7 Hz, $^2J_{7,8}$ = 15.4 Hz) were in accord with 2*E*, 5*Z*, and 7*E* double-bond configurations. However, H-4 shifted to δ_H 5.08 in **6**, compared to the corresponding chemical shift for H-4 at δ_H 4.90 in **5**. Meanwhile, the coupling constants ($^2J_{3,4}$ = 6.2 Hz, $^2J_{4,5}$ = 3.8 Hz) in **6** were different from those in **5** ($^2J_{3,4}$ = 3.2 Hz, $^2J_{4,5}$ = 7.0 Hz), suggesting **6** to be the 4-epimer of **5**. In the ROESY spectrum, correlations between H-3/H-7, H-7/H-9, H-5/H-6, and H-6/H-8 were observed in both **5** and **6**. However, H-4 showed an NOE correlation to H-2 but not to H-7 in compound **5**, in contrast to the NOE correlation from H-4 to H-7 but not to H-2 in compound **6** (Figure 5). Because the absolute configuration of C-9 in **5** was determined to be *R* by

DOI: 10.1021/acs.jnatprod.6b00473
J. Nat. Prod. 2016, 79, 2332−2340

Table 2. ^{1}H and ^{13}C NMR Data for Compounds 5−8

	5[a]		6[a]		7[b]		8[a]	
position	δ_C, type	δ_H (J in Hz)	δ_C, type	δ_H (J in Hz)	δ_C, type	δ_H (J in Hz)	δ_C, type	δ_H (J in Hz)
1	167.7, C		168.3, C		171.7, C		173.0, C	
2	120.4, CH	6.06, dd (15.8, 2.3)	121.6, CH	6.03, dd (15.7, 1.2)	30.4, CH_2	2.67, m	30.5, CH_2	2.68, m
						2.51, m		2.53, m
3	154.3, CH	7.27, dd (15.8, 3.2)	151.2, CH	7.11, dd (15.7, 6.2)	39.0, CH_2	2.78, m	38.7, CH_2	2.76, m
						2.71, m		2.69,m
4	68.9, CH	4.90, ddd (7.0, 3.2, 2.3)	70.4, CH	5.08, ddd (6.2, 3.8, 1.2)	202.5, C		204.5, C	
5	130.6, CH	5.71, dd (11.3, 7.0)	133.9, CH	5.55, dd (11.7, 3.8)	129.4, CH	6.15, d (11.5)	129.4, CH	6.19, d (11.6)
6	132.0, CH	6.14, dd (11.3, 10.7)	129.3, CH	6.02, dd (11.7, 10.9)	136.8, CH	6.45, dd (11.5, 10.7)	137.1, CH	6.50, dd (11.6, 10.7)
7	128.6, CH	6.44, dd (15.6, 10.7)	129.0, CH	6.40, dd (15.4, 10.9)	126.5, CH	6.55, dd (15.8, 10.7)	129.5, CH	6.70, dd (15.9, 10.7)
8	139.2, CH	5.51, dd (15.6, 6.8)	138.3, CH	5.47, dd (15.4, 7.6)	143.6, CH	5.77, dd (15.8, 7.4)	141.3, CH	5.70, dd (15.9, 7.8)
9	72.4, CH	4.04, m	72.7, CH	4.04, m	72.2, CH	4.17, m	82.7, CH	3.75, m
10	35.7, CH_2	1.55, m	36.0, CH_2	1.51, m	35.9, CH_2	1.71, m	33.2, CH_2	1.73, m
						1.36, m		1.36, m
11	18.5, CH_2	1.48, m	21.5, CH_2	1.42, m	19.4, CH_2	1.38, m	19.4, CH_2	1.36, m
		1.36, m		1.01, m		1.19, m		1.18, m
12	35.1, CH_2	1.71, m	37.1, CH_2	1.65, m	34.6, CH_2	1.66, m	34.4, CH_2	1.69, m
		1.52, m		1.58, m		1.37, m		1.35, m
13	71.6, CH	5.15, m	72.7, CH	4.90, m	70.9, CH	4.95, m	72.0, CH	4.99, m
14	19.0, CH_3	1.28, d (6.5)	21.0, CH_3	1.29, d (6.3)	19.3, CH_3	1.12, d (6.4)	18.9, CH_3	1.15, d (6.5)
9-OH						3.97, d (3.5)		
9-OMe							56.6, CH_3	3.29, s

[a]Recorded at 600 MHz (^{1}H) and 150 MHz (^{13}C) in CD_3OD. [b]Recorded at 600 MHz (^{1}H) and 150 MHz (^{13}C) in CD_3COCD_3.

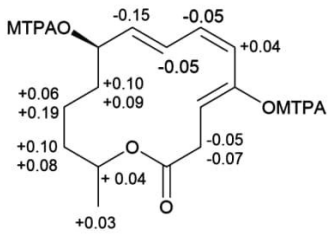

Figure 4. $\Delta\delta^{SR}$ ($\delta_S - \delta_R$) values of (*S*)-MTPA ester **5a** and (*R*)-MTPA ester **5b**.

Mosher's method, the above findings indicated the 4*S* configuration for **5** and the 4*R* configuration for **6**, respectively.

The TDDFT-ECD approach was pursued to confirm the above assignment. A conjugated diene and an α,β-unsaturated lactone chromophore can be found in **5**, which gave rise to a strong positive Cotton effect (CE) at 235 nm (Figure 6). DFT reoptimization of the initial 217 MMFF conformers of (4*S*,9*R*,13*S*)-**5** resulted in 18 and 15 conformers at the B3LYP/6-31G(d) in vacuo and B97D/TZVP PCM/MeCN levels, respectively. The ECD spectra computed for the above conformers reproduced the intense positive CE at 234 nm and the negative one below 195 nm, while the weak low-energy positive n−π* shoulder could not be reproduced well. On the basis of the good overall agreement of the π−π* transitions, the absolute configuration of **5** could be assigned as (4*S*, 9*R*, 13*S*).

DFT reoptimization of the initial 274 MMFF conformers of (4*R*,9*R*,13*S*)-**6** resulted in 15, 20, and 20 conformers at the B3LYP/6-31G(d) in vacuo, B97D/TZVP PCM/MeCN, and CAM-B3LYP/TZVP PCM/MeCN levels, respectively. All the ECD calculations performed on all sets of conformers

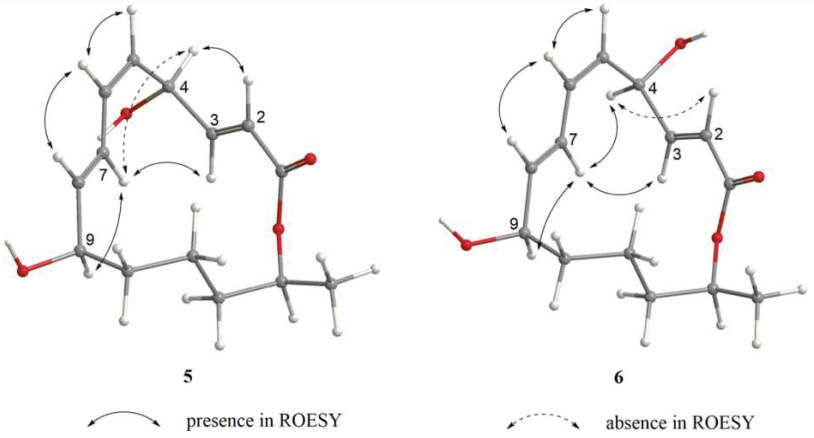

Figure 5. Key NOE correlations in compounds **5** and **6**.

DOI: 10.1021/acs.jnatprod.6b00473
J. Nat. Prod. 2016, 79, 2332−2340

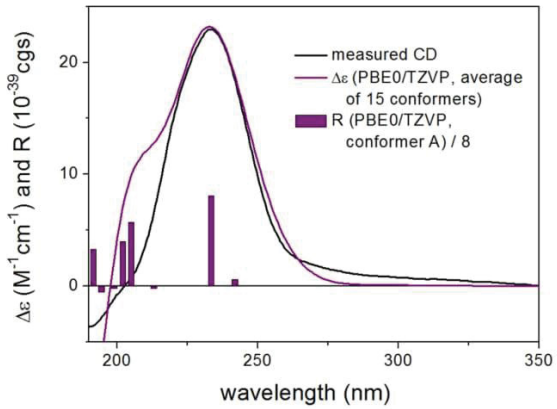

Figure 6. Experimental ECD spectrum of **5** in MeCN compared with the Boltzmann-weighted PBE0/TZVP PCM/MeCN ECD spectrum of (4*S*,9*R*,13*S*)-**5** computed for the B97D/TZVP PCM/MeCN conformers. Bars represent the rotational strength of the lowest energy conformer.

reproduced the strong $\pi-\pi^*$ transitions at 233 and 207 nm, while the weak negative transition at 288 nm could be reproduced only by the in vacuo calculations performed on the B3LYP/6-31G(d)-reoptimized conformers and the weak positive n$-\pi^*$ transition at 351 nm could not be reproduced at any applied level (Figure 7). The good agreement of the high-energy ECD transitions allowed the safe elucidation of the absolute configuration of **6** as (4*R*, 9*R*, 13*S*).

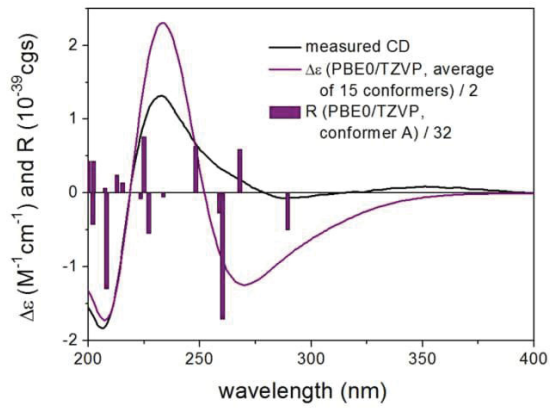

Figure 7. Experimental ECD spectrum of **6** in MeCN compared with the Boltzmann-weighted PBE0/TZVP ECD spectrum of (4*R*,9*R*,13*S*)-**6** computed for the B3LYP/6-31G(d) in vacuo conformers. Bars represent the rotational strength of the lowest energy conformer.

Pestalotioprolide G (**7**) was obtained as a colorless oil, possessing the molecular formula $C_{14}H_{20}O_4$ as determined from the HRESIMS spectrum. Comparison of the ^{1}H and ^{13}C NMR data revealed that the segment from C-1 to C-4 of **7** was the same as that of **4**, whereas the substructure from C-5 to C-14 was compatible with that of **5** and **6**, which was further confirmed by analysis of 2D NMR spectra. The configurations of C-7 and C-13 in **7** were assumed to be the same as those of **5** and **6** due to their similar NMR data and the biogenetic relationship of the respective compounds.

Compound **8** was elucidated as the C-9 *O*-methyl derivative of **7**, as evident from the appearance of an additional methoxy group (δ_C 56.6, δ_H 3.29) in **8** and the HMBC correlation from its protons to the obvious deshielded C-9 (δ_C 82.7). The similarity of the NMR data including NOE correlations between **7** and **8** suggested the same configurations for both compounds.

The remaining three known compounds were identified as seiricuprolide (**9**),[3] nigrosporolide (**10**),[13] and 4,7-dihydroxy-13-tetradeca-2,5,8-trienolide (**11**),[15,16] respectively. All substances (**1**−**11**) were tested for their cytotoxicity against the L5178Y mouse lymphoma cell line using the MTT assay (Table 3). Among them, **3** exhibited potent activity with an IC_{50} value of 0.7 μM, which was even stronger than that of the positive control kahalalide F (IC_{50} 4.3 μM). Compounds **4**, **5**, **6**, and **8** were less active, with IC_{50} values of 5.6, 3.4, 3.9, and 11 μM, respectively, whereas the other macrolides showed weak or no activity (IC_{50} > 20 μM). On the basis of these bioassay data, some preliminary structure−activity relationships can be concluded. The epoxy group at C-5/C-6 (**1** vs **11**; **9** vs **10**) apparently resulted in total loss of cytotoxicity. The rearrangement of the double bond from C-2/C-3 to the C-3 ketone (**3** vs **4**; **5** and **6** vs **7**) decreased the cytotoxicity. The 8*Z* or 8*E* configuration (**9** vs **1**; **10** vs **11**) and 4*R* or 4*S* configuration (**6** vs **5**) had little influence on the cytotoxicity. Moreover, the hydroxy group replaced by the methoxy substituent at C-7 (**10** vs **3**) or C-9 (**7** vs **8**) led to a strong increase of cytotoxicity. In addition to the experiments with the murine lymphoma cell line, cytotoxicity of all isolated macrolides was also evaluated against the human ovarian cancer cell line A2780 (Table 3). Only compound **5** showed significant activity, with an IC_{50} value of 1.2 μM, which was comparable to that of the positive control cisplatin (IC_{50} 1.2 μM). Compound **6** (IC_{50} 12 μM) was less active, and the others (IC_{50} > 20 μM) exhibited weak or no activity. These differences in activity may reflect species specific (murine vs human) or cell line specific (blood cancer vs solid cancer) differences in susceptibility against the studied compounds.

Coculture experiments of *P. microspora* employing different inoculation volumes of *S. lividans* were carried out (Figure 8). Compared with the axenic fungal control, strong enhancements of compounds **5** (9.0-fold increase) and **6** (10.4-fold increase) were found in the coculture with 0.2 g of *S. lividans* per flask (Table 4). However, for Δ^8 isomers **10** and **11**, only a small increase (1.3-fold) was observed. Meanwhile, some unidentified macrolides were also detected in the coculture extracts as suggested by comparison of their UV patterns and MS data with those of the isolated macrolides. The structures of these compounds were not elucidated due to their small amounts.

Table 3. Cytotoxicity (IC_{50}, μM) of 1−11 against the L5178Y and A2780 Cell Lines

	1	2	3	4	5	6	7	8	9	10	11
L5178Y[a]	–[c]	39	0.7	5.6	3.4	3.9	–	11	–	21	21
A2780[b]	–	–	28	–	1.2	12	36	–	–	43	–

[a]Kahalalide F (IC_{50} 4.3 μM) as positive control. [b]Cisplatin (IC_{50} 1.2 μM) as positive control. [c]IC_{50} > 50 μM.

DOI: 10.1021/acs.jnatprod.6b00473
J. Nat. Prod. 2016, 79, 2332−2340

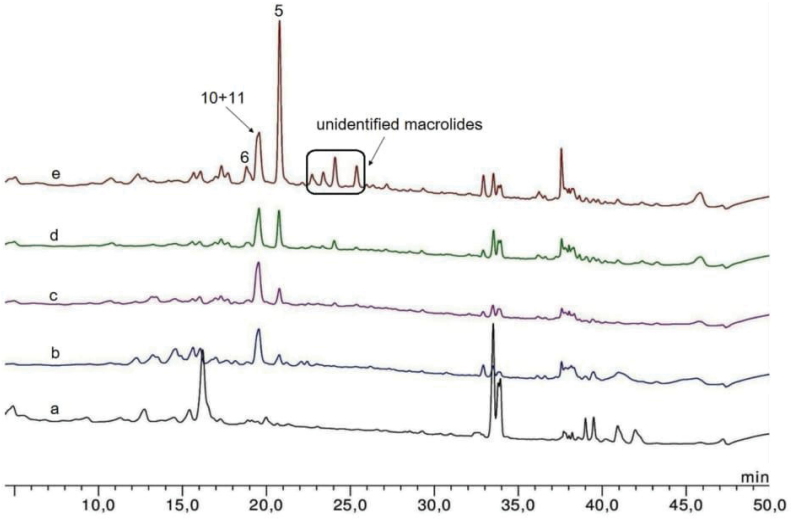

Figure 8. HPLC analysis of the EtOAc extract from cocultivation experiments detected at UV 235 nm: (a) axenic control of *S. lividans*, (b) axenic control of *P. microspora*, (c) coculture of *P. microspora* with *S. lividans* (0.05 g/flask), (d) coculture of *P. microspora* with *S. lividans* (0.1 g/flask), (e) coculture of *P. microspora* with *S. lividans* (0.2 g/flask).

Table 4. Yield of Macrolides per Flask during Coculture of *P. microspora* with Different Inoculation Volumes of *S. lividans* (n = 3) vs Axenic Controls of *P. microspora* (n = 3)[a]

	5	6	10 + 11
control of *P. microspora*	0.52 ± 0.11	0.10[b]	5.35 ± 1.09
coculture of *P. microspora* with *S. lividans* (0.05 g/flask)	0.53 ± 0.05	not detected	5.21 ± 0.49
coculture of *P. microspora* with *S. lividans* (0.1 g/flask)	1.17 ± 0.14	0.44 ± 0.05	4.32 ± 0.52
coculture of *P. microspora* with *S. lividans* (0.2 g/flask)	4.70 ± 0.97	1.04 ± 0.22	6.71 ± 1.39
coculture of *P. microspora* with *S. lividans* (0.2 g/flask) vs control of *P. microspora* (fold)	9.0	10.4	1.3

[a]Amounts of compounds are reported in mg/1 L flask. [b]Calculation was performed using the actual isolated amount because it could not be detected by HPLC.

These experiments suggested that the production of fungal secondary metabolites can be induced by cocultivation with *S. lividans*, and higher inoculation volumes of bacteria seemed to be more effective in provoking this induction.

In summary, chemical examination of the endophytic fungus *P. microspora* resulted in the isolation of 11 14-membered macrolides, including seven new compounds, pestalotioprolides C (**2**) and D–H (**4**–**8**) and 7-*O*-methylnigrosporolide (**3**). All compounds are suggested to have the 13*S* configuration, as demonstrated by X-ray crystallography for compounds **1**, **2**, and **10** and by ECD calculations for compounds **5** and **6**. Compounds **3**–**6** showed potent cytotoxicity against the L5178Y murine lymphoma cell line with IC_{50} values of 0.7, 5.6, 3.4, and 3.9 μM, respectively. The presence of an epoxy group, the rearrangement of the double bond, and the methoxy substituent influenced their cytotoxicity differently, whereas the configuration of the C-8/C-9 double bond and the absolute configuration of C-4 had little influence with regard to the bioactivity of the respective metabolites. In addition, compound **5** exhibited significant activity against the human ovarian cancer cell line A2780 with an IC_{50} value of 1.2 μM. Moreover, when *P. microspora* was cocultured with *S. lividans*, the production of macrolides **5** and **6** strongly increased in comparison to the axenically grown fungus.

EXPERIMENTAL SECTION

General Experimental Procedures. Optical rotations were measured with a P-1020 polarimeter (JASCO). UV spectra were obtained from a PerkinElmer Lambda 25 UV/vis spectrometer. IR spectra were measured in ATR-mode (Platinum ATR-QL, Diamond) on a Bruker TENSOR 37 IR spectrometer. The melting point was determined using a Büchi melting point apparatus B-540. ^{1}H, ^{13}C, and 2D NMR spectra were recorded on Bruker Avance III 600 or 700 NMR spectrometers (Bruker). HRESIMS data were obtained from a UHR-QTOF Maxis 4G mass spectrometer (Bruker Daltonics). HPLC analysis was undertaken with a Dionex P580 system (Dionex Softron), employing a 125 × 4 mm i.d., 5 μm, Eurospher C_{18} analytical column (Knauer). Semipreparative HPLC was achieved on a Lachrom-Merck Hitachi system (Merck), using a 300 × 8 mm i.d., 10 μm, Eurospher C_{18} column (Knauer). Thin-layer chromatography was performed on precoated silica gel 60 F_{254} plates (Merck) with detection at 254 or 365 nm or by spraying anisaldehyde reagent followed by heating. Column chromatography was carried out using silica gel 60 M (Merck) or Sephadex LH-20.

Fungal Material and Identification. Following standard procedures,[17] the endophytic fungus was isolated from fresh, healthy fruits of *Drepanocarpus lunatus* (Fabaceae), which were collected in August 2013 from Douala, Cameroon. It was identified as *Pestalotiopsis microspora* (GenBank accession number KU255793) according to DNA amplification and sequencing of the fungal ITS region as described before.[18] A voucher fungal strain was kept in one of the authors' lab (P.P.) with the code number DL-F-3.

Fermentation, Extraction, and Isolation. Twenty 1 L Erlenmeyer flasks with solid rice medium (100 g of rice, 3.5 g of sea salt, and 110 mL of demineralized water, each) were used for fermentation. They were autoclaved at 121 °C for 20 min and cooled to room temperature, followed by inoculation with the fungus. After cultivation at 20 °C under static conditions for 4 weeks, 500 mL of EtOAc was added to each flask to stop the fermentation. The flasks were shaken at 150 rpm for 8 h on a shaker, and then the EtOAc solution was evaporated to dryness. The obtained brown extract (15.4 g) was subjected to a 20 × 8 cm i.d. silica gel vacuum liquid chromatography column, using solvents in a gradient of increasing

DOI: 10.1021/acs.jnatprod.6b00473
J. Nat. Prod. 2016, 79, 2332–2340

polarity (*n*-hexane−EtOAc, 9:1, 7:3, 1:1, 3:7; CH_2Cl_2−MeOH, 15:1, 9:1, 7:3, 0:10; 600 mL each gradient) to yield 11 fractions in total. Fractions C, E, and F, which showed bioactivity against the mouse lymphoma cell line, were selected for further separation. Fraction C (153.3 mg) was subjected to a 60 × 3 cm i.d. Sephadex LH-20 column with MeOH as mobile phase to remove pigments, then purified by semipreparative HPLC (MeOH−H_2O: 0−5 min, 45%; 5−15 min, from 45% to 58%; 16−19 min, 100%) to give **3** (2.1 mg), **4** (0.4 mg), and **8** (0.9 mg). Following the same protocol, a mixture (15.1 mg) of **1** and **9** was obtained from fraction E (149.8 mg) (HPLC sequence, MeOH−H_2O: 0−10 min, from 20% to 40%; 10−25 min, from 40% to 60%; 26−30 min, 100%). The mixture was subsequently separated by a Phenomenex chiral-phase column (250 × 4.6 mm i.d., 5 μm, Lux Amylose-2) using CH_3CN−H_2O (45:55), to afford **9** (9.3 mg) and **1** (3.2 mg). Meanwhile, **2** (5.4 mg), **5** (13.4 mg), **7** (3.4 mg), **6** (1.9 mg), and a mixture (51.2 mg) of **10** and **11** were obtained from fraction F (240.0 mg) (HPLC sequence, methanol−H_2O: 0−10 min, from 10% to 30%; 10−23 min, from 40% to 60%; 24−28 min, 100%). After separation by chiral-phase column as mentioned above, 10 mg of this mixture yielded **10** (4.5 mg) and **11** (4.5 mg).

*Pestalotioprolide B (**1**):* colorless crystals; mp 111−115 °C; $[\alpha]^{20}_D$ +72 (*c* 1.0, $CHCl_3$); UV (MeOH) λ_{max} (log ε) 214 (3.55) nm; IR ν_{max} 3373, 2939, 1714, 1687, 1368, 1241, 1043, 971 cm^{-1}; ^1H and ^{13}C NMR data, Table 1; HRESIMS *m*/*z* 291.1207 $[M + Na]^+$ (calcd for $C_{14}H_{20}NaO_5$, 291.1203).

*Pestalotioprolide C (**2**):* colorless crystals; mp 124−126 °C; $[\alpha]^{20}_D$ +40 (*c* 1.4, MeOH); UV (MeOH) λ_{max} (log ε) 218 (3.66) nm; IR ν_{max} 3294, 2933, 1704, 1644, 1483, 1265, 1127, 1058, 966 cm^{-1}; ^1H and ^{13}C NMR data, Table 1; HRESIMS *m*/*z* 257.1748 $[M + H]^+$ (calcd for $C_{14}H_{25}O_4$, 257.1747).

*7-O-Methylnigrosporolide (**3**):* colorless oil; $[\alpha]^{20}_D$ +67 (*c* 0.2, MeOH); UV (MeOH) λ_{max} (log ε) 214 (3.54) nm; IR ν_{max} 3298, 2934, 1704, 1645, 1482, 1352, 1264, 1127, 1058, 1027 cm^{-1}; ^1H and ^{13}C NMR data, Table 1; HRESIMS *m*/*z* 289.1407 $[M + Na]^+$ (calcd for $C_{15}H_{22}NaO_4$, 289.1410).

*Pestalotioprolide D (**4**):* colorless oil; $[\alpha]^{20}_D$ −30 (*c* 0.1, MeOH); UV (MeOH) λ_{max} (log ε) 220 (3.45) nm; IR ν_{max} 3300, 2935, 1705, 1645, 1483, 1266, 1108, 1059, 966 cm^{-1}; ^1H and ^{13}C NMR data, Table 1; HRESIMS *m*/*z* 289.1408 $[M + Na]^+$ (calcd for $C_{15}H_{22}NaO_4$, 289.1410).

*Pestalotioprolide E (**5**):* colorless oil; $[\alpha]^{20}_D$ +222 (*c* 1.8, MeOH); ECD (MeCN) λ_{max} ($\Delta\varepsilon$) 295 (sh) (+0.86), 234 (+22.97), negative CE below 202 nm; UV (MeOH) λ_{max} (log ε) 214 (4.25), 230 (4.15) nm; IR ν_{max} 3379, 2939, 1696, 1642, 1453, 1265, 1081, 989 cm^{-1}; ^1H and ^{13}C NMR data, Table 2; HRESIMS *m*/*z* 270.1698 $[M + NH_4]^+$ (calcd for $C_{14}H_{24}NO_4$, 270.1700).

*Pestalotioprolide F (**6**):* colorless oil; $[\alpha]^{20}_D$ +9 (*c* 0.5, MeOH); ECD (MeCN) λ_{max} ($\Delta\varepsilon$) 351 (+0.09), 288 (−0.07), 233 (+1.31), 207 (−1.83) nm; UV (MeOH) λ_{max} (log ε) 211 (4.24), 229 (4.14) nm; IR ν_{max} 3380, 2934, 1703, 1650, 1451, 1259, 1108, 979 cm^{-1}; ^1H and ^{13}C NMR data, Table 2; HRESIMS *m*/*z* 270.1701 $[M + NH_4]^+$ (calcd for $C_{14}H_{24}NO_4$, 270.1700).

*Pestalotioprolide G (**7**):* colorless oil; $[\alpha]^{20}_D$ −177 (*c* 0.2, MeOH); UV (MeOH) λ_{max} (log ε) 265 (4.33) nm; IR ν_{max} 3420, 2938, 1714, 1584, 1451, 1360, 1254, 1110, 976 cm^{-1}; ^1H and ^{13}C NMR data, Table 2; HRESIMS *m*/*z* 253.1436 $[M + H]^+$ (calcd for $C_{14}H_{21}O_4$, 253.1434).

*Pestalotioprolide H (**8**):* colorless oil; $[\alpha]^{20}_D$ −38 (*c* 0.2, MeOH); UV (MeOH) λ_{max} (log ε) 264 (4.34) nm; ^1H and ^{13}C NMR data, Table 2; HRESIMS *m*/*z* 267.1586 $[M + H]^+$ (calcd for $C_{15}H_{23}O_4$, 267.1591).

*Seiricuprolide (**9**):* white powder; $[\alpha]^{20}_D$ +40 (*c* 2.7, MeOH), lit.[3] $[\alpha]^{25}_D$ +67 (*c* 1.5, MeOH).

*Nigrosporolide (**10**):* colorless crystals; mp 142−145 °C; $[\alpha]^{20}_D$ +81 (*c* 0.9, MeOH).

*4,7-Dihydroxy-13-tetradeca-2,5,8-trienolide (**11**):* white powder; $[\alpha]^{20}_D$ +174 (*c* 0.4, $CHCl_3$), lit.[15] $[\alpha]^{28}_D$ +188 (*c* 0.7, $CHCl_3$).

X-ray Crystallographic Analysis of 1, 2, and 10. *Crystallization Conditions.* X-ray quality crystals of **1**, **2**, and **10** were obtained by slow evaporation from an acetone solution. A suitable single crystal was carefully selected under a polarizing microscope. Data collection: Bruker Kappa APEX2 CCD diffractometer with a microfocus tube, Cu Kα radiation (λ = 1.541 78 Å) for **1**, **2**, and the first data set of **10** or Mo Kα radiation (λ = 0.710 73 Å) for the second data set of **10**, multilayer mirror, ω- and ϕ-scan; data collection with APEX2, cell refinement and data reduction with SAINT,[19] experimental absorption correction with SADABS.[20] Structure analysis and refinement: The structure was solved by direct methods using SHELXS-97; refinement was done by full-matrix least-squares on F^2 using the SHELXL-97 program suite.[21] All non-hydrogen positions were refined with anisotropic displacement parameters. Hydrogen atoms were positioned geometrically (with C−H = 0.95 Å for aromatic CH, 1.00 Å for tertiary CH, 0.99 Å for CH_2, and 0.98 Å for CH_3) and refined using riding models (AFIX 43, 13, 23, and 137, respectively), with $U_{iso}(H) = 1.2U_{eq}(CH, CH_2)$ and $1.5U_{eq}(CH_3)$. The hydrogen atoms in the hydroxy groups were positioned geometrically with AFIX 148 in **1** and were found and refined with $U_{iso}(H) = 1.5U_{eq}(O)$ in **2** and **10**. Hydrogen atoms in the solvent water molecule in **1** were found and refined with $U_{iso}(H) = 1.5U_{eq}(O)$.

During refinement of the data set for compound **2**, SHELX reported warnings regarding the Flack parameter. The Flack parameter calculated by classical fit to all intensities gave a value of −0.0(9), and the Flack parameter calculated by Parsons' method gave 0.25(15) together with the message "Friedel differences statistically dubious - Flack x unreliable". The refinement as a two-component inversion twin using the TWIN/BASF instructions in SHELXL led to a Flack parameter of 0.00, a negative BASF, and continuing errors. Therefore, the analysis of the absolute configuration was performed using likelihood methods[22] with the command "ByvoetPair" in PLATON for Windows.[23] The resulting value for the Hooft parameter was given as 0.17(12), which indicated that the absolute configuration was probably determined correctly. The method calculated the probability that the absolute configuration of the model was correct as 1.00 P2(true).[22]

For compound **10** the Mo Kα data set was collected for the bond length and angle information, while the Cu Kα data set was crucial for the absolute configuration.

Graphics were drawn with DIAMOND,[24] and analyses of the inter- and intramolecular hydrogen-bonding interactions were done with PLATON for Windows.[23] The structural data have been deposited in the Cambridge Crystallographic Data Center (CCDC Nos. 1479850 for **1**, 1479851 for **2**, 1479852 and 1479853 for **10**).

*Crystal data of **1**:* $C_{14}H_{22}O_6$, *M* = 286.31, triclinic system, space group *P*1, *a* = 6.3082(4) Å, *b* = 7.5108(5) Å, *c* = 8.1100(5) Å, *V* = 374.29(4) Å^3, *Z* = 1, D_{calc} = 1.270 g/cm^3, crystal size 0.11 × 0.09 × 0.05 mm^3, μ(Cu Kα) = 0.827 mm^{-1}, 5.5° < θ < 65.3°, N_t = 3068, *N* = 1630 (R_{int} = 0.0449), R_1 = 0.0342, wR_2 = 0.0878, *S* = 1.026, Flack parameter[25] = −0.03(19).

*Crystal data of **2**:* $C_{14}H_{24}O_4$, *M* = 256.33, orthorhombic system, space group $P2_12_12_1$, *a* = 36.533(4) Å, *b* = 4.9693(6) Å, *c* = 7.6479(9) Å, *V* = 1388.4(3) Å^3, *Z* = 4, D_{calc} = 1.226 g/cm^3, crystal size 0.30 × 0.08 × 0.04 mm^3, μ(Cu Kα) = 0.717 mm^{-1}, 2.4° < θ < 71.9°, N_t = 17343, *N* = 2418 (R_{int} = 0.0668), R_1 = 0.0867, wR_2 = 0.2408, *S* = 1.161, Hooft parameter = 0.17(12).

*Crystal data of **10** (Cu Kα):* $C_{14}H_{20}O_4$, *M* = 252.30, orthorhombic system, space group $P2_12_12_1$, *a* = 4.8106(3) Å, *b* = 7.6079(5) Å, *c* = 37.246(2) Å, *V* = 1363.13(15) Å^3, *Z* = 4, D_{calc} = 1.229 g/cm^3, crystal size 0.80 × 0.10 × 0.02 mm^3, μ(Cu Kα) = 0.730 mm^{-1}, 2.4° < θ < 44.5°, N_t = 4063, *N* = 928 (R_{int} = 0.0541), R_1 = 0.0287, wR_2 = 0.0687, *S* = 1.159, Flack parameter = 0.14(8).

*Crystal data of **10** (Mo Kα):* $C_{14}H_{20}O_4$, *M* = 252.30, orthorhombic system, space group $P2_12_12_1$, *a* = 4.8042(3) Å, *b* = 7.6036(4) Å, *c* = 37.247(2) Å, *V* = 1360.59(13) Å^3, *Z* = 4, D_{calc} = 1.232 g/cm^3, crystal size 0.80 × 0.10 × 0.02 mm^3, μ(Mo Kα) = 0.089 mm^{-1}, 2.2° < θ < 26.5°, N_t = 21569, *N* = 2786 (R_{int} = 0.0294), R_1 = 0.0316, wR_2 = 0.0797, *S* = 1.088.

Preparation of (*S*)- and (*R*)-MTPA Esters 5a and 5b. Compound **5** (0.8 mg) was treated with (*R*)-MTPACl (8 μL) and DMAP (0.1 mg) in 0.5 mL of pyridine. The mixture was stirred at room temperature for 12 h. The crude product was purified by semipreparative HPLC (MeOH−H_2O: 0−5 min, 60%; 5−15 min,

DOI: 10.1021/acs.jnatprod.6b00473
J. Nat. Prod. 2016, 79, 2332−2340

from 60% to 90%; 16−19 min, 100%), to yield (*S*)-MTPA ester **5a** (1.6 mg). In a similar way, (*R*)-MTPA ester **5b** (1.6 mg) was prepared after compound **5** reacted with (*S*)-MTPACl.

*(S)-MTPA ester **5a**:* ^{1}H NMR (CD_3OD, 600 MHz) δ 7.62−7.41 (10H, m, phenyl protons), 6.70 (1H, dd, J = 15.8, 10.1 Hz, H-7), 6.40 (1H, dd, J = 10.7, 10.1 Hz, H-6), 5.90 (1H, d, J = 10.7 Hz, H-5), 5.72 (1H, dd, J = 15.8, 5.3 Hz, H-8), 5.69 (1H, m, H-9), 5.49 (1H, dd, J = 10.1, 5.7 Hz, H-3), 5.03 (1H, m, H-13), 3.63 (3H, s, OMe of MTPA), 3.55 (3H, s, OMe of MTPA), 2.99 (1H, dd, J = 15.1, 5.7 Hz, H-2a), 2.90 (1H, dd, J = 15.1, 10.1 Hz, H-2b), 1.92 (1H, m, H-10a), 1.82 (1H, m, H-10b), 1.76 (1H, m, H-12a), 1.64 (1H, m, H-12b), 1.57 (2H, m, H_2-11), 1.24 (3H, d, J = 6.4 Hz, H_3-14); HRESIMS m/z 702.2501 $[M + NH_4]^+$ (calcd for $C_{34}H_{38}F_6NO_8$, 702.2496).

*(R)-MTPA ester **5b**:* ^{1}H NMR (CD_3OD, 600 MHz) δ 7.58−7.43 (10H, m, phenyl protons), 6.75 (1H, dd, J = 16.2, 10.2 Hz, H-7), 6.45 (1H, dd, J = 10.7, 10.2 Hz, H-6), 5.87 (1H, dd, J = 16.2, 5.1 Hz, H-8), 5.86 (1H, d, J = 10.7 Hz, H-5), 5.71 (1H, m, H-9), 5.50 (1H, dd, J = 9.8, 6.1 Hz, H-3), 4.99 (1H, m, H-13), 3.61 (3H, s, OMe of MTPA), 3.57 (3H, s, OMe of MTPA), 3.04 (1H, dd, J = 15.0, 6.1 Hz, H-2a), 2.97 (1H, dd, J = 15.0, 9.8 Hz, H-2b), 1.82 (1H, m, H-10a), 1.73 (1H, m, H-10b), 1.66 (1H, m, H-12a), 1.56 (1H, m, H-12b), 1.51 (1H, m, H-11a), 1.38 (1H, m, H-11b), 1.21 (3H, d, J = 6.3 Hz, H_3-14); HRESIMS m/z 702.2496 $[M + NH_4]^+$ (calcd for $C_{34}H_{38}F_6NO_8$, 702.2496).

Cocultivation Experiment of *P. microspora* with *S. lividans*. *P. microspora* and *S. lividans* were cocultured in 15 1-L Erlenmeyer flasks (three for axenic *P. microspora*, three for axenic *S. lividans*, three for coculture of *P. microspora* and 0.05 g of *S. lividans*, three for coculture of *P. microspora* and 0.1 g of *S. lividans*, three for coculture of *P. microspora* and 0.2 g of *S. lividans*) containing 60 mL of yeast malt (YM) medium and 50 g of commercially available rice each. An overnight culture of *S. lividans* was inoculated to prewarmed YM medium, which was then incubated at 37 °C and shaken at 200 rpm for 15 h. The resulting *S. lividans* balls were separated from the broth after centrifugation at 6000 rpm for 5 min. After weighing, 1.4 g of *S. lividans* balls was suspended with 7 mL of fresh YM medium and then added to the coculture flasks (0.05, 0.1, or 0.2 g/flask), which were further incubated at 30 °C for 7 days. After this preincubation, *P. microspora* grown on malt agar was added under sterile conditions. Then all flasks were kept at 20 °C under static conditions until they reached the stationary growth phase (3 weeks for control of *P. microspora* and *S. lividans*, 5 weeks for coculture). The fermentation was stopped by adding 500 mL of EtOAc to each flask. After evaporation, the dry extract was dissolved in 20 mL of MeOH, and 25 μL of this solution was injected for HPLC analysis.

Cytotoxicity Assay. Cytotoxicity against the mouse lymphoma cell line L5178Y and the human ovarian cancer cell line A2780 was evaluated using the MTT method with kahalalide F (for L5178Y) or cisplatin (for A2780) as positive control and media with 0.1% DMSO as negative control as described previously.[26,27]

Computational Section. Mixed torsional/low-frequency mode conformational searches were carried out by means of the Macromodel 9.9.223 software using the Merck Molecular Force Field (MMFF) with an implicit solvent model for $CHCl_3$.[28] Geometry reoptimizations were carried out at the B3LYP/6-31G(d) level in vacuo and at the B97D/TZVP[29,30] and CAM-B3LYP/TZVP[31,32] levels with the PCM solvent model for MeCN. TDDFT-ECD calculations were run with various functionals (B3LYP, BH&HLYP, CAM-B3LYP, PBE0) and the TZVP basis set as implemented in the Gaussian 09 package with the same or no solvent model as in the preceding DFT optimization step.[33] ECD spectra were generated as sums of Gaussians with 3000 and 4200 cm^{-1} widths at half-height (corresponding to ca. 16 and 22 at 230 nm, respectively), using dipole-velocity-computed rotational strength values.[34] Boltzmann distributions were estimated from the ZPVE-corrected B3LYP/6-31G(d) energies in the gas-phase calculations and from the B97D/TZVP and CAM-B3LYP/TZVP energies in the solvated ones. The MOLEKEL software package was used for visualization of the results.[35]

■ ASSOCIATED CONTENT

Supporting Information

The Supporting Information is available free of charge on the ACS Publications website at DOI: 10.1021/acs.jnatprod.6b00473.

UV, HRESIMS, and NMR spectra of compounds **1**−**8** and MTPA esters **5a** and **5b**, and structure and population of the low-energy conformers (>1%) of compounds **5** and **6** as well as results of X-ray analysis of compounds **1**, **2**, and **10** (PDF)

Crystallographic data (CIF)

Crystallographic data (CIF)

Crystallographic data (CIF)

■ AUTHOR INFORMATION

Corresponding Authors

*Tel: +49 211 81 15979. Fax: +49 211 81 11923. E-mail: zhenfeizi0@sina.com (Z. Liu).

*Tel: +49 211 81 14163. Fax: +49 211 81 11923. E-mail: proksch@uni-duesseldorf.de (P. Proksch).

Notes

The authors declare no competing financial interest.

■ ACKNOWLEDGMENTS

S.L. thanks the China Scholarship Council for financial support. P.P. wishes to thank the Manchot Foundation and the DFG (GRK 2158) for support. T.K. and A.M. thank the Hungarian National Research Foundation (OTKA K105871) for financial support and the National Information Infrastructure Development Institute (NIIFI 10038) for CPU time. We furthermore wish to thank S. H. Akone (Institute of Pharmaceutical Biology and Biotechnology, Heinrich-Heine-Universität Düsseldorf, Germany) for collection of the plant material.

■ REFERENCES

(1) McGuire, J. M.; Bunch, R. L.; Anderson, R. C.; Boaz, H. E.; Flynn, E. H.; Powell, H. M.; Smith, J. W. *Antibiot. Chemother.* **1952**, *2*, 281−283.

(2) Harvey, R. J.; Wallwork, B. D.; Lund, V. J. *Immunol. Allergy Clin. North Am.* **2009**, *29*, 689−703.

(3) Ballio, A.; Evidente, A.; Graniti, A.; Randazzo, G.; Sparapano, L. *Phytochemistry* **1988**, *27*, 3117−3121.

(4) Zinedine, A.; Soriano, J. M.; Moltó, J. C.; Mañes, J. *Food Chem. Toxicol.* **2007**, *45*, 1−18.

(5) Kito, K.; Ookura, R.; Yoshida, S.; Namikoshi, M.; Ooi, T.; Kusumi, T. *Org. Lett.* **2008**, *10*, 225−228.

(6) Xu, J.; Kjer, J.; Sendker, J.; Wray, V.; Guan, H.; Edrada, R.; Lin, W.; Wu, J.; Proksch, P. *J. Nat. Prod.* **2009**, *72*, 662−665.

(7) Bara, R.; Zerfass, I.; Aly, A. H.; Goldbach-Gecke, H.; Raghavan, V.; Sass, P.; Mándi, A.; Wray, V.; Polavarapu, P. L.; Pretsch, A.; Lin, W.; Kurtán, T.; Debbab, A.; Brötz-Oesterhelt, H.; Proksch, P. *J. Med. Chem.* **2013**, *56*, 3257−3272.

(8) El Amrani, M.; Lai, D.; Debbab, A.; Aly, A. H.; Siems, K.; Seidel, C.; Schnekenburger, M.; Gaigneaux, A.; Diederich, M.; Feger, D.; Lin, W.; Proksch, P. *J. Nat. Prod.* **2014**, *77*, 49−56.

(9) Liu, S.; Dai, H.; Orfali, R. S.; Lin, W.; Liu, Z.; Proksch, P. *J. Agric. Food Chem.* **2016**, *64*, 3127−3132.

(10) Ola, A. R. B.; Thomy, D.; Lai, D.; Brötz-Oesterhelt, H.; Proksch, P. *J. Nat. Prod.* **2013**, *76*, 2094−2099.

(11) Chen, H.; Daletos, G.; Abdel-Aziz, M. S.; Thomy, D.; Dai, H.; Brötz-Oesterhelt, H.; Lin, W.; Proksch, P. *Phytochem. Lett.* **2015**, *12*, 35−41.

(12) Rukachaisirikul, V.; Rodglin, A.; Phongpaichit, S.; Buatong, J.; Sakayaroj, J. *Phytochem. Lett.* **2012**, *5*, 13−17.

DOI: 10.1021/acs.jnatprod.6b00473
J. Nat. Prod. 2016, 79, 2332−2340

(13) Harwooda, J. S.; Cutler, H. G.; Jacyno, J. M. *Nat. Prod. Lett.* **1995**, *6*, 181−185.
(14) Jiao, P.; Swenson, D. C.; Gloer, J. B.; Wicklow, D. T. *J. Nat. Prod.* **2006**, *69*, 636−639.
(15) Kobayashi, H.; Kanematsu, M.; Yoshida, M.; Shishido, K. *Chem. Commun.* **2011**, *47*, 7440−7442.
(16) Khamthong, N.; Rukachaisirikul, V.; Phongpaichit, S.; Preedanon, S.; Sakayroj, J. *Phytochem. Lett.* **2014**, *10*, 5−9.
(17) Debbab, A.; Aly, A. H.; Edrada-Ebel, R.; Wray, V.; Müller, W. E. G.; Totzke, F.; Zirrgiebel, U.; Schächtele, C.; Kubbutat, M. H. G.; Lin, W. H.; Mosaddak, M.; Hakiki, A.; Proksch, P.; Ebel, R. *J. Nat. Prod.* **2009**, *72*, 626−631.
(18) Kjer, J.; Debbab, A.; Aly, A. H.; Proksch, P. *Nat. Protoc.* **2010**, *5*, 479−490.
(19) *Apex2, Data Collection Program for the CCD Area-Detector System*; *SAINT, Data Reduction and Frame Integration Program for the CCD Area-Detector System*; Bruker Analytical X-ray Systems: Madison, WI, USA, 1997−2006.
(20) Sheldrick, G. M. *SADABS: Area-detector absorption correction*; University of Göttingen: Germany, 1996.
(21) Sheldrick, G. M. *Acta Crystallogr., Sect. A: Found. Crystallogr.* **2008**, *64*, 112−122.
(22) (a) Hooft, R. W. W.; Straver, L. H.; Spek, A. L. *J. Appl. Crystallogr.* **2008**, *41*, 96−103. (b) Hooft, R. W. W.; Straver, L. H.; Spek, A. L. *Acta Crystallogr., Sect. A: Found. Crystallogr.* **2009**, *65*, 319−321. (c) Hooft, R. W. W.; Straver, L. H.; Spek, A. L. *J. Appl. Crystallogr.* **2010**, *43*, 665−668.
(23) (a) Spek, A. L. *Acta Crystallogr., Sect. D: Biol. Crystallogr.* **2009**, *65*, 148−155. (b) Spek, A. L. *J. Appl. Crystallogr.* **2003**, *36*, 7−13. (c) Spek, A. L. *PLATON - A Multipurpose Crystallographic Tool*; Utrecht University: Utrecht, The Netherlands, 2008. (d) Farrugia, L. J. *Windows implementation*, Version 40608; University of Glasgow: Scotland, 2008.
(24) Brandenburg, K. *Diamond (Version 3.2), Crystal and Molecular Structure Visualization, Crystal Impact − K*; Brandenburg & H. Putz Gbr: Bonn, Germany, 2009.
(25) (a) Flack, H. D.; Sadki, M.; Thompson, A. L.; Watkin, D. J. *Acta Crystallogr., Sect. A: Found. Crystallogr.* **2011**, *67*, 21−34. (b) Flack, H. D.; Bernardinelli, G. *Chirality* **2008**, *20*, 681−690. (c) Flack, H. D.; Bernardinelli, G. *Acta Crystallogr., Sect. A: Found. Crystallogr.* **1999**, *55*, 908−915. (d) Flack, H. *Acta Crystallogr., Sect. A: Found. Crystallogr.* **1983**, *39*, 876−881.
(26) Ashour, M.; Edrada, R.; Ebel, R.; Wray, V.; Wätjen, W.; Padmakumar, K.; Müller, W. E. G.; Lin, W. H.; Proksch, P. *J. Nat. Prod.* **2006**, *69*, 1547−1553.
(27) Rönsberg, D.; Debbab, A.; Mandi, A.; Vasylyeva, V.; Böhler, P.; Stork, B.; Engelke, L.; Hamacher, A.; Sawadogo, R.; Diederich, M.; Wray, V.; Lin, W.; Kassack, M. U.; Janiak, C.; Scheu, S.; Wesselborg, S.; Kurtan, T.; Aly, A. H.; Proksch, P. *J. Org. Chem.* **2013**, *78*, 12409−12425.
(28) *MacroModel*; Schrödinger, LLC, 2012, http://www.schrodinger.com/MacroModel.
(29) Sun, P.; Xu, D. X.; Mándi, A.; Kurtán, T.; Li, T. J.; Schulz, B.; Zhang, W. *J. Org. Chem.* **2013**, *78*, 7030−7047.
(30) Grimme, S. *J. Comput. Chem.* **2006**, *27*, 1787−1799.
(31) Yanai, T.; Tew, D.; Handy, N. *Chem. Phys. Lett.* **2004**, *393*, 51−57.
(32) Pescitelli, G.; Di Bari, L.; Berova, N. *Chem. Soc. Rev.* **2011**, *40*, 4603−4625.
(33) Frisch, M. J.; Trucks, G. W.; Schlegel, H. B.; Scuseria, G. E.; Robb, M. A.; Cheeseman, J. R.; Scalmani, G.; Barone, V.; Mennucci, B.; Petersson, G. A.; Nakatsuji, H.; Caricato, M.; Li, X.; Hratchian, H. P.; Izmaylov, A. F.; Bloino, J.; Zheng, G.; Sonnenberg, J. L.; Hada, M.; Ehara, M.; Toyota, K.; Fukuda, R.; Hasegawa, J.; Ishida, M.; Nakajima, T.; Honda, Y.; Kitao, O.; Nakai, H.; Vreven, T.; Montgomery, J. A., Jr.; Peralta, J. E.; Ogliaro, F.; Bearpark, M.; Heyd, J. J.; Brothers, E.; Kudin, K. N.; Staroverov, V. N.; Kobayashi, R.; Normand, J.; Raghavachari, K.; Rendell, A.; Burant, J. C.; Iyengar, S. S.; Tomasi, J.; Cossi, M.; Rega, N.; Millam, J. M.; Klene, M.; Knox, J. E.; Cross, J. B.; Bakken, V.; Adamo, C.; Jaramillo, J.; Gomperts, R.; Stratmann, R. E.; Yazyev, O.; Austin, A. J.; Cammi, R.; Pomelli, C.; Ochterski, J. W.; Martin, R. L.; Morokuma, K.; Zakrzewski, V. G.; Voth, G. A.; Salvador, P.; Dannenberg, J. J.; Dapprich, S.; Daniels, A. D.; Farkas, O.; Foresman, J. B.; Ortiz, J. V.; Cioslowski, J.; Fox, D. J. *Gaussian 09*, revision B.01; Gaussian, Inc.: Wallingford, CT, 2010.
(34) Stephens, P. J.; Harada, N. *Chirality* **2010**, *22*, 229−233.
(35) Varetto, U. *MOLEKEL*, v. 5.4; Swiss National Supercomputing Centre: Manno, Switzerland, 2009.

DOI: 10.1021/acs.jnatprod.6b00473
J. Nat. Prod. 2016, 79, 2332−2340

Supporting Information

Cytotoxic 14-Membered Macrolides from a Mangrove-Derived Endophytic Fungus, *Pestalotiopsis microspora*

Shuai Liu,[†] Haofu Dai,[‡] Gamall Makhloufi,[§] Christian Heering,[§] Christoph Janiak,[§] Rudolf Hartmann,[⊥] Attila Mándi,[#] Tibor Kurtán,[#] Werner E.G. Müller,[∥] Matthias U. Kassack,[○] Wenhan Lin,[△] Zhen Liu,[*,†] Peter Proksch[*,†]

[†]Institute of Pharmaceutical Biology and Biotechnology, Heinrich-Heine-Universität Düsseldorf, Universitätsstrasse 1, 40225 Düsseldorf, Germany

[‡]Key Laboratory of Biology and Genetic Resources of Tropical Crops, Ministry of Agriculture, Institute of Tropical Bioscience and Biotechnology, Chinese Academy of Tropical Agricultural Sciences, Haikou 571101, China

[§]Institute of Inorganic and Structural Chemistry, Heinrich-Heine-Universität Düsseldorf, Universitätsstrasse 1, 40225 Düsseldorf, Germany

[⊥]Institute of Complex Systems: Strukturbiochemie, Forschungszentrum Juelich, Wilhelm-Johnen-Straße, 52428 Juelich, Germany

[#]Department of Organic Chemistry, University of Debrecen, P.O. Box 400, H-4002 Debrecen, Hungary

[∥]Institute of Physiological Chemistry, Universitätsmedizin der Johannes Gutenberg-Universität Mainz, Duesbergweg 6, 55128 Mainz, Germany

[○]Institute of Pharmaceutical and Medicinal Chemistry, Heinrich-Heine-Universität Düsseldorf, Universitätsstrasse 1, 40225 Düsseldorf, Germany

[△]State Key Laboratory of Natural and Biomimetic Drugs, Peking University, Beijing 100191, China

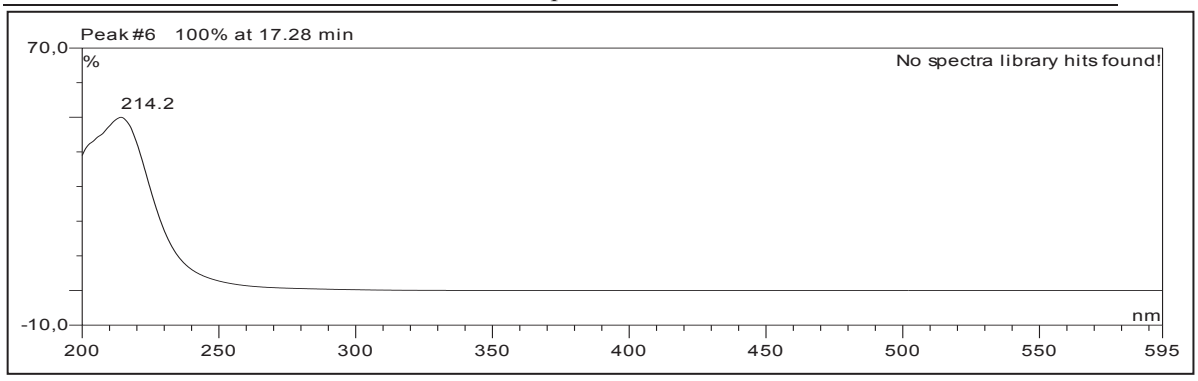

S1. UV spectrum of compound **1**.

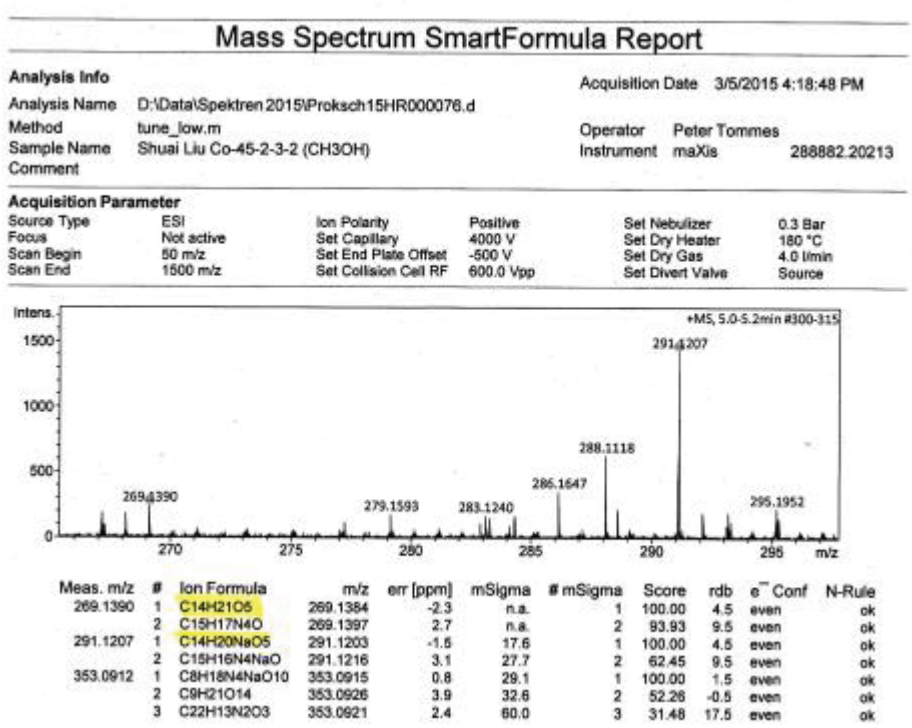

S2. HRESIMS spectrum of compound **1.**

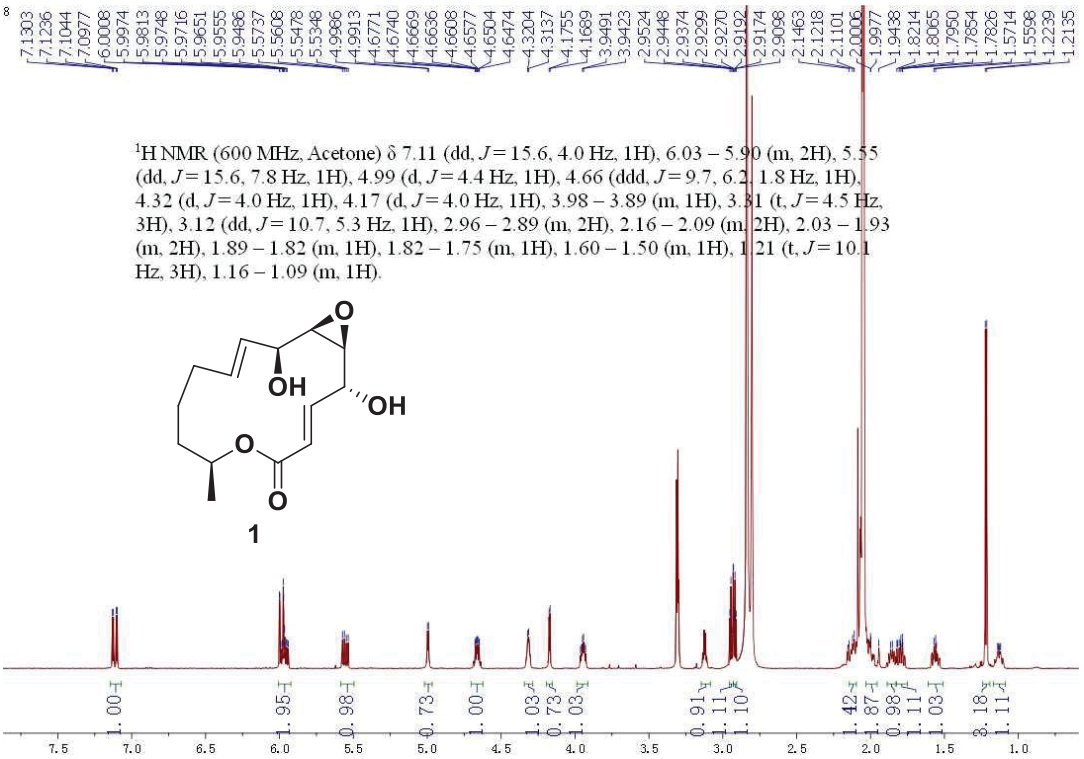

S3. ^{1}H NMR (600 MHz, acetone-d_6) spectrum of compound **1**.

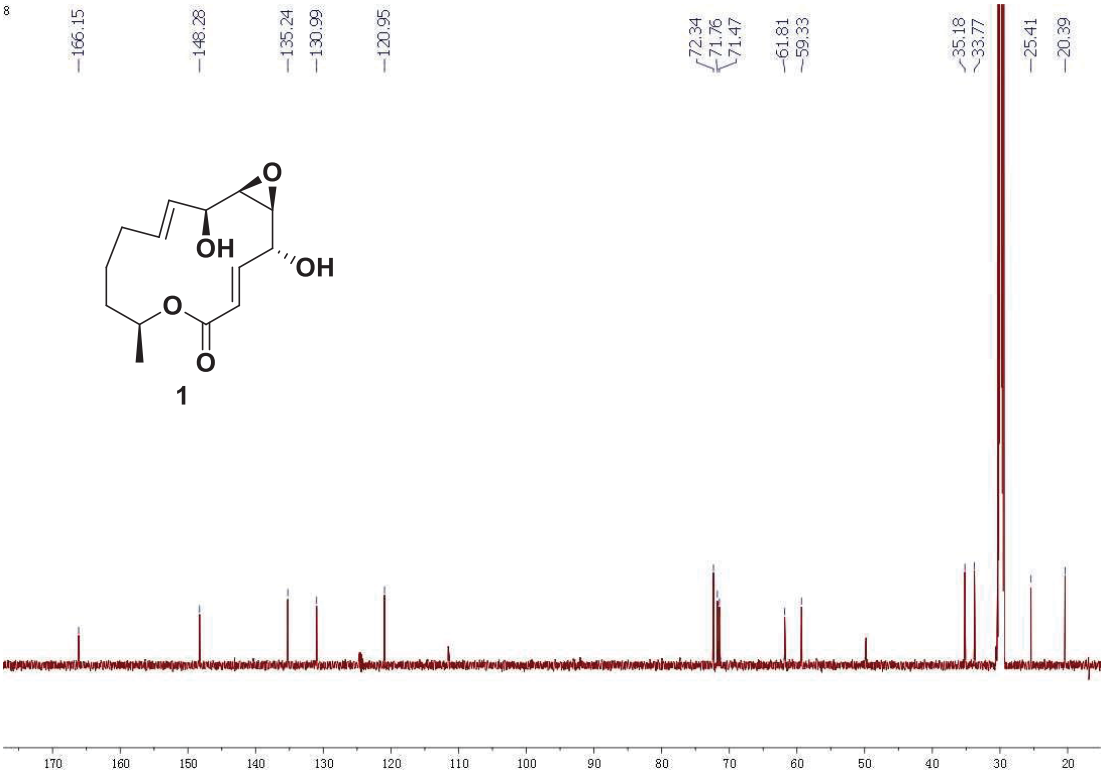

S4. ^{13}C NMR (150 MHz, acetone-d_6) spectrum of compound **1**.

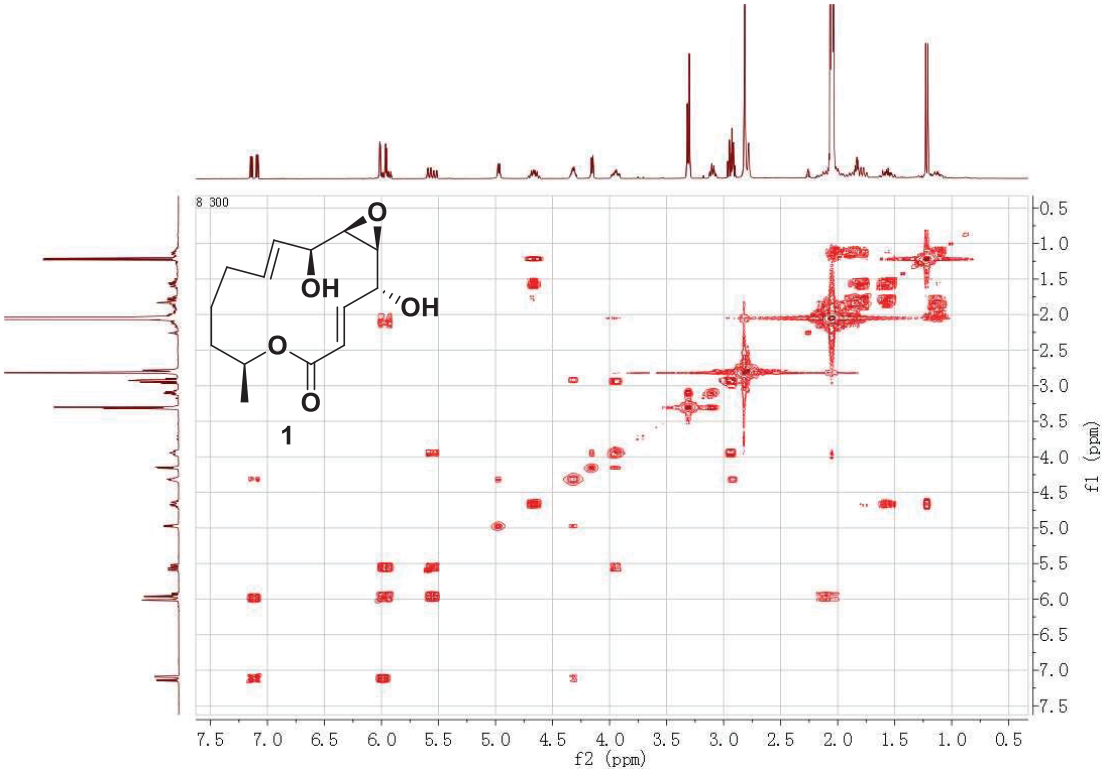

S5. ^{1}H-^{1}H COSY (300 MHz, acetone-d_6) spectrum of compound **1**.

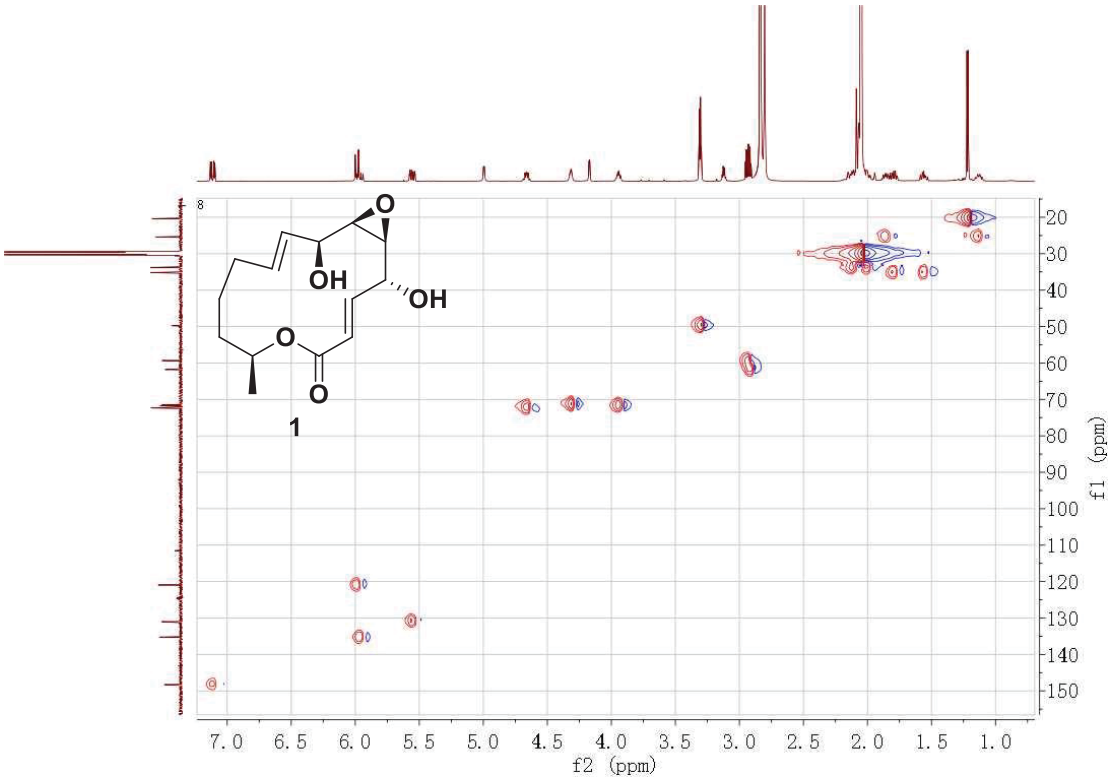

S6. HSQC (600 and 150 MHz, acetone-d_6) spectrum of compound **1**.

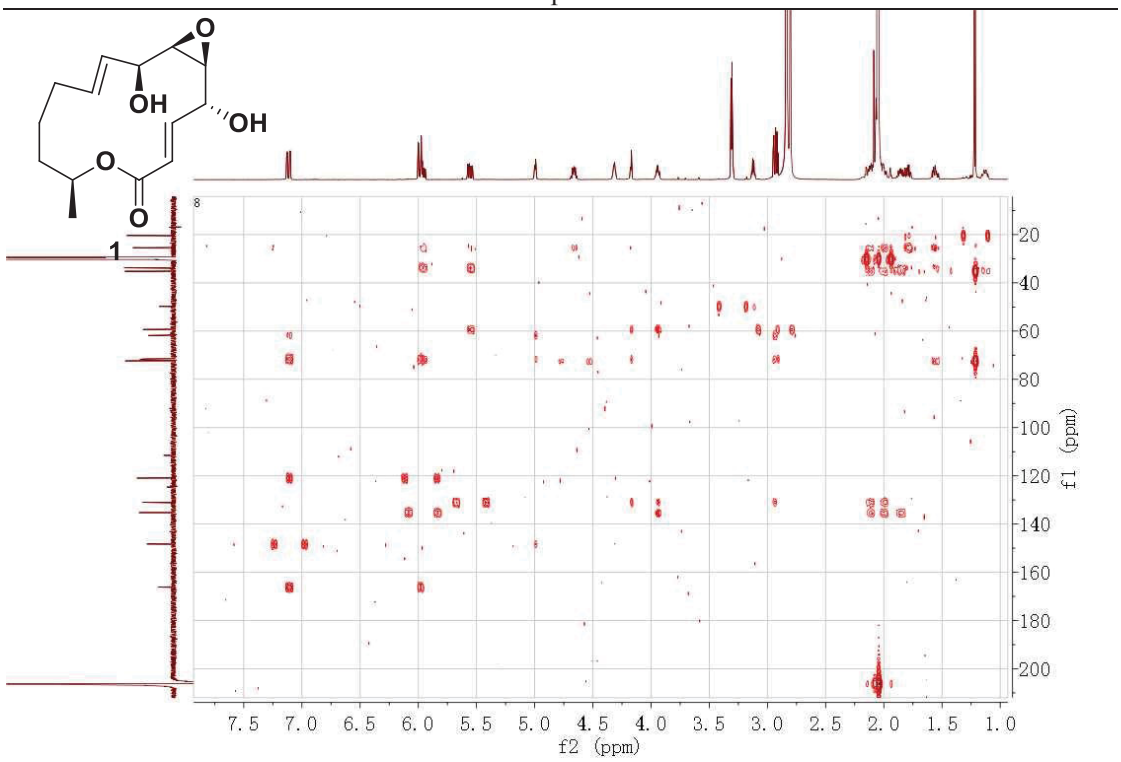

S7. HMBC (600 and 150 MHz, acetone-d_6) spectrum of compound **1**.

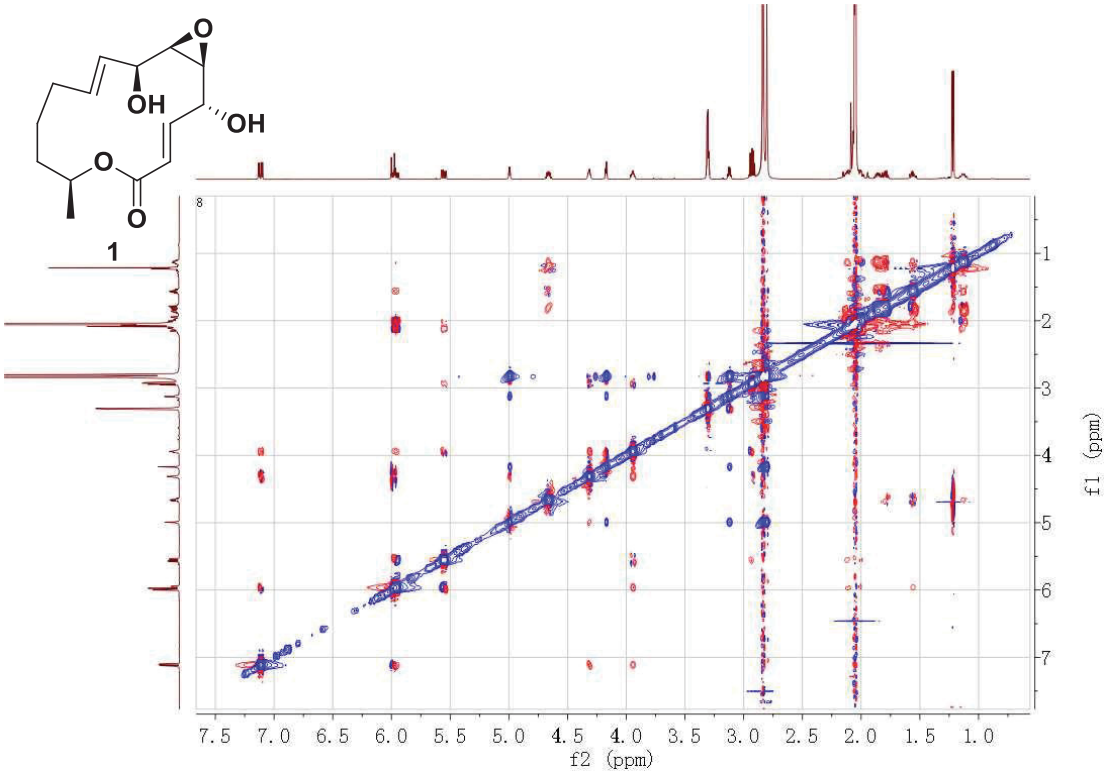

S8. ROESY (600 MHz, acetone-d_6) spectrum of compound **1**.

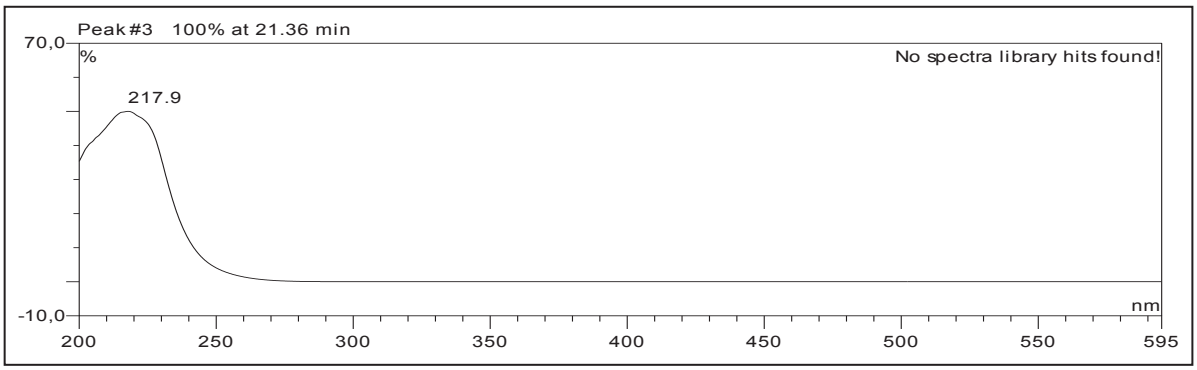

S9. UV spectrum of compound **2**.

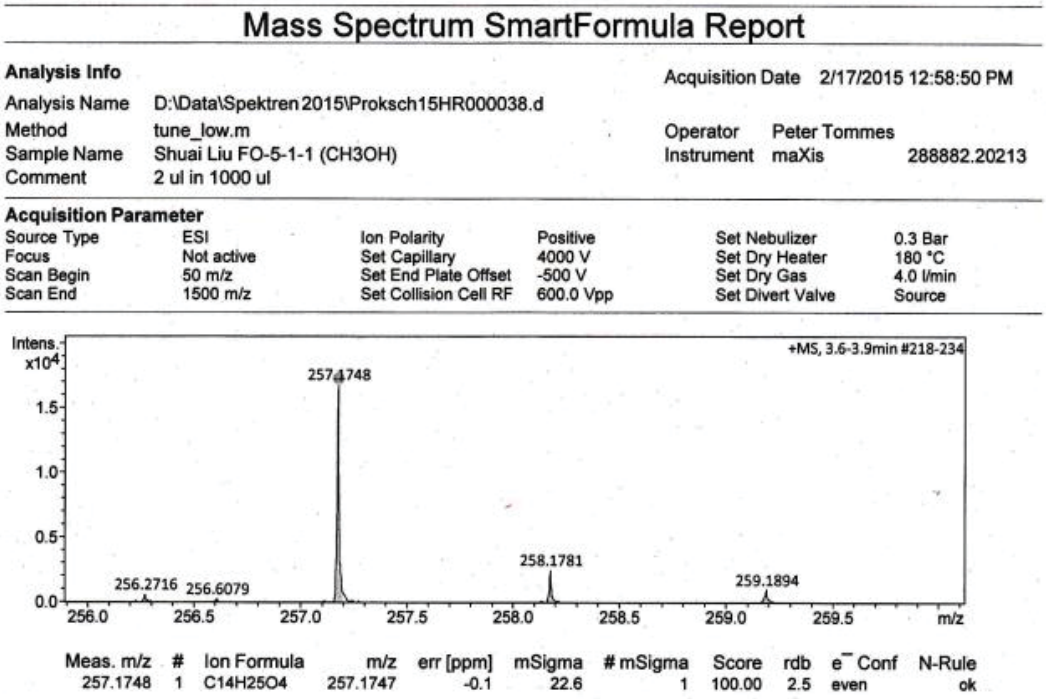

S10. HRESIMS spectrum of compound **2.**

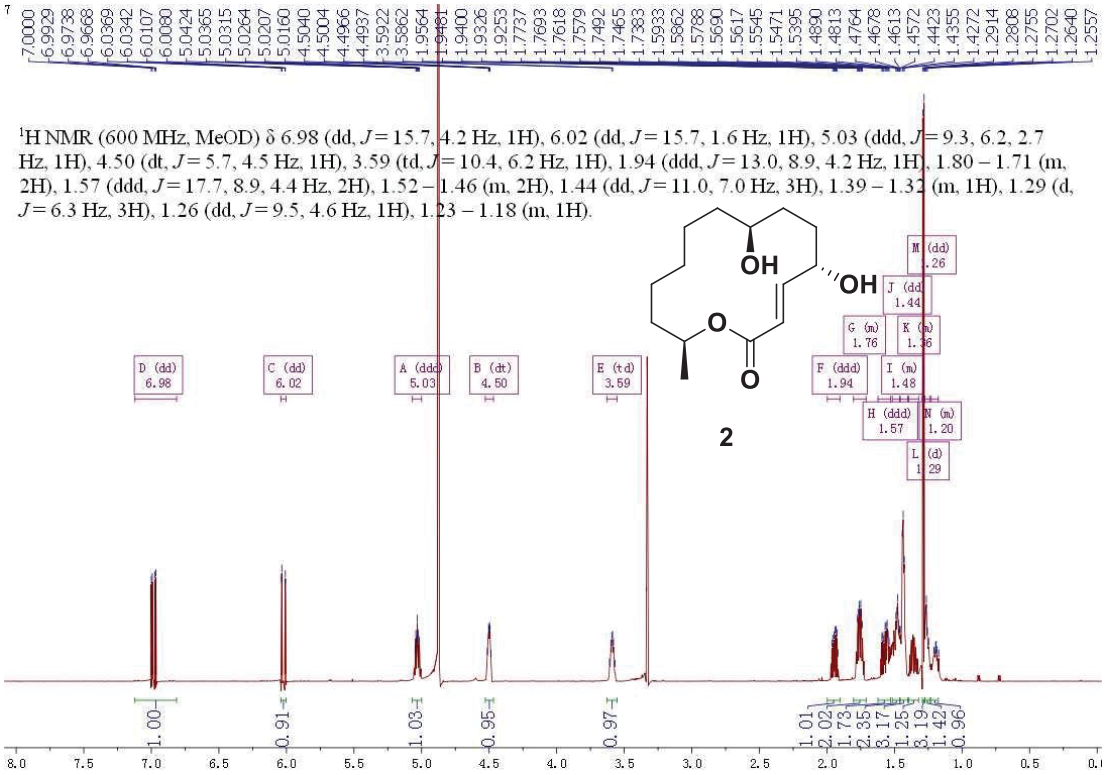

S11. ^{1}H NMR (600 MHz, CD_3OD) spectrum of compound **2**.

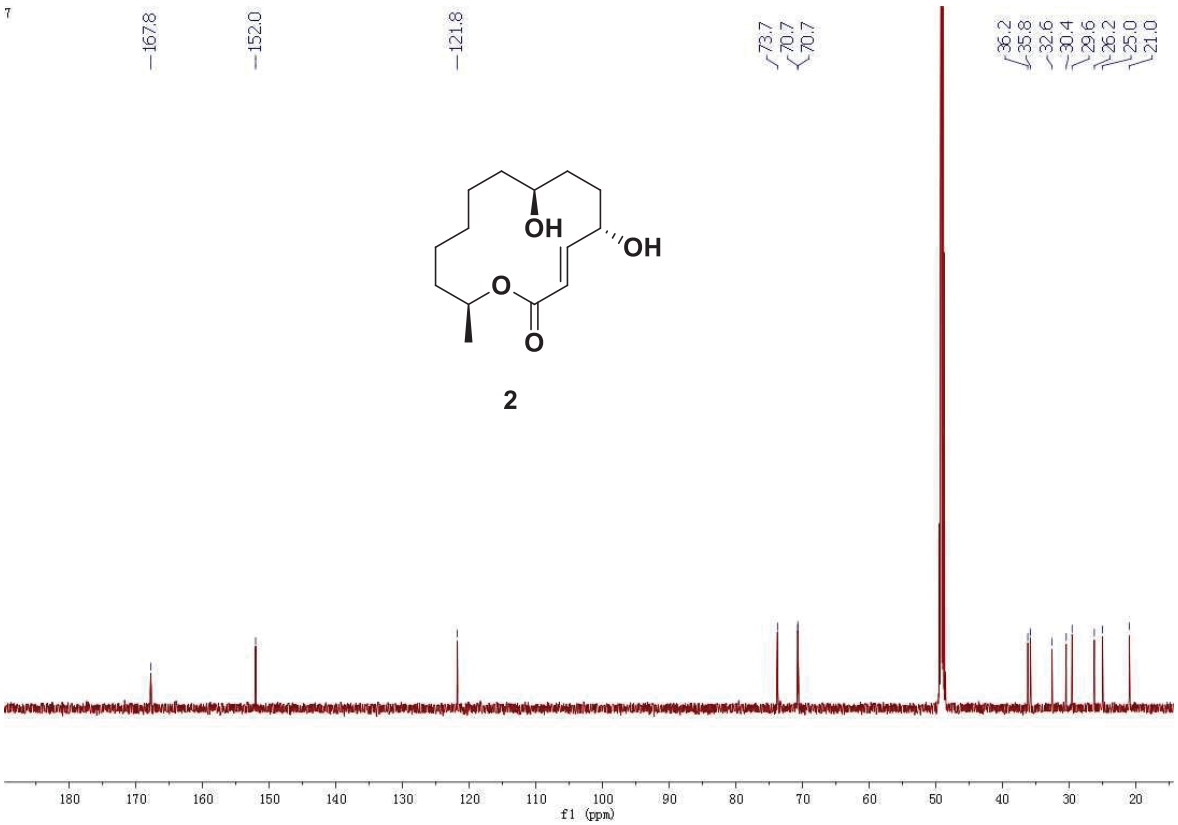

S12. ^{13}C NMR (150 MHz, CD_3OD) spectrum of compound **2**.

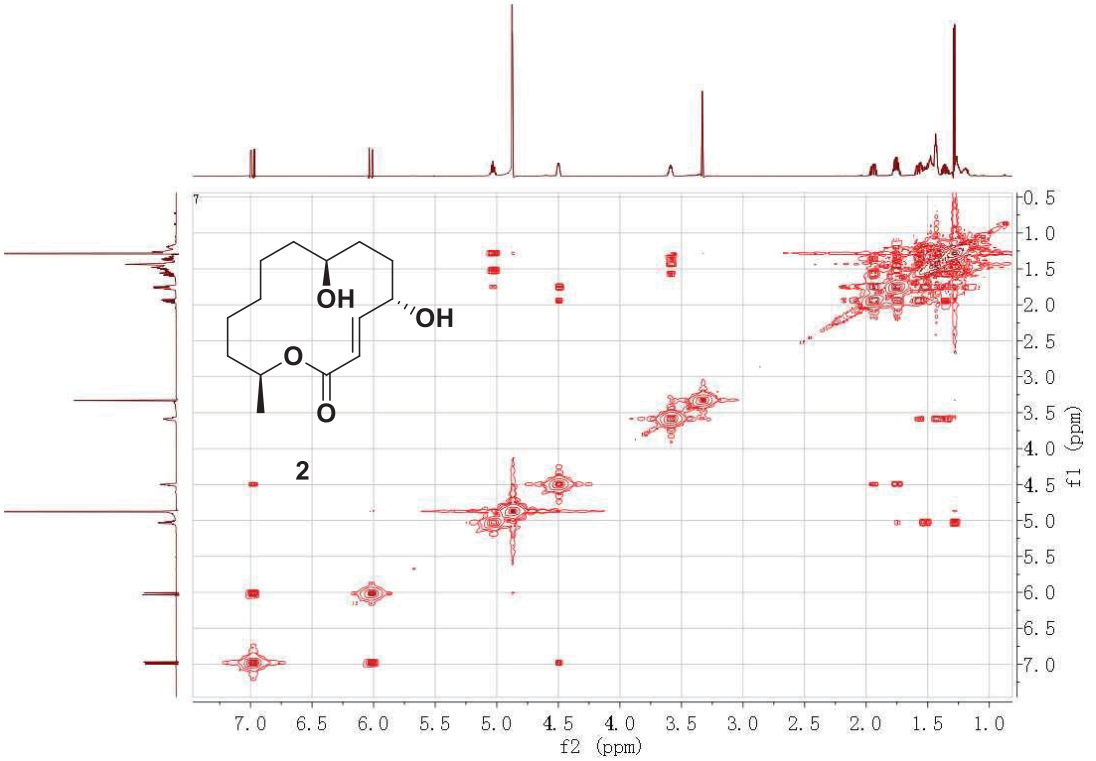

S13. ^{1}H-^{1}H COSY (600 MHz, CD_3OD) spectrum of compound **2**.

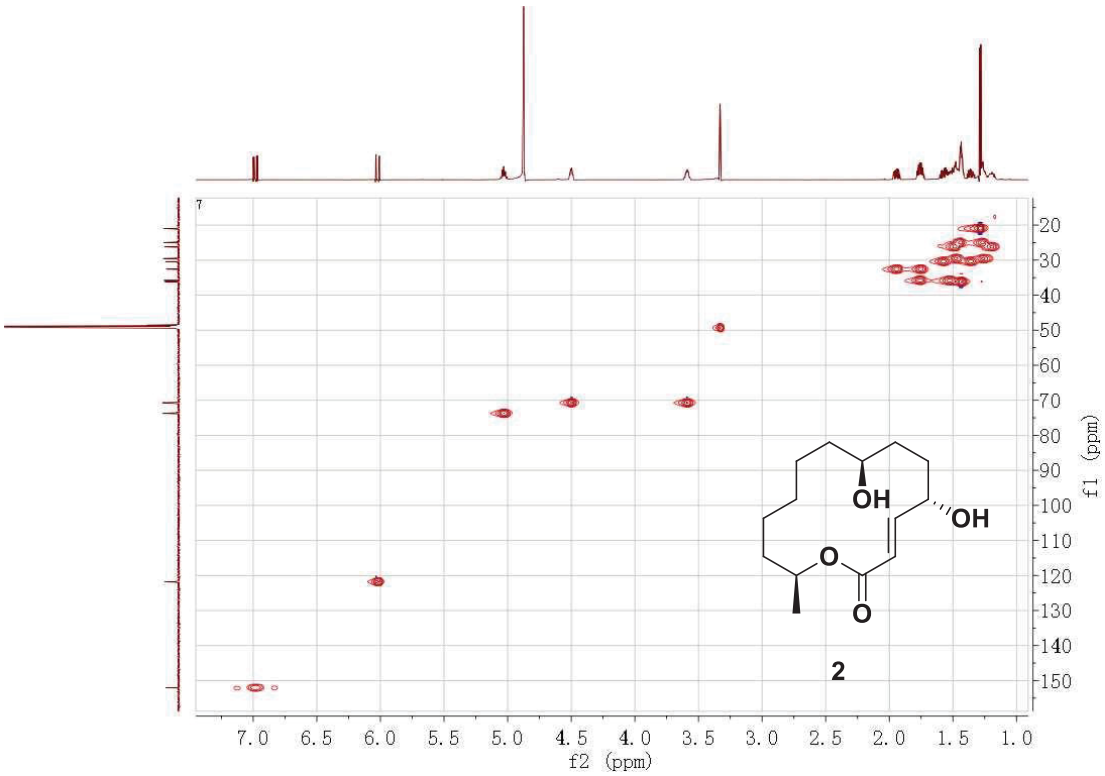

S14. HSQC (600 and 150 MHz, CD_3OD) spectrum of compound **2**.

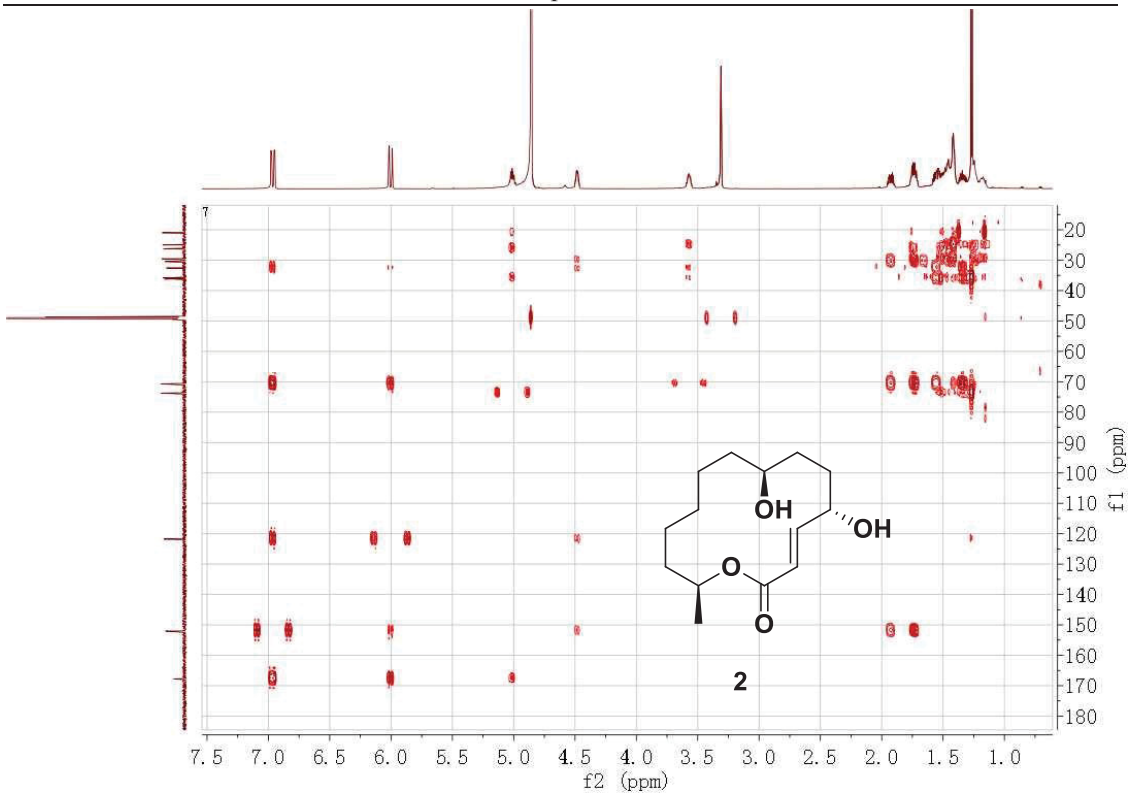

S15. HMBC (600 and 150 MHz, CD_3OD) spectrum of compound **2**.

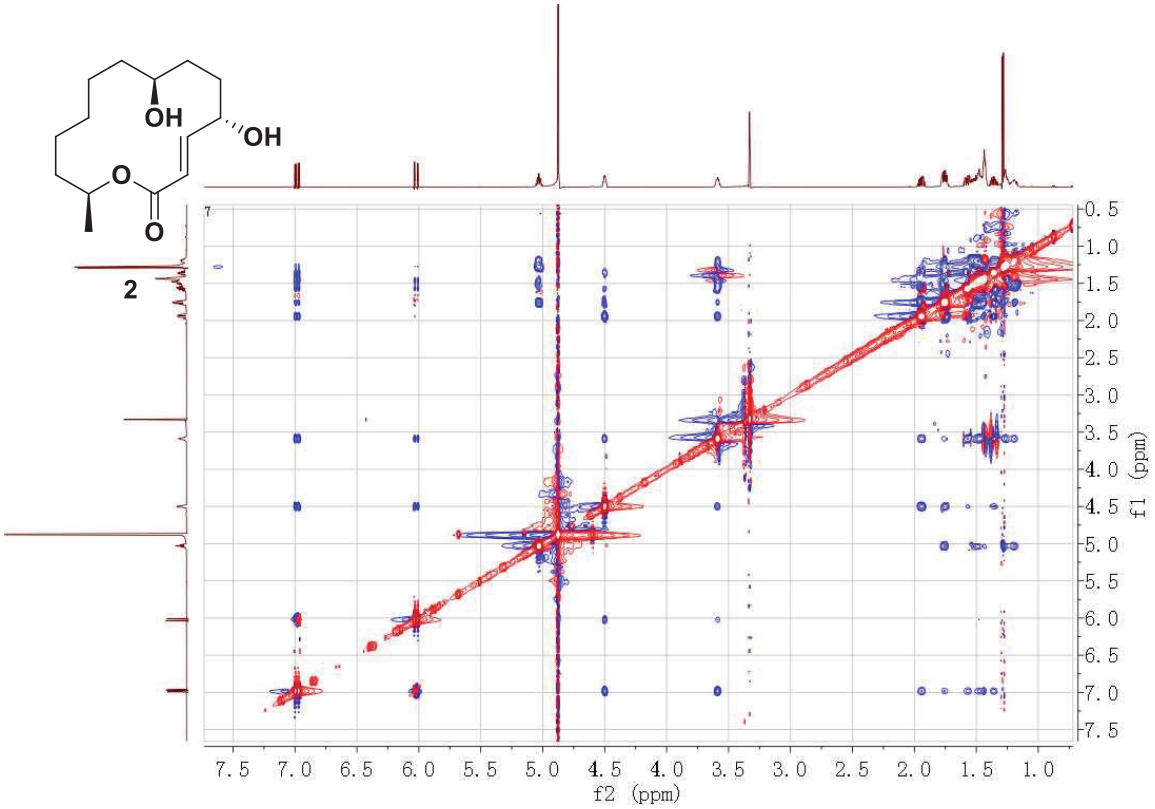

S16. ROESY (600 MHz, CD_3OD) spectrum of compound **2**.

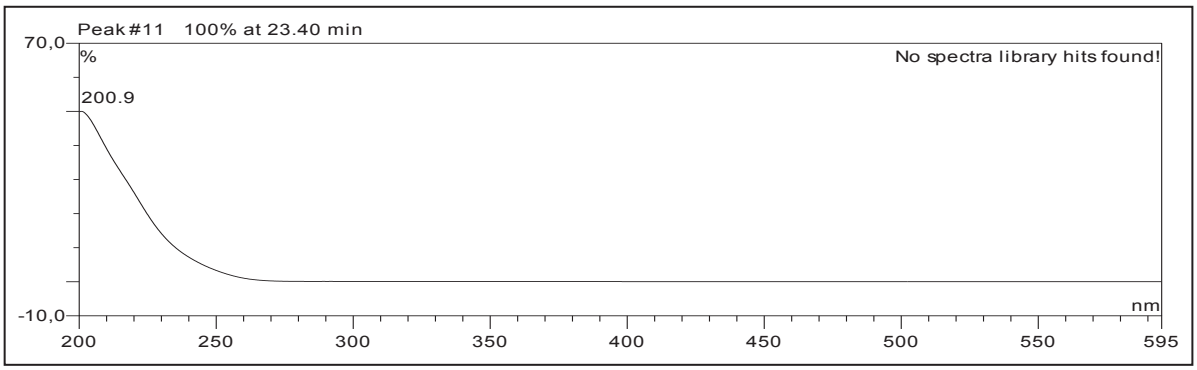

S17. UV spectrum of compound **3**.

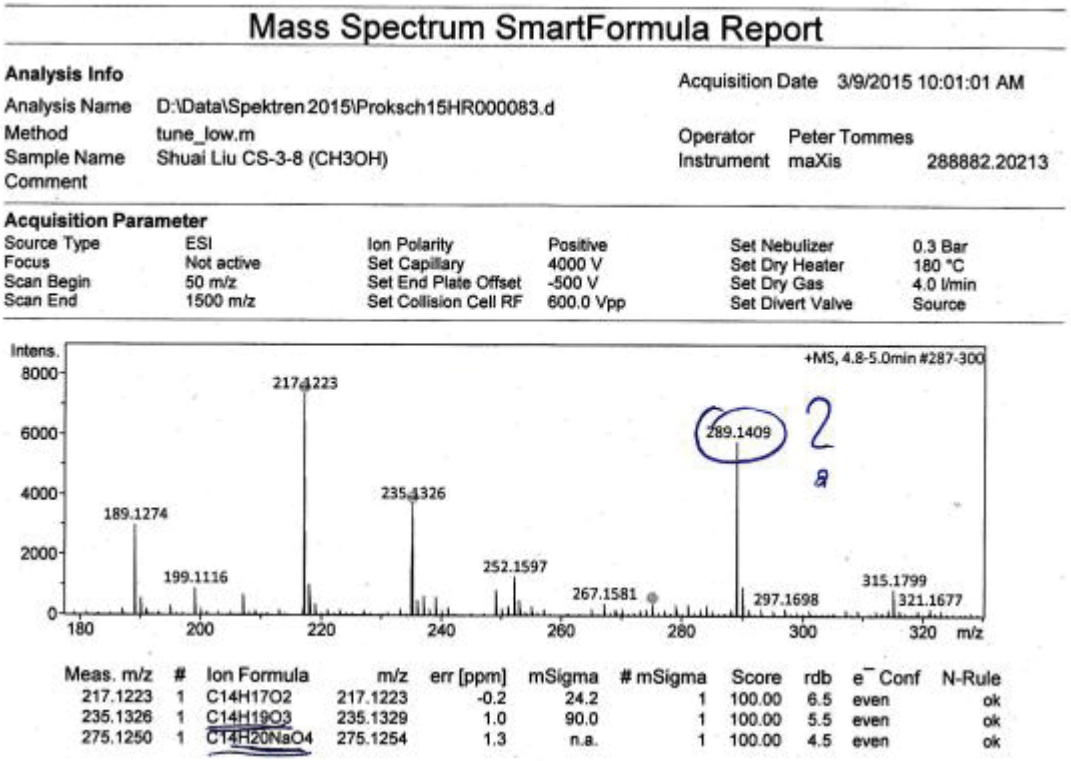

S18. HRESIMS spectrum of compound **3.**

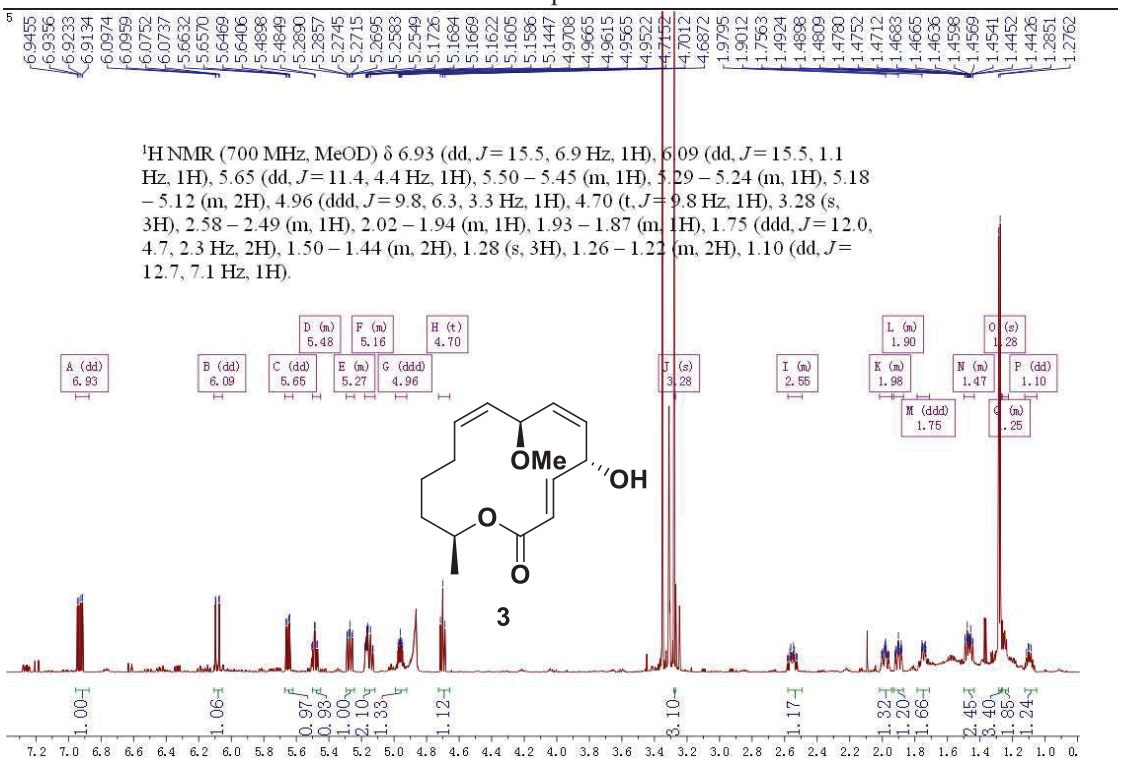

S19. ^{1}H NMR (700 MHz, CD_3OD) spectrum of compound **3**.

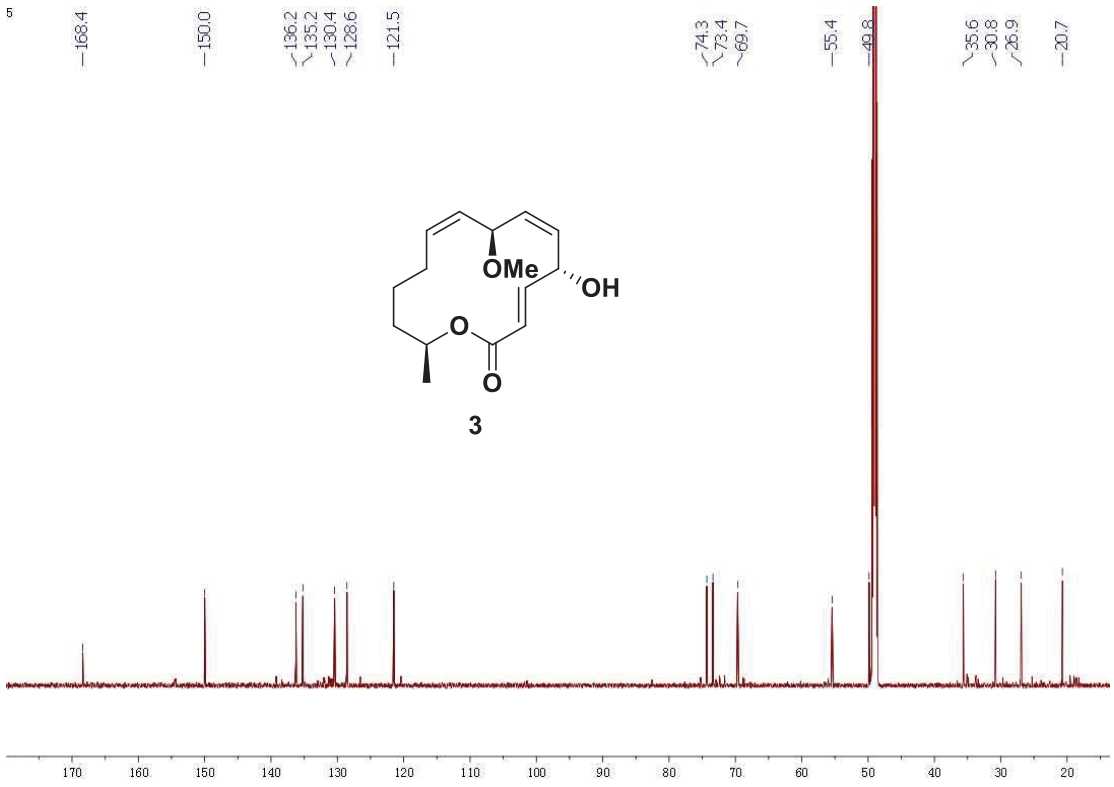

S20. ^{13}C NMR (175 MHz, CD_3OD) spectrum of compound **3**.

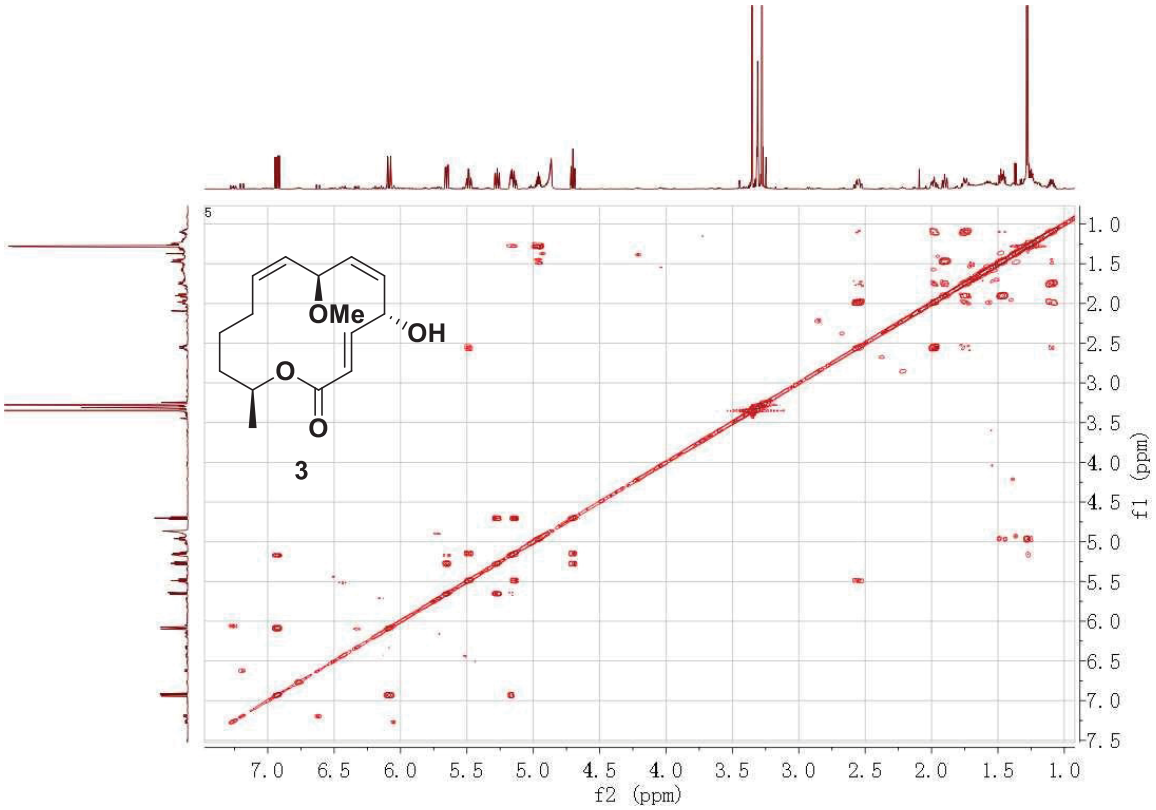

S21. ^{1}H-^{1}H COSY (700 MHz, CD_3OD) spectrum of compound **3**.

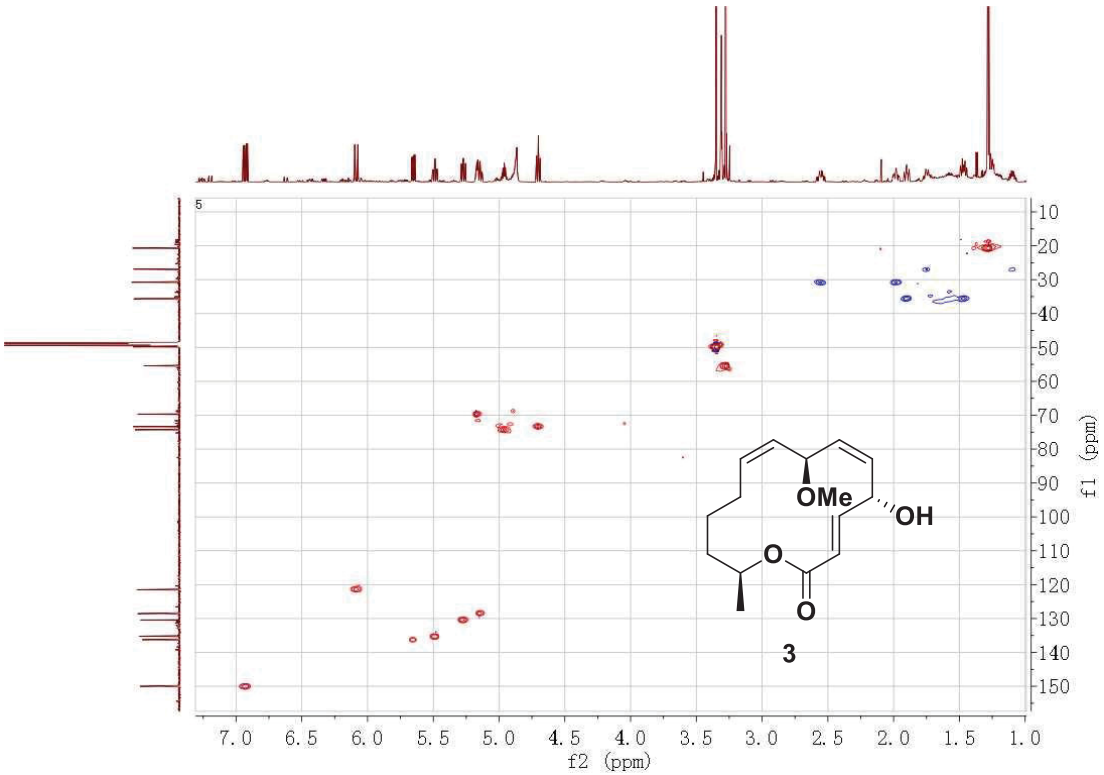

S22. HSQC (700 and 175 MHz, CD_3OD) spectrum of compound **3**.

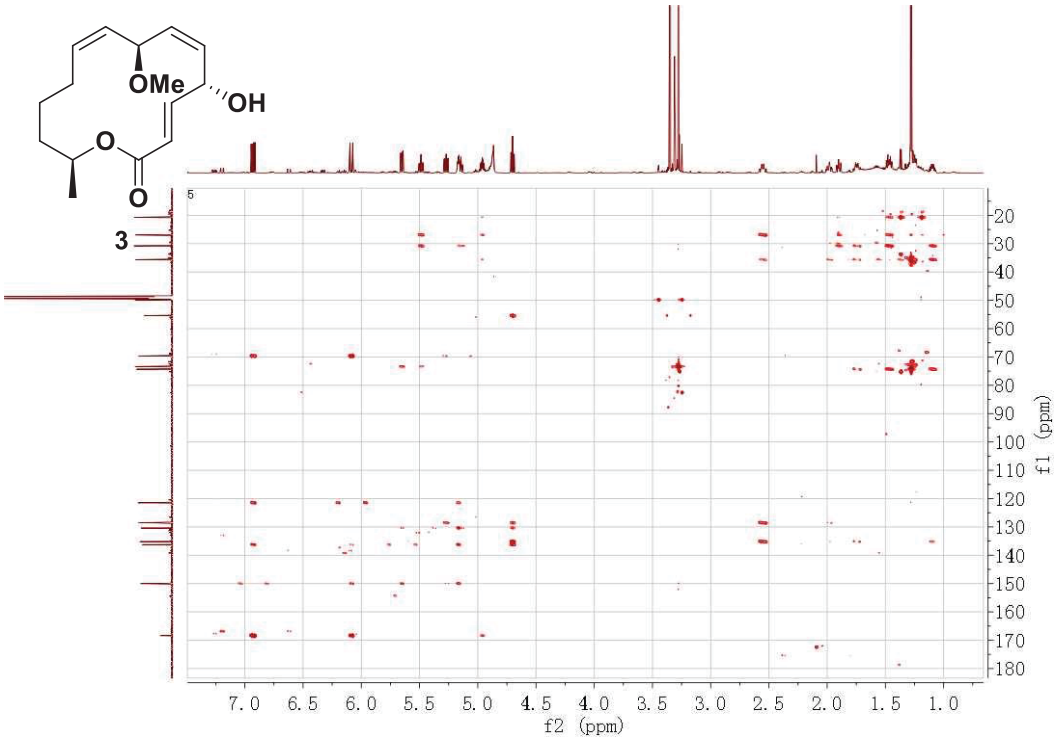

S23. HMBC (700 and 175 MHz, CD_3OD) spectrum of compound **3**.

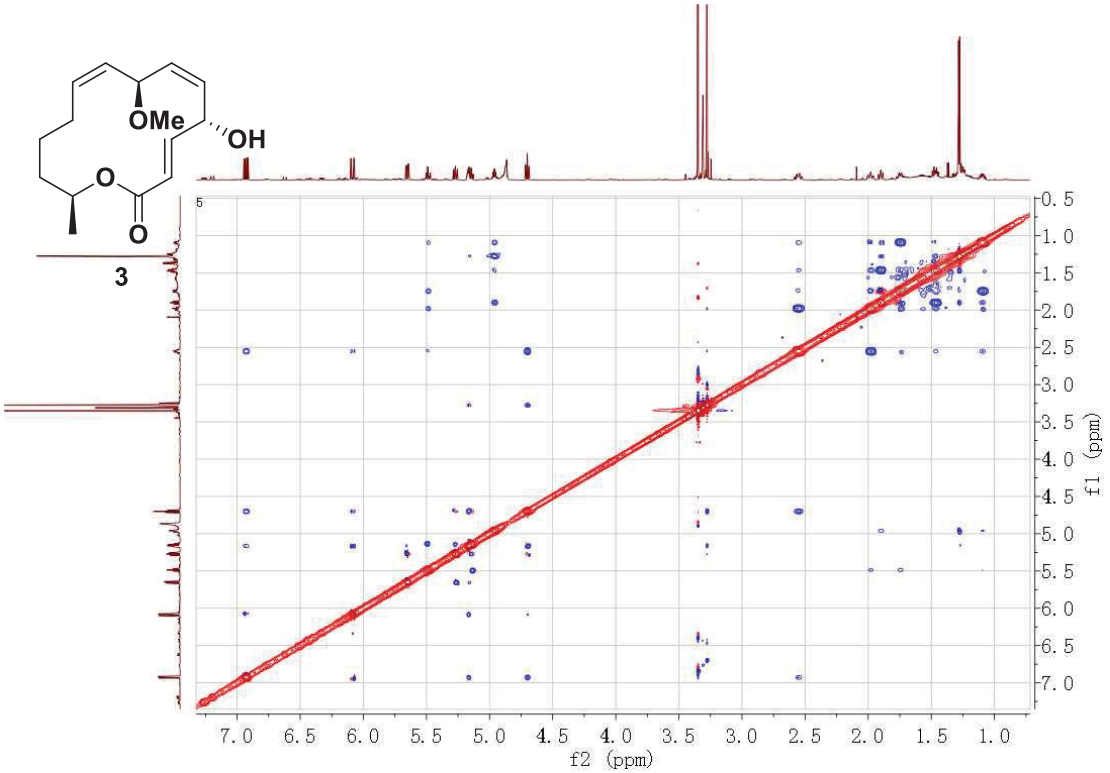

S24. ROESY (700 MHz, CD_3OD) spectrum of compound **3**.

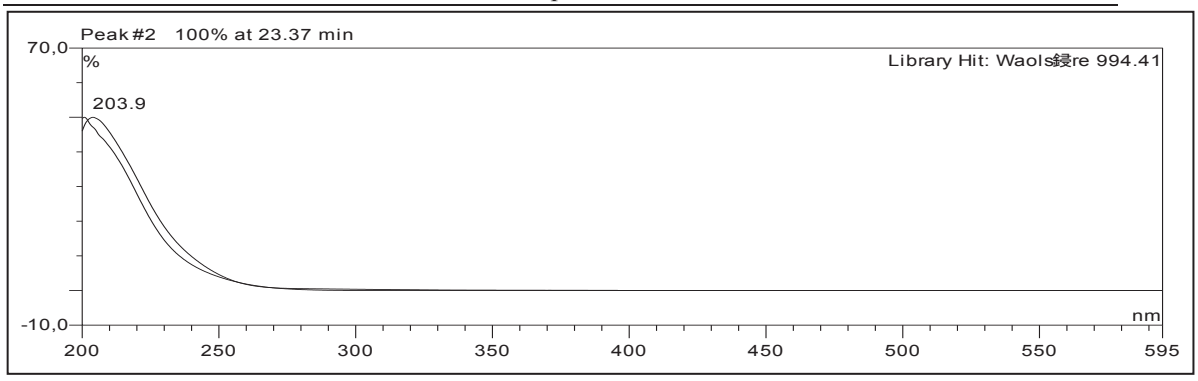

S25. UV spectrum of compound **4.**

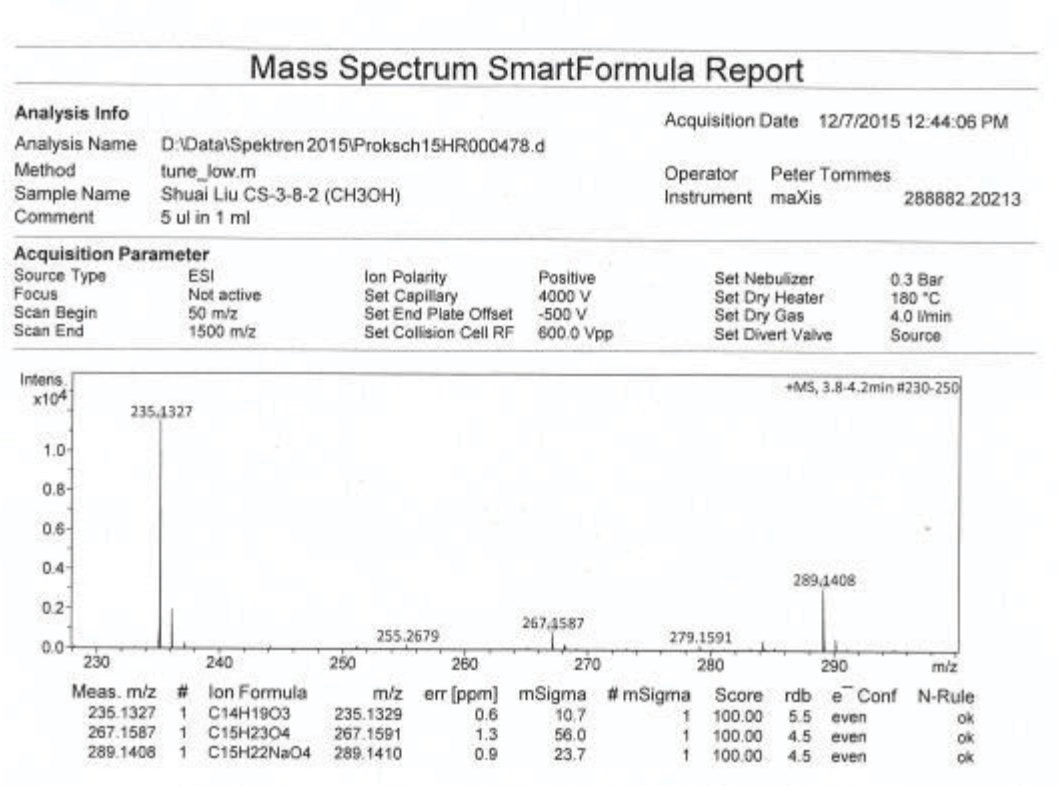

S26. HRESIMS spectrum of compound **4.**

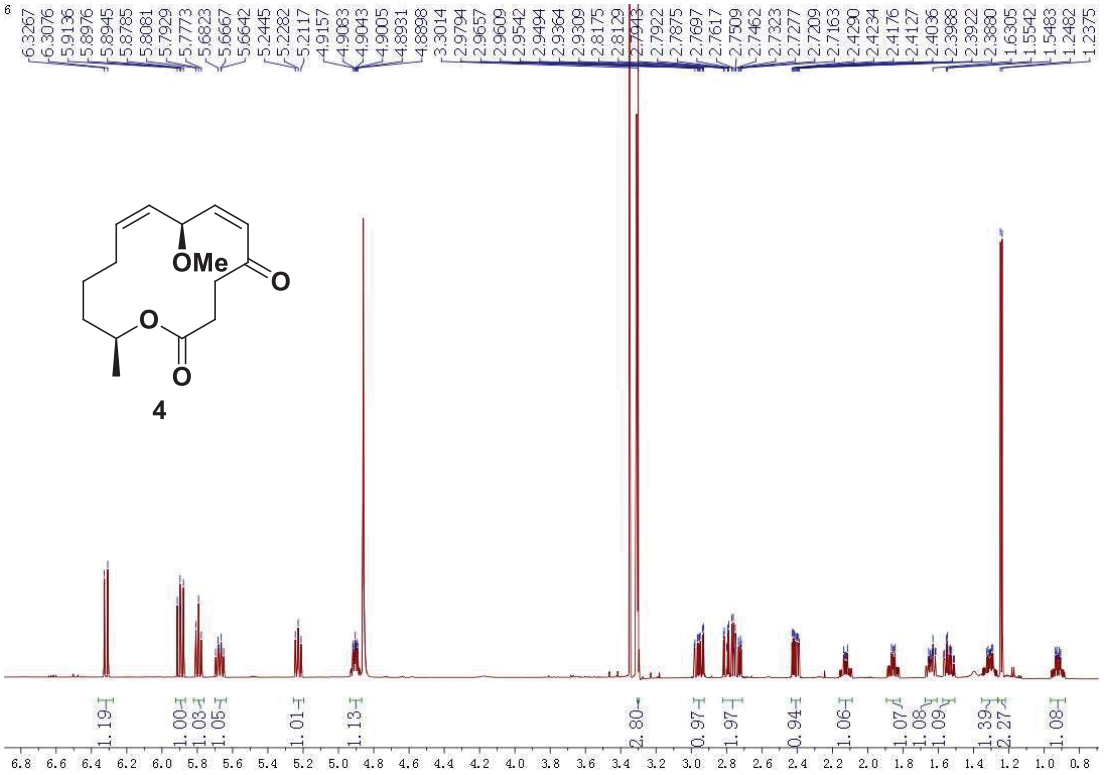

S27. ^{1}H NMR (600 MHz, CD_3OD) spectrum of compound **4.**

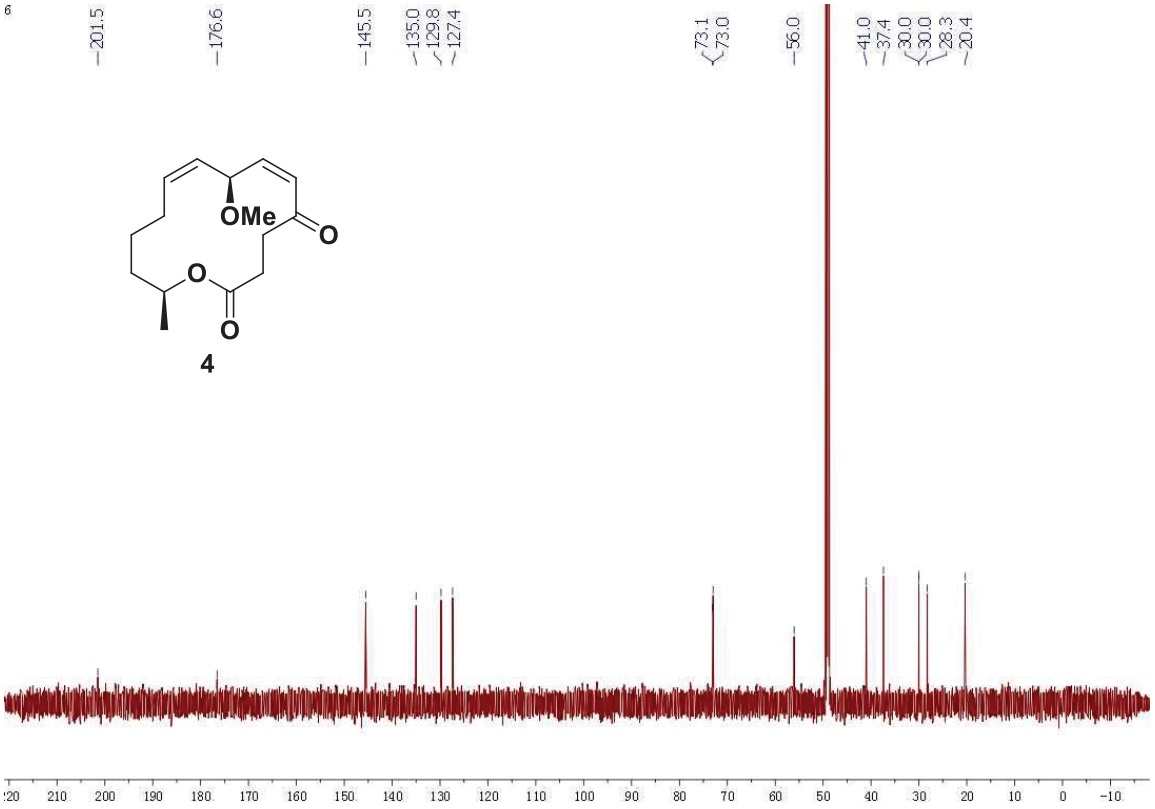

S28. ^{13}C NMR (150 MHz, CD_3OD) spectrum of compound **4.**

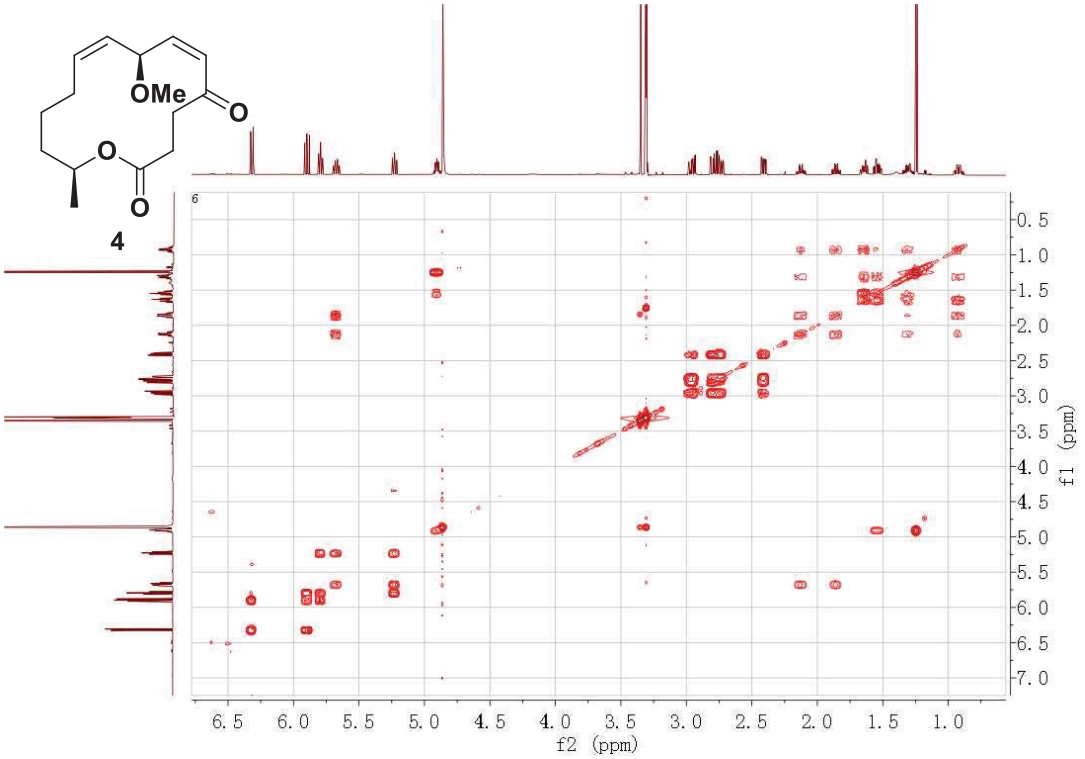

S29. ^{1}H-^{1}H COSY (600 MHz, CD_3OD) spectrum of compound **4.**

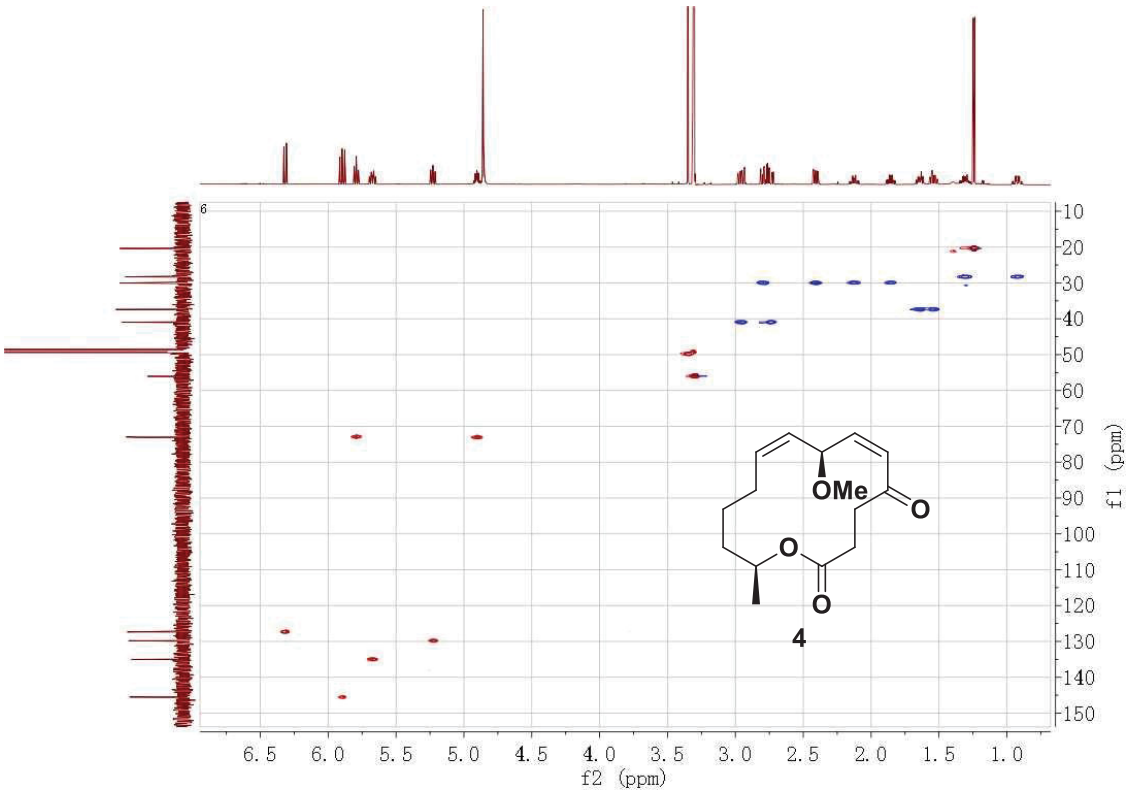

S30. HSQC (600 and 150 MHz, CD_3OD) spectrum of compound **4.**

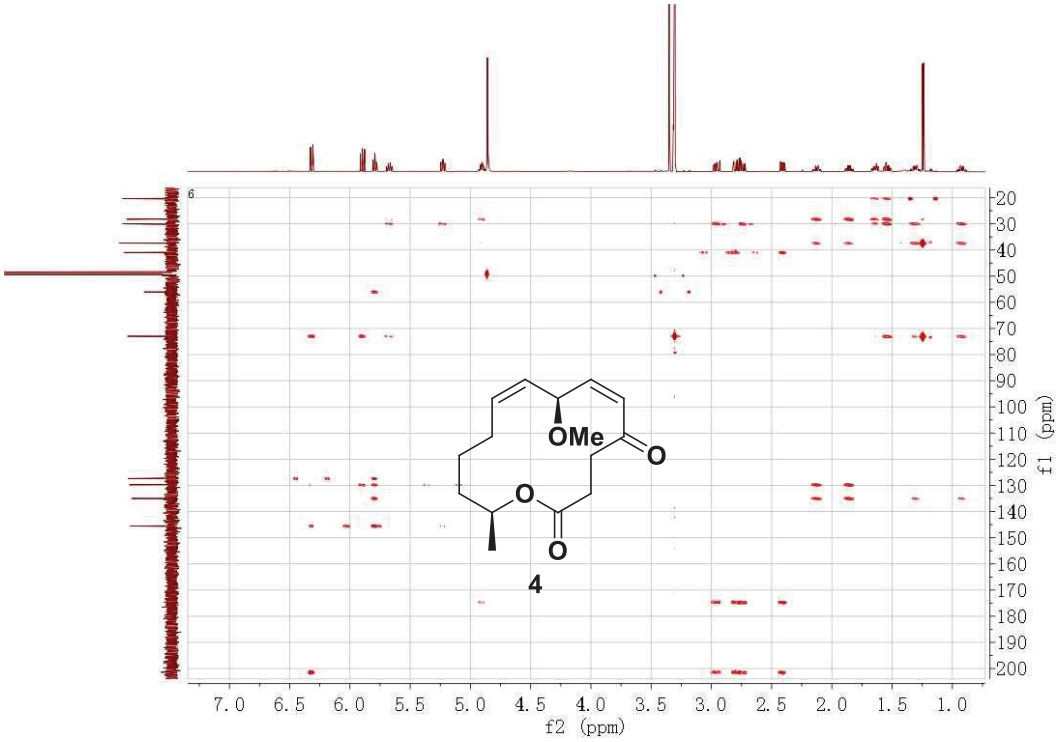

S31. HMBC (600 and 150 MHz, CD_3OD) spectrum of compound **4.**

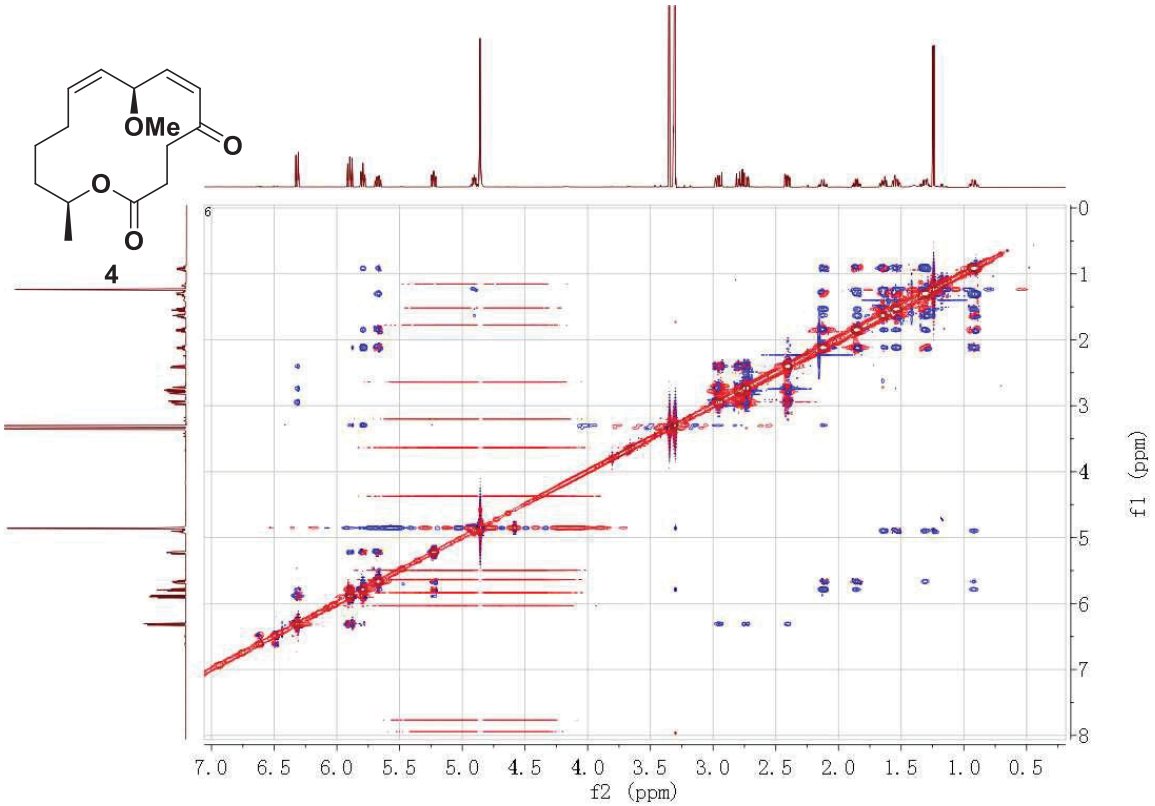

S32. ROESY (600 MHz, CD_3OD) spectrum of compound **4.**

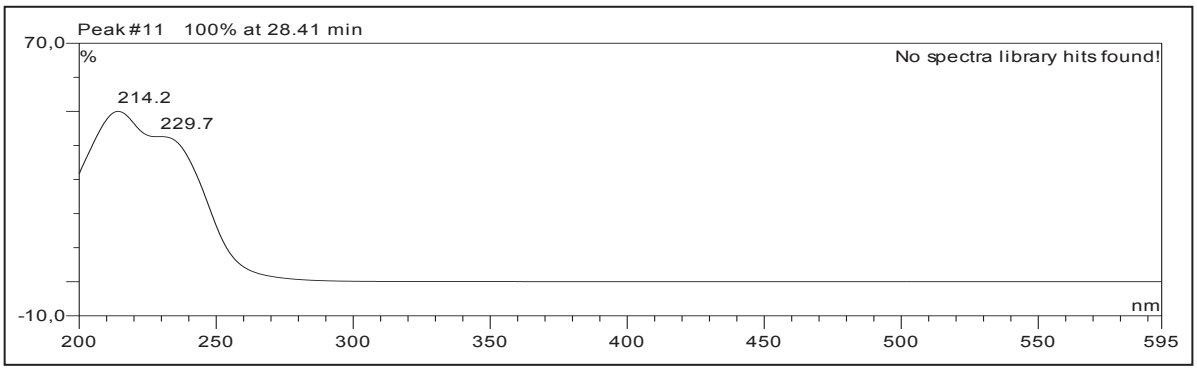

S33. UV spectrum of compound **5**.

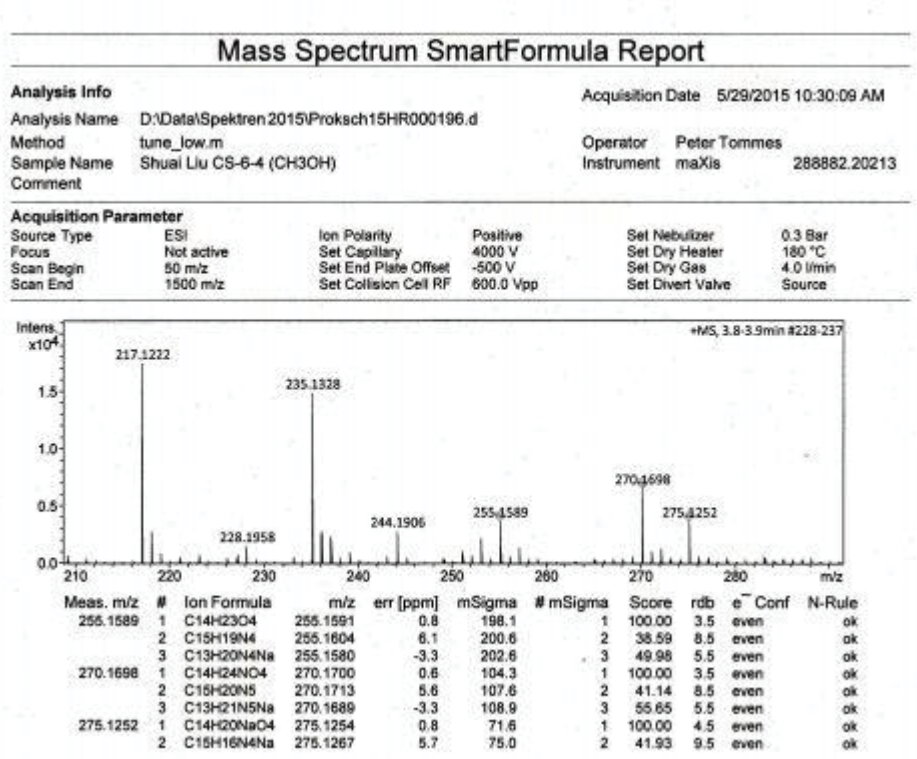

S34. HRESIMS spectrum of compound **5.**

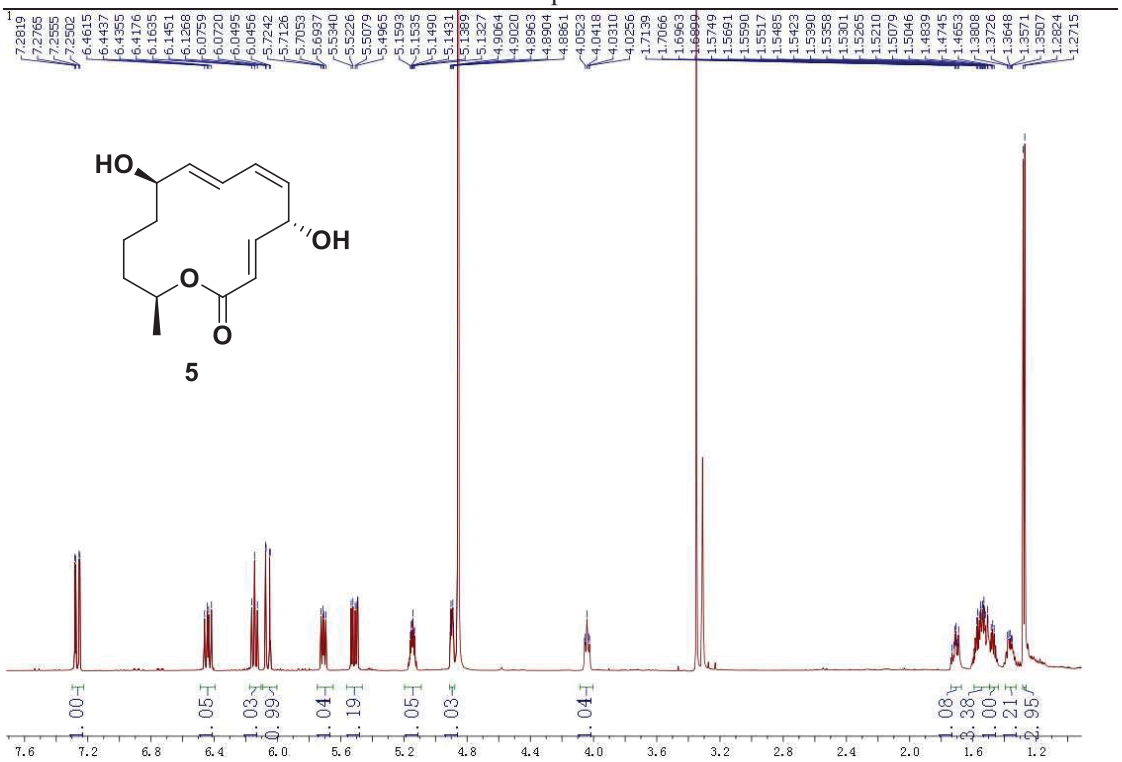

S35. ^{1}H NMR (600 MHz, CD_3OD) spectrum of compound **5.**

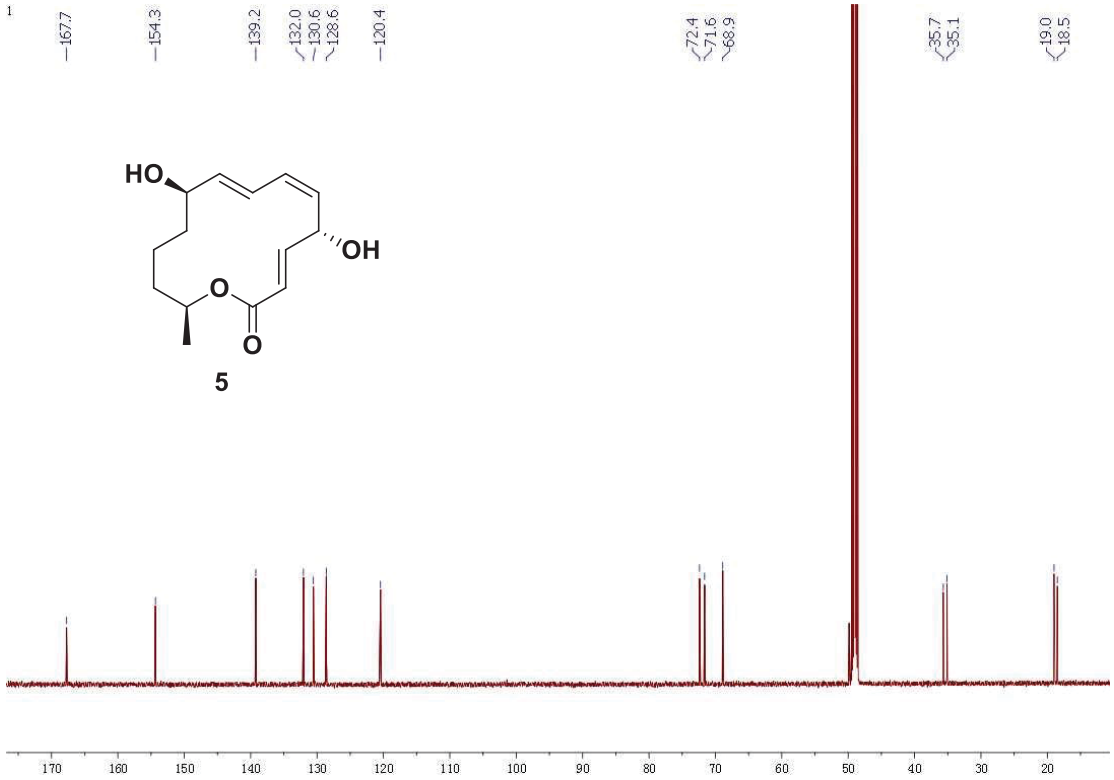

S36. ^{13}C NMR (150 MHz, CD_3OD) spectrum of compound **5.**

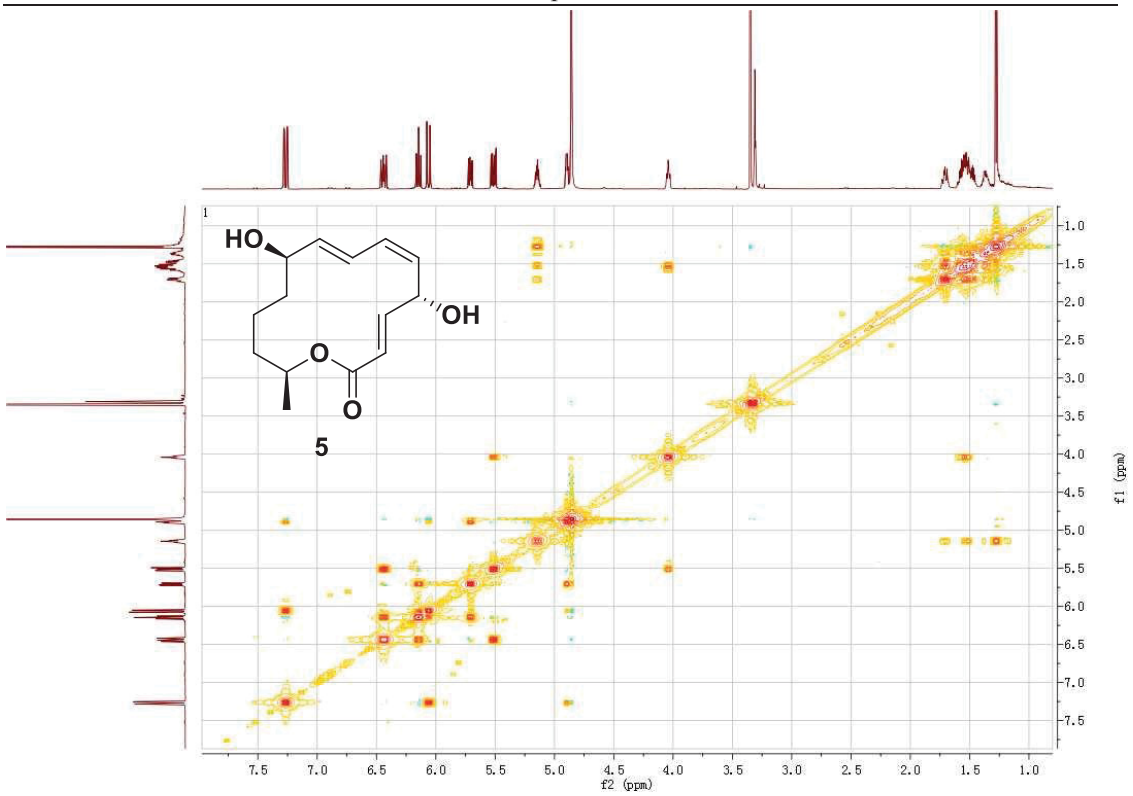

S37. ^{1}H-^{1}H COSY (600 MHz, CD_3OD) spectrum of compound **5.**

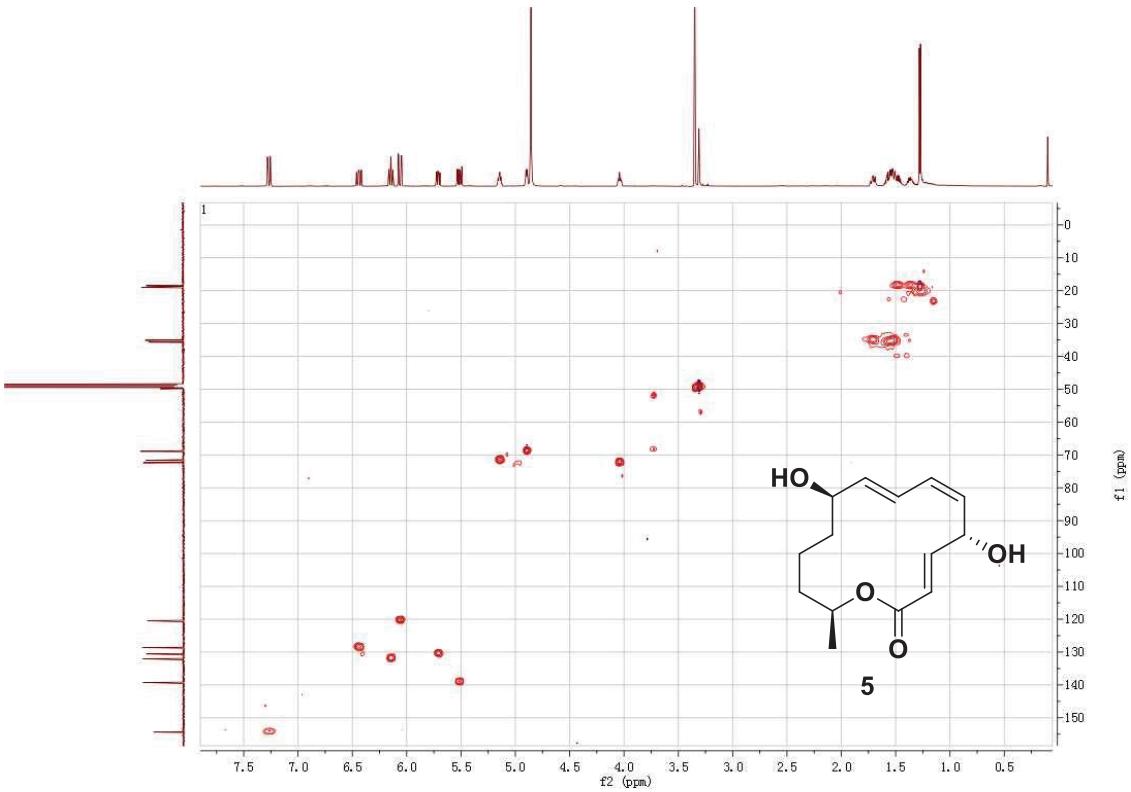

S38. HSQC (600 and 150 MHz, CD_3OD) spectrum of compound **5.**

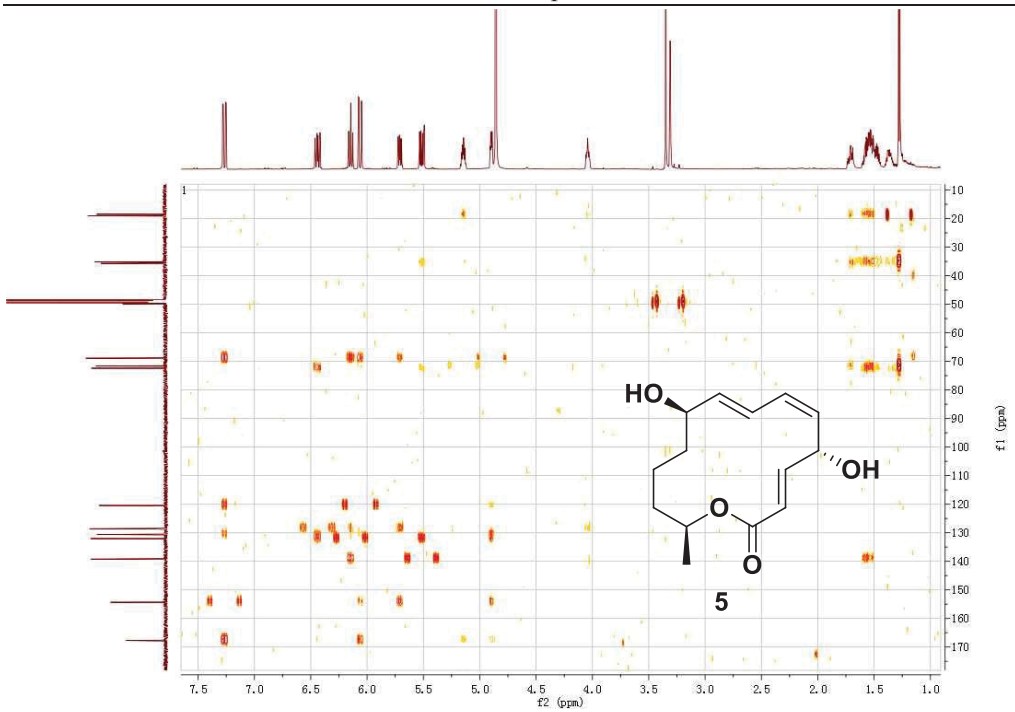

S39. HMBC (600 and 150 MHz, CD_3OD) spectrum of compound **5.**

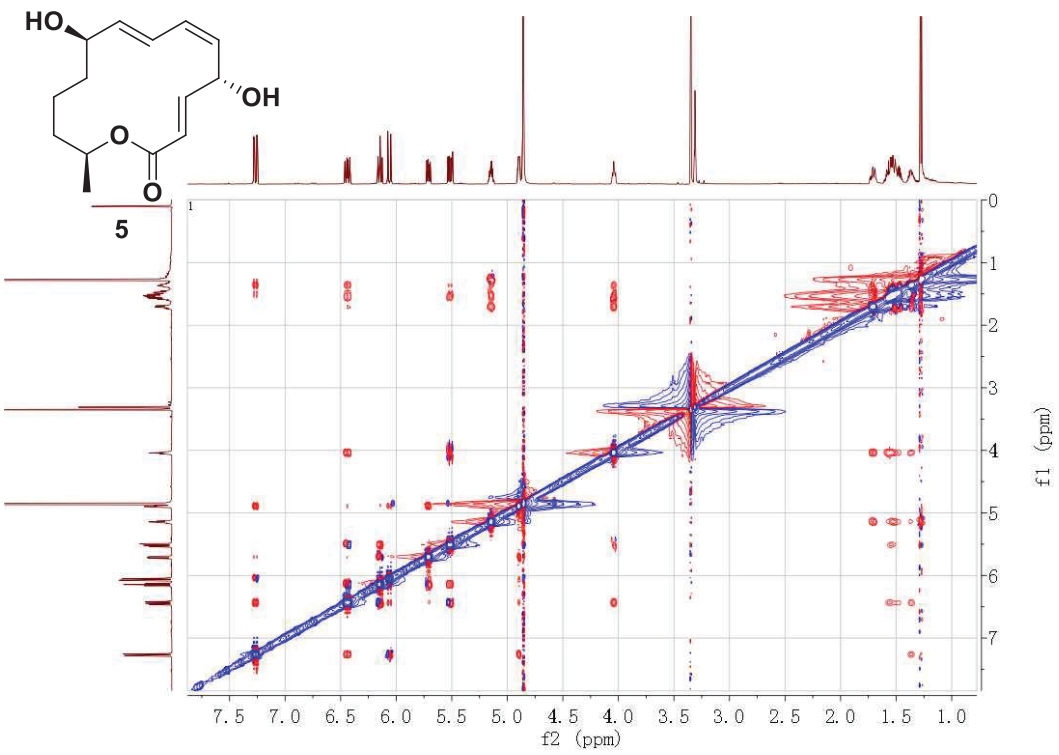

S40. ROESY (600 MHz, CD_3OD) spectrum of compound **5.**

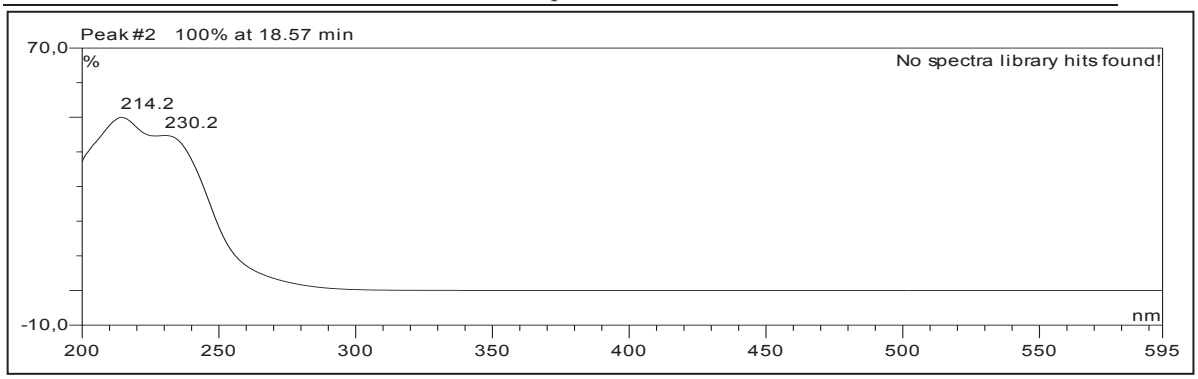

S41. UV spectrum of compound **6**.

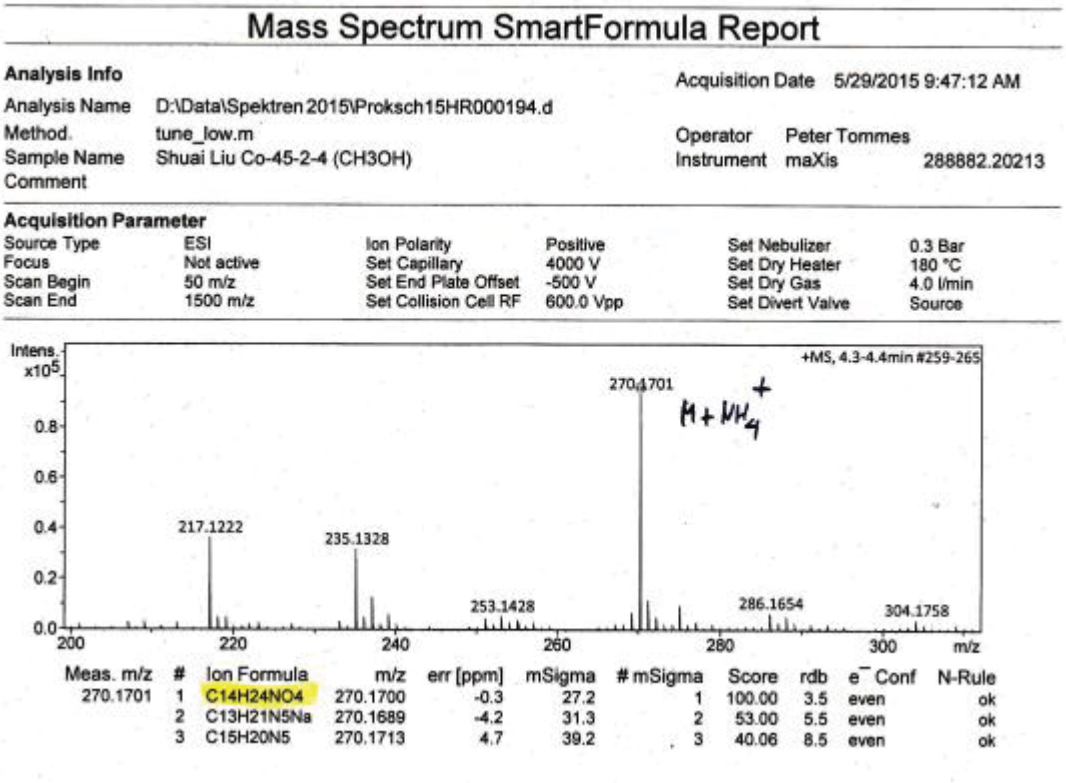

S42. HRESIMS spectrum of compound **6.**

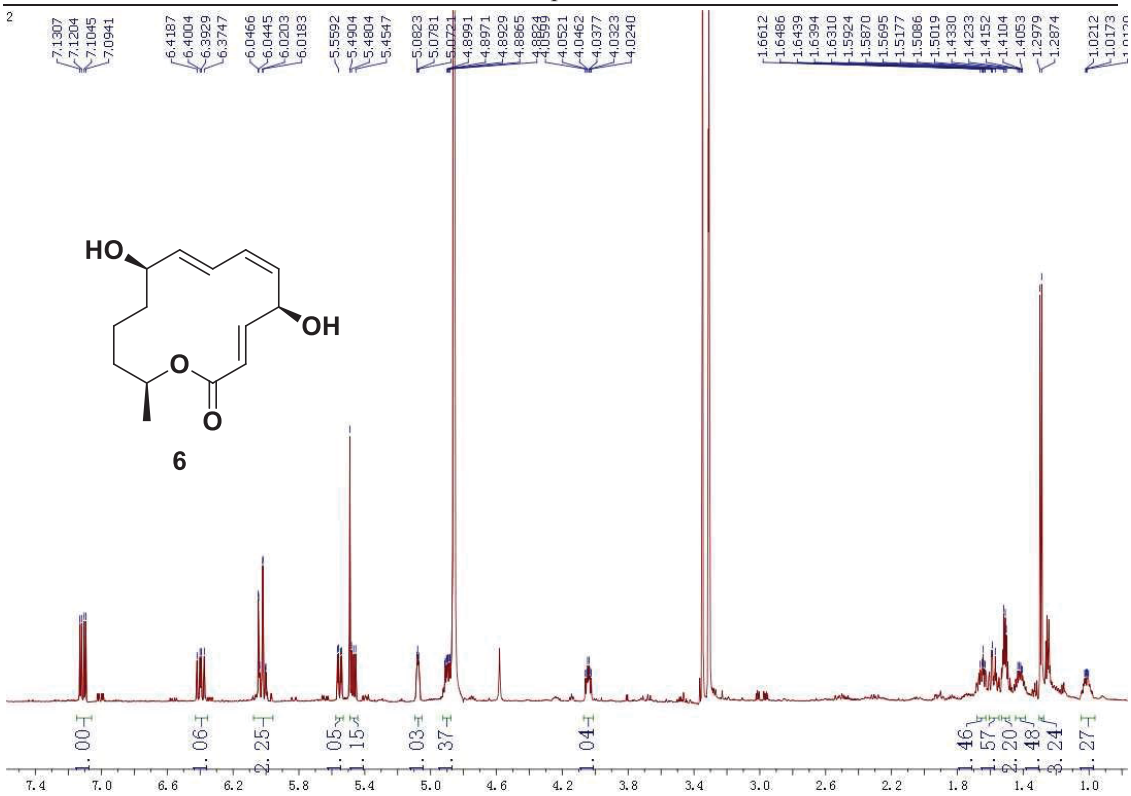

S43. ^{1}H NMR (600 MHz, CD_3OD) spectrum of compound **6**.

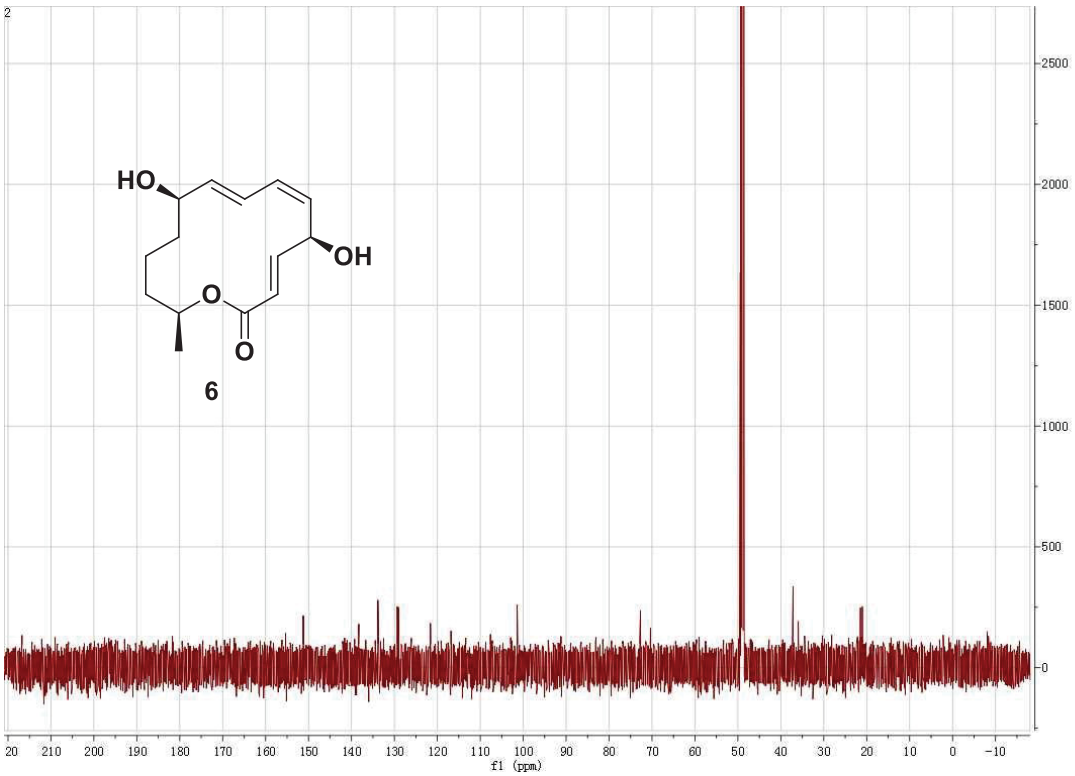

S44. ^{13}C NMR (125 MHz, CD_3OD) spectrum of compound **6**.

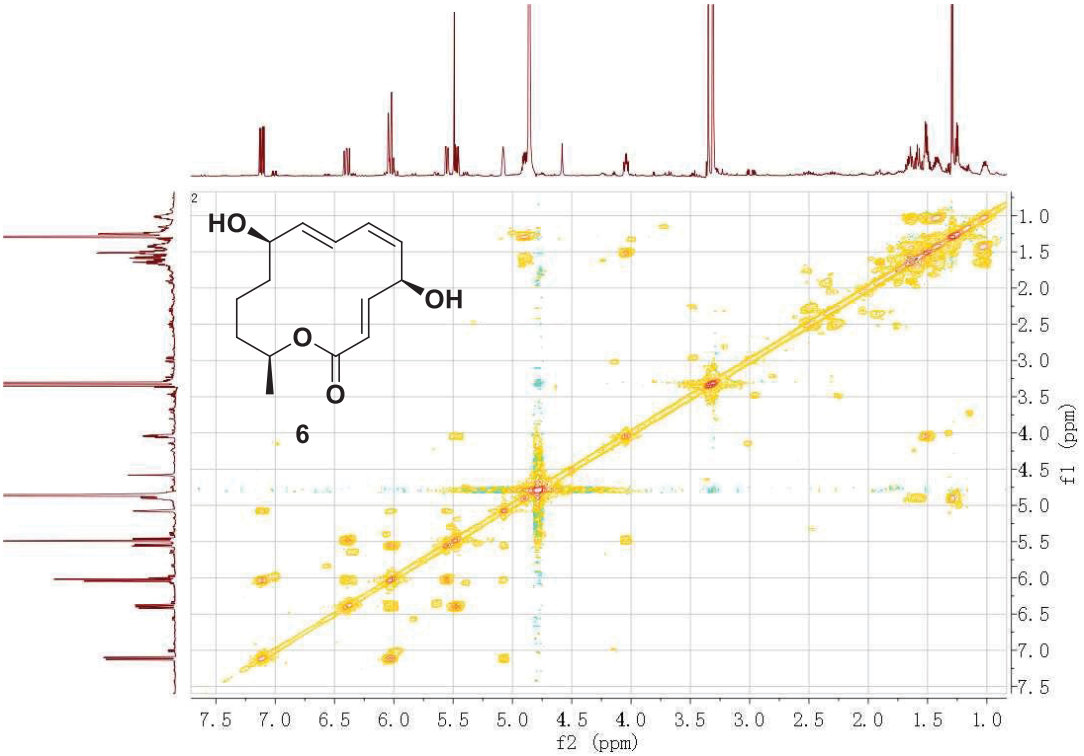

S45. ^{1}H-^{1}H COSY (600 MHz, CD_3OD) spectrum of compound **6**.

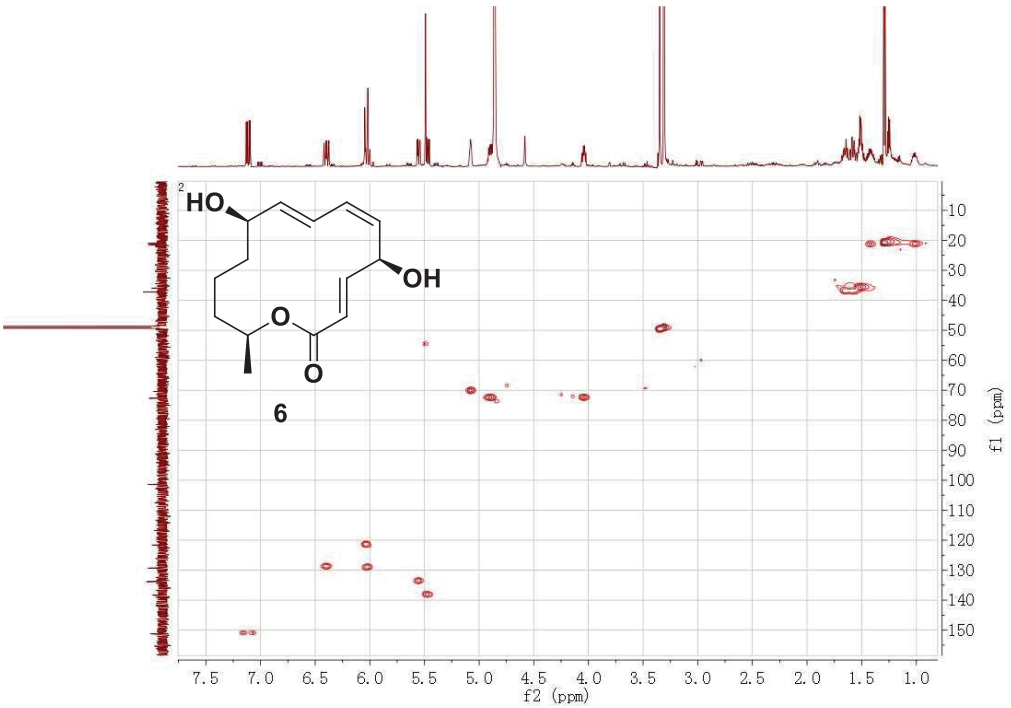

S46. HSQC (600 and 150 MHz, CD_3OD) spectrum of compound **6**.

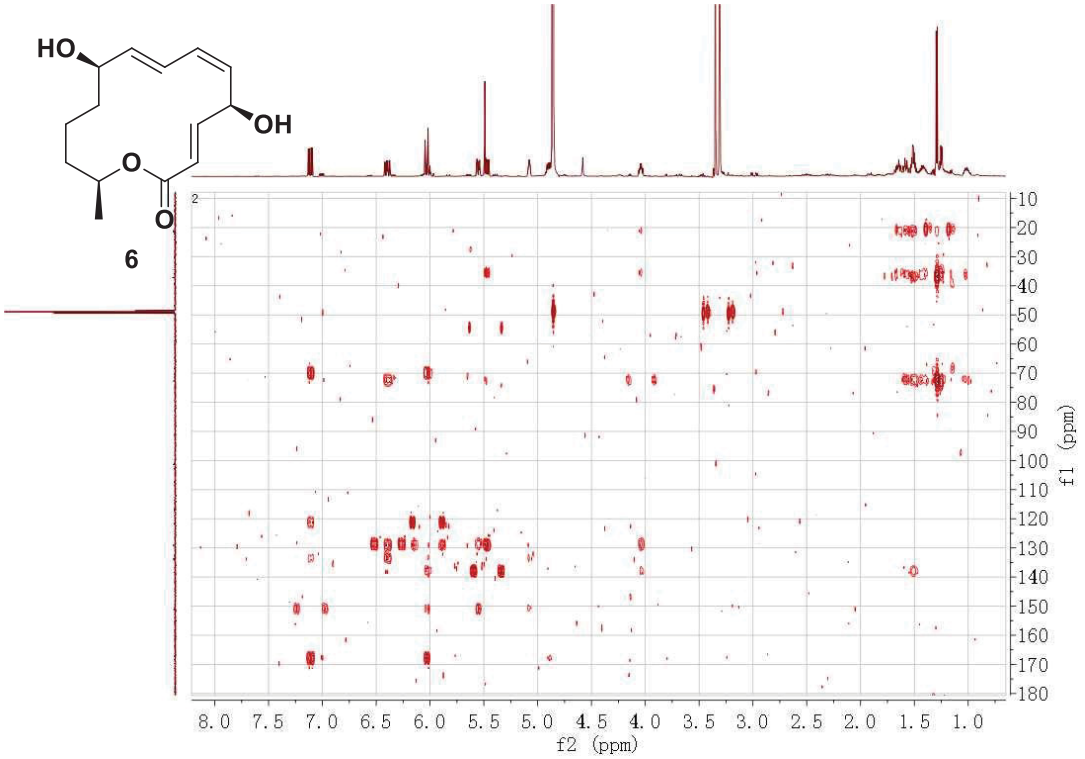

S47. HMBC (600 and 150 MHz, CD_3OD) spectrum of compound **6**.

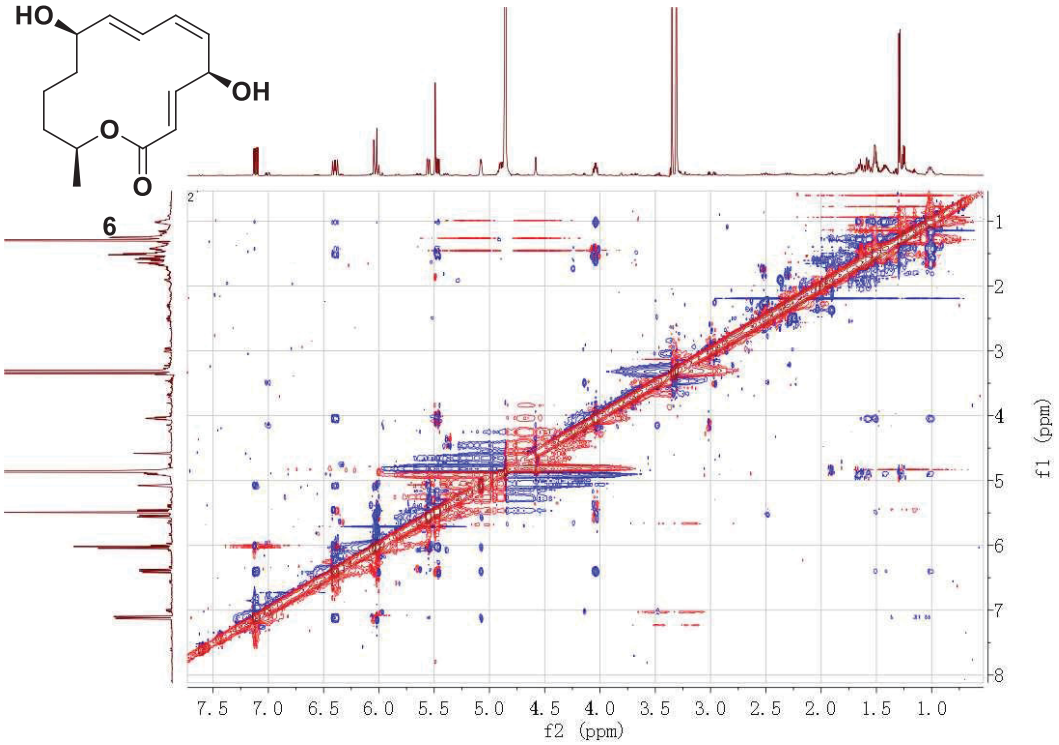

S48. ROESY (600 MHz, CD_3OD) spectrum of compound **6.**

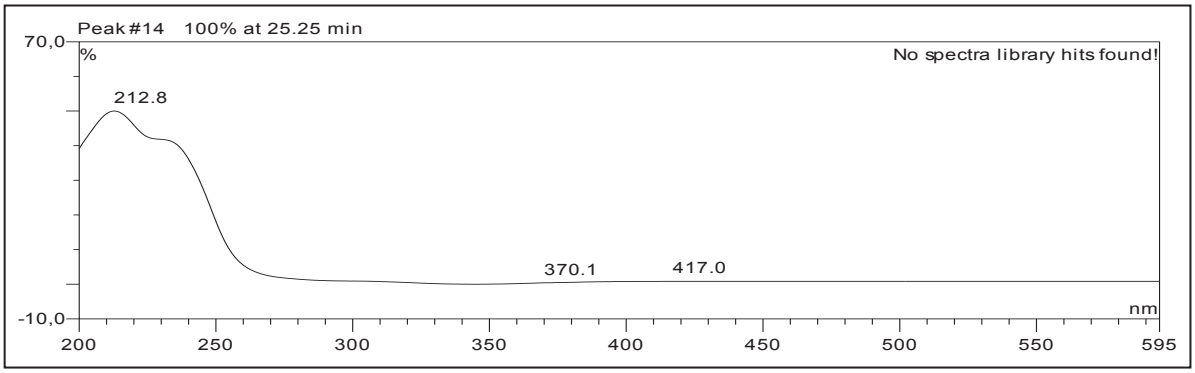

S49. UV spectrum of compound **7**.

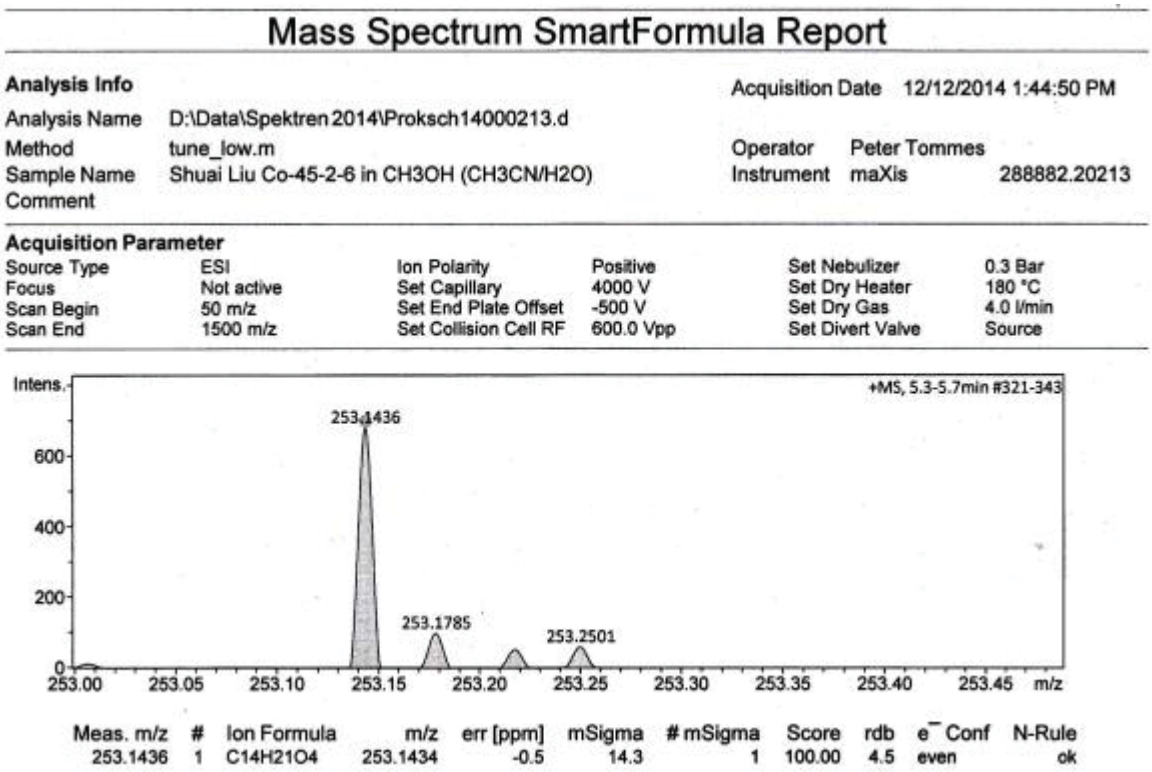

S50. HRESIMS spectrum of compound **7.**

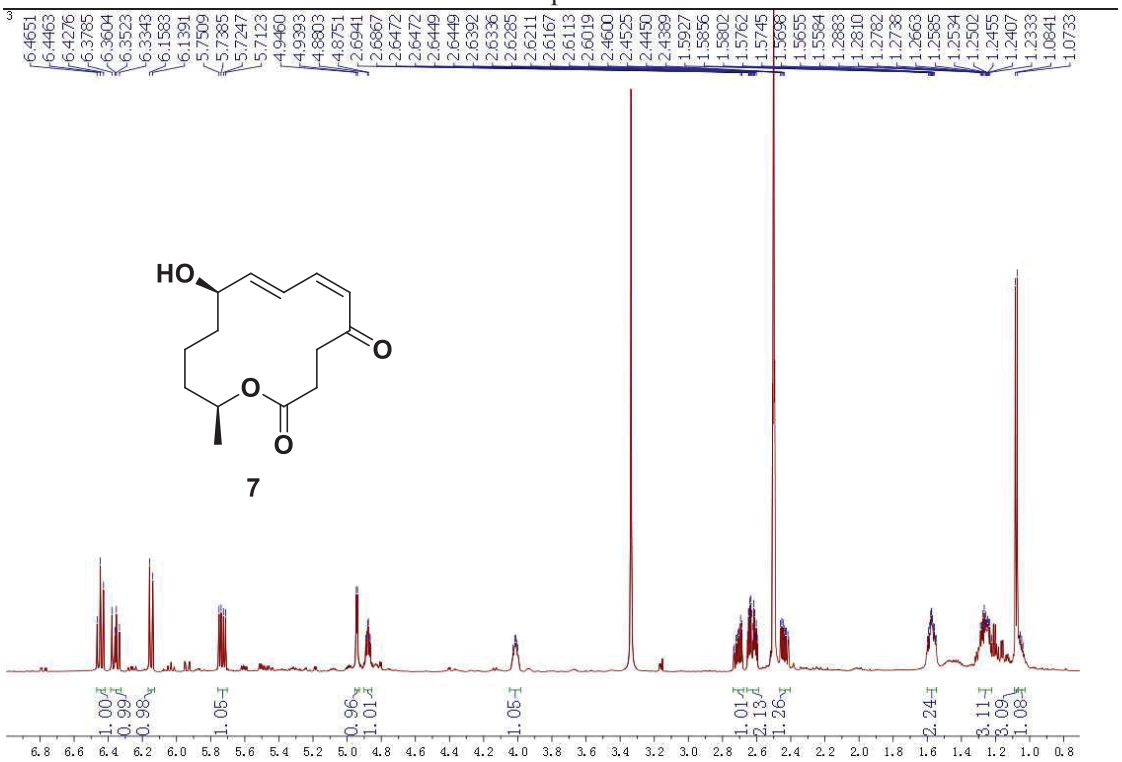

S51. ^{1}H NMR (600 MHz, CD_3OD) spectrum of compound **7**.

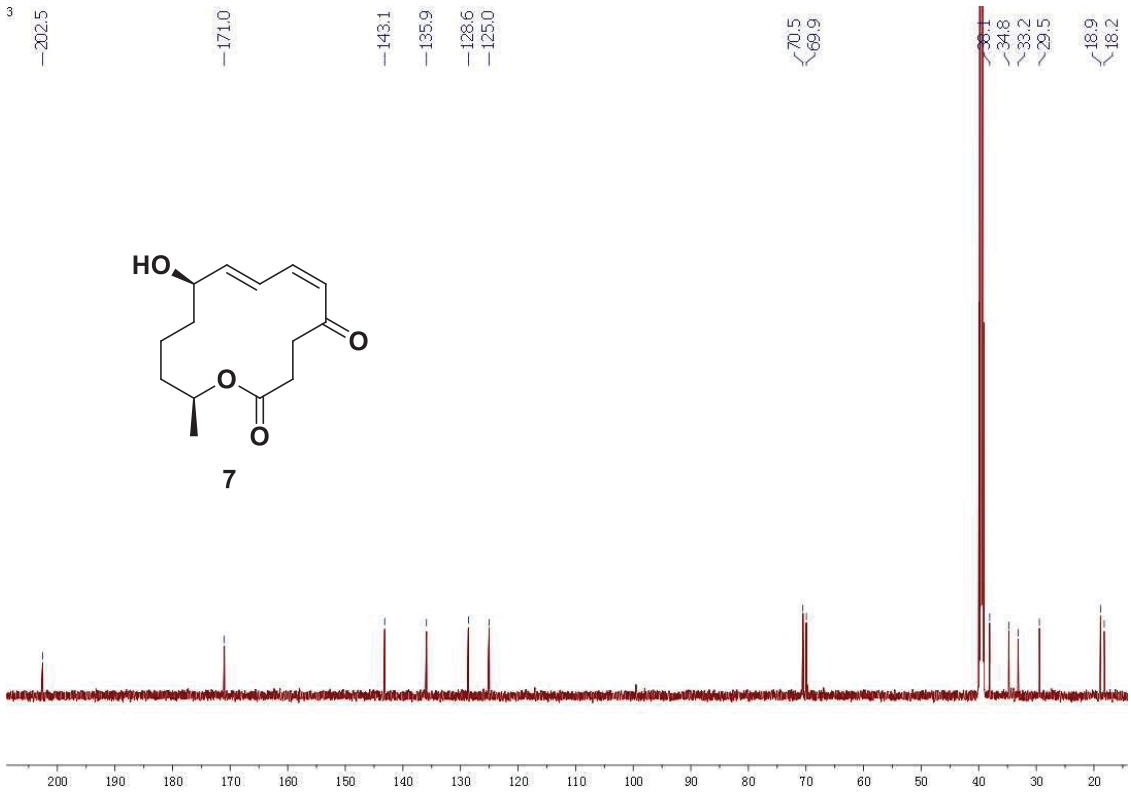

S52. ^{13}C NMR (125 MHz, DMSO-d_6) spectrum of compound **7**.

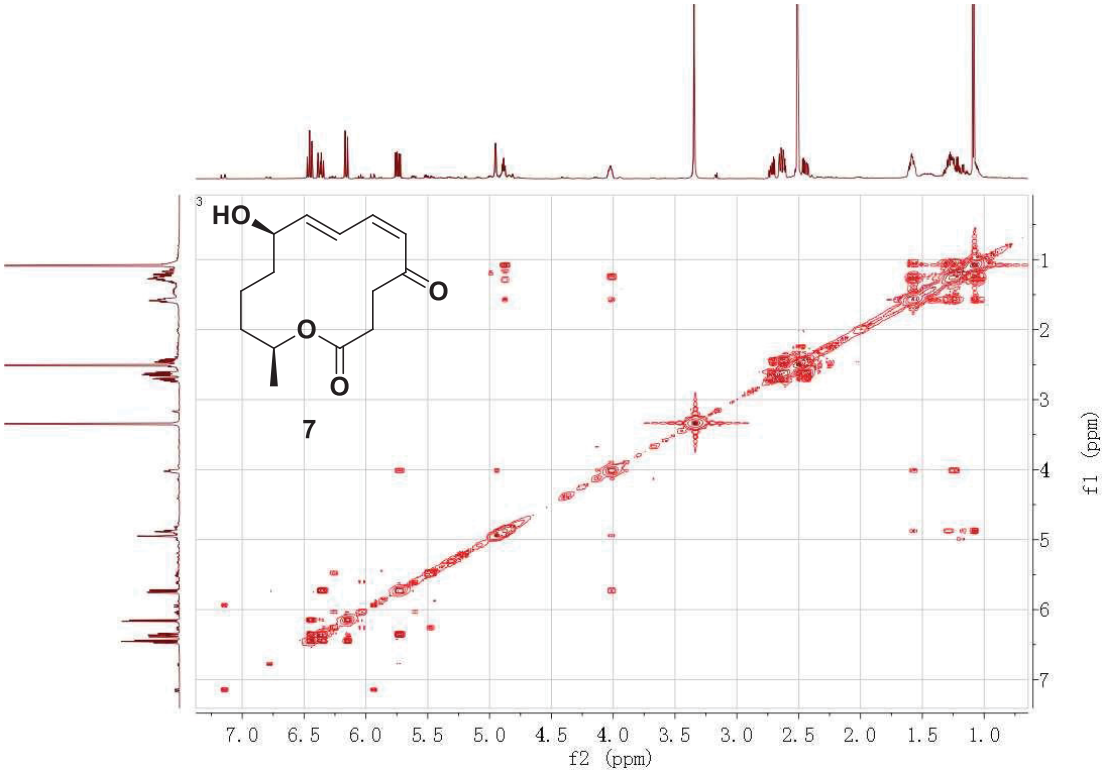

S53. ^{1}H-^{1}H COSY (600 MHz, DMSO-d_6) spectrum of compound **7**.

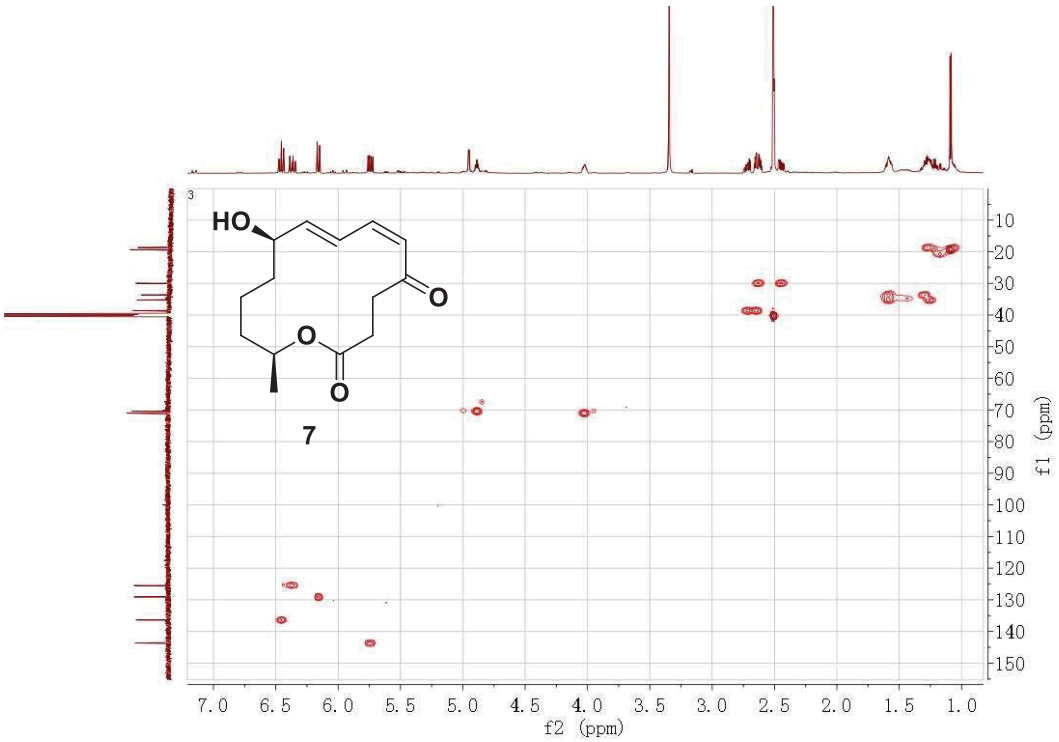

S54. HSQC (600 and 150 MHz, DMSO-d_6) spectrum of compound **7**.

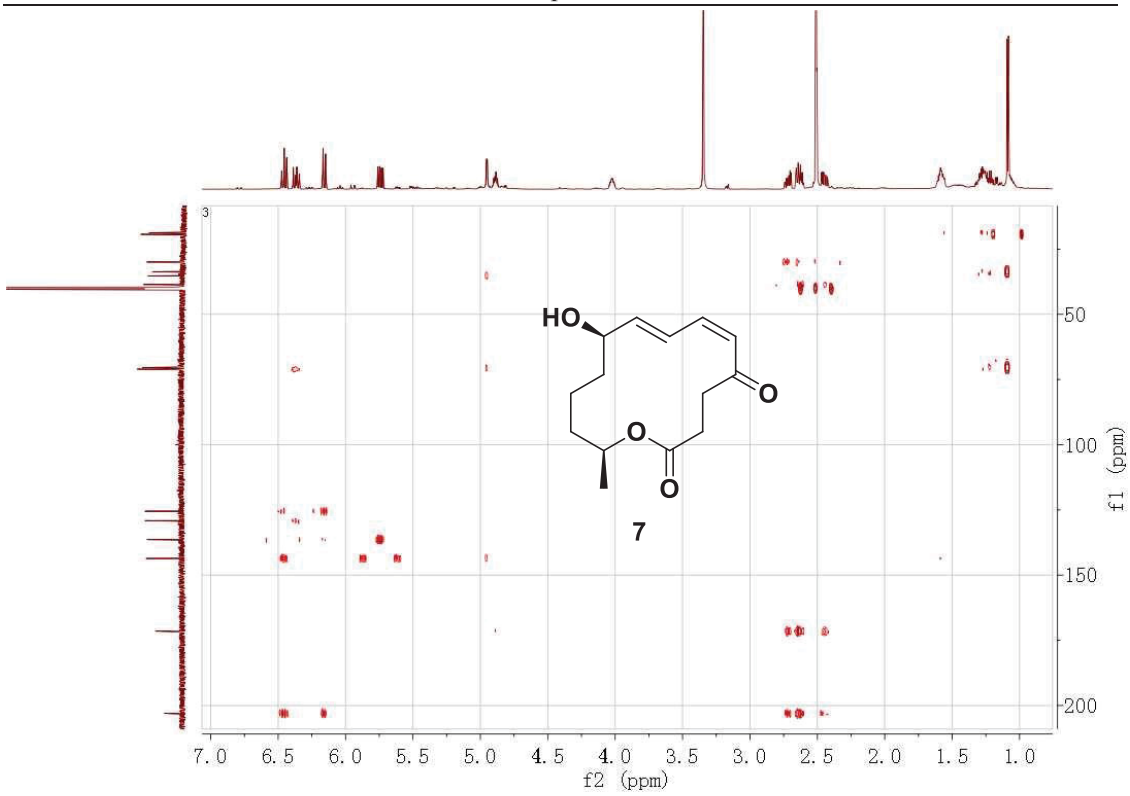

S55. HMBC (600 and 150 MHz, DMSO-d_6) spectrum of compound **7**.

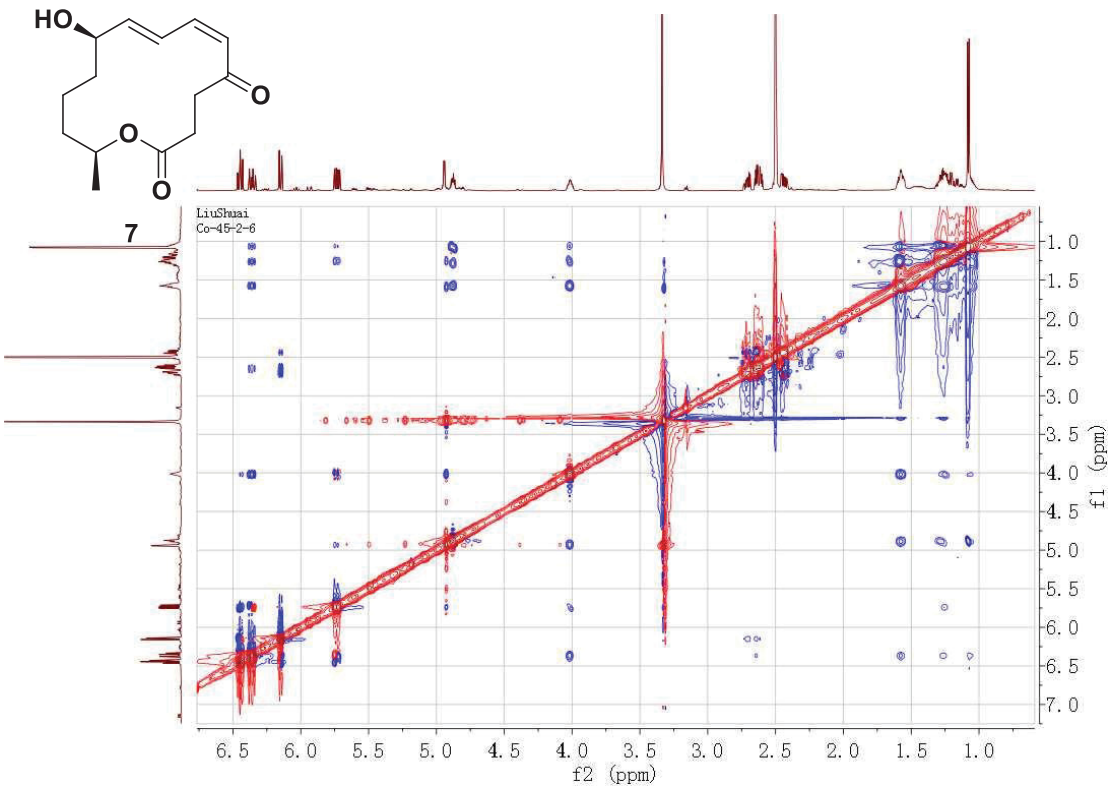

S56. ROESY (600 MHz, DMSO-d_6) spectrum of compound **7.**

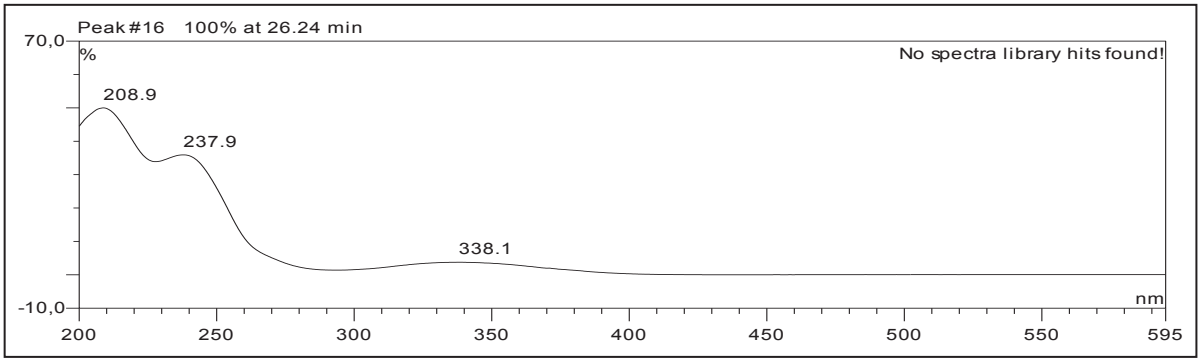

S57. UV spectrum of compound **8**.

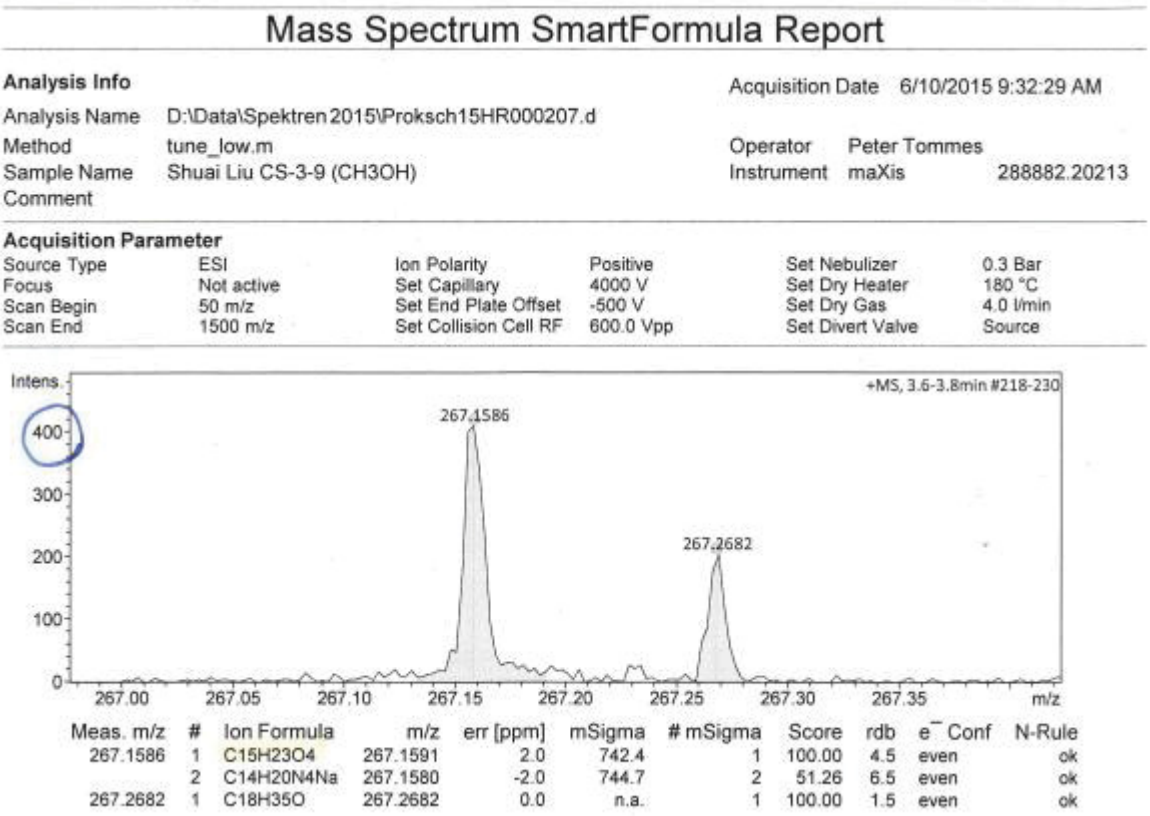

S58. HRESIMS spectrum of compound **8.**

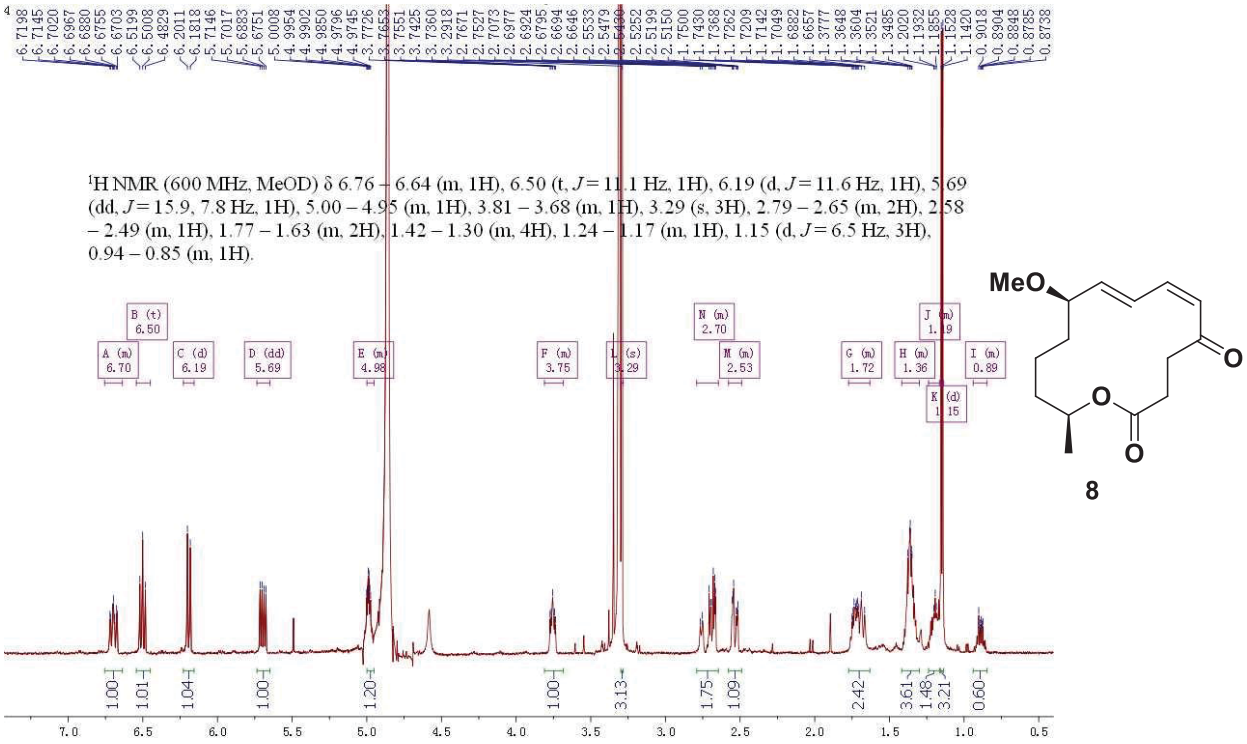

S59. ^{1}H NMR (600 MHz, CD_3OD) spectrum of compound **8**.

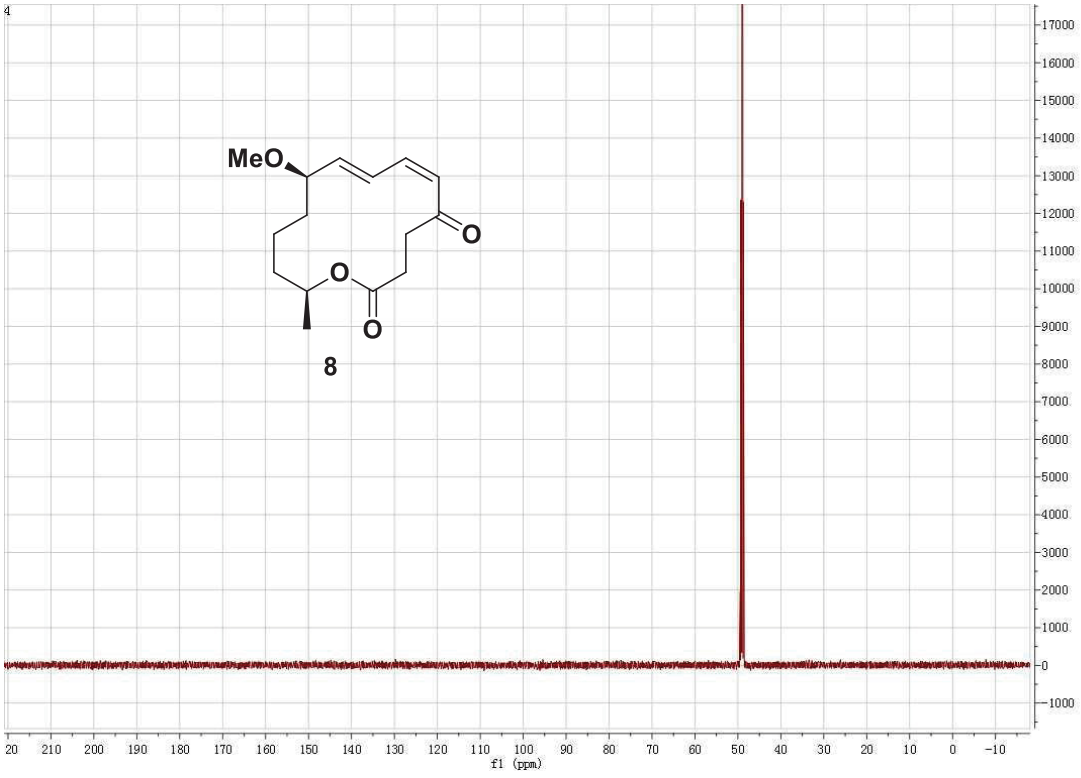

S60. ^{13}C NMR (125 MHz, CD_3OD) spectrum of compound **8**.

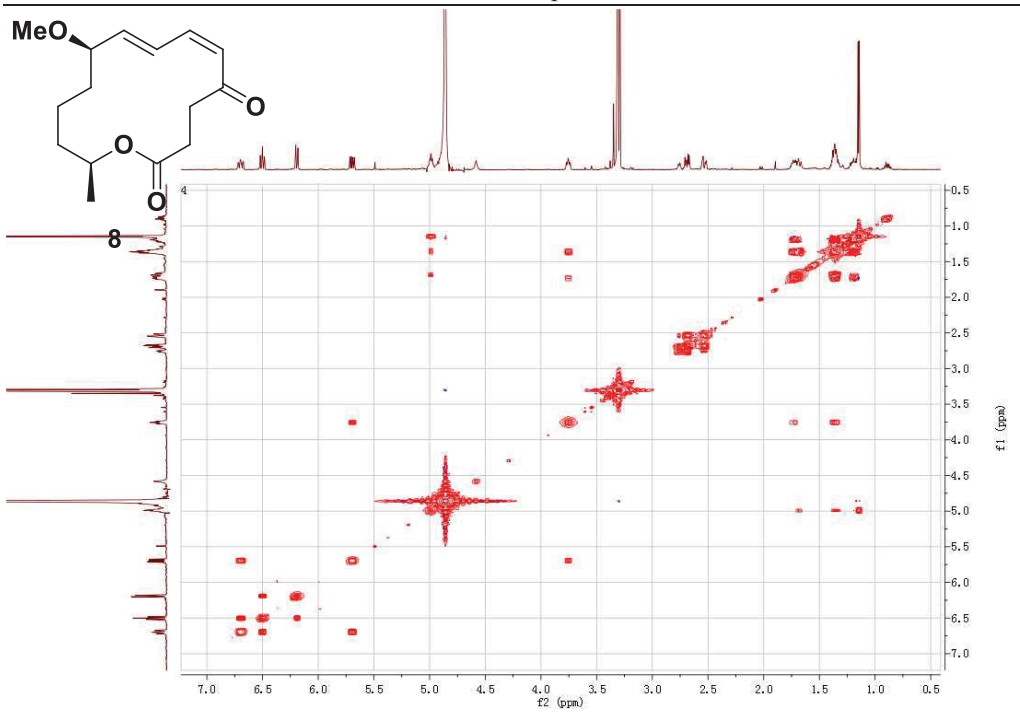

S61. ^{1}H-^{1}H COSY (600 MHz, CD_3OD) spectrum of compound **8**.

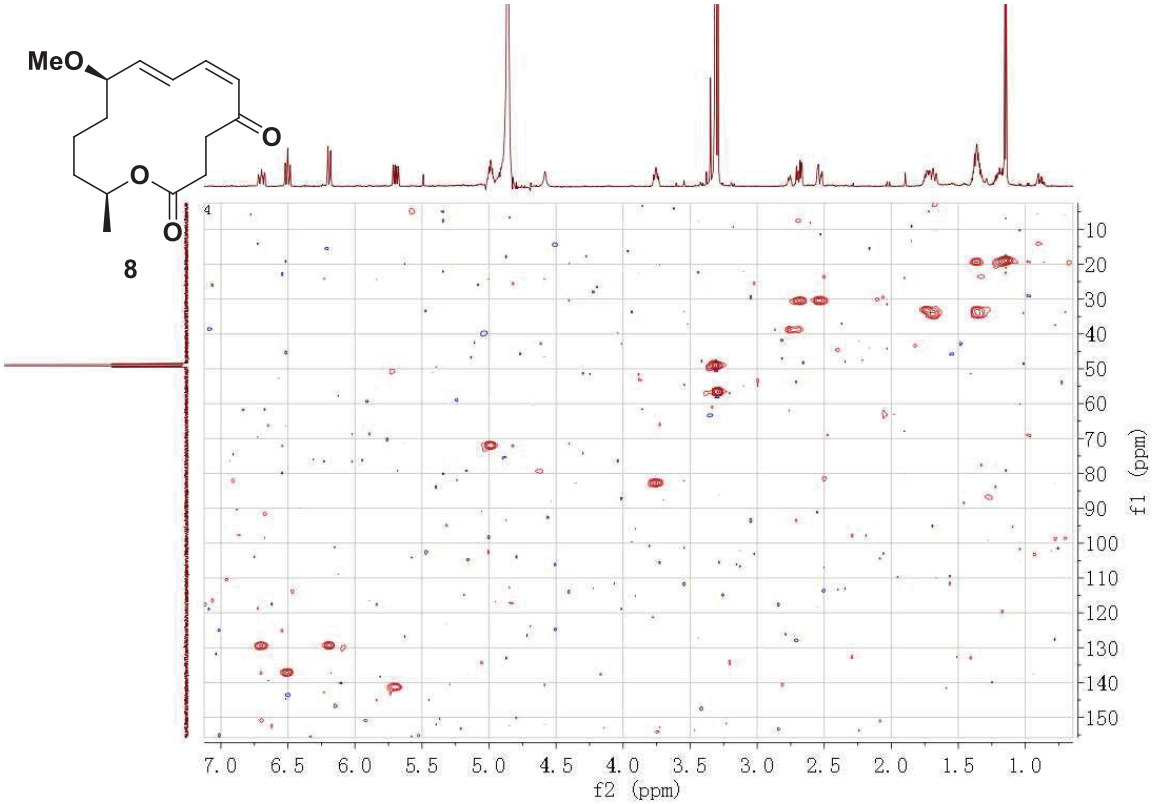

S62. HSQC (600 and 150 MHz, CD_3OD) spectrum of compound **8**.

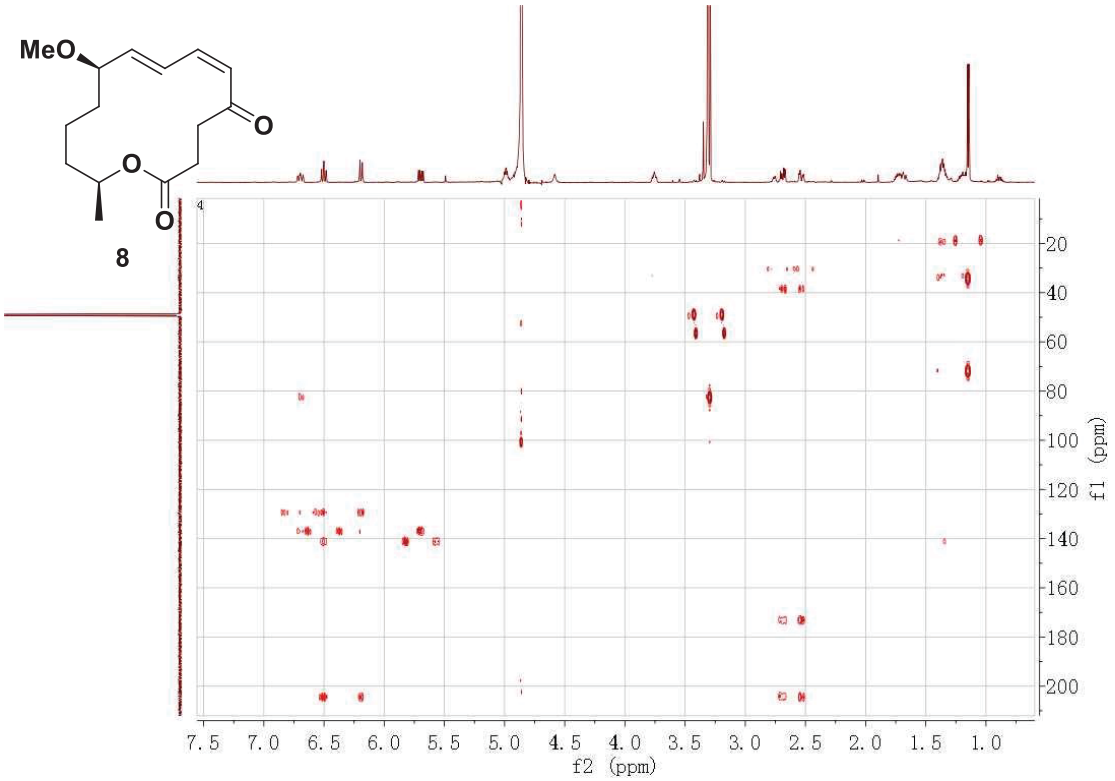

S63. HMBC (600 and 150 MHz, CD_3OD) spectrum of compound **8**.

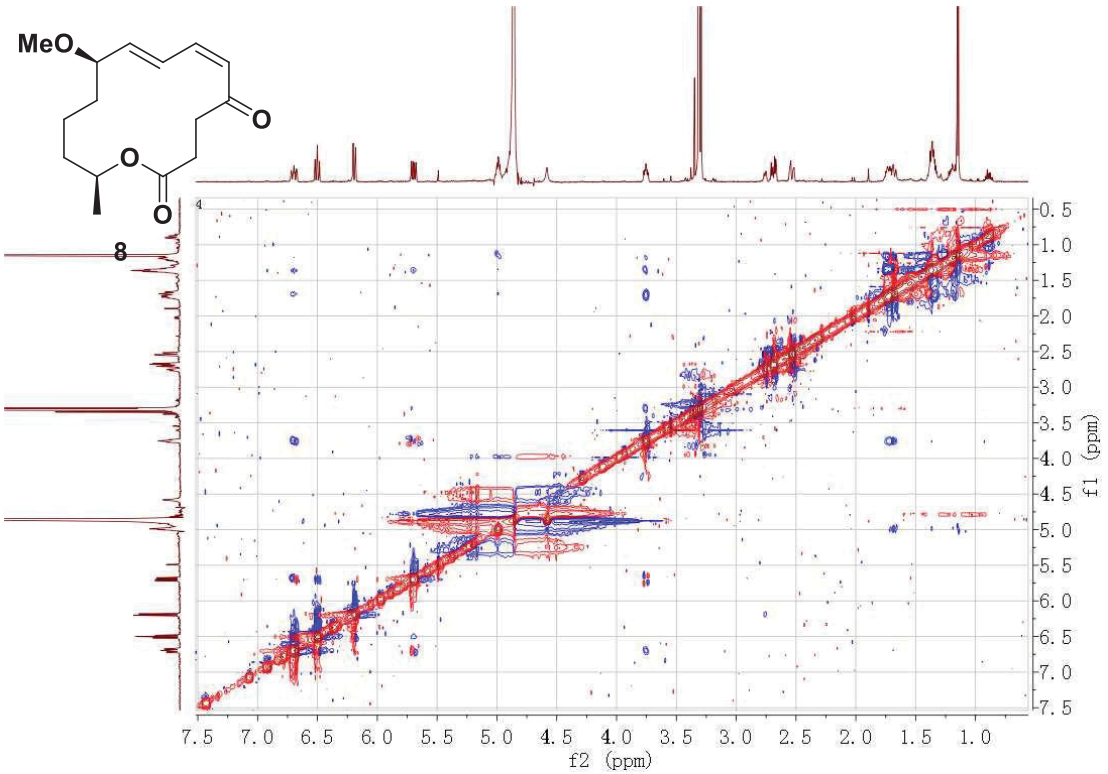

S64. ROESY (600 MHz, CD_3OD) spectrum of compound **8.**

Mass Spectrum SmartFormula Report

Analysis Info

Analysis Name	D:\Data\Spektren 2015\Proksch15HR000184.d	Acquisition Date	5/26/2015 9:09:18 AM
Method	tune_low.m	Operator	Peter Tommes
Sample Name	Shuai Liu CS-6-4(+) (CH3OH)	Instrument	maXis 288882.20213
Comment			

Acquisition Parameter

Source Type	ESI	Ion Polarity	Positive	Set Nebulizer	0.3 Bar
Focus	Not active	Set Capillary	4000 V	Set Dry Heater	180 °C
Scan Begin	50 m/z	Set End Plate Offset	-500 V	Set Dry Gas	4.0 l/min
Scan End	1500 m/z	Set Collision Cell RF	600.0 Vpp	Set Divert Valve	Source

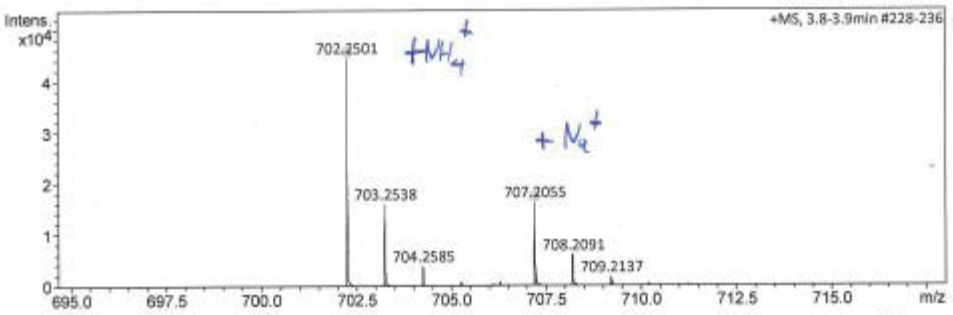

Meas. m/z	#	Ion Formula	m/z	err [ppm]	mSigma	# mSigma	Score	rdb	e⁻ Conf	N-Rule
702.2501	1	C34H38F6NO8	702.2496	-0.8	10.4	1	100.00	13.5	even	ok
	2	C31H30F6N11O2	702.2483	-2.7	12.3	2	42.38	19.5	even	ok
	3	C35H34F6N5O4	702.2510	1.1	22.2	3	68.52	18.5	even	ok
707.2055	1	C34H34F6NaO8	707.2050	-0.7	9.4	1	100.00	14.5	even	ok
	2	C31H26F6N10NaO2	707.2037	-2.6	15.4	2	39.68	20.5	even	ok
	3	C35H30F6N4NaO4	707.2063	1.2	18.1	3	69.28	19.5	even	ok

S65. HRESIMS spectrum of compound **5a.**

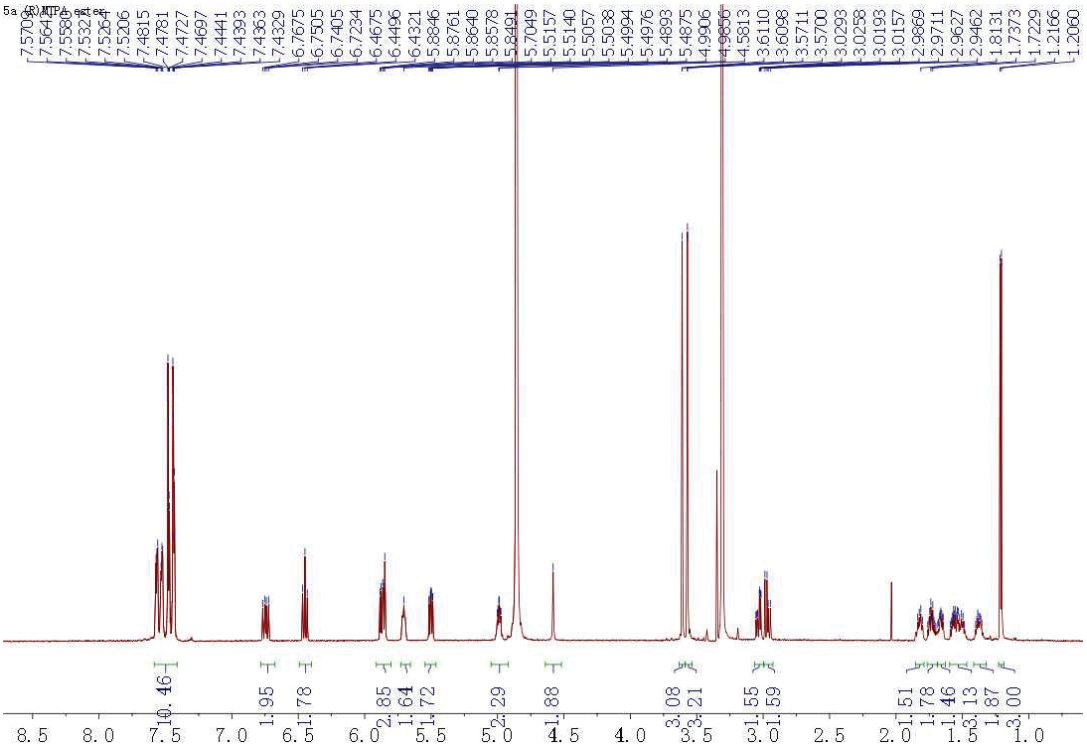

S66. ^{1}H NMR (600 MHz, CD_3OD) spectrum of compound **5a**.

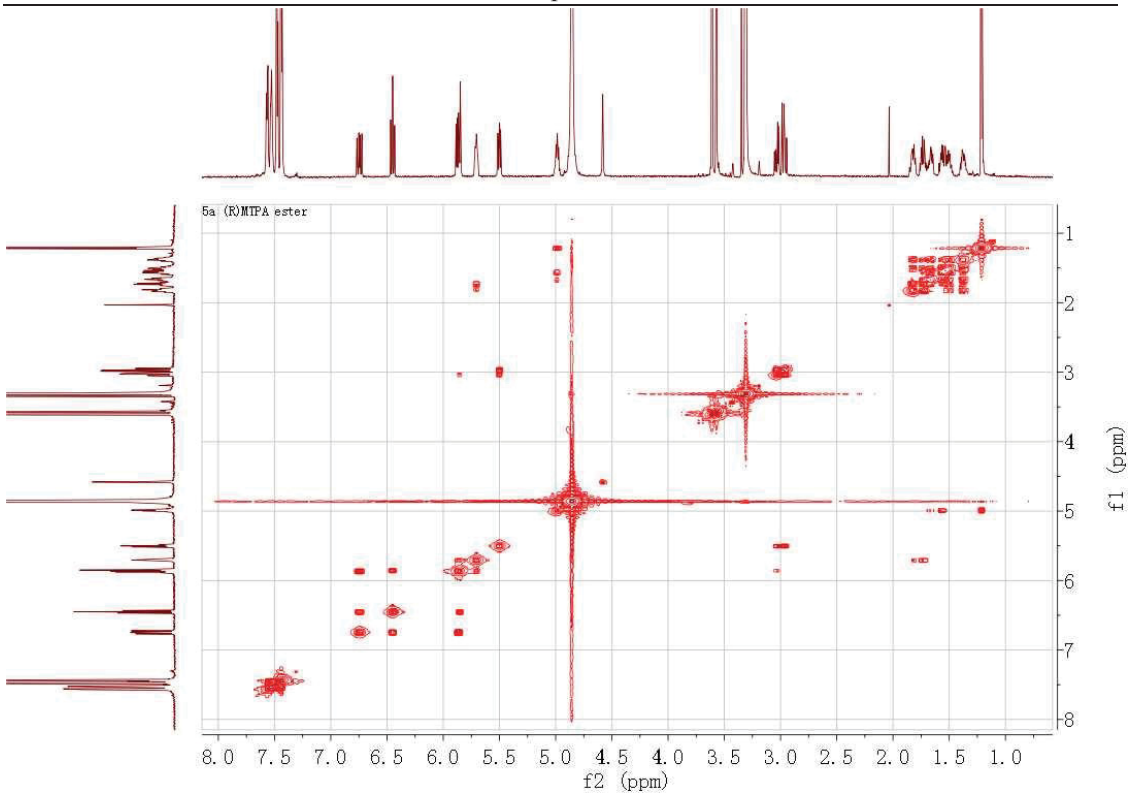

S67. ^{1}H-^{1}H COSY (600 MHz, CD_3OD) spectrum of compound **5a**.

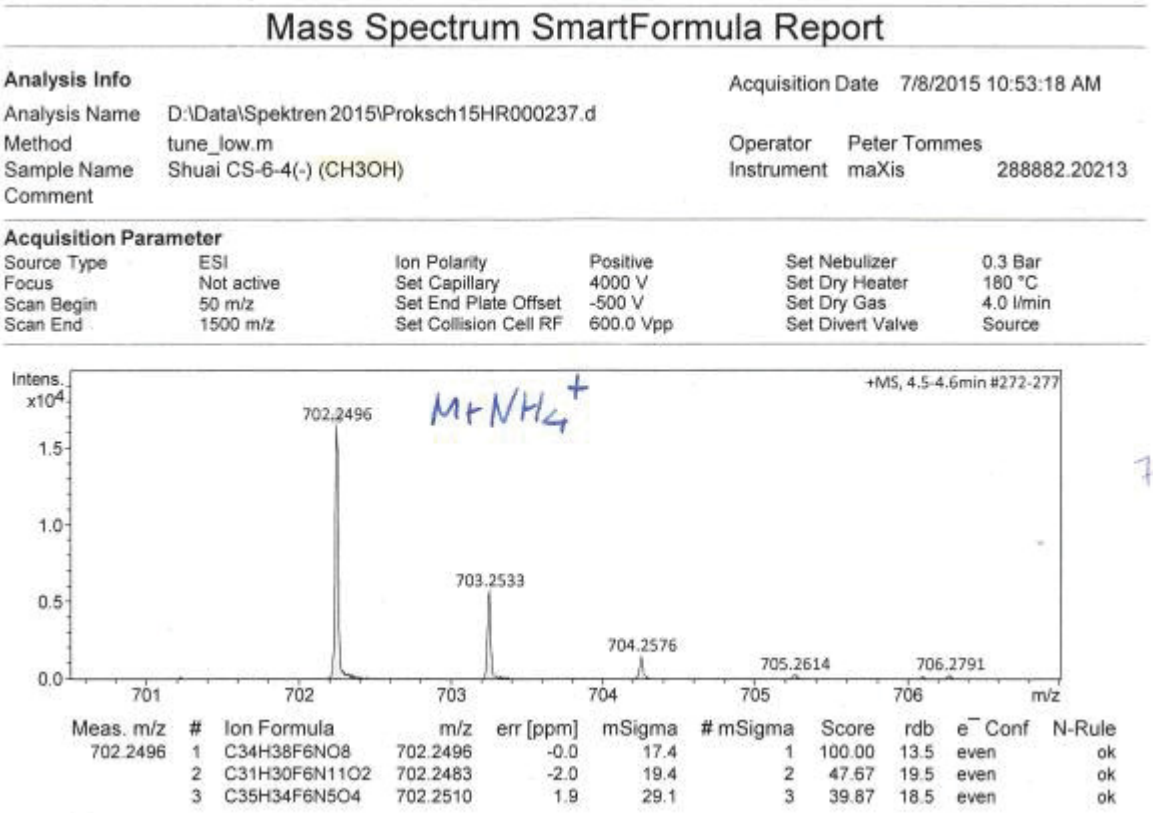

S68. HRESIMS spectrum of compound **5b.**

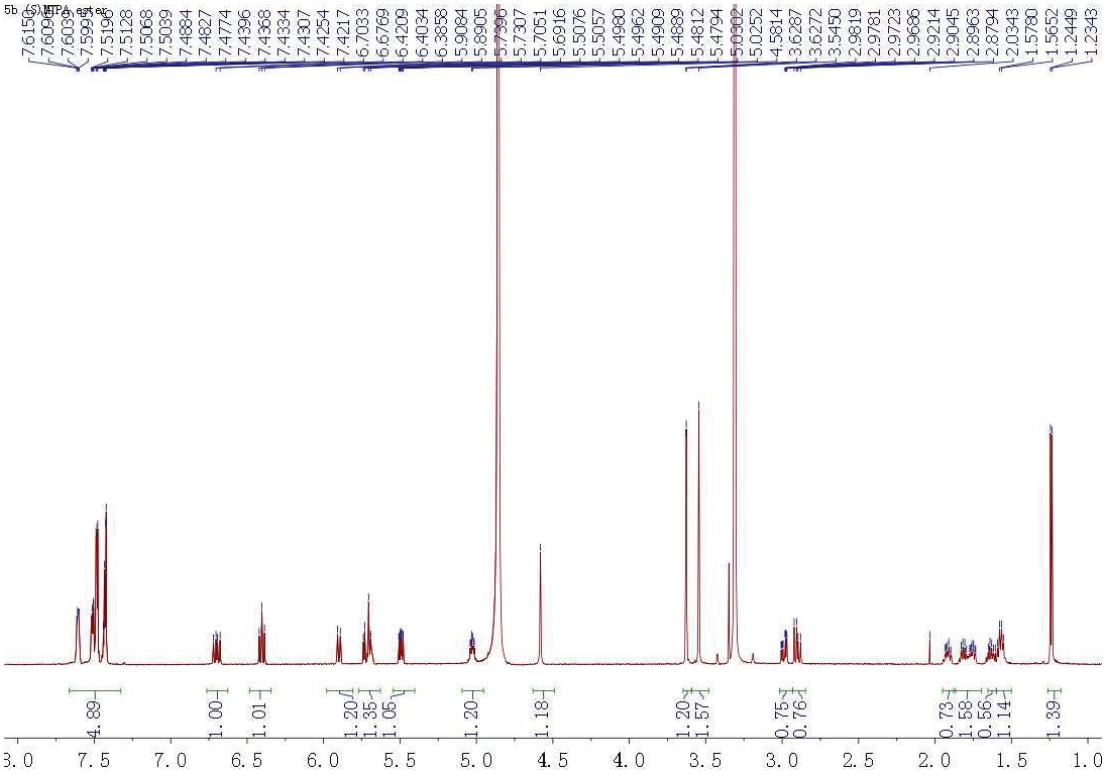

S69. ^{1}H NMR (600 MHz, CD_3OD) spectrum of compound **5b**.

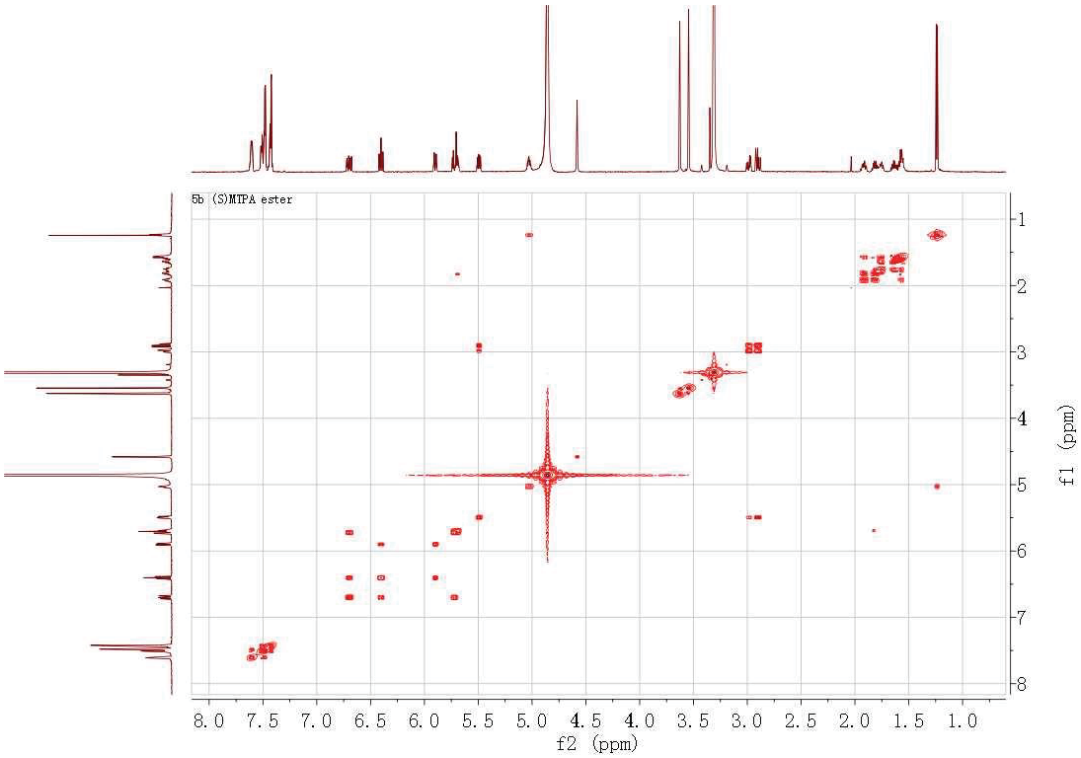

S70. ^{1}H-^{1}H COSY (600 MHz, CD_3OD) spectrum of compound **5b**.

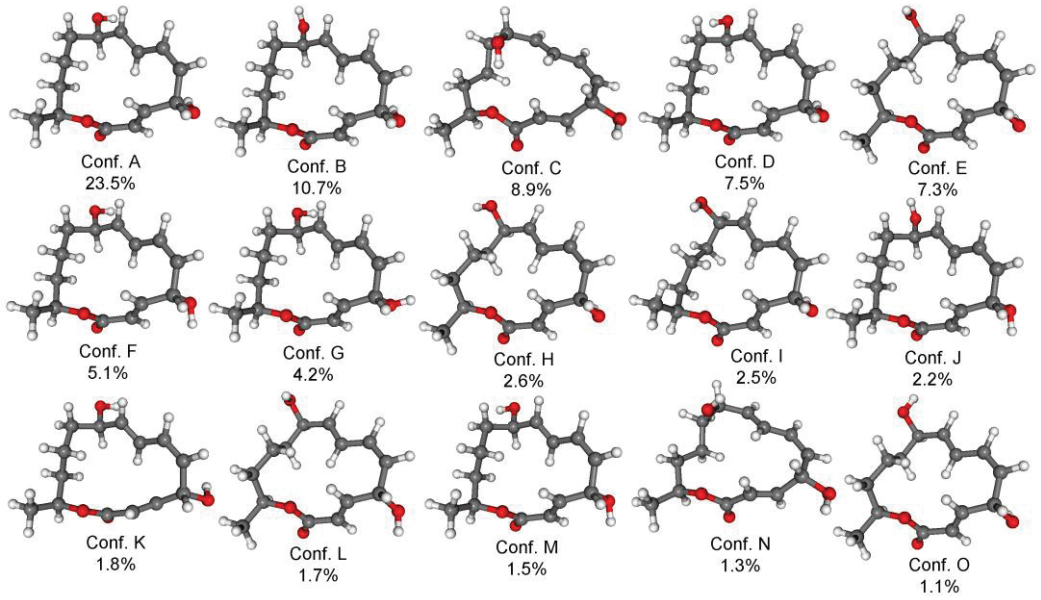

S71. Structure and population of the low-energy B97D /TZVP PCM/MeCN conformers (>1%) of (4*S*,9*R*,13*S*)-**5**.

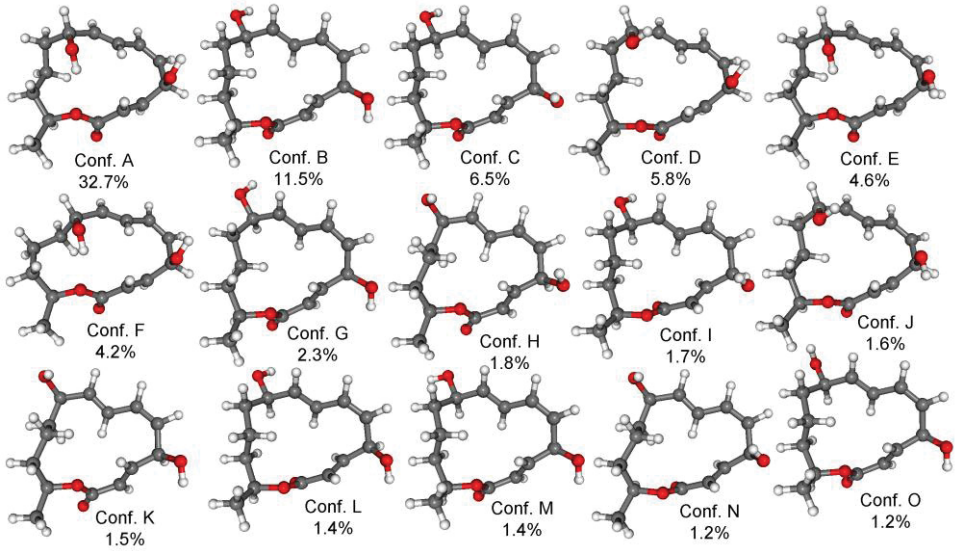

S72. Structure and population of the low-energy B3LYP/6-31G(d) conformers (>1%) of (4*R*,9*R*,13*S*)-**6**.

Results of X-ray analysis of compound **1**

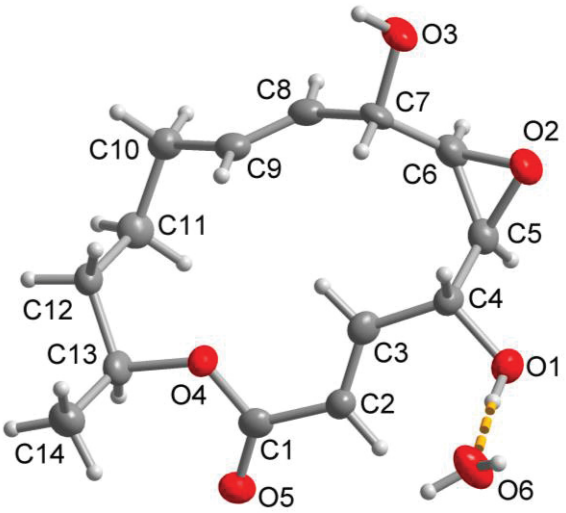

Molecular structure of pestalotioprolide B (**1**) from single-crystal X-ray diffractometry (70% thermal ellipsoids, H atoms of arbitrary radii). Compound **1** crysttallizes with a crystal water molecule. The hydrogen bond from the hydroxyl group with O1 to the crystal water molecule is depicted as a dashed orange line.

Fractional atomic coordinates and isotropic or equivalent isotropic displacement parameters (Å^2) for ***1***

	x	*y*	*z*	U_{iso}*/U_{eq}
O1	0.5785 (4)	0.5551 (3)	0.3997 (3)	0.0225 (5)
H1	0.708 (6)	0.501 (3)	0.366 (5)	0.034*
C1	0.9284 (5)	0.6016 (4)	0.8310 (4)	0.0180 (7)
H1S	1.072 (8)	0.383 (7)	0.317 (7)	0.061 (15)*
O2	0.2443 (3)	0.9457 (3)	0.3743 (2)	0.0247 (5)
C2	0.8146 (5)	0.5865 (4)	0.6815 (4)	0.0182 (6)
H2	0.8169	0.4689	0.6395	0.022*
H2S	1.003 (9)	0.402 (7)	0.150 (8)	0.070 (15)*
O3	0.3097 (4)	1.3146 (3)	0.4532 (3)	0.0262 (5)
H3A	0.400 (5)	1.394 (4)	0.442 (4)	0.039*
C3	0.7102 (5)	0.7303 (4)	0.6045 (3)	0.0192 (7)
H3	0.7180	0.8457	0.6466	0.023*
O4	0.9551 (3)	0.7707 (2)	0.8549 (2)	0.0197 (5)

C4	0.5807 (5)	0.7320 (4)	0.4583 (3)	0.0183 (6)
H4	0.6442	0.8007	0.3666	0.022*
O5	0.9902 (3)	0.4744 (3)	0.9214 (3)	0.0223 (5)
C5	0.3457 (5)	0.8251 (4)	0.4989 (4)	0.0202 (6)
H51	0.2522	0.7451	0.5538	0.024*
O6	0.9632 (4)	0.4005 (3)	0.2642 (3)	0.0311 (6)
C6	0.2674 (5)	1.0204 (4)	0.5325 (4)	0.0207 (7)
H6	0.1288	1.0496	0.6057	0.025*
C7	0.4096 (5)	1.1567 (4)	0.5420 (4)	0.0197 (7)
H7	0.5592	1.1061	0.4900	0.024*
C8	0.4185 (5)	1.2013 (4)	0.7206 (4)	0.0199 (7)
H8	0.2834	1.2454	0.7826	0.024*
C9	0.5963 (5)	1.1852 (4)	0.8004 (4)	0.0198 (7)
H9	0.7329	1.1454	0.7390	0.024*
C10	0.5972 (5)	1.2255 (4)	0.9810 (4)	0.0214 (7)
H10A	0.4450	1.2615	1.0297	0.026*
H10B	0.6680	1.3299	0.9924	0.026*
C11	0.7157 (5)	1.0633 (4)	1.0784 (4)	0.0231 (7)
H11A	0.6529	0.9562	1.0584	0.028*
H11B	0.6880	1.0919	1.1980	0.028*
C12	0.9636 (5)	1.0119 (4)	1.0349 (4)	0.0198 (6)
H12A	1.0008	1.0791	0.9341	0.024*
H12B	1.0376	1.0513	1.1262	0.024*
C13	1.0492 (5)	0.8104 (4)	1.0058 (4)	0.0206 (7)
H13	0.9953	0.7401	1.1006	0.025*
C14	1.2936 (5)	0.7557 (4)	0.9803 (4)	0.0265 (7)
H14A	1.3357	0.6283	0.9448	0.040*
H14B	1.3565	0.7699	1.0844	0.040*
H14C	1.3476	0.8334	0.8952	0.040*

*Atomic displacement parameters (Å^2) for **1***

	U^{11}	U^{22}	U^{33}	U^{12}	U^{13}	U^{23}
O1	0.0247 (12)	0.0212 (11)	0.0216 (11)	-0.0035 (8)	-0.0041 (9)	-0.0045 (8)
C1	0.0162 (15)	0.0176 (16)	0.0180 (15)	-0.0003 (12)	0.0020 (12)	-0.0009 (13)
O2	0.0288 (12)	0.0256 (12)	0.0200 (12)	-0.0036 (9)	-0.0100 (9)	0.0014 (9)
C2	0.0186 (15)	0.0160 (15)	0.0202 (15)	-0.0035 (12)	-0.0028 (11)	-0.0015 (12)
O3	0.0276 (12)	0.0234 (12)	0.0293 (13)	-0.0061 (10)	-0.0120 (9)	0.0097 (9)
C3	0.0230 (16)	0.0194 (15)	0.0144 (14)	-0.0035 (13)	0.0008 (11)	-0.0035 (12)
O4	0.0260 (12)	0.0163 (11)	0.0179 (11)	-0.0053 (8)	-0.0063 (8)	0.0001 (8)
C4	0.0229 (16)	0.0158 (14)	0.0168 (14)	-0.0041 (12)	-0.0038 (11)	-0.0004 (12)
O5	0.0260 (12)	0.0196 (11)	0.0201 (11)	-0.0014 (8)	-0.0033 (8)	0.0021 (8)
C5	0.0218 (15)	0.0234 (16)	0.0165 (15)	-0.0059 (12)	-0.0039 (11)	0.0006 (12)
O6	0.0261 (14)	0.0433 (14)	0.0203 (14)	0.0029 (11)	-0.0064 (10)	-0.0018 (10)
C6	0.0194 (16)	0.0235 (16)	0.0183 (16)	-0.0014 (12)	-0.0042 (12)	0.0010 (12)
C7	0.0180 (15)	0.0174 (15)	0.0223 (17)	0.0015 (12)	-0.0069 (12)	0.0043 (11)
C8	0.0199 (16)	0.0143 (14)	0.0238 (16)	-0.0006 (11)	0.0000 (12)	0.0019 (12)
C9	0.0208 (16)	0.0152 (14)	0.0221 (16)	-0.0015 (12)	-0.0009 (12)	0.0013 (11)
C10	0.0222 (16)	0.0192 (15)	0.0218 (17)	-0.0017 (13)	-0.0017 (12)	-0.0020 (12)
C11	0.0272 (17)	0.0246 (16)	0.0172 (15)	-0.0050 (13)	-0.0008 (12)	0.0010 (12)
C12	0.0240 (16)	0.0185 (14)	0.0182 (15)	-0.0055 (12)	-0.0073 (11)	0.0006 (11)
C13	0.0273 (17)	0.0215 (16)	0.0144 (15)	-0.0066 (13)	-0.0068 (12)	0.0012 (12)
C14	0.0251 (18)	0.0253 (16)	0.0289 (17)	-0.0031 (13)	-0.0068 (13)	0.0008 (13)

*Geometric parameters (Å, º) for **1***

O1—C4	1.423 (3)	C6—H6	1.0000
O1—H1	0.86 (4)	C7—C8	1.501 (4)
C1—O5	1.212 (4)	C7—H7	1.0000
C1—O4	1.335 (3)	C8—C9	1.325 (5)
C1—C2	1.479 (4)	C8—H8	0.9500
O2—C6	1.441 (4)	C9—C10	1.502 (4)
O2—C5	1.444 (4)	C9—H9	0.9500
C2—C3	1.318 (4)	C10—C11	1.533 (5)
C2—H2	0.9500	C10—H10A	0.9900
O3—C7	1.434 (4)	C10—H10B	0.9900

O3—H3A	0.90 (4)	C11—C12	1.541 (4)
C3—C4	1.495 (4)	C11—H11A	0.9900
C3—H3	0.9500	C11—H11B	0.9900
O4—C13	1.467 (3)	C12—C13	1.512 (4)
C4—C5	1.511 (4)	C12—H12A	0.9900
C4—H4	1.0000	C12—H12B	0.9900
C5—C6	1.469 (4)	C13—C14	1.507 (4)
C5—H51	1.0000	C13—H13	1.0000
O6—H1S	0.83 (5)	C14—H14A	0.9800
O6—H2S	0.94 (6)	C14—H14B	0.9800
C6—C7	1.503 (4)	C14—H14C	0.9800
C4—O1—H1	109.5	C6—C7—H7	110.3
O5—C1—O4	124.0 (3)	C9—C8—C7	126.4 (3)
O5—C1—C2	123.6 (2)	C9—C8—H8	116.8
O4—C1—C2	112.5 (2)	C7—C8—H8	116.8
C6—O2—C5	61.24 (19)	C8—C9—C10	124.6 (3)
C3—C2—C1	122.4 (2)	C8—C9—H9	117.7
C3—C2—H2	118.8	C10—C9—H9	117.7
C1—C2—H2	118.8	C9—C10—C11	113.1 (2)
C7—O3—H3A	109.5	C9—C10—H10A	109.0
C2—C3—C4	127.2 (2)	C11—C10—H10A	109.0
C2—C3—H3	116.4	C9—C10—H10B	109.0
C4—C3—H3	116.4	C11—C10—H10B	109.0
C1—O4—C13	118.8 (2)	H10A—C10—H10B	107.8
O1—C4—C3	113.6 (2)	C10—C11—C12	114.7 (2)
O1—C4—C5	106.4 (2)	C10—C11—H11A	108.6
C3—C4—C5	111.2 (2)	C12—C11—H11A	108.6
O1—C4—H4	108.5	C10—C11—H11B	108.6
C3—C4—H4	108.5	C12—C11—H11B	108.6
C5—C4—H4	108.5	H11A—C11—H11B	107.6
O2—C5—C6	59.27 (18)	C13—C12—C11	113.7 (2)
O2—C5—C4	116.6 (2)	C13—C12—H12A	108.8

C6—C5—C4	125.3 (3)	C11—C12—H12A	108.8
O2—C5—H51	114.6	C13—C12—H12B	108.8
C6—C5—H51	114.6	C11—C12—H12B	108.8
C4—C5—H51	114.6	H12A—C12—H12B	107.7
H1S—O6—H2S	111 (5)	O4—C13—C14	109.2 (2)
O2—C6—C5	59.49 (18)	O4—C13—C12	104.8 (2)
O2—C6—C7	119.5 (2)	C14—C13—C12	114.2 (2)
C5—C6—C7	125.3 (3)	O4—C13—H13	109.5
O2—C6—H6	113.9	C14—C13—H13	109.5
C5—C6—H6	113.9	C12—C13—H13	109.5
C7—C6—H6	113.9	C13—C14—H14A	109.5
O3—C7—C8	110.9 (2)	C13—C14—H14B	109.5
O3—C7—C6	106.4 (2)	H14A—C14—H14B	109.5
C8—C7—C6	108.7 (2)	C13—C14—H14C	109.5
O3—C7—H7	110.3	H14A—C14—H14C	109.5
C8—C7—H7	110.3	H14B—C14—H14C	109.5
O5—C1—C2—C3	165.7 (3)	C4—C5—C6—C7	-4.0 (5)
O4—C1—C2—C3	-14.2 (4)	O2—C6—C7—O3	64.8 (3)
C1—C2—C3—C4	-176.7 (3)	C5—C6—C7—O3	136.5 (3)
O5—C1—O4—C13	-4.9 (4)	O2—C6—C7—C8	-175.8 (2)
C2—C1—O4—C13	175.0 (2)	C5—C6—C7—C8	-104.1 (3)
C2—C3—C4—O1	-1.0 (4)	O3—C7—C8—C9	-119.7 (3)
C2—C3—C4—C5	119.0 (3)	C6—C7—C8—C9	123.7 (3)
C6—O2—C5—C4	-117.0 (3)	C7—C8—C9—C10	-177.8 (3)
O1—C4—C5—O2	-97.6 (3)	C8—C9—C10—C11	123.1 (3)
C3—C4—C5—O2	138.2 (2)	C9—C10—C11—C12	68.1 (3)
O1—C4—C5—C6	-167.4 (3)	C10—C11—C12—C13	-132.4 (3)
C3—C4—C5—C6	68.5 (4)	C1—O4—C13—C14	82.8 (3)
C5—O2—C6—C7	115.9 (3)	C1—O4—C13—C12	-154.4 (2)
C4—C5—C6—O2	102.5 (3)	C11—C12—C13—O4	66.5 (3)
O2—C5—C6—C7	-106.5 (3)	C11—C12—C13—C1	-174.1 (3)

		4	

Hydrogen-bond geometry (Å, º) for ***1***

D—H···*A*	*D*—H	H···*A*	*D*···*A*	*D*—H···*A*
O1—H1···O6	0.86	1.77	2.617 (3)	170
O6—H1*S*···O3^{i}	0.83 (5)	1.92 (5)	2.737 (3)	172 (5)
O6—H2*S*···O5^{ii}	0.94 (6)	1.93 (6)	2.822 (3)	159 (5)
O3—H3*A*···O1^{iii}	0.90	1.83	2.731 (3)	175
C8—H8···O5^{iv}	0.95	2.46	3.347 (3)	156
C10—H10*B*···O5^{iii}	0.99	2.52	3.403 (4)	149

Symmetry codes: (i) *x*+1, *y*-1, *z*; (ii) *x*, *y*, *z*-1; (iii) *x*, *y*+1, *z*; (iv) *x*-1, *y*+1, *z*;

Figures for packing diagram and hydrogen-bonding network in **1**:

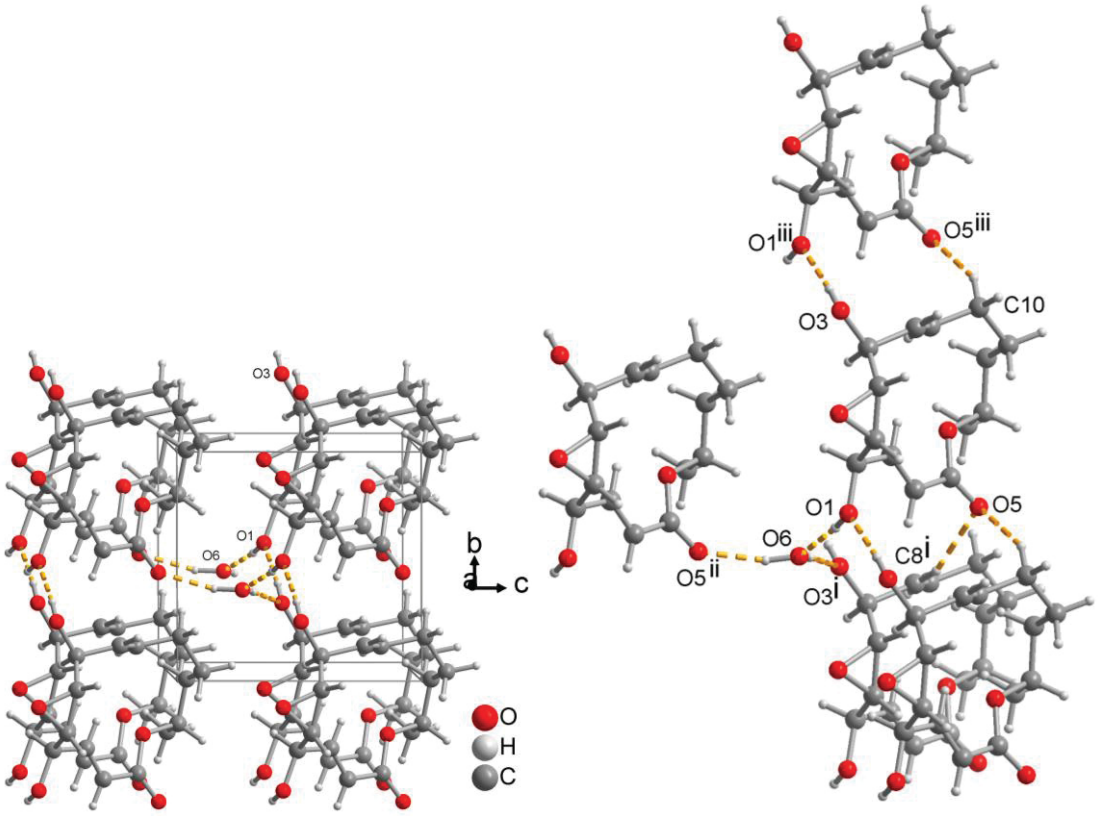

Results of X-ray analysis of compound **2**

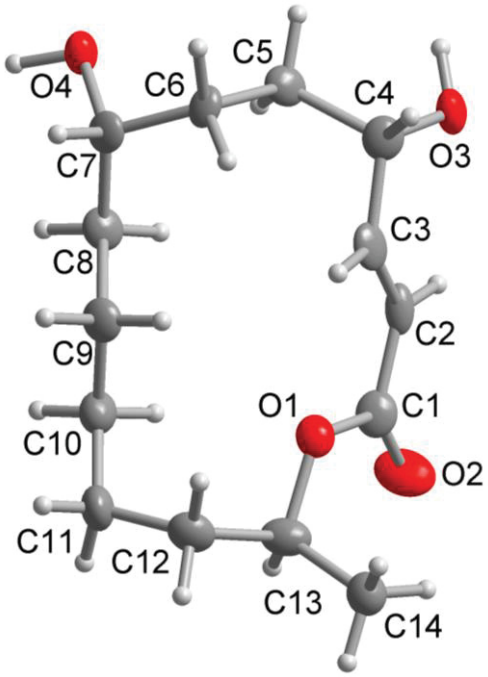

Molecular structure of pestalotioprolide C (**2**) from single-crystal X-ray diffractometry (50% thermal ellipsoids, H atoms of arbitrary radii).

Fractional atomic coordinates and isotropic or equivalent isotropic displacement parameters (Å^2) for ***2***

	x	*y*	*z*	U_{iso}*/U_{eq}
O1	0.41196 (13)	0.3777 (10)	0.4915 (7)	0.0301 (12)
O2	0.41352 (16)	0.7715 (12)	0.6378 (10)	0.0505 (17)
O3	0.28404 (14)	0.4453 (11)	0.7020 (7)	0.0305 (12)
H3O	0.259 (2)	0.48 (2)	0.675 (13)	0.046*
O4	0.27184 (13)	0.2761 (11)	0.0400 (6)	0.0297 (12)
H4O	0.275 (2)	0.35 (2)	-0.081 (13)	0.045*
C1	0.3970 (2)	0.5736 (14)	0.5904 (11)	0.0323 (17)
C2	0.3579 (2)	0.5253 (15)	0.6241 (9)	0.0286 (16)
H2	0.3442	0.6603	0.6831	0.034*
C3	0.3408 (2)	0.3014 (15)	0.5756 (10)	0.0300 (17)
H3	0.3554	0.1625	0.5266	0.036*
C4	0.30074 (19)	0.2479 (15)	0.5909 (10)	0.0307 (16)
H4	0.2973	0.0668	0.6456	0.037*
C5	0.28227 (18)	0.2460 (15)	0.4104 (10)	0.0292 (16)

H5A	0.2849	0.4273	0.3582	0.035*
H5B	0.2558	0.2122	0.4270	0.035*
C6	0.2972 (2)	0.0370 (14)	0.2787 (10)	0.0255 (15)
H6A	0.3200	-0.0419	0.3265	0.031*
H6B	0.2791	-0.1101	0.2665	0.031*
C7	0.30522 (18)	0.1518 (15)	0.0988 (10)	0.0284 (16)
H7	0.3111	-0.0007	0.0183	0.034*
C8	0.33654 (19)	0.3526 (15)	0.0923 (11)	0.0308 (16)
H8A	0.3334	0.4826	0.1893	0.037*
H8B	0.3348	0.4546	-0.0186	0.037*
C9	0.37489 (19)	0.2305 (16)	0.1053 (11)	0.0329 (17)
H9A	0.3772	0.1309	0.2168	0.039*
H9B	0.3785	0.1011	0.0084	0.039*
C10	0.4042 (2)	0.4462 (17)	0.0965 (11)	0.0364 (18)
H10A	0.4000	0.5761	0.1925	0.044*
H10B	0.4015	0.5449	-0.0152	0.044*
C11	0.4436 (2)	0.342 (2)	0.1098 (11)	0.041 (2)
H11A	0.4604	0.4937	0.0845	0.050*
H11B	0.4473	0.2054	0.0173	0.050*
C12	0.4549 (2)	0.2176 (18)	0.2857 (11)	0.0389 (19)
H12A	0.4403	0.0519	0.3033	0.047*
H12B	0.4809	0.1631	0.2776	0.047*
C13	0.45040 (19)	0.3943 (16)	0.4477 (11)	0.0349 (19)
H13	0.4567	0.5845	0.4173	0.042*
C14	0.4734 (2)	0.3051 (17)	0.6018 (11)	0.0365 (18)
H14A	0.4677	0.4173	0.7035	0.055*
H14B	0.4994	0.3237	0.5726	0.055*
H14C	0.4680	0.1165	0.6289	0.055*

Atomic displacement parameters (Å^2) for ***2***

	U^{11}	U^{22}	U^{33}	U^{12}	U^{13}	U^{23}

O1	0.038 (3)	0.021 (2)	0.031 (3)	-0.001 (2)	0.002 (2)	-0.002 (2)
O2	0.049 (3)	0.024 (3)	0.078 (5)	-0.006 (3)	0.011 (3)	-0.005 (3)
O3	0.039 (3)	0.033 (3)	0.019 (3)	0.008 (2)	0.003 (2)	0.001 (2)
O4	0.036 (2)	0.031 (3)	0.022 (3)	0.006 (2)	0.0006 (19)	0.001 (2)
C1	0.046 (4)	0.016 (4)	0.035 (4)	0.004 (3)	-0.001 (3)	0.002 (3)
C2	0.051 (4)	0.018 (4)	0.017 (4)	0.011 (3)	0.002 (3)	0.002 (3)
C3	0.045 (4)	0.023 (4)	0.022 (4)	0.006 (3)	0.003 (3)	0.013 (3)
C4	0.039 (4)	0.019 (3)	0.035 (4)	0.007 (3)	-0.001 (3)	0.002 (3)
C5	0.034 (3)	0.021 (3)	0.033 (4)	0.002 (3)	0.002 (3)	0.010 (4)
C6	0.037 (4)	0.016 (3)	0.023 (4)	0.002 (3)	-0.004 (3)	-0.006 (3)
C7	0.034 (4)	0.023 (4)	0.028 (4)	0.007 (3)	0.002 (3)	-0.011 (3)
C8	0.038 (4)	0.021 (4)	0.033 (4)	0.002 (3)	0.002 (3)	0.008 (4)
C9	0.039 (4)	0.027 (4)	0.033 (4)	0.005 (3)	0.004 (3)	-0.008 (4)
C10	0.041 (4)	0.040 (4)	0.028 (4)	-0.006 (3)	0.000 (3)	0.004 (4)
C11	0.043 (4)	0.058 (6)	0.023 (4)	-0.003 (4)	0.004 (3)	-0.001 (4)
C12	0.031 (4)	0.040 (5)	0.046 (5)	0.004 (4)	0.003 (3)	0.003 (4)
C13	0.029 (4)	0.023 (4)	0.053 (5)	0.001 (3)	0.002 (3)	0.001 (4)
C14	0.040 (4)	0.037 (5)	0.033 (4)	-0.002 (3)	0.002 (3)	-0.002 (4)

Geometric parameters (Å, º) for ***2***

O1—C1	1.349 (10)	C7—H7	1.0000
O1—C13	1.446 (8)	C8—C9	1.530 (9)
O2—C1	1.210 (10)	C8—H8A	0.9900
O3—C4	1.434 (9)	C8—H8B	0.9900
O3—H3O	0.95 (9)	C9—C10	1.518 (11)
O4—C7	1.440 (8)	C9—H9A	0.9900
O4—H4O	0.99 (10)	C9—H9B	0.9900
C1—C2	1.472 (11)	C10—C11	1.533 (11)
C2—C3	1.328 (11)	C10—H10A	0.9900
C2—H2	0.9500	C10—H10B	0.9900
C3—C4	1.492 (10)	C11—C12	1.537 (12)
C3—H3	0.9500	C11—H11A	0.9900
C4—C5	1.537 (10)	C11—H11B	0.9900

C4—H4	1.0000	C12—C13	1.527 (12)
C5—C6	1.546 (10)	C12—H12A	0.9900
C5—H5A	0.9900	C12—H12B	0.9900
C5—H5B	0.9900	C13—C14	1.514 (11)
C6—C7	1.517 (11)	C13—H13	1.0000
C6—H6A	0.9900	C14—H14A	0.9800
C6—H6B	0.9900	C14—H14B	0.9800
C7—C8	1.519 (10)	C14—H14C	0.9800
C1—O1—C13	118.8 (6)	C7—C8—H8B	108.5
C4—O3—H3O	113 (6)	C9—C8—H8B	108.5
C7—O4—H4O	110 (5)	H8A—C8—H8B	107.5
O2—C1—O1	123.6 (7)	C10—C9—C8	111.4 (7)
O2—C1—C2	124.4 (7)	C10—C9—H9A	109.4
O1—C1—C2	112.0 (6)	C8—C9—H9A	109.4
C3—C2—C1	122.9 (7)	C10—C9—H9B	109.4
C3—C2—H2	118.5	C8—C9—H9B	109.4
C1—C2—H2	118.5	H9A—C9—H9B	108.0
C2—C3—C4	126.0 (7)	C9—C10—C11	115.0 (7)
C2—C3—H3	117.0	C9—C10—H10A	108.5
C4—C3—H3	117.0	C11—C10—H10A	108.5
O3—C4—C3	110.0 (6)	C9—C10—H10B	108.5
O3—C4—C5	110.5 (5)	C11—C10—H10B	108.5
C3—C4—C5	111.2 (6)	H10A—C10—H10B	107.5
O3—C4—H4	108.4	C10—C11—C12	116.4 (6)
C3—C4—H4	108.4	C10—C11—H11A	108.2
C5—C4—H4	108.4	C12—C11—H11A	108.2
C4—C5—C6	115.8 (6)	C10—C11—H11B	108.2
C4—C5—H5A	108.3	C12—C11—H11B	108.2
C6—C5—H5A	108.3	H11A—C11—H11B	107.4
C4—C5—H5B	108.3	C13—C12—C11	116.8 (7)
C6—C5—H5B	108.3	C13—C12—H12A	108.1
H5A—C5—H5B	107.4	C11—C12—H12A	108.1

C7—C6—C5	114.0 (6)	C13—C12—H12B	108.1
C7—C6—H6A	108.8	C11—C12—H12B	108.1
C5—C6—H6A	108.8	H12A—C12—H12B	107.3
C7—C6—H6B	108.8	O1—C13—C14	110.0 (6)
C5—C6—H6B	108.8	O1—C13—C12	105.0 (6)
H6A—C6—H6B	107.7	C14—C13—C12	113.8 (6)
O4—C7—C6	106.3 (5)	O1—C13—H13	109.3
O4—C7—C8	110.2 (6)	C14—C13—H13	109.3
C6—C7—C8	115.0 (6)	C12—C13—H13	109.3
O4—C7—H7	108.4	C13—C14—H14A	109.5
C6—C7—H7	108.4	C13—C14—H14B	109.5
C8—C7—H7	108.4	H14A—C14—H14B	109.5
C7—C8—C9	115.3 (6)	C13—C14—H14C	109.5
C7—C8—H8A	108.5	H14A—C14—H14C	109.5
C9—C8—H8A	108.5	H14B—C14—H14C	109.5
C13—O1—C1—O2	3.9 (11)	C5—C6—C7—C8	66.8 (8)
C13—O1—C1—C2	-179.5 (6)	O4—C7—C8—C9	-164.8 (6)
O2—C1—C2—C3	-177.6 (8)	C6—C7—C8—C9	75.1 (8)
O1—C1—C2—C3	5.9 (10)	C7—C8—C9—C10	179.7 (7)
C1—C2—C3—C4	-174.3 (7)	C8—C9—C10—C11	179.6 (7)
C2—C3—C4—O3	-13.3 (10)	C9—C10—C11—C12	-66.6 (10)
C2—C3—C4—C5	109.4 (8)	C10—C11—C12—C13	-56.6 (10)
O3—C4—C5—C6	-178.7 (6)	C1—O1—C13—C14	78.4 (8)
C3—C4—C5—C6	58.8 (8)	C1—O1—C13—C12	-158.7 (6)
C4—C5—C6—C7	-132.0 (6)	C11—C12—C13—O1	80.0 (8)
C5—C6—C7—O4	-55.4 (7)	C11—C12—C13—C14	-159.6 (7)

Hydrogen-bond geometry (Å, º) for ***2***

D—H···*A*	*D*—H	H···*A*	*D*···*A*	*D*—H···*A*
O3—H3···O4^{i}	0.95 (9)	1.96 (10)	2.760 (7)	140 (8)
O4—H4···O3^{ii}	0.99 (10)	1.76 (10)	2.754 (7)	175 (9)

C14—H14···O2^{iii}	0.98	2.63	3.448 (10)	141

Symmetry codes: (i) -*x*+1/2, -*y*+1, *z*+1/2; (ii) *x*, *y*, *z*-1; (iii) *x*, *y*-1, *z*.

Figures for packing diagram and hydrogen-bonding network in **2**:

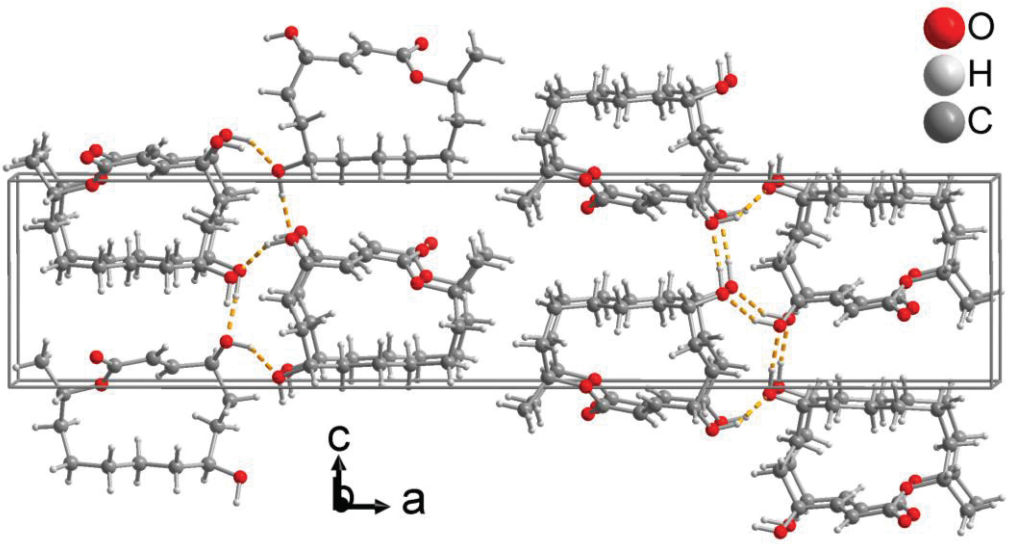

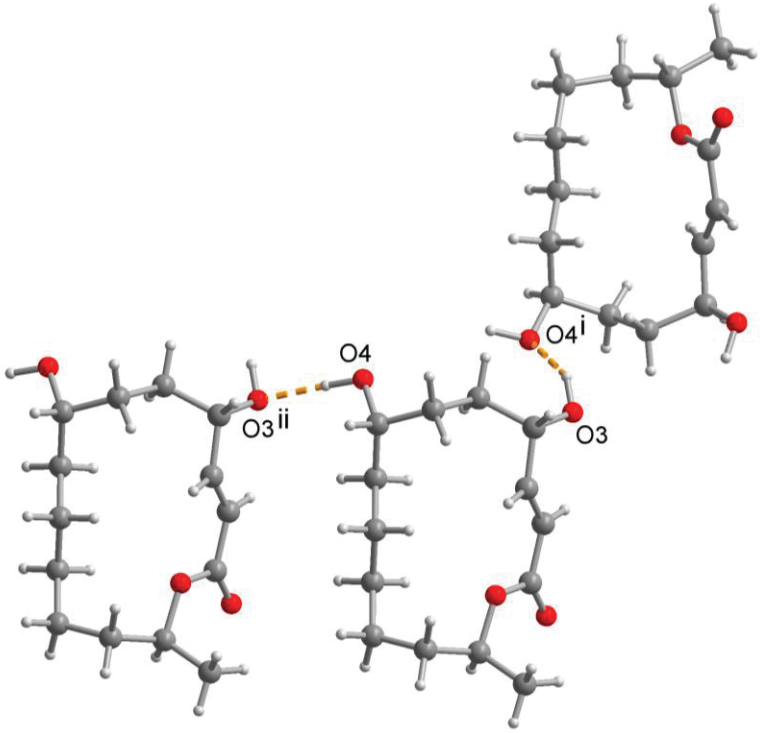

Results of X-ray analysis of compound **10**

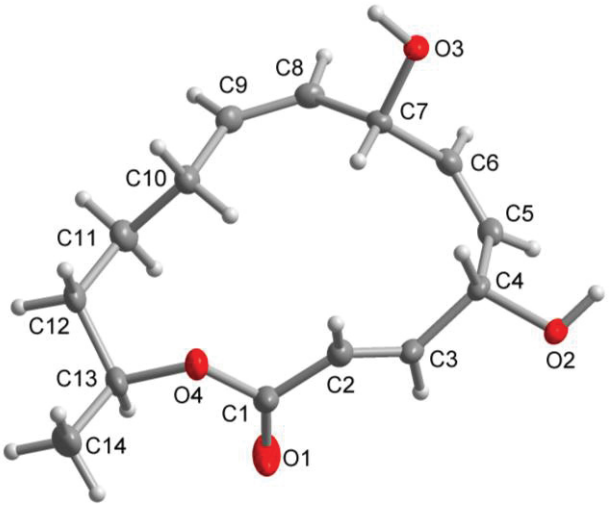

Molecular structure of nigrosporolide (**10**) from single-crystal X-ray diffractometry (50% thermal ellipsoids, H atoms of arbitrary radii).

The following data is from the Mo-Kα data set.

*Fractional atomic coordinates and isotropic or equivalent isotropic displacement parameters (Å^2) for **10** (Mo-Kα data set)*

	x	*y*	*z*	U_{iso}*/U_{eq}
O1	0.6715 (5)	0.8228 (2)	0.58066 (4)	0.0679 (7)
H2	1.064 (9)	0.873 (5)	0.7339 (10)	0.102*
C1	0.8334 (5)	0.7146 (2)	0.59127 (5)	0.0327 (5)
O2	1.0135 (3)	0.90000 (16)	0.71121 (3)	0.0230 (3)
C2	0.9594 (4)	0.7057 (2)	0.62752 (5)	0.0262 (4)
H2A	1.1256	0.6400	0.6309	0.031*
O3	0.8506 (3)	0.24890 (17)	0.72354 (3)	0.0211 (3)
C3	0.8462 (4)	0.7868 (2)	0.65523 (5)	0.0231 (4)
H3A	0.7118	0.8760	0.6509	0.028*
C11	0.5045 (4)	0.2839 (3)	0.57786 (5)	0.0291 (4)
H11A	0.3766	0.3830	0.5830	0.035*
H11B	0.3887	0.1801	0.5720	0.035*
C4	0.9218 (4)	0.7434 (2)	0.69313 (5)	0.0188 (4)
H4A	1.0747	0.6542	0.6933	0.023*
C5	0.6690 (4)	0.6689 (2)	0.71196 (5)	0.0206 (4)
H5A	0.5567	0.7508	0.7247	0.025*

C10	0.6708 (4)	0.2438 (3)	0.61197 (5)	0.0235 (4)
H10A	0.8032	0.1469	0.6071	0.028*
H10B	0.7800	0.3489	0.6189	0.028*
H3	0.883 (5)	0.141 (3)	0.7160 (6)	0.035*
O4	0.9118 (3)	0.57165 (17)	0.57269 (3)	0.0264 (3)
C8	0.5034 (4)	0.2359 (2)	0.67693 (5)	0.0207 (4)
H8A	0.3619	0.1903	0.6921	0.025*
C6	0.5863 (4)	0.5033 (2)	0.71281 (5)	0.0198 (4)
H6A	0.4227	0.4799	0.7263	0.024*
C9	0.4843 (4)	0.1925 (2)	0.64248 (5)	0.0224 (4)
H9A	0.3317	0.1190	0.6363	0.027*
C12	0.6790 (5)	0.3309 (3)	0.54476 (5)	0.0287 (4)
H12A	0.8545	0.2627	0.5456	0.034*
H12B	0.5762	0.2934	0.5230	0.034*
C7	0.7200 (4)	0.3478 (2)	0.69495 (4)	0.0175 (4)
H7	0.8624	0.3876	0.6771	0.021*
C14	0.9229 (6)	0.5653 (3)	0.50810 (5)	0.0399 (6)
H14A	0.8200	0.5308	0.4865	0.060*
H14B	1.0987	0.5001	0.5092	0.060*
H14C	0.9618	0.6917	0.5073	0.060*
C13	0.7507 (5)	0.5239 (3)	0.54099 (5)	0.0269 (4)
H13A	0.5752	0.5946	0.5404	0.032*

*Atomic displacement parameters (Å^2) for **10** (Mo-Kα data set)*

	U^{11}	U^{22}	U^{33}	U^{12}	U^{13}	U^{23}
O1	0.135 (2)	0.0358 (9)	0.0327 (9)	0.0399 (12)	-0.0350 (11)	-0.0127 (7)
C1	0.0597 (14)	0.0180 (9)	0.0204 (9)	0.0036 (10)	-0.0040 (9)	-0.0015 (7)
O2	0.0341 (7)	0.0145 (6)	0.0204 (6)	0.0004 (6)	-0.0077 (6)	-0.0022 (5)
C2	0.0373 (10)	0.0197 (9)	0.0215 (9)	-0.0009 (8)	-0.0026 (8)	-0.0015 (7)
O3	0.0280 (6)	0.0165 (6)	0.0190 (6)	0.0037 (6)	-0.0036 (5)	-0.0001 (5)
C3	0.0335 (10)	0.0142 (8)	0.0215 (9)	0.0022 (8)	-0.0068 (8)	-0.0010 (7)
C11	0.0351 (10)	0.0297 (10)	0.0225 (10)	-0.0021 (9)	-0.0073 (8)	-0.0006 (8)
C4	0.0243 (9)	0.0127 (8)	0.0194 (8)	0.0017 (7)	-0.0029 (7)	-0.0027 (7)

C5	0.0215 (8)	0.0210 (9)	0.0194 (8)	0.0064 (7)	-0.0001 (7)	-0.0022 (7)
C10	0.0287 (9)	0.0222 (9)	0.0197 (9)	0.0007 (8)	-0.0038 (7)	-0.0016 (7)
O4	0.0368 (8)	0.0243 (7)	0.0181 (6)	0.0017 (6)	-0.0015 (6)	-0.0056 (5)
C8	0.0185 (8)	0.0199 (9)	0.0236 (9)	-0.0014 (7)	0.0008 (7)	0.0030 (7)
C6	0.0184 (8)	0.0248 (9)	0.0163 (8)	0.0022 (7)	0.0003 (7)	0.0013 (7)
C9	0.0225 (8)	0.0196 (8)	0.0250 (9)	-0.0022 (7)	-0.0055 (7)	-0.0001 (7)
C12	0.0447 (12)	0.0259 (9)	0.0157 (8)	0.0018 (9)	-0.0066 (8)	-0.0040 (7)
C7	0.0188 (8)	0.0176 (8)	0.0160 (8)	0.0010 (7)	0.0011 (7)	0.0026 (7)
C14	0.0658 (16)	0.0329 (12)	0.0211 (10)	0.0003 (11)	0.0063 (11)	-0.0010 (8)
C13	0.0418 (11)	0.0244 (9)	0.0146 (8)	0.0051 (9)	-0.0034 (8)	-0.0032 (7)

*Geometric parameters (Å, º) for **10** (Mo-Kα data set)*

O1—C1	1.199 (3)	C10—C9	1.499 (3)
C1—O4	1.343 (2)	C10—H10A	0.9900
C1—C2	1.481 (3)	C10—H10B	0.9900
O2—C4	1.437 (2)	O4—C13	1.458 (2)
O2—H2	0.90 (4)	C8—C9	1.328 (2)
C2—C3	1.320 (3)	C8—C7	1.503 (2)
C2—H2A	0.9500	C8—H8A	0.9500
O3—C7	1.447 (2)	C6—C7	1.501 (2)
O3—H3	0.88 (3)	C6—H6A	0.9500
C3—C4	1.495 (2)	C9—H9A	0.9500
C3—H3A	0.9500	C12—C13	1.514 (3)
C11—C10	1.532 (2)	C12—H12A	0.9900
C11—C12	1.533 (3)	C12—H12B	0.9900
C11—H11A	0.9900	C7—H7	1.0000
C11—H11B	0.9900	C14—C13	1.512 (3)
C4—C5	1.512 (3)	C14—H14A	0.9800
C4—H4A	1.0000	C14—H14B	0.9800
C5—C6	1.321 (3)	C14—H14C	0.9800
C5—H5A	0.9500	C13—H13A	1.0000
O1—C1—O4	124.56 (19)	C9—C8—C7	128.30 (17)

O1—C1—C2	126.68 (18)	C9—C8—H8A	115.8
O4—C1—C2	108.54 (17)	C7—C8—H8A	115.8
C4—O2—H2	109 (3)	C5—C6—C7	127.69 (17)
C3—C2—C1	121.50 (19)	C5—C6—H6A	116.2
C3—C2—H2A	119.3	C7—C6—H6A	116.2
C1—C2—H2A	119.3	C8—C9—C10	128.82 (17)
C7—O3—H3	109.1 (16)	C8—C9—H9A	115.6
C2—C3—C4	122.35 (17)	C10—C9—H9A	115.6
C2—C3—H3A	118.8	C13—C12—C11	115.13 (16)
C4—C3—H3A	118.8	C13—C12—H12A	108.5
C10—C11—C12	115.34 (17)	C11—C12—H12A	108.5
C10—C11—H11A	108.4	C13—C12—H12B	108.5
C12—C11—H11A	108.4	C11—C12—H12B	108.5
C10—C11—H11B	108.4	H12A—C12—H12B	107.5
C12—C11—H11B	108.4	O3—C7—C6	105.59 (13)
H11A—C11—H11B	107.5	O3—C7—C8	109.55 (14)
O2—C4—C3	109.52 (14)	C6—C7—C8	110.35 (14)
O2—C4—C5	109.83 (14)	O3—C7—H7	110.4
C3—C4—C5	109.01 (15)	C6—C7—H7	110.4
O2—C4—H4A	109.5	C8—C7—H7	110.4
C3—C4—H4A	109.5	C13—C14—H14A	109.5
C5—C4—H4A	109.5	C13—C14—H14B	109.5
C6—C5—C4	127.59 (16)	H14A—C14—H14B	109.5
C6—C5—H5A	116.2	C13—C14—H14C	109.5
C4—C5—H5A	116.2	H14A—C14—H14C	109.5
C9—C10—C11	111.64 (16)	H14B—C14—H14C	109.5
C9—C10—H10A	109.3	O4—C13—C14	108.30 (18)
C11—C10—H10A	109.3	O4—C13—C12	106.67 (15)
C9—C10—H10B	109.3	C14—C13—C12	113.65 (16)
C11—C10—H10B	109.3	O4—C13—H13A	109.4
H10A—C10—H10B	108.0	C14—C13—H13A	109.4
C1—O4—C13	118.05 (16)	C12—C13—H13A	109.4

O1—C1—C2—C3	20.0 (4)	C7—C8—C9—C10	-0.5 (3)
O4—C1—C2—C3	-154.8 (2)	C11—C10—C9—C8	-140.2 (2)
C1—C2—C3—C4	163.55 (18)	C10—C11—C12—C13	-87.9 (2)
C2—C3—C4—O2	124.28 (19)	C5—C6—C7—O3	106.6 (2)
C2—C3—C4—C5	-115.5 (2)	C5—C6—C7—C8	-135.07 (19)
O2—C4—C5—C6	-152.95 (18)	C9—C8—C7—O3	-123.2 (2)
C3—C4—C5—C6	87.0 (2)	C9—C8—C7—C6	121.0 (2)
C12—C11—C10—C9	-177.77 (16)	C1—O4—C13—C14	107.8 (2)
O1—C1—O4—C13	-13.2 (3)	C1—O4—C13—C12	-129.56 (19)
C2—C1—O4—C13	161.68 (17)	C11—C12—C13—O4	60.7 (2)
C4—C5—C6—C7	-0.8 (3)	C11—C12—C13—C14	179.95 (19)

*Hydrogen-bond geometry (Å, º) for **10** (Mo-Kα data set)*

D—H···*A*	*D*—H	H···*A*	*D*···*A*	*D*—H···*A*
O2—H2···O3^{i}	0.90 (4)	1.89 (4)	2.7662 (18)	163 (4)
O3—H3···O2^{ii}	0.88 (3)	1.94 (3)	2.8038 (18)	165 (2)

Symmetry codes: (i) -*x*+2, *y*+1/2, -*z*+3/2; (ii) *x*, *y*-1, *z*.

Figures for packing diagram and hydrogen-bonding network in **10** (Mo-Kα data set):

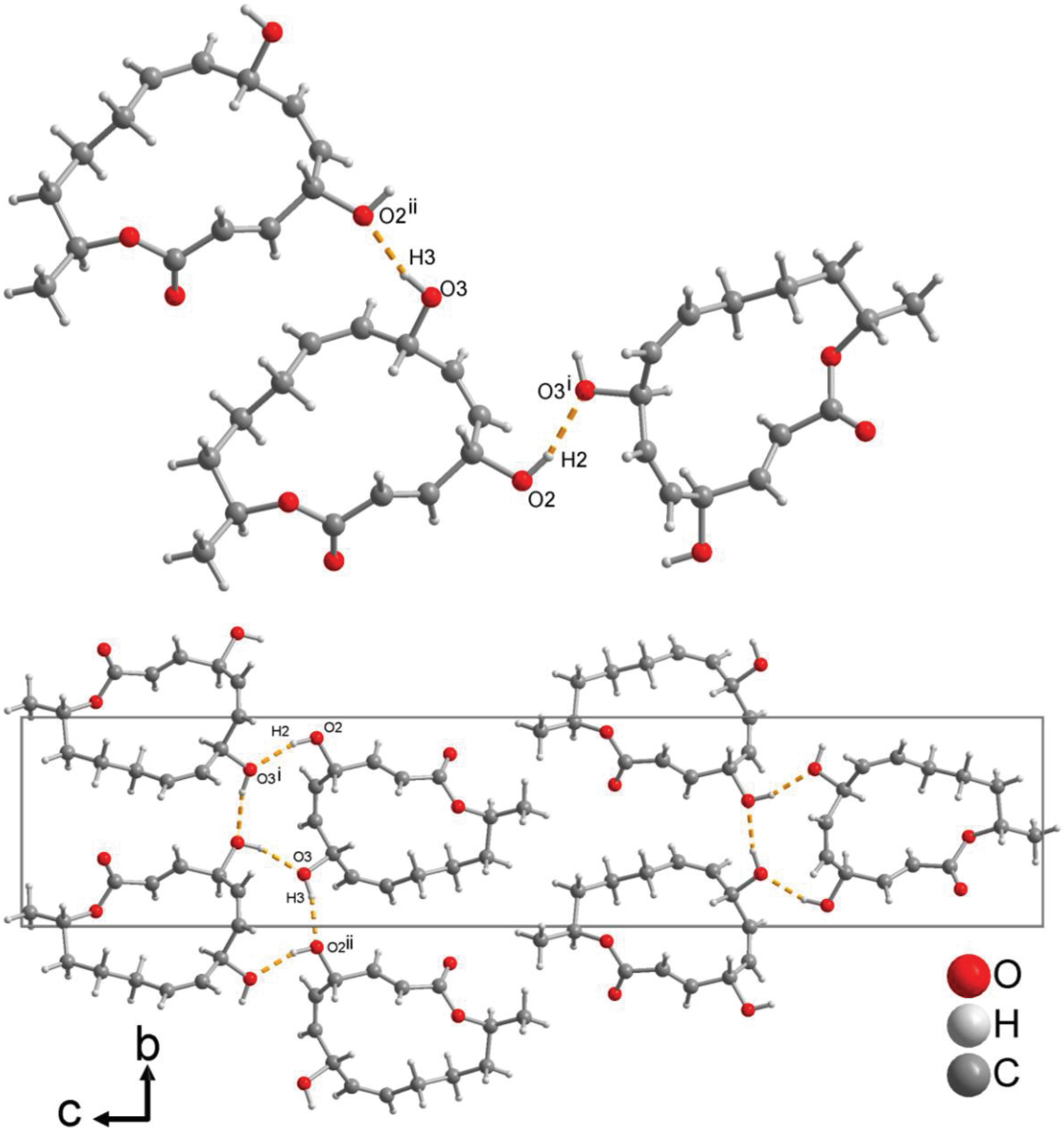

The following data is from the Cu-Kα data set.

Fractional atomic coordinates and isotropic or equivalent isotropic displacement parameters (Å^2) for ***10*** *(Cu-Kα data set)*

	x	*y*	*z*	U_{iso}*/U_{eq}
O1	0.8250 (8)	0.1768 (3)	0.08055 (7)	0.0818 (13)
H2	0.422 (12)	0.133 (6)	0.2347 (10)	0.123*
C1	0.6670 (9)	0.2858 (5)	0.09135 (9)	0.0461 (11)
C2	0.5427 (8)	0.2944 (4)	0.12770 (10)	0.0373 (10)

H2A	0.3777	0.3609	0.1312	0.045*
O2	0.4873 (5)	0.1002 (2)	0.21127 (5)	0.0373 (7)
C3	0.6543 (8)	0.2126 (3)	0.15543 (9)	0.0344 (10)
H3A	0.7874	0.1225	0.1513	0.041*
O3	0.6487 (4)	0.7511 (3)	0.22359 (5)	0.0342 (7)
C4	0.5769 (8)	0.2577 (4)	0.19305 (8)	0.0325 (10)
H4A	0.4238	0.3467	0.1931	0.039*
O4	0.5899 (4)	0.4283 (3)	0.07265 (5)	0.0377 (7)
C5	0.8284 (8)	0.3311 (5)	0.21182 (9)	0.0344 (10)
H5A	0.9396	0.2490	0.2246	0.041*
C6	0.9133 (7)	0.4976 (4)	0.21264 (7)	0.0312 (9)
H6A	1.0770	0.5207	0.2261	0.037*
C7	0.7809 (6)	0.6524 (4)	0.19481 (8)	0.0266 (10)
H7A	0.6392	0.6127	0.1769	0.032*
C8	0.9966 (7)	0.7631 (4)	0.17704 (9)	0.0350 (10)
H8A	1.1384	0.8084	0.1922	0.042*
C9	1.0142 (8)	0.8061 (4)	0.14257 (9)	0.0352 (9)
H9A	1.1664	0.8798	0.1365	0.042*
C10	0.8302 (8)	0.7556 (4)	0.11199 (8)	0.0375 (10)
H10A	0.6984	0.8526	0.1071	0.045*
H10B	0.7205	0.6506	0.1188	0.045*
H3	0.638 (8)	0.868 (4)	0.2149 (8)	0.056*
C11	0.9957 (8)	0.7155 (4)	0.07792 (7)	0.0414 (9)
H11A	1.1231	0.6164	0.0830	0.050*
H11B	1.1114	0.8192	0.0721	0.050*
C12	0.8196 (8)	0.6687 (4)	0.04470 (8)	0.0417 (10)
H12A	0.6435	0.7358	0.0458	0.050*
H12B	0.9209	0.7071	0.0229	0.050*
C13	0.7514 (8)	0.4759 (4)	0.04097 (7)	0.0399 (10)
H13A	0.9270	0.4056	0.0403	0.048*
C14	0.5768 (9)	0.4360 (3)	0.00800 (7)	0.0540 (11)
H14A	0.6817	0.4668	-0.0137	0.081*

H14B	0.4049	0.5049	0.0089	0.081*
H14C	0.5313	0.3105	0.0075	0.081*

*Atomic displacement parameters (Å^2) for **10** (Cu-Kα data set)*

	U^{11}	U^{22}	U^{33}	U^{12}	U^{13}	U^{23}
O1	0.153 (3)	0.0486 (16)	0.0438 (19)	0.044 (2)	0.0371 (19)	0.0126 (14)
C1	0.073 (3)	0.033 (2)	0.032 (3)	0.002 (2)	0.004 (2)	0.000 (2)
C2	0.051 (2)	0.0312 (19)	0.030 (2)	0.003 (2)	0.007 (2)	0.0012 (18)
O2	0.0539 (15)	0.0282 (12)	0.0297 (13)	-0.0011 (14)	0.0074 (12)	0.0046 (12)
C3	0.049 (2)	0.0212 (18)	0.033 (2)	-0.001 (2)	0.005 (2)	0.0048 (19)
O3	0.0441 (14)	0.0317 (11)	0.0267 (15)	0.0065 (12)	0.0049 (12)	0.0014 (12)
C4	0.046 (2)	0.030 (2)	0.022 (2)	0.003 (2)	0.0044 (19)	0.0024 (18)
O4	0.0468 (16)	0.0371 (15)	0.0292 (14)	0.0012 (13)	0.0007 (13)	0.0095 (12)
C5	0.037 (2)	0.039 (2)	0.027 (2)	0.006 (2)	-0.0027 (17)	0.0080 (18)
C6	0.029 (2)	0.037 (2)	0.0276 (19)	-0.001 (2)	-0.0038 (14)	-0.002 (2)
C7	0.026 (2)	0.0313 (18)	0.023 (2)	0.001 (2)	-0.0025 (17)	0.0014 (19)
C8	0.042 (2)	0.034 (2)	0.029 (3)	-0.003 (2)	0.0018 (18)	-0.0009 (18)
C9	0.0383 (19)	0.0302 (18)	0.037 (2)	-0.005 (2)	0.005 (2)	-0.0021 (19)
C10	0.047 (2)	0.0348 (19)	0.031 (2)	0.001 (2)	0.0056 (18)	-0.0025 (18)
C11	0.052 (2)	0.0413 (19)	0.031 (2)	-0.003 (2)	0.004 (2)	0.0007 (18)
C12	0.059 (2)	0.036 (2)	0.029 (2)	0.002 (2)	0.0078 (18)	0.0040 (18)
C13	0.058 (2)	0.037 (2)	0.024 (2)	0.006 (2)	0.004 (2)	0.006 (2)
C14	0.084 (3)	0.046 (2)	0.0317 (19)	-0.003 (2)	-0.007 (2)	0.0029 (19)

*Geometric parameters (Å, º) for **10** (Cu-Kα data set)*

O1—C1	1.195 (4)	C7—H7A	1.0000
C1—O4	1.341 (4)	C8—C9	1.328 (4)
C1—C2	1.481 (5)	C8—H8A	0.9500
C2—C3	1.320 (4)	C9—C10	1.493 (4)
C2—H2A	0.9500	C9—H9A	0.9500
O2—C4	1.443 (3)	C10—C11	1.529 (4)
O2—H2	0.96 (4)	C10—H10A	0.9900
C3—C4	1.490 (4)	C10—H10B	0.9900

C3—H3A	0.9500	C11—C12	1.541 (4)
O3—C7	1.455 (3)	C11—H11A	0.9900
O3—H3	0.94 (3)	C11—H11B	0.9900
C4—C5	1.504 (5)	C12—C13	1.510 (5)
C4—H4A	1.0000	C12—H12A	0.9900
O4—C13	1.459 (3)	C12—H12B	0.9900
C5—C6	1.331 (4)	C13—C14	1.518 (4)
C5—H5A	0.9500	C13—H13A	1.0000
C6—C7	1.495 (4)	C14—H14A	0.9800
C6—H6A	0.9500	C14—H14B	0.9800
C7—C8	1.492 (4)	C14—H14C	0.9800
O1—C1—O4	124.2 (3)	C8—C9—C10	129.6 (4)
O1—C1—C2	126.6 (3)	C8—C9—H9A	115.2
O4—C1—C2	109.1 (3)	C10—C9—H9A	115.2
C3—C2—C1	122.0 (3)	C9—C10—C11	112.1 (3)
C3—C2—H2A	119.0	C9—C10—H10A	109.2
C1—C2—H2A	119.0	C11—C10—H10A	109.2
C4—O2—H2	108 (3)	C9—C10—H10B	109.2
C2—C3—C4	121.7 (3)	C11—C10—H10B	109.2
C2—C3—H3A	119.2	H10A—C10—H10B	107.9
C4—C3—H3A	119.2	C10—C11—C12	115.2 (3)
C7—O3—H3	104.9 (19)	C10—C11—H11A	108.5
O2—C4—C3	109.0 (2)	C12—C11—H11A	108.5
O2—C4—C5	109.3 (3)	C10—C11—H11B	108.5
C3—C4—C5	108.8 (3)	C12—C11—H11B	108.5
O2—C4—H4A	109.9	H11A—C11—H11B	107.5
C3—C4—H4A	109.9	C13—C12—C11	114.7 (3)
C5—C4—H4A	109.9	C13—C12—H12A	108.6
C1—O4—C13	118.3 (3)	C11—C12—H12A	108.6
C6—C5—C4	127.6 (3)	C13—C12—H12B	108.6
C6—C5—H5A	116.2	C11—C12—H12B	108.6

C4—C5—H5A	116.2	H12A—C12—H12B	107.6
C5—C6—C7	127.5 (3)	O4—C13—C12	106.4 (3)
C5—C6—H6A	116.2	O4—C13—C14	108.1 (3)
C7—C6—H6A	116.2	C12—C13—C14	112.9 (3)
O3—C7—C8	109.8 (2)	O4—C13—H13A	109.8
O3—C7—C6	105.4 (2)	C12—C13—H13A	109.8
C8—C7—C6	110.2 (3)	C14—C13—H13A	109.8
O3—C7—H7A	110.4	C13—C14—H14A	109.5
C8—C7—H7A	110.4	C13—C14—H14B	109.5
C6—C7—H7A	110.4	H14A—C14—H14B	109.5
C9—C8—C7	127.8 (4)	C13—C14—H14C	109.5
C9—C8—H8A	116.1	H14A—C14—H14C	109.5
C7—C8—H8A	116.1	H14B—C14—H14C	109.5
O1—C1—C2—C3	20.5 (5)	C5—C6—C7—C8	-135.4 (4)
O4—C1—C2—C3	-155.1 (3)	O3—C7—C8—C9	-123.0 (3)
C1—C2—C3—C4	163.6 (3)	C6—C7—C8—C9	121.2 (3)
C2—C3—C4—O2	125.5 (3)	C7—C8—C9—C10	-0.9 (5)
C2—C3—C4—C5	-115.5 (3)	C8—C9—C10—C11	-140.0 (3)
O1—C1—O4—C13	-14.4 (5)	C9—C10—C11—C12	-177.9 (3)
C2—C1—O4—C13	161.3 (3)	C10—C11—C12—C13	-88.5 (4)
O2—C4—C5—C6	-153.6 (3)	C1—O4—C13—C12	-130.1 (3)
C3—C4—C5—C6	87.6 (4)	C1—O4—C13—C14	108.4 (3)
C4—C5—C6—C7	-0.6 (6)	C11—C12—C13—O4	61.4 (4)
C5—C6—C7—O3	106.1 (4)	C11—C12—C13—C14	179.7 (3)

Hydrogen-bond geometry (Å, º) for ***10*** *(Cu-K*α *data set)*

D—H···*A*	*D*—H	H···*A*	*D*···*A*	*D*—H···*A*
O2—H2···O3^{i}	0.96 (4)	1.83 (4)	2.762 (3)	164 (5)
O3—H3···O2^{ii}	0.94 (3)	1.92 (3)	2.805 (3)	156 (3)

Symmetry codes: (i) -*x*+1, *y*-1/2, -*z*+1/2; (ii) *x*, *y*+1, *z*.

Chapter 4

Phenolic Bisabolanes from the Sponge-Derived Fungus *Aspergillus* sp.

Published in “Phytochemistry Letters”.

Impact Factor: 1.353.

Phytochemistry Letters 18 (2016) 187–191

Contents lists available at ScienceDirect

Phytochemistry Letters

journal homepage: www.elsevier.com/locate/phytol

Phenolic bisabolanes from the sponge-derived fungus *Aspergillus* sp.

Shuai Liu[a], Haofu Dai[b], Belma Konuklugil[c], Raha S. Orfali[d], Wenhan Lin[e], Rainer Kalscheuer[a], Zhen Liu[a,*], Peter Proksch[a,*]

[a] Institute of Pharmaceutical Biology and Biotechnology, Heinrich-Heine-Universität Düsseldorf, Universitätsstrasse 1, 40225 Düsseldorf, Germany
[b] Key Laboratory of Biology and Genetic Resources of Tropical Crops, Ministry of Agriculture, Institute of Tropical Bioscience and Biotechnology, Chinese Academy of Tropical Agricultural Sciences, Haikou 571101, China
[c] Department of Pharmacognosy, Faculty of Pharmacy, Ankara University, Ankara 06110, Turkey
[d] Department of Pharmacognosy, Faculty of Pharmacy, King Saud University, Riyadh, Saudi Arabia
[e] State Key Laboratory of Natural and Biomimetic Drugs, Peking University, Beijing 100191, China

ARTICLE INFO

Article history:
Received 8 August 2016
Received in revised form 22 September 2016
Accepted 11 October 2016
Available online xxx

Keywords:
Sponge-derived fungus
Aspergillus sp.
Phenolic bisabolanes
Antibacterial
Co-cultivation

ABSTRACT

Two new phenolic bisabolane sesquiterpenes, asperchondols A (**1**) and B (**2**), together with seven known analogues (**3**–**9**) and four known diphenyl ethers (**10**–**13**) were obtained from *Aspergillus* sp., that had been isolated from the marine sponge *Chondrilla nucula*. Their structures were elucidated through NMR and MS analysis, and by comparison with literature data. All isolated compounds were evaluated for their antibacterial activity against eight human pathogenic bacteria. Co-cultivation experiment of *Aspergillus* sp. with *Bacillus subtilis* was also conducted.

1. Introduction

Marine-derived fungi have attracted considerable interest in the pharmaceutical community as promising producers for a wide range of metabolites with unique structures and pharmacological activities as exemplified by plinabulin that is currently in clinical studies phase III as a new anticancer drug (Ebada and Proksch, 2015). Plinabulin is a synthetic analogue of phenylahistin, the latter being derived from a marine strain of *Aspergillus ustus* (Kanoh et al., 1997). Phenolic bisabolane metabolites are sesquiterpenoids, which have hitherto mainly been reported from two genera of marine-derived fungi: *Aspergillus* and *Penicillium* isolated from different marine organisms including sponges (Li et al., 2012; Wang et al., 2015), corals (Wei et al., 2010; Zhuang et al., 2011) and mangroves (Lu et al., 2010; Wang et al., 2012), and from deep sea sediment (Li et al., 2015). Phenolic bisabolanes have received considerable attention due to their various biological activities such as antioxidant (Trisuwan et al., 2011), cytotoxic (Sun et al., 2012), or antibacterial activities (Chen et al., 2013).

In our ongoing studies on bioactive secondary metabolites from sponge-associated fungi (Zhou et al., 2014; Chen, Aktas et al., 2015; Elnaggar et al., 2016), we investigated the fungus *Aspergillus* sp., which was isolated from the marine sponge *Chondrilla nucula*. The crude extract of this fungus showed antibacterial activity against *E. faecium* ATCC35667 with MIC (Minimum Inhibitory Concentration) value of 50 μM. After fractionation by VLC (vacuum liquid chromatography), only subfractions 4 and 5 showed inhibitory effect against *E. faecium* ATCC35667 with MIC values of 25 μM and 50 μM, respectively. From these two subfractions, two new phenolic bisabolane sesquiterpenes, asperchondols A (**1**) and B (**2**), and eleven known compounds **3**–**13** were isolated (Fig. 1). The antimicrobial activities against eight human pathogenic bacteria were determined for all isolated compounds. In order to trigger the expression of silent biosynthetic pathways of this fungus, co-cultivation of this fungus with the bacterium *Bacillus subtilis* was also conducted on the basis of our previous study (Chen, Daletos et al., 2015; Ola et al., 2013).

2. Results and discussion

Compound **1** was obtained as a white amorphous powder. Its molecular formula was determined as $C_{22}H_{30}O_4$ by HRESIMS data (*m*/*z* 381.2038 $[M+Na]^+$), implying eight degrees of unsaturation. The ^1H NMR spectrum of **1** (Table 1) showed characteristic signals

* Corresponding authors.
E-mail addresses: zhenfeizi0@sina.com (Z. Liu), proksch@uni-duesseldorf.de (P. Proksch).

http://dx.doi.org/10.1016/j.phytol.2016.10.015
1874-3900/

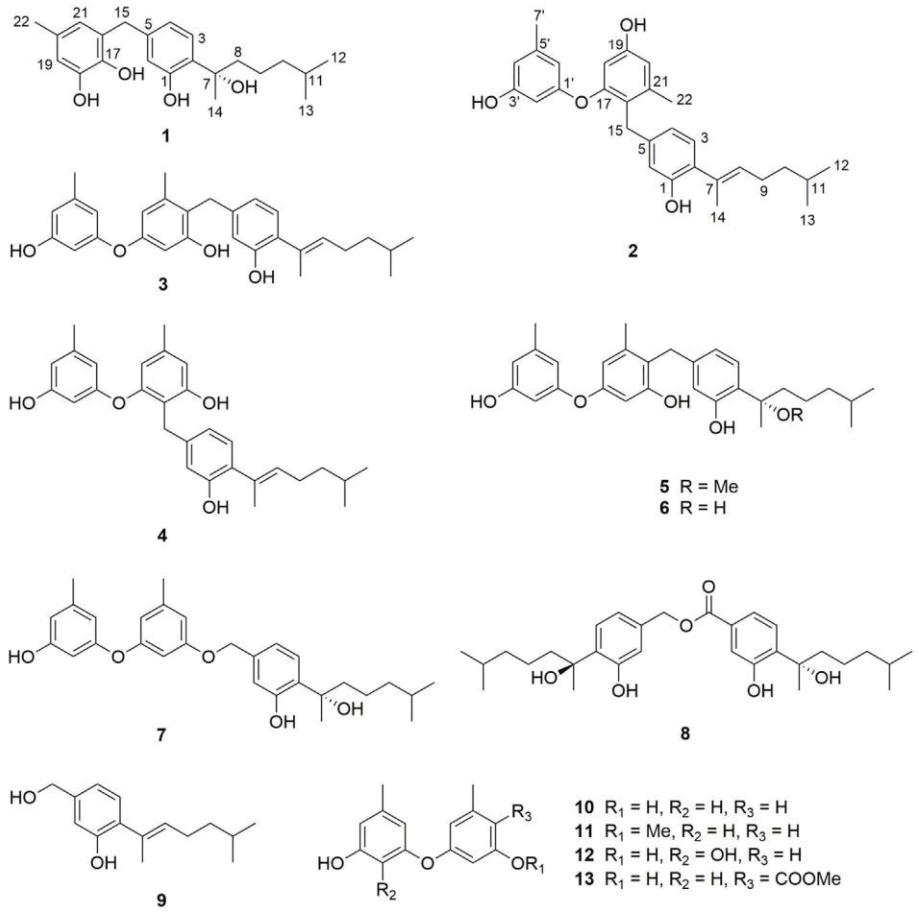

Fig. 1. Structures of compounds isolated from *Aspergillus* sp.

of an ABX aromatic spin system at δ_H 6.97 (d, J = 8.0 Hz, H-3), 6.65 (dd, J = 8.0, 1.4 Hz, H-4), and 6.59 (d, J = 1.4 Hz, H-6). The HMBC correlations from H-4 and H-6 to C-2 (δ_C 129.2), from H-3 to C-1 (δ_C 156.6) and C-5 (δ_C 142.4), and from H_2-15 to C-4 (δ_C 120.4), C-5 and C-6 (δ_C 117.5) indicated the presence of a 1,2,5-trisubstituted benzene ring with a hydroxy group attached at the C-1 position (Fig. 2). A 2-hydroxy-6-methylheptan-2-yl substituent at the C-2 position was established by the COSY correlations between H_{ab}-8 (δ_H 1.84 and 1.76)/H_2-9 (δ_H 1.27), H_2-9/H_2-10 (δ_H 1.11), H_2-10/H-11 (δ_H 1.48), and H-11/Me-12(13) (δ_H 0.82) together with the HMBC correlations from H-3 to C-7 (δ_C 77.7) and from Me-14 (δ_H 1.55) to C-2, C-7, and C-8 (δ_C 43.7). In addition, two *meta*-coupled aromatic protons at δ_H 6.47 (d, J = 1.5 Hz, H-19) and 6.32 (d, J = 1.5 Hz, H-21), an aromatic methyl at δ_H 2.12 (s, Me-22), and a methylene at δ_H 3.80 (s, H_2-15) were observed in the ^{1}H NMR spectrum of **1**. The HMBC correlations from H-19 to C-17 (δ_C 141.4), C-18 (δ_C 145.6) and C-21 (δ_C 122.4), from H-21 to C-17 and C-19 (δ_C 114.3), and from Me-22 to C-19, C-20 (δ_C 129.4) and C-21 indicated the presence of another benzene ring with a methyl and two hydroxy groups attached at the C-20, C-17 and C-18 positions, respectively. Furthermore, the HMBC correlations from H_2-15 to C-4, C-5, C-6, C-16 (δ_C 128.7), C-17 and C-21 indicated the linkage between the two bezene rings via C-15. Thus, the planar structure of **1** was elucidated as shown in Fig. 1 and the compound was named asperchondol A, representing a new phenolic bisabolane sesquiterpene derivative. The chiral center at C-7 in **1** was suggested to be *S* by comparison of optical rotation of **1** with that of the known compound expansol B (**6**), whose absolute configuration was determined by specific rotation calculation (Lu et al., 2010).

The molecular formula of compound **2** was determined to be $C_{29}H_{34}O_4$ on the basis of HRESIMS data, being identical to those of expansols D (**3**) and F (**4**) (Wang et al., 2012). Comparison of the NMR data of **2** (Table 1) with those of **3** and **4**, suggested that **2** was an isomer of the latter compounds, showing chemical shift differences for some aromatic protons and for the methylene group (CH_2-15). Detailed analysis of the 2D NMR data of **2** (Fig. 3) established two substructures including a phenolic bisabolane sesquiterpene (from C-1 to C-15) and a diphenyl ether (from C-16 to C-22 and from C-1′ to C-7′), which are identical to those found in **3** and **4**. The ROESY correlation between H_3-14 (δ_H 1.93) and H_2-9 (δ_H 2.15) was in accordance with the *E*-configuration of the double bond at C-7/C-8 in **2**. Furthermore, key HMBC correlations from H_2-15 (δ_H 3.82) to C-4 (δ_C 120.2), C-5 (δ_C 142.3), C-6 (δ_C 115.9), C-16 (δ_C 122.6), C-17 (δ_C 156.8) and C-21 (δ_C 140.4) indicated the connection between the phenolic bisabolane sesquiterpene and the diphenyl ether moieties via C-15 in **2**. Thus, compound **2** was identified as shown and named asperchondol B.

The remaining known compounds were identified as expansols D (**3**), F (**4**) (Wang et al., 2012), A (**5**), and B (**6**) (Lu et al., 2010), peniciaculins A (**7**) and B (**8**) (Li et al., 2015), aspergillusene A (**9**) (Trisuwan et al., 2011), and four known diphenyl ethers diorcinol (**10**) (Itabashi et al., 1993), cordyols E (**11**) (Wang et al., 2012) and C

Table 1
^{1}H and ^{13}C NMR Data of **1** and **2** in CD_3OD.

Position	**1**[a]		**2**[b]	
	δ_H (J in Hz)	δ_C, type	δ_H (J in Hz)	δ_C, type
1		156.6, C		154.8, C
2		129.2, C		127.3, C
3	6.97, d (8.0)	126.7, CH	6.85, d (7.7)	129.7, CH
4	6.65, dd (8.0, 1.4)	120.4, CH	6.53, d (7.7)	120.2, CH
5		142.4, C		142.3, C
6	6.59, d (1.4)	117.5, CH	6.51, brs	115.9, CH
7		77.7, C		135.5, C
8	1.84, m; 1.76, m	43.7, CH_2	5.37, t (7.3)	130.4, CH
9	1.27, m	22.5, CH_2	2.15, m	26.8, CH_2
10	1.11, m	40.2, CH_2	1.32, m	39.7, CH_2
11	1.48, m	28.5, CH	1.62, m	28.7, CH
12,13	0.82, d (6.6)	22.6, CH_3	0.93, d (6.6)	22.7, CH_3
14	1.55, s	28.6, CH_3	1.93, s	17.0, CH_3
15	3.80, s	35.6, CH_2	3.82, s	31.6, CH_2
16		128.7, C		122.6, C
17		141.4, C		156.8, C
18		145.6, C	6.13, br s	103.0, CH
19	6.47, d (1.5)	114.3, CH		159.8, C
20		129.4, C	6.17, br s	110.6, CH
21	6.32, d (1.5)	122.4, CH		140.4, C
22	2.12, s	20.4, CH_3	2.19, s	19.9, CH_3
1′				157.3, C
2′			6.23, br s	105.3, CH
3′				156.7, C
4′			6.30, br s	111.3. CH
5′				141.9, C
6′			6.45, br s	113.6, CH
7′			2.18, s	21.3, CH_3

[a] Recoreded at 500 MHz for ^{1}H and 125 MHz for ^{13}C.
[b] Recoreded at 600 MHz for ^{1}H and 150 MHz for ^{13}C.

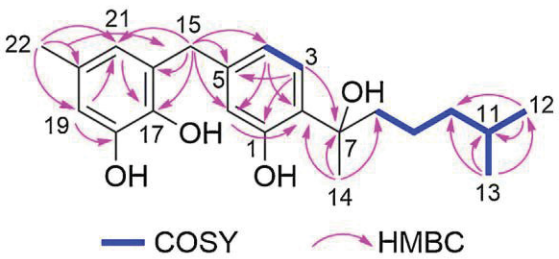

Fig. 2. Key COSY and HMBC correlations of **1.**

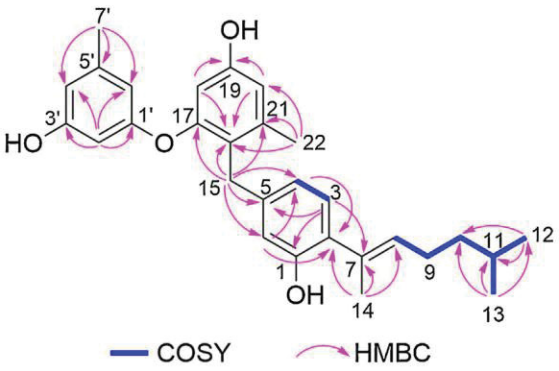

Fig. 3. Key COSY and HMBC correlations of **2.**

(**12**) (Bunyapaiboonsri et al., 2007), 4-methoxycarbonyldiorcinol (**13**) (Gong et al., 2011) by comparison of their spectroscopic data with those reported in the literature.

Diorcinol (**10**) has been reported to exhibited antibacterial activities against *Staphylococcus epidermidis* ATCC 12228 and *Staphylococcus aureus* ATCC 27154 with MIC values of 27.2 and 54.3 μM (Chen et al., 2013). All metabolites isolated in this study were evaluated for their antibacterial activities against *Mycobacterium tuberculosis* and seven antibiotic-resistant bacteria which belong to the so called ESKAPE (Pendleton et al., 2013) pathogens including the gram-positive bacteria *Staphylococcus aureus*, *Enterococcus faecium* and *Enterococcus faecalis*, and the gram-negative strain *Acinetobacter baumannii* (Table 2). The bisabolane diphenyl ethers (**2**–**7**) showed inhibitory activity against five of the analyzed bacterial strains including *S. aureus* ATCC700699, *E. faecalis* ATCC29212, *E. faecalis* ATCC51299, *E. faecium* ATCC35667 and *E. faecium* ATCC700221 with MIC values ranging from 6.25 to 50 μM. Especially the activity of **3** against *E. faecium* ATCC700221 was even more active than the positive control moxifloxacin. Compounds **1**, **2**, **3**, **4** and **10** exhibited weak inhibitory activity against *S. aureus* ATCC25923 with MIC values of 50, 25, 50, 50 and 50 μM, repectively. However, only the diphenyl ether **10** showed very weak inhibitory activity against *M. tuberculosis* with MIC value of 100 μM. Compound **10** was also active against *S. aureus* ATCC700699, *E. faecium* ATCC35667 and *E. faecium* ATCC 700221 with MIC values of 25, 50 and 25 μM, respectively. Compounds **8**, **9**, **11**, **12** and **13** showed no activity (MIC > 100 μM) against all the eight analyzed bacterial strains. None of these compounds was active against the gram-negative strain *A. baumannii* ATCCBAA1605.

A preliminary structure-activity relationship for the antibacterial activity is proposed. The coexistence of the phenolic bisabolane sesquiterpene and the diphenyl ether moieties seems to be very important since the hybirds (**2–7**) were more active than phenolic bisabolane sesquiterpenoids (**1**, **8** and **9**) and the phenyl esters (**10**–**13**). The positions (**2**, **3** vs. **4**) and the nature (C-bridged **6** vs. O-bridged **7**) of the linkage between the phenolic bisabolane sesquiterpene and the diphenyl ether moieties have no obvious influence on the antibacterial activity. Oxidation (**6** vs. **3**) and methylation (**5** vs. **6**) in the side chain led to slight decrease of activity. For diphenyl ether derivatives (**10**–**13**), any additional substituent led to decrease of activity.

When *Aspergillus* sp. was co-cultured with *Bacillus subtilis*, an obvious enhancement of compound **12** (5.4-fold increase) and **13** (3.5-fold increase) compared with the axenic fungal control was detected, whereas the amount of compound **10** decreased by about one third. The above data indicated that co-culture of *Aspergillus* sp. with *B. subtilis* can be an effective way to increase the accumulation of some secondary metabolites produced by the fungus. Furthermore, the complex and far unknown interactions between the fungus and the bacterium still need to be studied.

3. Experimental section

3.1. General experimental procedures

Optical rotation values were measured on a JASCO p-1020 polarimeter. HRESIMS spectra were recorded on an UHR-QTOF maxis 4G mass spectrometer. ^{1}H, ^{13}C and 2D NMR spectra were recorded on a Bruker Avance III 500 or 600 spectrometer. The Dionex P580 system, which was coupled to a photodiode array detector (UVD340s) and a separation column (125 mm × 4 mm i.d., 5 μm, Eurospher C_{18}), was used for HPLC analysis. Semi-preparative HPLC Lachrom-Merck Hitachi system was comprised of the L7100 pump, the L7400 UV detector and a 300 mm × 8 mm i.d., 10 μm, Eurospher C_{18} column. Sephadex LH-20 or MN silica gel 60 M was applied to column chromatography. The pre-coated silica gel 60 F_{254} plates (Merck) was used to thin layer chromatography (TLC) with detection at 254 and 365 nm.

Table 2
Antimicrobial Activities (MIC, μM).

strains	Compounds									
	1	**2**	**3**	**4**	**5**	**6**	**7**	**10**	Moxifloxacin[a]	Rifampicin[b]
M. tuberculosis	–[c]	–	–	–	–	–	–	100		<0.78
S. aureus ATCC25923	50	25	50	50	–	100	–	50	<0.97	
S. aureus ATCC700699	–	25	25	25	50	50	50	25	3.89	
E. faecalis ATCC29212	–	25	25	12.5	50	25	25	100	<0.97	
E. faecalis ATCC51299	–	25	12.5	12.5	25	12.5	12.5	100	<0.97	
E. faecium ATCC35667	–	25	6.25	12.5	25	12.5	12.5	50	1.95	
E. faecium ATCC700221	–	25	6.25	12.5	12.5	12.5	12.5	25	7.78	
A. baumannii ATCCBAA1605	–	–	–	–	–	–	–	–		12.5

[a] Moxifloxacin as the positive control for the gram-positive strains (*S. aureus* ATCC25923, *S. aureus* ATCC700699, *E. faecalis* ATCC29212, *E. faecalis* ATCC51299, *E. faecium* ATCC35667, *E. faecium* ATCC700221).
[b] rifampicin as the positive control for *M. tuberculosis* and the gram-negative strain *A.baumannii* ATCCBAA1605.
[c] MIC > 100 μM.

3.2. Fungal material and identification

The *Aspergillus* sp. strain was isolated from the sponge *Chondrilla nucula*, collected at Ayvalık of Aegean Sea (10 m depth), Turkey in 2014. A voucher specimen was deposited at Ankara University, Faculty of Pharmacy, Ankara, Turkey. The sponge's surface was immersed in 70% ethanol with 30 s for sterilization, followed by rinsing in sterilized artificial sea water for three times. Then the sponge material was cut into small pieces (ca. 1.5 × 1.5 mm), which were subsequently transferred to a potato/carrot agar medium for incubation (25 °C). After several days, hyphae on the sponge material were transferred to fresh plates for further purification. The fungal identification was conducted by DNA amplification and sequencing of the ITS region (GenBank accession No. KU921704) according to the protocol described before (Kjer et al., 2010). A voucher strain (CN-3-1) was deposited at one of the authors' lab (P. P.)

3.3. Extraction and isolation

Aspergillus sp. was cultivated in 18 Erlenmeyer flasks on solid rice medium (100 g rice, 3.5 g sea salt and 110 mL water) at 20 °C under static conditions. After four weeks, 500 mL EtOAc were added to each flask. The obtained crude extract (30.2 g) was subjected to vacuum liquid chromatography (VLC) using a gradient of *n*-hexane-EtOAc followed by a gradient of CH_2Cl_2-MeOH, to yield 13 subfractions (F1-F13). Subfraction F4 (1.8 g), eluted with *n*-hexane-EtOAc (70:30), was submitted to a Sephadex LH-20 column using MeOH as mobile phase. Fractions were combined according to TLC monitoring and further purified by semi-preparative HPLC with MeOH-H_2O to yield **10** (3.8 mg), **13** (3.0 mg), **11** (2.0 mg), **5** (2.1 mg), **3** (1.3 mg) and **4** (2.5 mg). Following a similar procedure, **1** (1.1 mg), **2** (0.7 mg), **12** (3.1 mg), **9** (1.0 mg), **6** (1.0 mg), **7** (1.0 mg) and **8** (1.8 mg) were obtained from subfraction F5 (636.5 mg).

3.3.1. Asperchondol A (*1*)

White amorphous powder; $[\alpha]^{20}_D$ +5.8 (*c* 0.2, MeOH); UV (MeOH) λ_{max} (log ε) 213 (5.08), 282 (2.02) nm; ^1H and ^{13}C NMR data, see Table 1; HRESIMS *m/z* 381.2038 $[M+Na]^+$ (calcd for $C_{22}H_{30}O_4Na$, 381.2036).

3.3.2. Asperchondol B (*2*)

White amorphous powder; UV (MeOH) λ_{max} (log ε) 204(5.12), 282 (2.01) nm; ^1H and ^{13}C NMR data, see Table 1; HRESIMS *m/z* 447.2527 $[M+H]^+$ (calcd for $C_{29}H_{35}O_4$, 447.2530)

3.4. Co-cultivation experiments of Aspergillus sp. with B. subtilis

Co-cultivation experiments were carried out in nine 1L Erlenmeyer flasks (three for co-culture of *Aspergillus* sp. with *B. subtilis*, three for axenic *Aspergillus* sp., and one for axenic *B. subtilis*) containing 110 mL of distilled water and 100 g of commercially available milk rice (Milch-Reis, ORYZA) each. *B. subtilis* was grown in Mueller Hinton (MH) broth. An overnight culture of *B. subtilis* was used to inoculate prewarmed MH medium (100 mL in 500 mL flask), which was then incubated at 37 °C with shaking at 200 rpm to mid exponential growth phase (optical density 0.2–0.4 at 600 nm). 10 mL of the bacteria culture was added to the rice medium, which was further incubated for 7 days at 37 °C. After this preincubation, *Aspergillus* sp. grown on malt agar (3 pieces, 1 cm × 1 cm) was added to the rice medium containing bacteria under sterile conditions. Fungal and bacterial controls were grown axenically on rice medium. All flasks were kept at 20 °C under static conditions. The axenic controls of *Aspergillus* sp. were kept for 20 days until it covered the bottom of the flasks, while for the co-cultivation of the fungus and the bacterium a time period of 28 days was necessary until the fungus had reached the bottom of the flasks. The fermentation was stopped by adding 500 mL of EtOAc to each flask. The extraction was completed after shaking the flasks on a laboratory shaker at 150 rpm for 8 h. After evaporation, each extract was dissolved in 5 mL of MeOH, and 50 μL of this solution was dissolved in 1.5 mL MeOH, then 30 μL of this solution was injected for HPLC analysis.

3.5. Antibacterial assay

Antibacterial assay against *M. tuberculosis* was carried out as described before with rifampicin as positive control (Datelos et al., 2015; Palomino et al., 2002). The broth microdilution assay was applied for the activity screening according to CLSI guidelines (CLSI, 2015). Mueller-Hinton broth (0.20%, w/v, beef extract; 1.75%, w/v, acid digest of casein; 0.15%, w/v, starch) was used to propagate

the 7 ESKAPE strains. After incubation at 37 °C for 24 h, the 96-well plates were checked by visual inspection. The MICs were determined as the lowest concentration for no visible growth of bacteria. Moxifloxacin and rifampicin were used as the positive control for the gram-positive and gram-negative strains, respectively. For the crude extract and all the 13 subfractions (F1-F13) obtained by VLC, their antibacterial activity against *M. tuberculosis*, *E. faecium* ATCC35667 and *A. baumannii* ATCCBAA1605 were tested.

Acknowledgements

Financial support of the Manchot Foundation to P.P. is gratefully acknowledged. Furthermore P.P. and B.K. wish to thank BMBF and Tubitak for support.

Appendix A. Supplementary data

Supplementary data (HRESIMS and NMR spectra of new compounds 1 and 2) associated with this article can be found, in the online version, at http://dx.doi.org/10.1016/j.phytol.2016.10.015.

References

Bunyapaiboonsri, T., Yoiprommarat, S., Intereya, K., Kocharin, K., 2007. New diphenyl ethers from the insect pathogenic fungus *Cordyceps* sp. Chem. Pharm. Bull. 55, 304–307.

CLSI, 2015. Methods for Dilution Antimicrobial Susceptibility Tests for Bacteria That Grow Aerobically. CLSI Document M07-A10, Approved Standard, Tenth ed. Clinical and Laboratory Standards Institute, Wayne, PA, USA.

Chen, M., Shao, C.L., Fu, X.M., Xu, R.F., Zheng, J.J., Zhao, D.L., She, Z.G., Wang, C.Y., 2013. Bioactive indole alkaloids and phenyl ether derivatives from a marine-derived *Aspergillus* sp. fungus. J. Nat. Prod. 76, 547–553.

Chen, H., Aktas, N., Konuklugil, B., Mándi, A., Daletos, G., Lin, W., Dai, H., Kurtan, T., Proksch, P., 2015. A new fusarielin analogue from *Penicillium* sp. isolated from the mediterranean sponge *Ircinia oros*. Tetrahedron Lett. 56, 5317–5320.

Chen, H., Daletos, G., Abdel-Aziz, M.S., Thomy, D., Dai, H., Brötz-Oesterhelt, H., Lin, W., Proksch, P., 2015. Inducing secondary metabolite production by the soil-dwelling fungus *Aspergillus terreus* through bacterial co-culture. Phytochem. Lett. 12, 35–41.

Datelos, G., Kalscheuer, R., Koliwer-Brandl, H., Hartmann, R., de Voogd, N.J., Wray, V., Lin, W.H., Proksch, P., 2015. Callyaerins from the marine sponge *Callyspongia aerizusa*: cyclic peptides with antitubercular activity. J. Nat. Prod. 78, 1910–1925.

Ebada, S.S., Proksch, P., 2015. Marine-derived fungal metabolites. Springer Handbook of Marine Biotechnology, vol. 32. , pp. 759–788.

Elnaggar, M.S., Ebada, S.S., Ashour, M.L., Ebrahim, W., Müller, W.E.G., Mándi, A., Kurtán, T., Singab, A., Lin, W., Liu, Z., Proksch, P., 2016. Xanthones and sesquiterpene derivatives from a marine-derived fungus *Scopulariopsis* sp. Tetrahedron 72, 2411–2419.

Gong, D.L., Wang, X.J., Xiang, Z.D., Wang, J.D., Zhang, H., Liu, C.X., Zhang, J., Xiang, W. S., 2011. Dipheyl etheric metabolites from *Streptomyces* sp. neau50. J. Antibiot. 64, 464–467.

Itabashi, T., Nozawa, K., Nakajima, S., Kawai, K., 1993. A new azaphilone, falconensin H, from *Emericella falconensis*. Chem. Pharm. Bull. 41, 2040–2041.

Kanoh, K., Kohno, S., Asari, T., Harada, T., Katada, J., Muramatsu, M., Kawashima, H., Sekiya, H., Uno, I., 1997. (−)-Phenylahistin: a new mammalian cell cycle inhibitor produced by *Aspergillus ustus*. Bioorg. Med. Chem. Lett. 7, 2847–2852.

Kjer, J., Debbab, A., Aly, A.H., Proksch, P., 2010. Methods for isolation of marine-derived endophytic fungi and their bioactive secondary products. Nat. Protoc. 5, 479–490.

Li, D., Xu, Y., Shao, C.L., Yang, R.Y., Zheng, C.J., Chen, Y.Y., Fu, X.M., Qian, P.Y., She, Z.G., de Voogd, N.J., Wang, C.Y., 2012. Antibacterial biasbolane-type sesquiterpenoids from the sponge-derived fungus *Aspergillus* sp. Mar. Drugs 10, 234–241.

Li, X.D., Li, X.M., Xu, G.M., Zhang, P., Wang, B.G., 2015. Antimicrobial phenolic bisabolanes and related derivatives from *Penicillium aculeatum* SD-321, a deep sea sediment-derived fungus. J. Nat. Prod. 78, 844–849.

Lu, Z., Zhu, H., Fu, P., Wang, Y., Zhang, Z., Lin, H., Liu, P., Zhuang, Y., Hong, K., Zhu, W., 2010. Cytotoxic polyphenols from the marine-derived fungus *Penicillium expansum*. J. Nat. Prod. 73, 911–914.

Ola, A.R.B., Thomy, D., Lai, D., Brötz-Oesterhelt, H., Proksch, P., 2013. Inducing secondary metabolite production by the endophytic fungus *Fusarium tricintum* through coculture with *Bacillus subtilis*. J. Nat. Prod. 76, 2094–2099.

Palomino, J.C., Martin, A., Camacho, M., Guerra, H., Swings, J., Portaels, F., 2002. Resazurin microtiter assay plate: simple and inexpensive method to detection of drug resistance in *Mycobacterium tuberculosis*. Antimicrob. Agents Chemother. 46, 2720–2722.

Pendleton, J.N., Gorman, S.P., Gilmore, B.F., 2013. Clinical relevance of the ESKAPE pathogens. Expert Rev. Anti Infect. Ther. 11, 297–308.

Sun, L.L., Shao, C.L., Chen, J.F., Guo, Z.Y., Fu, X.M., Chen, M., Chen, Y.Y., Li, R., de Voogd, N.J., She, Z.G., Lin, Y.C., Wang, C.Y., 2012. New bisabolane sesquiterpenoids from a marine-derived fungus *Asperigillus* sp. isolated from the sponge *Xestospongia testudinaria*. Bioorg. Med. Chem. Lett. 22, 1326–1329.

Trisuwan, K., Rukachaisirikul, V., Kaewpet, M., Phongpaichit, S., Hutadilok-Towatana, N., Preedanon, S., Sakayaroj, J., 2011. Sesquiterpene and xanthone derivatives from the sea fan-derived fungus *Aspergillus sydowii* PSU-F154. J. Nat. Prod. 74, 1663–1667.

Wang, J., Lu, Z., Liu, P., Wang, Y., Li, J., Hong, K., Zhu, W., 2012. Cytotoxic polyphenols from the fungus *Penicillium expansum* 091006 endogenous with the mangrove plant *Excoecaria agallocha*. Planta Med. 78, 1861–1866.

Wang, J., Qin, X., Xu, F., Zhang, T., Liao, S., Lin, X., Yang, B., Liu, J., Wang, L., Tu, Z., Liu, Y., 2015. Tetramic acid derivatives and polyphenols from sponge-derived fungus and their biological evaluation. Nat. Prod. Res. 29, 1761–1765.

Wei, M.Y., Wang, C.Y., Liu, Q.A., Shao, C.L., She, Z.G., Lin, Y.C., 2010. Five sesquiterpenoids from a marine-derived fungus *Aspergillus* sp. isolated from a gorgonian *Dichotella gemmacea*. Mar. Drugs 8, 941–949.

Zhou, Y., Debbab, A., Wray, V., Lin, W., Schulz, B., Trepos, R., Pile, C., Hellio, C., Proksch, P., Aly, A.H., 2014. Marine bacterial inhibitors from the sponge-derived fungus *Aspergillus* sp. Tetrahedron Lett. 55, 2789–2792.

Zhuang, Y., Teng, X., Wang, Y., Liu, P., Wang, H., Li, J., Li, G., Zhu, W., 2011. Cyclopeptides and polyketides from coral-associated fungus, *Aspergillus versicolor* LCJ-5-4. Tetrahedron 67, 7085–7089.

Supplementary data

Phenolic bisabolanes from the sponge-derived fungus *Aspergillus* sp.

Shuai Liu,[a] Haofu Dai,[b] Belma Konuklugil,[c] Raha S. Orfali,[d] Wenhan Lin,[e] Rainer Kalscheuer,[a] Zhen Liu,[a,*] Peter Proksch[a,*]

[a] Institute of Pharmaceutical Biology and Biotechnology, Heinrich-Heine-Universität Düsseldorf, Universitätsstrasse 1, 40225 Düsseldorf, Germany

[b] Key Laboratory of Biology and Genetic Resources of Tropical Crops, Ministry of Agriculture, Institute of Tropical Bioscience and Biotechnology, Chinese Academy of Tropical Agricultural Sciences, Haikou 571101, China

[c] Department of Pharmacognosy, Faculty of Pharmacy, Ankara University, Ankara 06110, Turkey

[d] Department of Pharmacognosy, Faculty of Pharmacy, King Saud University, Riyadh, Saudi Arabia

[e] State Key Laboratory of Natural and Biomimetic Drugs, Peking University, Beijing 100191, China

*Corresponding authors.

Tel.: +49 211 81 14163; fax: +49 211 81 11923;

e-mail: zhenfeizi0@sina.com (Z. Liu),

proksch@uni-duesseldorf.de (P. Proksch)

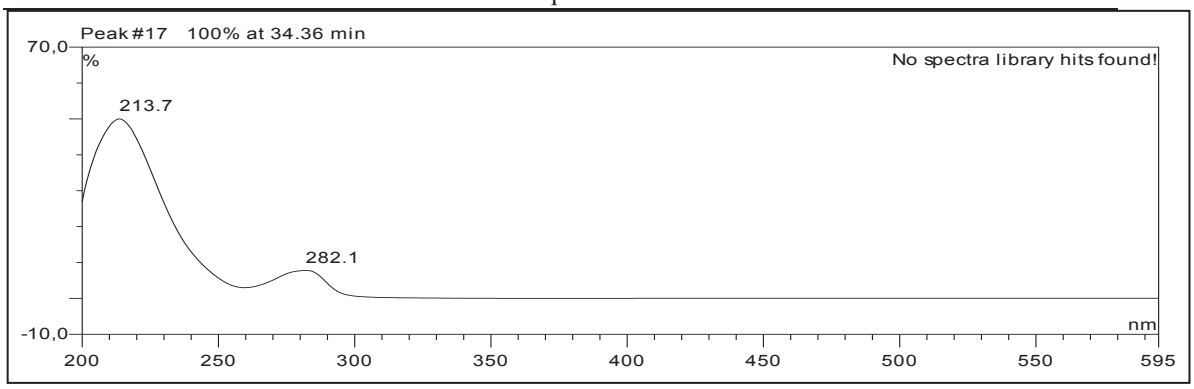

S1. UV spectrum of compound **1**.

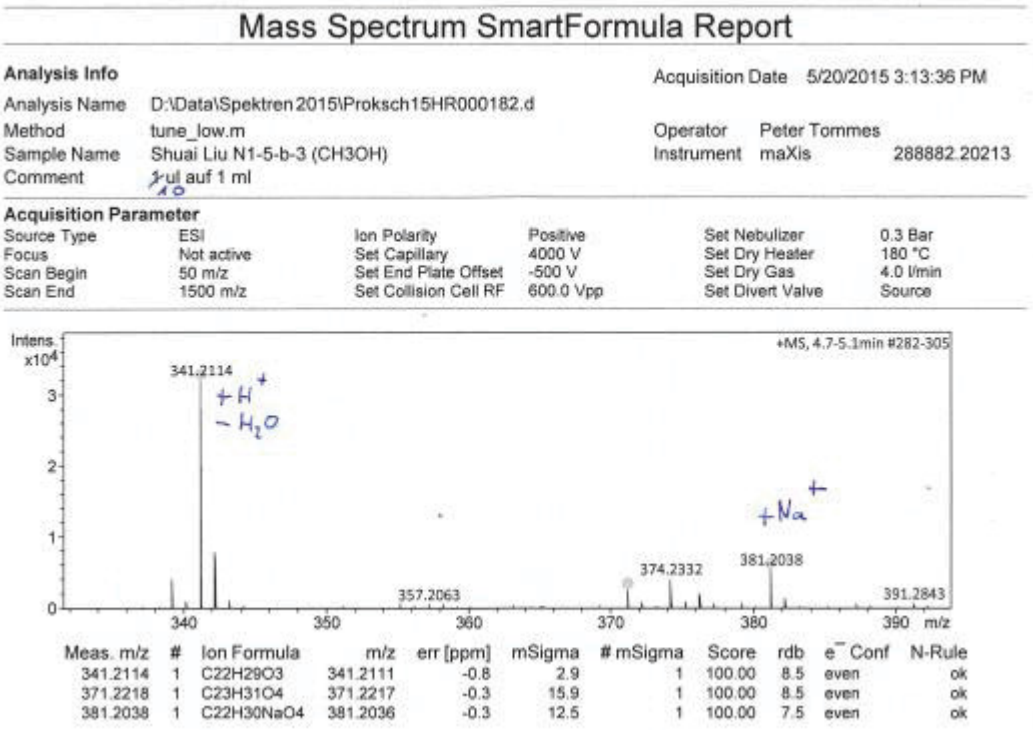

S2. HRESIMS spectrum of compound **1.**

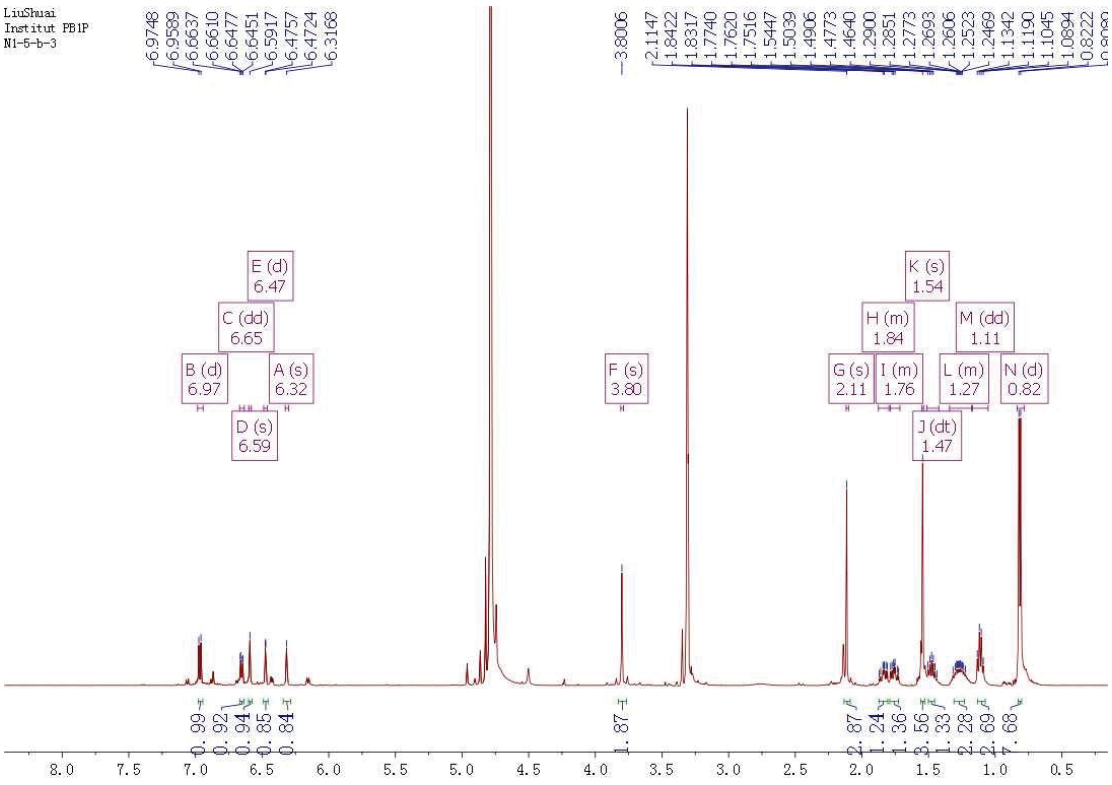

S3. ^{1}H NMR (500 MHz, CD_3OD) spectrum of compound **1**.

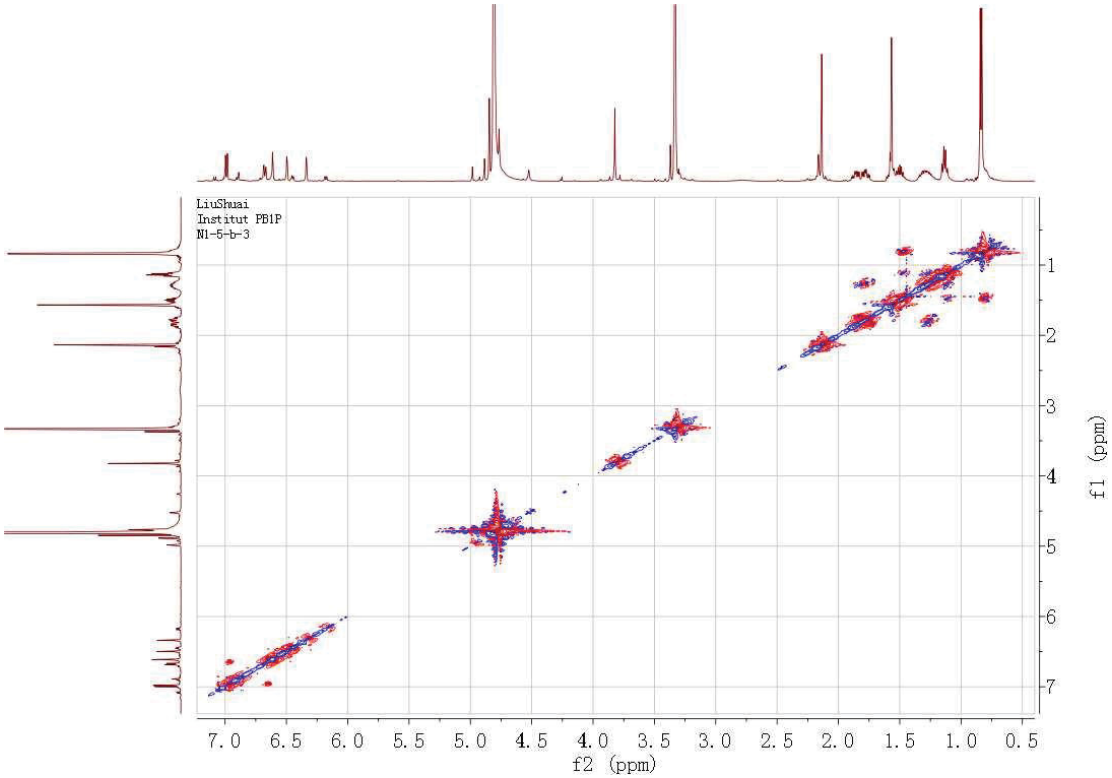

S4. COSY (500 MHz, CD_3OD) spectrum of compound **1**.

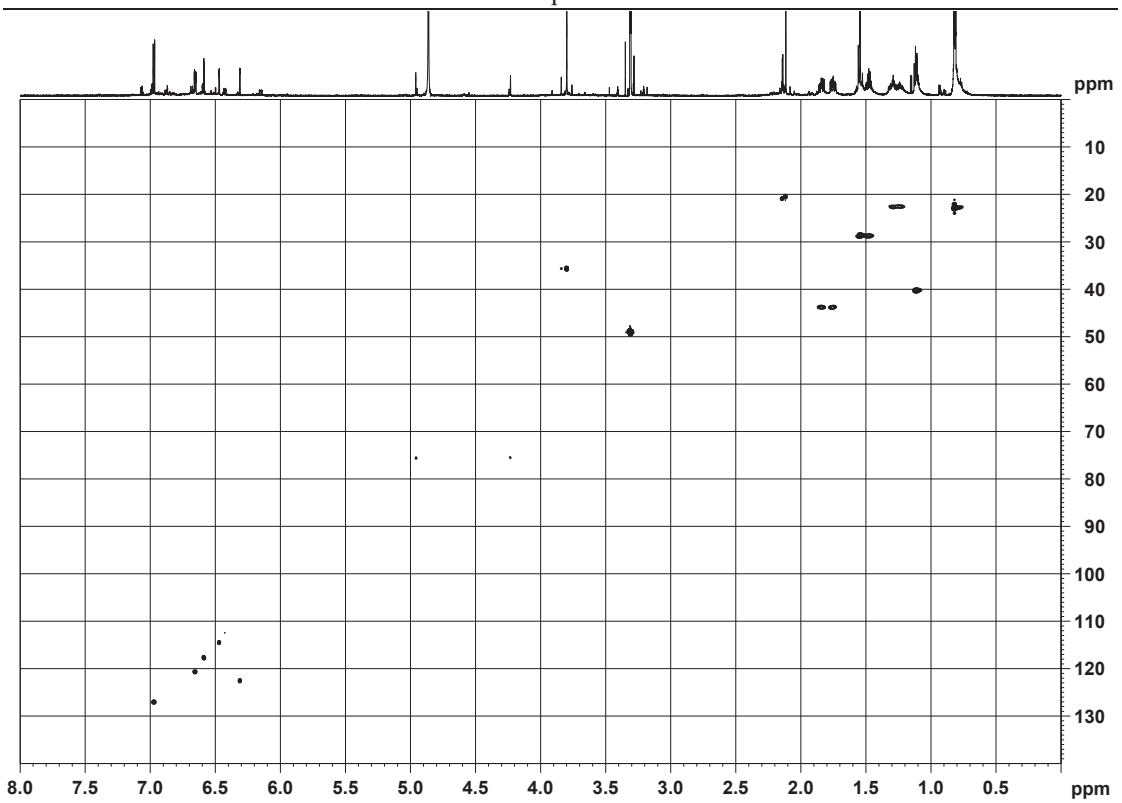

S5. HSQC (500 and 125 MHz, CD_3OD) spectrum of compound **1**.

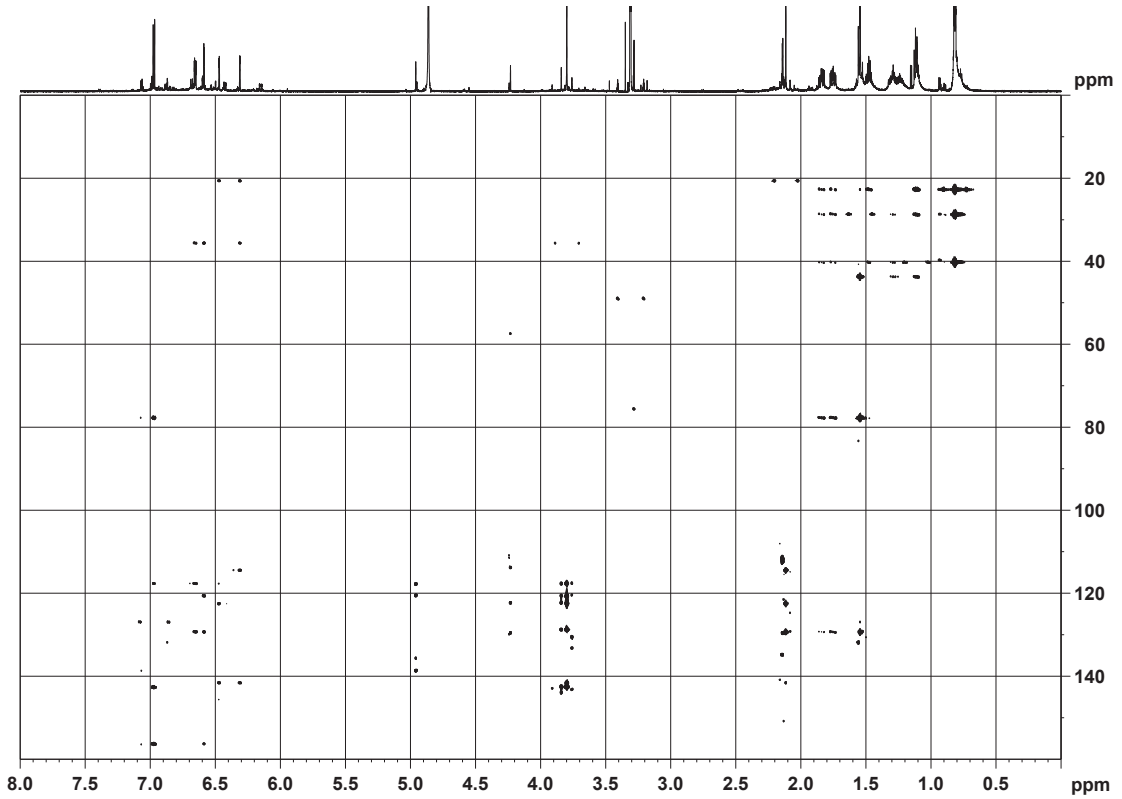

S6. HMBC (500 and 125 MHz, CD_3OD) spectrum of compound **1**.

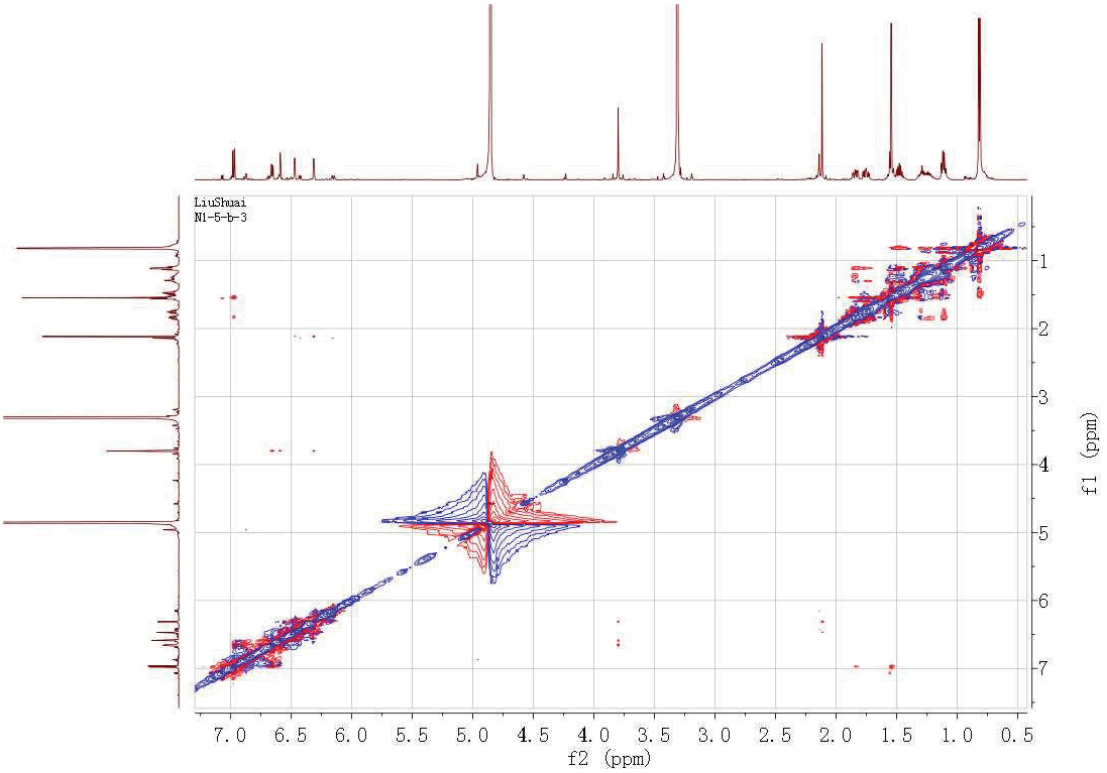

S7. ROESY (500 MHz, CD_3OD) spectrum of compound **1**.

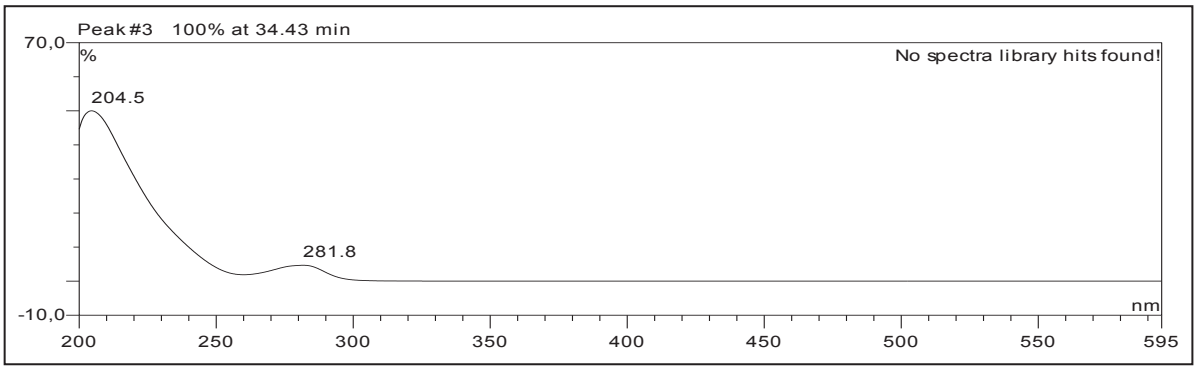

S8. UV spectrum of compound **2**.

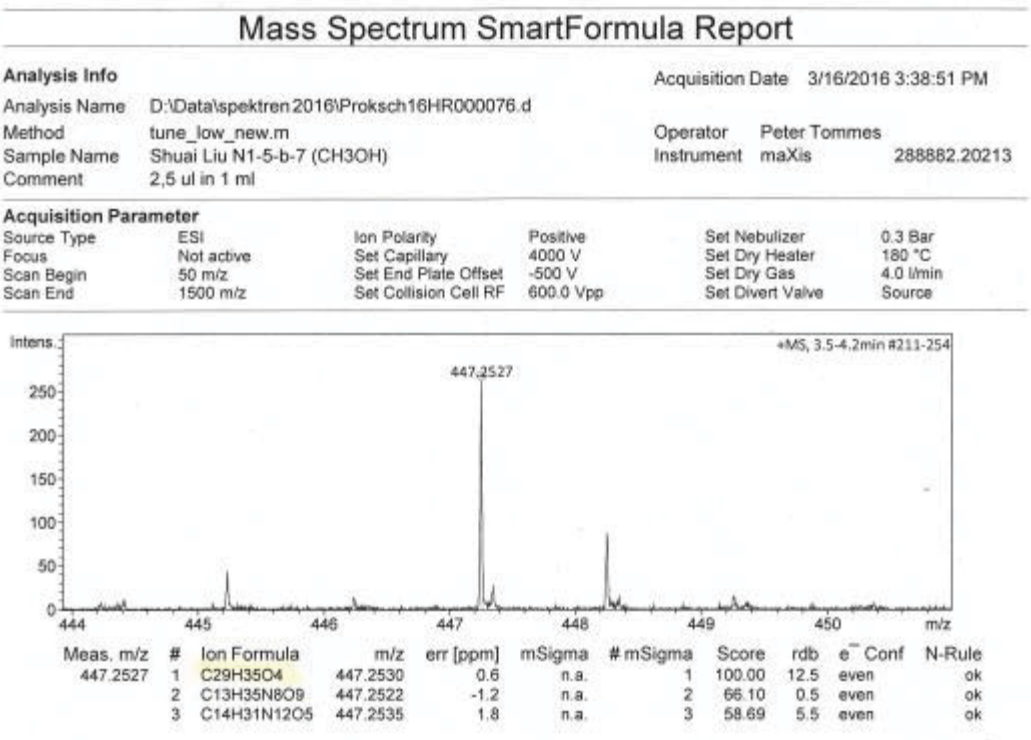

Mass Spectrum SmartFormula Report

Analysis Info

Analysis Name	D:\Data\spektren 2016\Proksch16HR000076.d	Acquisition Date	3/16/2016 3:38:51 PM
Method	tune_low_new.m	Operator	Peter Tommes
Sample Name	Shuai Liu N1-5-b-7 (CH3OH)	Instrument	maXis 288882.20213
Comment	2,5 ul in 1 ml		

Acquisition Parameter

Source Type	ESI	Ion Polarity	Positive	Set Nebulizer	0.3 Bar
Focus	Not active	Set Capillary	4000 V	Set Dry Heater	180 °C
Scan Begin	50 m/z	Set End Plate Offset	-500 V	Set Dry Gas	4.0 l/min
Scan End	1500 m/z	Set Collision Cell RF	600.0 Vpp	Set Divert Valve	Source

Meas. m/z	#	Ion Formula	m/z	err [ppm]	mSigma	# mSigma	Score	rdb	e⁻ Conf	N-Rule
447.2527	1	C29H35O4	447.2530	0.6	n.a.	1	100.00	12.5	even	ok
	2	C13H35N8O9	447.2522	-1.2	n.a.	2	66.10	0.5	even	ok
	3	C14H31N12O5	447.2535	1.8	n.a.	3	58.69	5.5	even	ok

S9. HRESIMS spectrum of compound **2.**

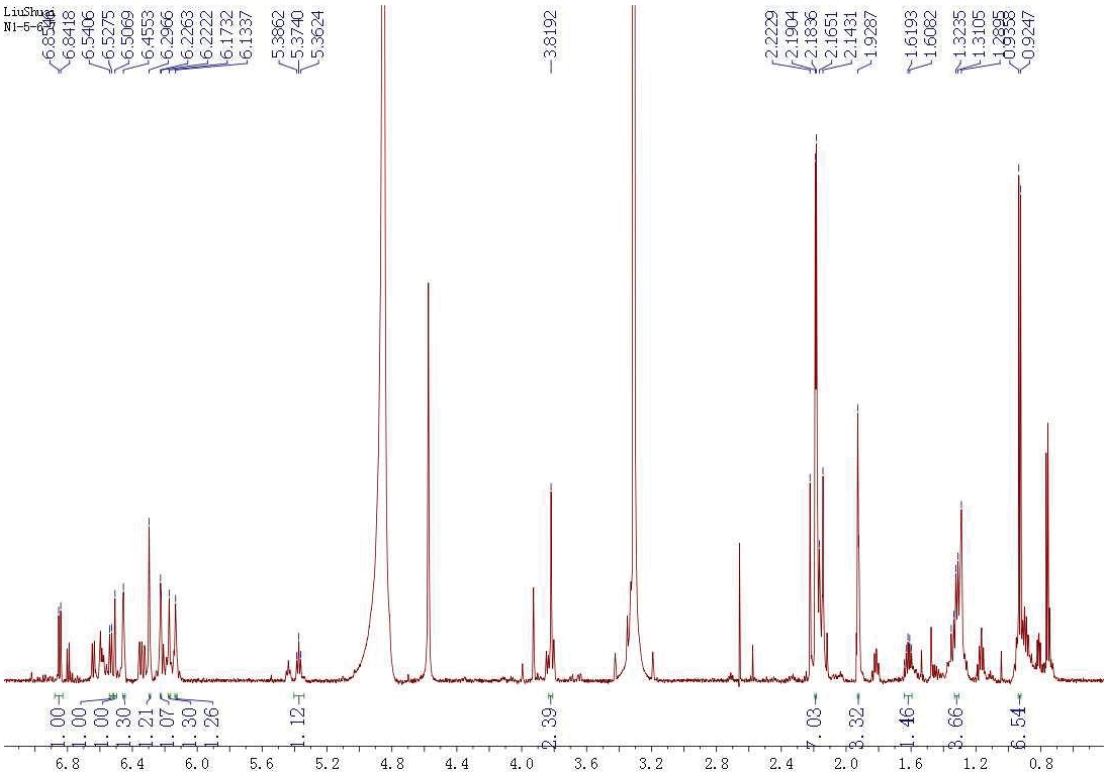

S10. ^{1}H NMR (600 MHz, CD_3OD) spectrum of compound **2**.

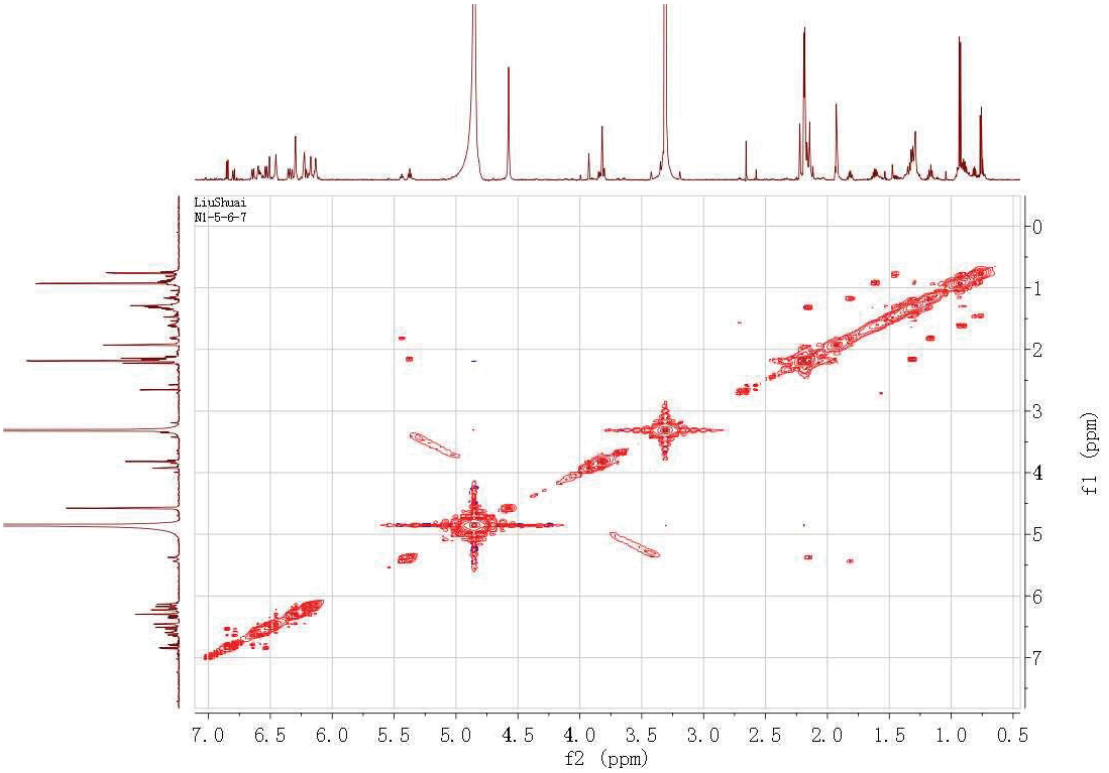

S11. COSY (600 MHz, CD_3OD) spectrum of compound **2**.

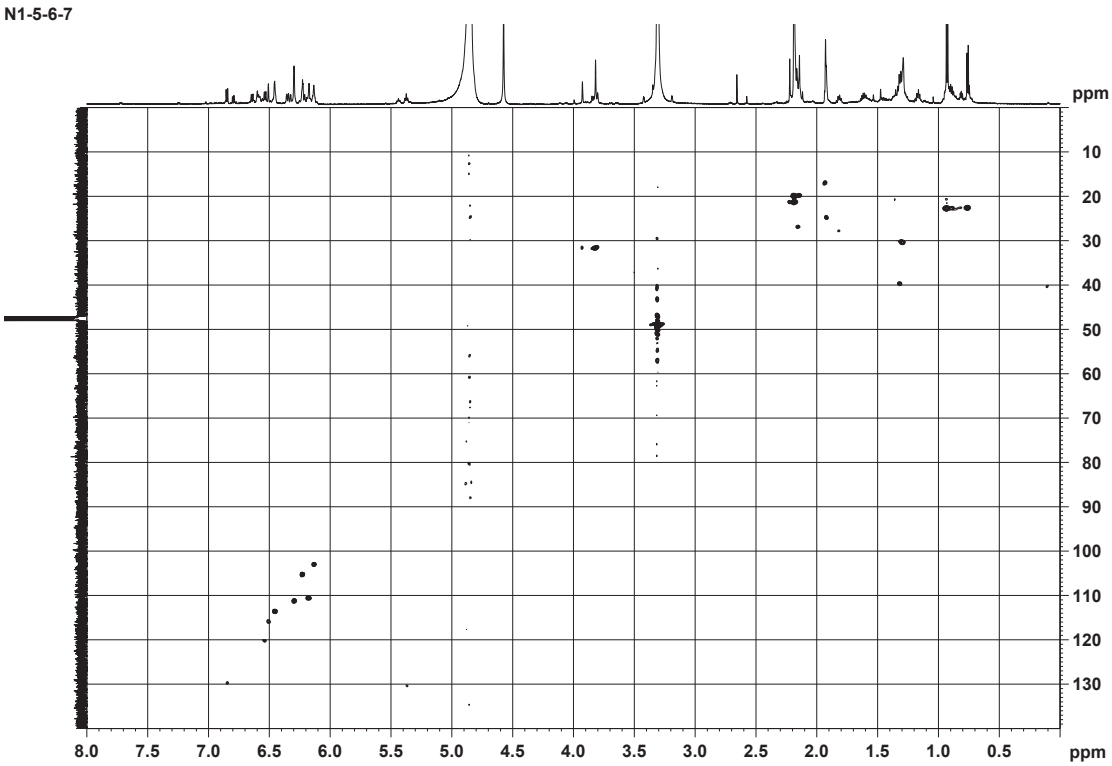

S12. HSQC (600 and 150 MHz, CD_3OD) spectrum of compound **2**.

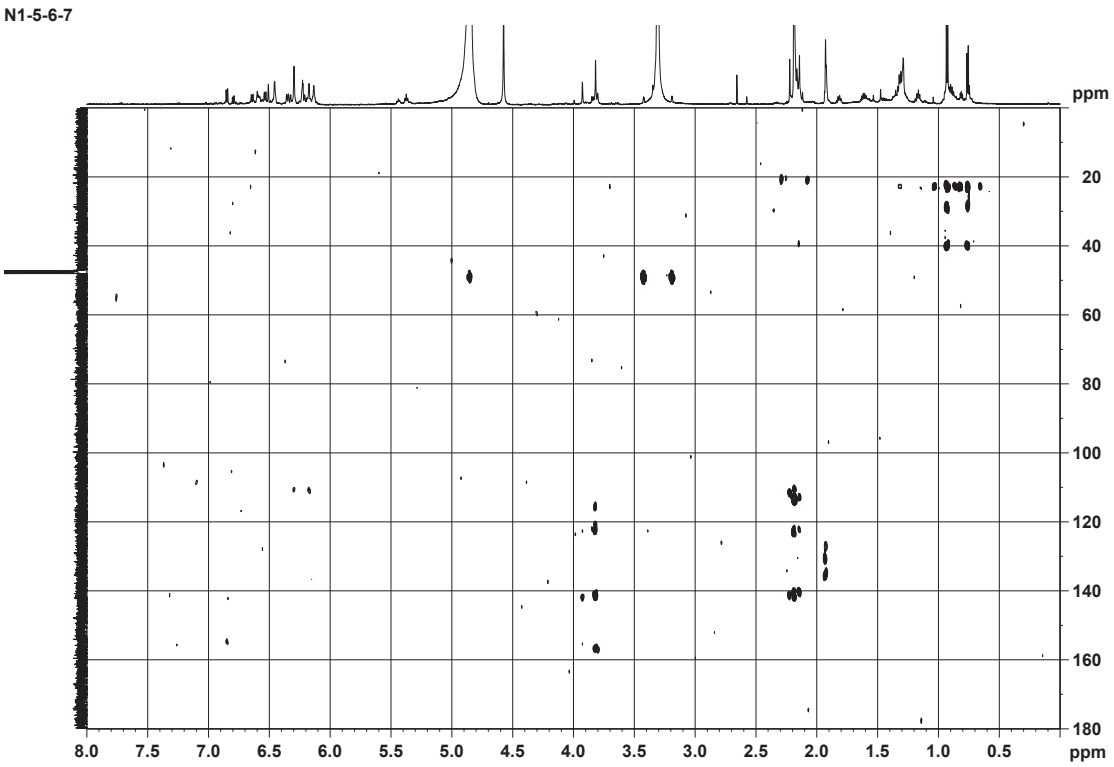

S13. HMBC (600 and 150 MHz, CD_3OD) spectrum of compound **2**.

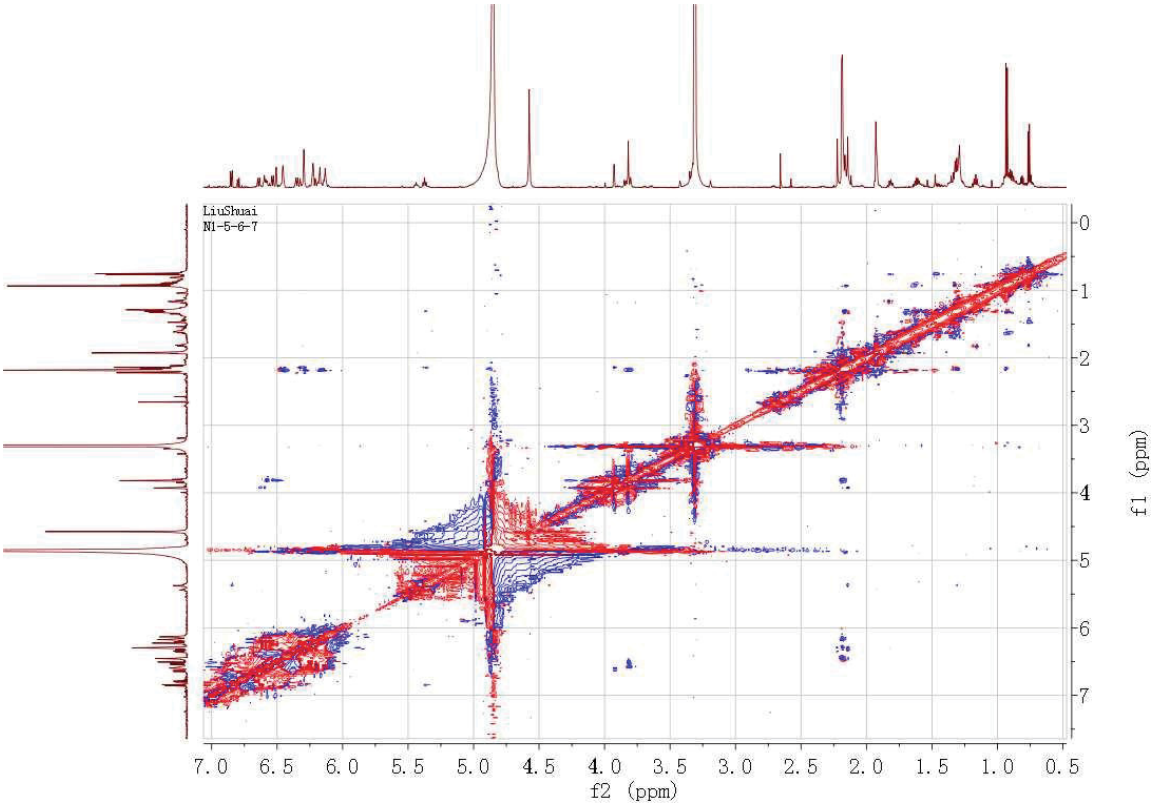

S14. ROESY (600 MHz, CD_3OD) spectrum of compound **2**.

Chapter 5

Inducing New Secondary Metabolites through the Co-Cultivation of the Fungus *Pestalotiopsis microspora* with the Bacterium *Bacillus subtilis*

Submitted to “Tetrahedron Letters”.

Impact Factor: 2.347.

Inducing new secondary metabolites through co-cultivation of the fungus *Pestalotiopsis microspora* with the bacterium *Bacillus subtilis*

Shuai Liu,[a] Haofu Dai,[b] Christian Heering,[c] Christoph Janiak,[c] Wenhan Lin,[d] Zhen Liu,[a,*] Peter Proksch[a,*]

[a] Institute of Pharmaceutical Biology and Biotechnology, Heinrich-Heine-Universität Düsseldorf, Universitätsstrasse 1, 40225 Düsseldorf, Germany

[b] Key Laboratory of Biology and Genetic Resources of Tropical Crops, Ministry of Agriculture, Institute of Tropical Bioscience and Biotechnology, Chinese Academy of Tropical Agricultural Sciences, Haikou 571101, China

[c] Institute of Inorganic and Structural Chemistry, Heinrich-Heine-Universität Düsseldorf, Universitätsstrasse 1, 40225 Düsseldorf, Germany

[d] State Key Laboratory of Natural and Biomimetic Drugs, Peking University, Beijing 100191, China

ABSTRACT:

Two new lactones pestalotioprolide J (**1**) and K (**2**), together with three known compounds (**3**-**5**) were isolated from the culture of the mangrove endophytic fungus *Pestalotiopsis microspora*. The co-cultivation of this fungus with *Bacillus subtilis* afforded two new sesquiterpenes pestabacillin A (**6**), B (**7**), and eight known copounds (**8**-**15**). All the structures of new compounds (**1**, **2**, **6**, and **7**) were determined from one- and two-dimensional NMR and HRESIMS spectra. As an unusual sesquiterpene, the structure of **6** was further confirmed by single crystal X-ray diffraction.

Keywords: *Pestalotiopsis microspora*, *Bacillus subtilis*, co-cultivation.

Introduction

Fungi and bacteria co-exist in many environments, such as in the oral cavity, on cheese surface, in cyanolichens, on medical devices, on mural paintings as well as in agricultural and forest environments.[1] The long evolutionary coexistence produced different scenarios of fungal-bacterial interactions. For example, *Penicillium* molds can produce *β*-lactam antibiotics (penicillin G) to inhibit the growth of *Staphylococcus* species,[2] while bacteria can produce lipopeptides (surfactin) to impair the fungal cell membranes.[3] Auxofuran produced by *Streptomyces* sp. can promote the extension of fungal mycelium.[4] On cheese surfaces, the lactate metabolism and alkaline production of the yeasts can create less acidic environment for the growth of some bacteria, which are very important for cheese ripening.[5] The fungus *Cryptococcus neoformans* can use the bacterial melanin precursor homogentisic acid to synthesize melanin to protect itself from UV and other environmental stress.[6]

In previous studies of our group, co-cultivation of fungi with bacteria was shown to induce the accumulation of new secondary fungal metabolites.[7–9] This paper reports the isolation and structure elucidation of metabolites from the mangrove-derived fungus *Pestalotiopsis microspora* in axenic culture and in co-culture with *Bacillus subtilis*. Two new lactones (**1**−**2**) and three known compounds (**3**−**5**) were isolated from the axenic culture of *P. microspora*, while two new sesquiterpenoids (**6**-**7**) and eight known compounds (**8**-**15**) were obtained from co-cultures of *P. microspora* and *B. subtilis* (Figure 1).

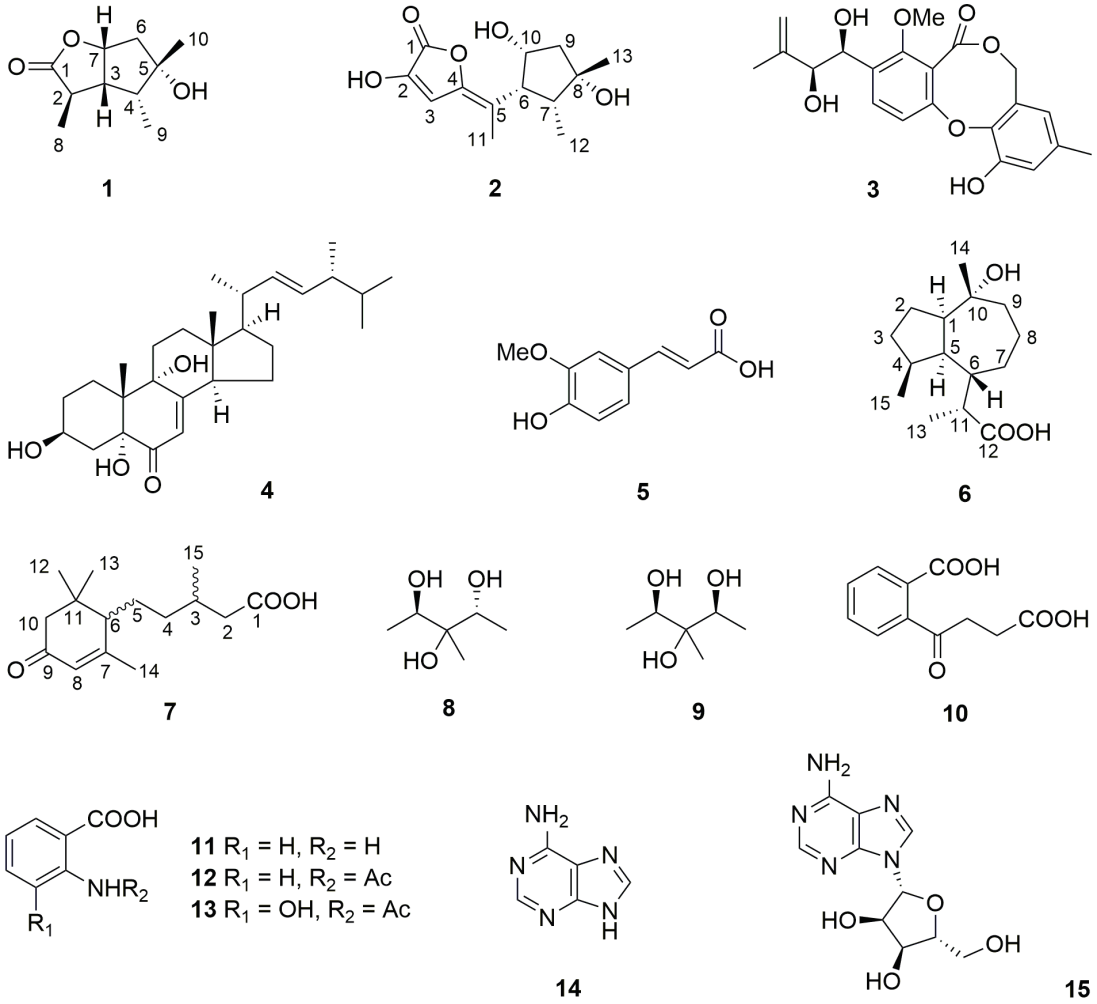

Figure 1. Structures of isolated compounds.

Results and Discussion

Compound **1** was isolated as colorless oil. The molecular formula $C_{10}H_{16}O_3$ was determined on the basis of the HR-ESIMS data, indicating three degrees of unsaturation. The ^{13}C NMR spectrum (Table 1) displayed ten signals including a carbonyl carbon at δ_C 181.6 (C-1), two oxygenated carbons at δ_C 79.5 (C-5) and 81.3 (C-7), three aliphatic methine carbons at δ_C 51.2 (C-3), 45.1 (C-4) and 36.1 (C-2), one aliphatic methylene carbon at δ_C 47.8 (C-6) and three methyl carbons at δ_C 25.6 (C-10), 18.8 (C-8) and 8.3 (C-9). The ^1H NMR spectrum of **1** (Table 1) exhibited signals of four methine groups at δ_H 4.96 (t, H-7), 2.97 (qd, H-2), 2.61 (ddd, H-3) and 1.86 (dq, H-4), signals of a methylene at δ_H 2.15 (d, H-6a) and 1.88 (dd, H-6b) as well as three methyls at δ_H 1.26 (d, Me-8), 1.25 (s, Me-10) and 1.05 (s, Me-9). These data suggested a bicyclic skeleton for **1**. The COSY correlations between Me-9/H-4, H-4/H-3, H-3/H-7 and H-7/H-6b along with key HMBC correlations from Me-10 to C-4, C-5 and C-6 established a cyclopentane ring with a hydroxy group at the C-5 position and two methyl groups at C-4 and C-5 (Figure 2). The

presence of an additional five-membered lactone ring was confirmed by the COSY correlations between H-3/H-2 and H-2/Me-8 in addition to key HMBC correlations from H-7 and Me-8 to C-1. The relative configuration of **1** was determined by ROESY data. The NOE relationships between H-7/H-6b, H-7/H-3, H-3/Me-8, H-3/H-4, H-4/Me-10, Me-10/H-6b suggested that these protons were *β*-oriented, while the NOE correlation between H-2 and Me-9 indicated their *α*-orientation (Figure 2). Thus, the structure of compound **1** was elucidated as shown, for which the name pestalotiolactone A is proposed.

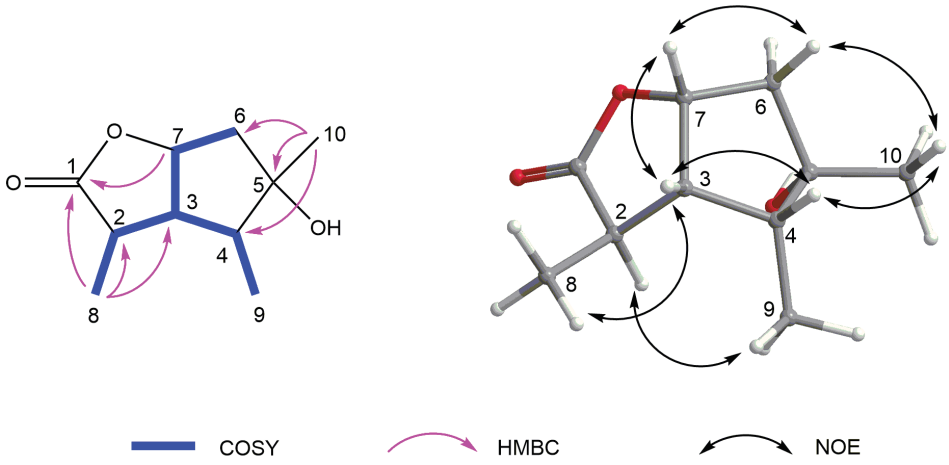

Figure 2. COSY, key HMBC and NOE correlations of compound **1**.

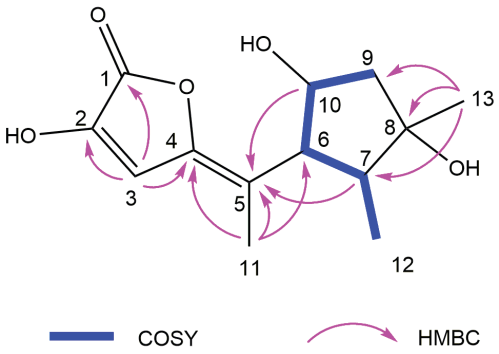

Figure 3. COSY and key HMBC correlations of compound **2**.

Table 1. ^{1}H (600 MHz) and ^{13}C (150 MHz) NMR data of **1** and **2**.

position	**1**[a]		**2**[b]	
	δ_H (J in Hz)	δ_C, type	δ_H (J in Hz)	δ_C, type
1		181.6, C		168.0, C
2	2.97, qd (7.6, 5.1)	36.1, CH		145.4, C
3	2.61, ddd (8.2, 7.8, 5.1)	51.2, CH	6.72, s	110.1, CH
4	1.86, dq (8.2, 7.0)	45.1, CH		145.5, C
5		79.5, C		121.8, C
6	2.15, d (15.3)	47.8, CH_2	3.71, dd (9.6, 6.6)	48.9, CH
	1.88, dd (15.3, 7.0)			
7	4.96, ddd (7.8, 7.0)	81.3, CH	2.16, dq (9.6, 7.5)	48.0, CH
8	1.26, d (7.6)	18.8, CH_3		79.1, C
9	1.05, d (7.0)	8.3, CH_3	2.09, dd (13.7, 6.6)	50.8, CH_2
			2.03, dd (13.7, 6.6)	
10	1.25, s	25.6, CH_3	4.34, q (6.6)	75.2, CH
11			2.08, s	17.0, CH_3
12			0.89, d (7.5)	10.8, CH_3
13			1.30, s	29.6, CH_3

[a] Recorded in $CDCl_3$. [b] Recorded in CD_3OD.

Pestalotiolactone B (**2**) possessed the molecular formula $C_{13}H_{18}O_5$ as determined by the HR-ESIMS data, with five degrees of unsaturation. In the ^{13}C NMR spectrum of **2** (Table 1), thirteen signals including a carbonyl carbon at δ_C 168.0 (C-1), four olefinic carbons at δ_C 145.5 (C-4), 145.4 (C-2), 121.8 (C-5) and 110.1 (C-3), two oxygenated aliphatic carbons at δ_C 79.1 (C-8) and 75.2 (C-10), two aliphatic methine carbons at δ_C 48.9 (C-6) and 48.0 (C-7), one aliphatic methylene carbon at δ_C 50.8 (C-9) and three methyl carbons at δ_C 29.6 (C-13), 17.0 (C-11) and 10.8 (C-12) were observed. The ^{1}H NMR spectrum of **2** (Table 1) showed one olefinic proton at δ_H 6.72 (t, H-3), one proton attached to an oxygenated carbon at δ_H 4.34 (q, H-10) and three methyls at δ_H 2.08 (s, Me-11), 1.30 (s, Me-13) and 0.89 (d, Me-12). The COSY correlation between H-9a (δ_H 2.09, dd)/H-10, H-9b (δ_H 2.03, dd)/H-10, H-10/H-6 (δ_H 3.71, dd), H-6/H-7 (δ_H 2.16, dd) and H-7/Me-12, together with the HMBC correlations from Me-13 to C-7, C-8 and C-9 indicated the

presence of a cyclopentane ring with a hydroxy group at the C-8 position and two methyl groups at the C-7 and C-8 positions in **2** (Figure 3). The partial structure from C-4 to C-6 was deduced by the HMBC correlations from Me-11 to C-4, C-5 and C-6 and from H-7 and H-10 to C-5. Combined with its molecular formula, the HMBC correlations from H-3 to C-1, C-2 and C-4 confirmed a lactone substructure from C-1 to C-4 with a hydroxyl group at C-2. The NOE correlation between H-3 and Me-11 was in accordance with a *Z*-configurated C-4/C-5 double bond. The NOE correlations between H-10/H-6, H-6/H-7 and H-7/Me-13 indicated that these protons were oriented on the same face of the ring.

In addition to these new natural products, three known compounds including pestalotiollide B (**3**),[10] 3*β*,5*α*,9*α*-trihydoxyergosta-7,22-diene-6-one (**4**)[11] and (*E*)-ferulic acid (**5**)[12] were also isolated from the axenic culture of the endophytic fungus *P*. *microspora*.

When the fungus was co-cultivated with *Bacillus subtilis*, the resulting HPLC chromatographic profiles were remarkably different from those of the axenic fungal culture. Ten compounds which were not present in the extract of the axenic fungal culture were isolated, including two new sesquiterpenoids pestabacillins A (**6**) and B (**7**).

Compound **6** was isolated as white amorphous powder. Its molecular formula $C_{15}H_{26}O_3$ was evident from the HRESIMS data. The ^{1}H NMR spectrum (Table 2) indicated the presence of three methyls at δ_H 1.24 (s, Me-14), 0.96 (d, Me-13) and 0.90 (d, Me-15) while the ^{13}C NMR spectrum exhibited fifteen signals including a carbonyl at δ_C 180.1 (C-12), an oxygenated quaternary carbon at δ_C 76.2 (C-10), five methines, five methylenes and three methyls at δ_C 29.6 (C-13), 17.0 (C-11) and 10.8 (C-12). The COSY correlations between Me-15/H-4 (δ_H 2.07, m), H-4/H_2-3, H_2-3/H_2-2, H_2-2/H-1 (δ_H 2.34, q) and H-1/H-5 (δ_H 2.08, m) as well as the HMBC correlations from Me-15 to C-3 (δ_C 33.7), C-4 (δ_C 37.0) and C-5 (δ_C 48.9) revealed the presence of a cyclopentane ring with a methyl substituent attached to C-4 in compound **6** (Figure 4). An additional seven-membered ring fused at the C-1 and C-5 positions was confirmed by the COSY correlations between H-5/H-6/H_2-7/H_2-8/H_2-9 and the HMBC correlation from Me-14 to C-1 (δ_C 52.7), C-9 (δ_C 49.0) and C-10. Furthermore, the COSY correlations between H-6 (δ_H 2.16, ddd)/H-11 (δ_H 2.59, qd) and H-11/Me-13 and the HMBC correlations from H-11 and Me-13 to C-12 indicated a 1-carboxyethyl group to be attached at the C-6 position. Thus, the planar structure of **6** was elucidated as shown, bearing a zierane-type sesquiterpene skeleton. In the ROESY spectrum of **6**,

H-1 showed correlations to H-2a (δ_H 1.87) and H-9b (δ_H 1.52), while Me-14 exhibited correlations to H-2b (δ_H 1.79) and H-9a (δ_H 1.84), suggesting a *trans* orientation of H-1 and Me-14. Assuming H-1 was oriented on the α-face of the ring, Me-14 was accordingly β-oriented (Figure 4). The NOE correlations between Me-14/H-6, Me-14/Me-15, H-6/Me-15 and H-1/H-5 indicated β-orientation of H-6 and Me-15 while H-4 and H-5 were α-oriented. In addition, the configuration at C-11 was deduced from the NOE correlations from H-11 to H-6 and Me-15 as well as from Me-13 to H-4 and H-5. Furthermore, the relative configuration of **6** was confirmed by X-ray diffraction (Figure 5).

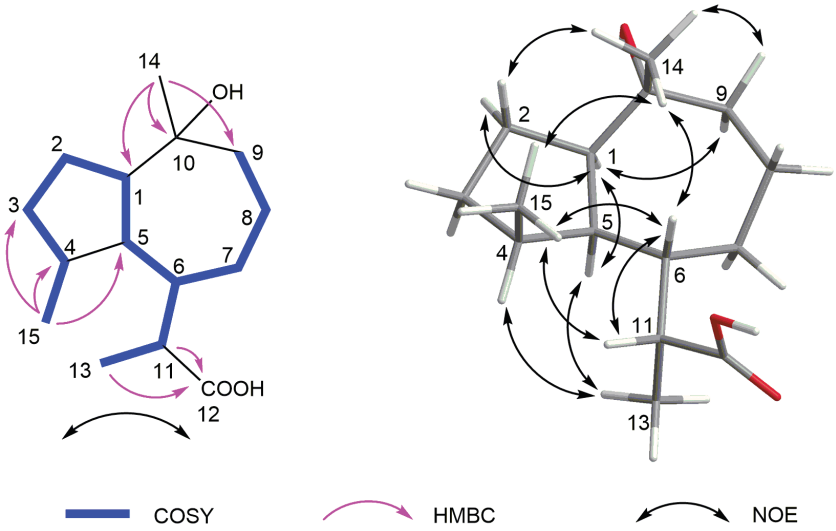

Figure 4. COSY, key HMBC and NOE correlations of compound **6**.

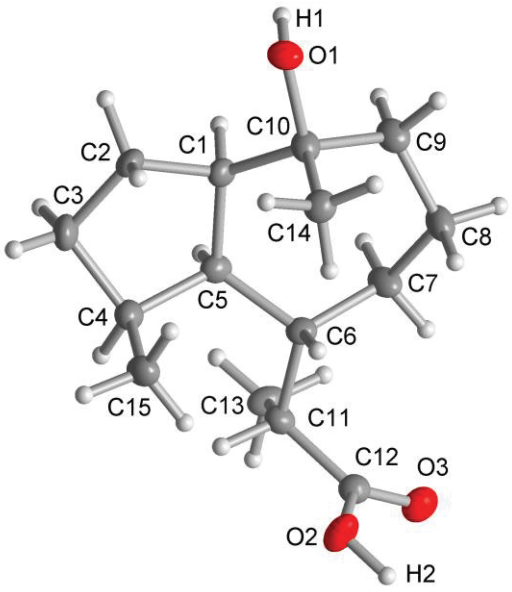

Figure 5. Molecular structure of **6** from single-crystal X-ray diffractometry.

Table 2. ^{1}H (600 MHz) and ^{13}C (150 MHz) NMR data of **6** and **7** in CD_3OD.

position	**6**		**7**	
	δ_H (J in Hz)	δ_C, type	δ_H (J in Hz)	δ_C, type
1	2.34, q (10.0)	52.7, CH		176.6, C
2	1.87, m	28.3, CH_2	2.28, dd (14.9. 6.7)	42.2, CH_2
	1.79, m		2.14, ddd (14.9. 7.4, 1.7)	
3	1.60, m	33.7, CH_2	1.91, m	31.8, CH
	1.49, m			
4	2.07, m	37.0, CH	1.51, m	37.1, CH_2
			1.32, m	
5	2.08, m	48.9, CH	1.81, m	28.6, CH_2
			1.48, m	
6	2.16, ddd (12.0, 10.0, 2.5)	41.1, CH	1.96, m	52.2, CH
7	1.56, m	31.5, CH_2		169.2, C
	1.16, m			
8	1.73, m	26.6, CH_2	5.81, s	125.0, CH
	1.39, m			
9	1.84, m	49.0, CH_2		201.9, C
	1.52, m			
10		76.2, C	2.45, d (17.4)	47.9, CH_2
			1.99, d (17.4)	
11	2.59, qd (7.0, 2.5)	43.3, CH		36.9, C
12		180.1, C	1.08, s	27.2, CH_3
13	0.96, d (7.0)	8.8, CH_3	1.02, s	28.8, CH_3
14	1.24, s	23.6, CH_3	2.03, s	24.5, CH_3
15	0.90, d (7.0)	14.7, CH_3	0.98, d (6.7)	19.7, CH_3

Compound **7** was isolated as a colorless oil. The molecular formula was determined to be $C_{15}H_{24}O_3$ based on the HR-ESIMS spectrum. The ^{1}H NMR spectrum of **7** (Table 2) showed an olefinic proton at δ_H 5.81 (s, H-8) and four methyl groups at δ_H 2.03 (s, Me-14), 1.08 (s, Me-12), 1.02 (s, Me-13) and 0.98 (d, Me-15), respectively. The HMBC correlations from Me-12 and

Me-13 to C-6 (δ_C 52.2), C-10 (δ_C 47.9) and C-11 (δ_C 36.9), from H-8 and H_2-10 (δ_H 2.45 and 1.99) to C-9 (δ_C 201.9) and from Me-14 to C-6, C-7 (δ_C 169.2) and C-8 (δ_C 125.0) established a cyclohexenone substructure with one methyl group at C-7 and two methyls at C-11 (Figure 5). In addition, a 3-methyl-4-carboxybutyl side chain at the C-6 position was deduced from the COSY correlations between H-6/H_2-5, H_2-5/H_2-4, H_2-4/H-3, H-3/H_2-2 and H-3/Me-15 as well as from the HMBC correlations from H_2-2 to C-1 (δ_C 176.6). Thus, the planar structure of **7** was elucidated as shown. Due to the conformational flexibility of the side-chain, the relative configuration of the two chiral centers at C-3 and C-6 remained unsolved.

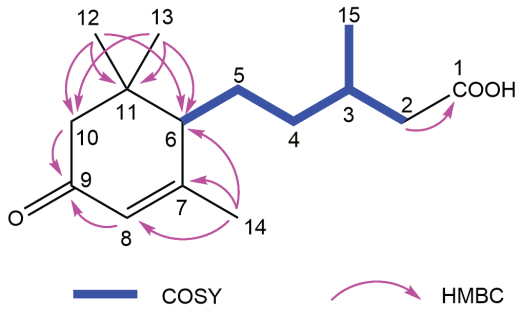

Figure 6. COSY and key HMBC correlations of compound **7**.

The additional known compounds were identified as 3-methyl-2*β*,3,4*α*-pentanetriol (**8**),[13] 3-methyl-2*β*,3,4*β*-pentanetriol (**9**),[14] *o*-succinylbenzoic acid (**10**),[15] anthranilic acid (**11**),[16] *N*-acetylanthranilic acid (**12**),[17] *N*-acetyl-3-hydroxyanthranilic acid (**13**),[18] adenine (**14**),[19] and adenosine (**15**).[20]

During the co-cultivation experiment with *B. subtilis*, the fungus *P. microspora* survived but showed a severe growth retardation compared with the axenic fungal control. It took the fungus close to 100 days to cover the surface of the solid rice medium completely, while for the axenic fungal control this time was only 28 days, indicating the severe stress for the fungus during the co-cultivation experiment. When *P. microspora* was co-cultured with *Streptomyces lividans*,[21] no such retardation of fungal had been observed suggesting that presence of *B. subtilis* causes a serious stress for the fungus when present in the same culture vessel. One reason for this might by the production of known fungicidal compounds such as iturins[22] by *B. subtilis* even though no attempt was made in this study to detect these metabolites in the culture flasks.

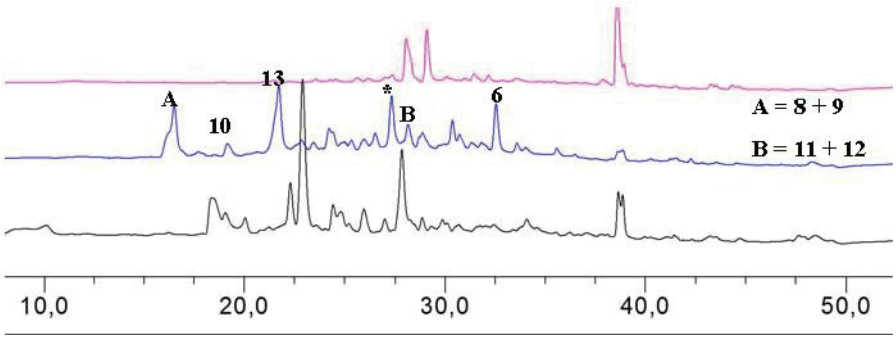

Figure 7. HPLC chromatograms of the EtOAc extracts from co-culture experiments detected at 235 nm: axenic control of *P. microspora* (pink), axenic control of *B. subtilis* (brown), co-culture of *P. microspora* with *B. subtilis* (blue) (* peak disappeared after VLC).

The extract resulting from co-cultivation of *P. microspora* with *B. subtilis* differed completely from that of axenic fungal control, but also from that of axenically grown *B. subtilis* as shown by HPLC analysis (Figure 7). Peak A turned out to be a mixture of the two diastereoisomers 3-methyl-2*β*,3,4*α*-pentanetriol (**8**) and 3-methyl-2*β*,3,4*β*-pentanetriol (**9**) with a ratio of 3:1. Since compound **9** was previously reported from the mangrove-derived bacterium *Bacillus* sp.,[14] the producer of **8** and **9** in the co-culture experiment conducted in this study is likewise suggested to be *B. subtilis*. *o*-Succinylbenzoic acid (**10**), which is a well-known intermediate during the biosynthetis of vitamin K_2 in several gram positive bacteria including *B. subtilis*,[15] is likewise proposed to be produced by *B. subtilis*. The same is suggested for the anthranilic acid derivatives (**11**-**13**) since anthranilic acid (**11**) was repeatedly obtained from co-cultures of different fungi with the same bacterial strain *B. subtilis* as employed in this study.[7-8] Adenine (**14**) and adenosine (**15**) are ubiquituous metabolites, hence no suggestion with regard to the possible producer can be made. Compound **6** is a novel zierane-type sesquiterpene derivative, whose analogues are only known from plants,[23] while compound **7** is a derivative of abscisic acid, which is a plant hormone that has also frequently been isolated from endophytic fungi.[24] Thus compounds **6** and **7** are suggested to be produced by the fungus *P. microspora*.

All isolated compounds were tested for their cytotoxicity against the L5178Y mouse lymphoma cell line. However, none of them showed activity at a dose of 10 μg/mL.

In summary, compounds **1** and **2** are bicyclic lactones isolated from the EtOAc extract of the axenically grown fungus *P. microspora* and they share the same 1,2-dimethylcyclopentane subunit. Since **1** is a monoterpenoid and **2** contained three additional carbons compared to **1**, the latter

compound is suggested to be formed through condensation of phosphoenolpyruvate (PEP) and a monoterpene moiety. Compounds **6** and **7** are sesquiterpenoids that were obtained from the co-culture of *P. microspora* and *B. subtilis*. Both are suggested to be produced by the fungus as a consequence of the presence of the bacterium that caused a severe retardation of the fungal growth.

Acknowledgments

S. L. thanks China Scholarship Council for financial support. P.P. wants to thank the Manchot Foundation for support.

Supplementary data

Supplementary data (UV, MS and NMR spectra of **1**, **2**, **6** and **7** as well as X-ray data of **6**) associated with this article can be found in the online version.

References

1. Frey-Klett, P.; Burlinson, P.; Deveau, A.; Barret, M.; Tarkka, M.; Sarniguet, A. *Microbiol. Mol. Biol. Rev.* **2011**, *75*, 583−609.
2. Fleming, A. *Br. J. Exp. Pathol.* **1929**, *10*, 226−236.
3. Heerklotz, H.; Seelig, J. *Eur. Biophys. J.* **2007**, *36*, 305−314.
4. Riedlinger, J.; Schrey, S. D.; Tarkka, M. T.; Hampp, R.; Kapur, M.; Fiedler, H. P. *Appl. Environ. Microbiol.* **2006**, *72*, 3550−3557.
5. Corsetti, A.; Rossi, J.; Gobbetti, M. *Int. J. Food Microbiol.* **2001**, *69*, 1−10.
6. Frases, S.; Salazar, A.; Dadachova, E.; Casadevall, A. *Appl. Environ. Microbiol.* **2007**, *73*, 615−621.
7. Ola, A. R. B.; Thomy, D.; Lai, D.; Brötz-Oesterhelt, H.; Proksch, P. *J. Nat. Prod.* **2013**, *76*, 2094−2099.
8. Chen, H.; Daletos, G.; Abdel-Aziz, M. S.; Thomy, D.; Dai, H.; Brötz-Oesterhelt, H.; Lin, W.; Proksch, P. *Phytochem. Lett.* **2015**, *12*, 35−41.
9. Ebrahim, W.; El-Neketi, M.; Lewald, L. I.; Orfali, R. S.; Lin, W.; Rehberg, N.; Kalscheuer, R.; Daletos, G.; Proksch, P. *J. Nat. Prod.* **2016**, *79*, 914−922.
10. Xu J.; Aly A. H.; Wray V.; Proksch P. *Tetrahedron Lett.* **2011**, *52*, 21−25.
11. Kawagishi, H.; Katsumi, R.; Sazawa, T.; Mizuno, T.; Hagiwara, T.; Nakamura T. *Phytochemistry* **1988**, *27*, 2777−2779.

12. Xing, X.; Ho, P.; Bourquin, G.; Yeh, L. A.; Cuny, G. D. *Tetrahedron* **2003**, *59*, 9961−9969.

13. Talontsi, F. M.; Kenla, T. J. N.; Dittrich, B.; Douanla-Meli, C.; Laatsch, H. *Planta Med.* **2012**, *78*, 1020−1023.

14. Tang, J.; Gao, H.; Hong, K.; Jiang, M.; Zhou, G.; Wang, N.; Yao, X. *Chin. J. Med. Chem.* **2008**, *18*, 206−209.

15. Plataniappan, C.; Taber, H.; Meganathan, R. *J. Bacteriol.* **1994**, *176*, 2648−2653.

16. Regulska, E.; Samsonowicz, M.; Świsłocka, R.; Lewandowski, W. *J. Mol. Struct.* **2009**, *936*, 162−170.

17. Giri, R.; Lam, J. K.; Yu, J. Q. *J. Am. Chem. Soc.* **2010**, *132*, 686−693.

18. Hund, H. K.; De Beyer, A.; Lingens, F. *Biol. Chem. Hoppe-Seyler* **1990**, *371*, 1005−1008.

19. Saladino, R.; Crestini, C.; Neri, V.; Ciciriello, F.; Costanzo, G.; Mauro, E. D. *ChemBioChem* **2006**, *7*, 1707−1714.

20. Patching, S. G.; Baldwin, S. A.; Baldwin, A. D.; Young, J. D.; Gallagher, M. P.; Henderson, P. J. F.; Herbert, R. B. *Org. Biomol. Chem.* **2005**, *3*, 462−470.

21. Liu, S.; Dai, H.; Makhloufi, G.; Heering, C.; Janiak, C.; Hartmann, R.; Mándi, A.; Kurtán, T.; Müller, W. E. G.; Kassack, M. U.; Lin, W.; Liu, Z.; Proksch P. *J. Nat. Prod.* **2016**, *79*, 2332–2340.

22. Gueldner, R. C.; Reilly, C. C.; Pusey, P. L.; Costello, C. E.; Arrendale, R. F.; Cox, R. H.; Himmelsbach, D. S.; Crumley, F. G.; Gulter, H. G. *J. Agric. Food Chem.* **1988**, *36*, 366−370.

23. Nakashima, K.; Oyama, M.; Ito, T.; Witono, J. R.; Darnaedi, D.; Tanaka, T.; Murata, J.; Iinuma, M. *Chem. Biodiversity* **2012**, *9*, 2195−2202.

24. Zeevaart, J. A. D. *Ann. Rev. Plant Physiol. Plant Mol. Biol.* **1988**, *39*, 439−473.

Supporting information

Inducing new secondary metabolites through the co-cultivation of the fungus *Pestalotiopsis microspora* with the bacterium *Bacillus subtilis*

Shuai Liu,[†] Haofu Dai,[‡] Wenhan Lin,[§] Zhen Liu,[*,†] Peter Proksch[*,†]

[†]Institute of Pharmaceutical Biology and Biotechnology, Heinrich-Heine-Universität Düsseldorf, Universitätsstrasse 1, 40225 Düsseldorf, Germany

[‡]Key Laboratory of Biology and Genetic Resources of Tropical Crops, Ministry of Agriculture, Institute of Tropical Bioscience and Biotechnology, Chinese Academy of Tropical Agricultural Sciences, Haikou 571101, China

[§]State Key Laboratory of Natural and Biomimetic Drugs, Peking University, Beijing 100191, China

Experimental Section

General Experimental Procedures. The optical rotations were measured on a JASCO p-1020 polarimeter. The HRESIMS spectra were recorded on a Bruker UHR-QTOF maxis 4G mass spectrometer. A Bruker Avance III 600 spectrometer was used to measure ^{1}H, ^{13}C and 2D NMR spectra. The HPLC analysis was conducted on the Dionex P580 system, coupled to a photodiode array detector (UVD340s) and an Eurospher C_{18} separation column (125 mm × 4 mm i.d., 5 μm). Column chromatography was conducted using Sephadex LH-20 or MN silica gel 60M as stationary phases. Thin layer chromatography (TLC) was performed on Merck pre-coated silica gel 60 F_{254} plates with detection at 254 and 365 nm. For semi-preparative HPLC, a Lachrom-Merck Hitachi system (L7100 pump and L7400 UV detector) and an Eurospher C_{18} column (300 mm × 8 mm i.d., 10 μm) were used.

Fungal Material, Identification, Fermentation and Extraction. The endophytic fungus was isolated from fresh, healthy fruits of *Drepanocarpus lunatus* (Fabaceae) collected in August 2013 from Douala, Cameroon. It was identified as *P. microspora* (GenBank accession number KU255793) according to DNA amplification and sequencing of the fungal ITS region as described before.[1] Twenty 1 L Erlenmeyer flasks with solid rice medium (100g rice, 3.5g sea salt, and 110 mL demineralized water, each) were used for fermentation. They were autoclaved at 121 °C for 20 min and cooled to room temperature, followed by inoculation with the fungus. After cultivation at 20 °C under static conditions for four weeks, 500 mL ethyl acetate were added to each flask to stop the fermentation. The flasks were shaken at 150 rpm for 8 h on a shaker, and then the ethyl acetate solution was evaporated to dryness, yielding

15.4 g EtOAc extract.

Isolation of Compounds 1-5. The EtOAc extract was first subjected to separation on silica gel by vacuum liquid chromatography using solvents (500 mL each gradient) in a gradient of increasing polarity (*n*-hexane−EtOAc, 9:1, 7:3, 7:3, 1:1, 1:1, 3:7, 3:7; dichloromethane (DCM)−methanol, 15:1, 9:1, 7:3, 0:10) to yield 11 fractions. Fraction 4 (175 mg) was subjected to a Sephadex LH-20 column using 100% MeOH as mobile phase to remove any pigments. Further purification was carried out by semi-preparative HPLC (MeOH in H_2O, 0-5 min, 50%; 5-15min, from 50% to 65%; 16-19 min, 100%) and yielded **1** (5.6 mg) and **5** (1.1 mg). With a similar purification processes, fraction 7 (100 mg) yielded **2** (3.0 mg), **3** (2.3 mg) and **4** (2.0 mg) (HPLC sequence, MeOH in H_2O: 0-10 min, from 30% to 35%; 10-25 min, from 35% to 50%; 26-30 min, 100%).

Co-cultivation Experiment of *P. microspora* with *B. subtilis.* Both microorganisms were co-cultured in seven Erlenmeyer flasks (1 L) containing 110 mL demineralized water, 3.8 g sea salt and 100 g rice (one flask for *P. microspora* alone; one for *B. subtilis* alone; five for co-cultures of *P. microspora* and *B. subtilis*) which had been autoclaved before inoculating the fungus and the bacterium.

The bacterial strain panel included laboratory strain *B. subtilis* 168 trpC2. *B. subtilis* was grown in Mueller-Hinton (MH) broth (0.20%, w/v, beef extract; 1.75%, w/v, acid digest of casein; 0.15%, w/v, starch). The bacteria were first inoculated to the prewarmed MH broth (50 mL in 250 mL flask), and then incubated at 37 ℃ for 15 h, shaking at 200 rpm to mid exponential growth phase. Afterwards the concentration of *B. subtilis* was diluted to OD_{600} of 0.2, 10 mL of the culture was further added to

the rice medium for another 5 days incubation at 37 ℃. After this preincubation, *P. microspora* grown on malt agar was added to the rice medium containing *B. subtilis* under sterile conditions. Next, all flasks were stored at 20 °C under static conditions. The axenic fungal control took 28 days to penetrate the rice medium completely, while the co-cultivation of the fungus and the bacterium lasted 98 days in total. The fermentation was stopped by adding 500 mL of EtOAc to each flask. The extraction was completed after shaking the flasks on a laboratory shaker at 150 rpm for 8 h. After evaporation, each extract was dissolved in 5 mL of MeOH, then 25 μL of this solution was injected into an analytical HPLC machine.

Isolation of Compounds 6-15. Five flasks of co-cultures of *P. microspora* and *B. subtilis* afforded 3.4 g brown extract. This extract was first subjected to silica gel vacuum liquid chromatography using solvents (500 mL each gradient) in a gradient of increasing polarity (*n*-hexane−EtOAc, 9:1, 7:3, 7:3, 1:1; dichloromethane−MeOH, 15:1, 9:1, 7:3, 0:10) to obtain 10 fractions in total. All fractions were analyzed by HPLC, and different compounds (Figure 4) were isolated from fractions 5, 6, 8, 10 and 11. Fraction 5 (169 mg) was subjected to a Sephadex LH-20 column with 100% MeOH to remove pigments followed by further purification using semi-preparative HPLC (MeOH in H_2O, 0-5 min, 45%; 5-15min, from 45% to 72%; 16-19 min, 100%), which yielded **6** (2.5 mg). Following the same procedure, fraction 6 (457 mg) gave **7** (3.0 mg) (HPLC sequence, MeOH in H_2O, 0-10 min, from 40% to 50%; 10-25 min, from 50% to 70%; 26-30 min, 100%), fraction 8 (572 mg) yielded a mixture of **8** and **9** (18.0 mg, 3:1) (HPLC sequence, MeOH in H_2O, 0-10 min, from 5% to 10%; 10-25 min, from 10% to 30%; 27-30 min, 100%), fraction 10 (385 mg) yielded **13** (1.0 mg),

14 (0.8 mg), **15** (0.9 mg) and the mixture of **11** and **12** (1.4 mg, 1:1) (HPLC sequence, MeOH in H_2O, 0-10 min, from 5% to 20%; 10-25 min, from 20% to 45%; 27-30 min, 100%), and fraction 11 (258.9 mg, MeOH 100%) yielded **10** (2.0 mg) (HPLC sequence, MeOH in H_2O, 0-10 min, from 5% to 10%; 10-25 min, from 10% to 25%; 27-30 min, 100%).

*Pestalotiolactone A (**1**):* colorless oil; $[\alpha]^{20}_D$ -36.1 (*c* 1.4, MeOH); UV (MeOH) λ_{max} (log ε) 234 (3.41); ^1H and ^{13}C NMR data, see **Table 1**; HRESIMS *m/z* 185.1172 $[M + H]^+$ (calcd for $C_{10}H_{17}O_3$, 185.1172).

*Pestalotiolactone B (**2**):* colorless oil; $[\alpha]^{20}_D$ -12.9 (*c* 0.7, MeOH); UV (MeOH) λ_{max} (log ε) 304 (4.82); ^1H and ^{13}C NMR data, see **Table 1**; HRESIMS *m/z* 255.1221 $[M + H]^+$ (calcd for $C_{13}H_{19}O_5$, 255.1227)

*Pestabacillin A (**6**):* white amorphous powder; $[\alpha]^{20}_D$ +58.7 (*c* 0.6, MeOH); UV (MeOH) λ_{max} (log ε) 216 (3.42); ^1H and ^{13}C NMR data, see **Table 2**; HRESIMS *m/z* 277.1774 $[M + Na]^+$ (calcd for $C_{15}H_{26}NaO_3$, 277.1774).

*Pestabacillin B (**7**):* colorless oil; $[\alpha]^{20}_D$ -43.7 (*c* 0.8, MeOH); UV (MeOH) λ_{max} (log ε) 242 (3.92); ^1H and ^{13}C NMR data, see **Table 2**; HRESIMS *m/z* 253.1800 $[M + H]^+$ (calcd for $C_{15}H_{25}O_3$, 253.1798).

X-ray Crystallographic Analysis of 6. *Crystallization conditions*: X-ray quality crystals of **6** were obtained by slow evaporation from a MeOH solution. A suitable single crystal was carefully selected under a polarizing microscope. *Data collection*: Bruker Kappa APEX2 CCD diffractometer (with microfocus tube), Mo-Kα radiation (λ = 0.71073 Å), multilayer mirror, ω- and ϕ-scan; data collection with APEX2, cell refinement and data reduction with SAINT,[2] experimental absorption correction with

SADABS.[3] *Structure Analysis and Refinement*: The structure was solved by direct methods using SHELXS-97; refinement was done by full-matrix least squares on F^2 using the SHELXL-97 program suite.[4] All non-hydrogen positions were refined with anisotropic displacement parameters. Hydrogen atoms were positioned geometrically (1.00 Å for tertiary CH, 0.99 Å for CH_2 and 0.98 Å for CH_3) and refined using riding models (AFIX 43, 13, 23 and 133 or 137, respectively), with $U_{iso}(H) = -1.2U_{eq}$(CH, CH_2) and $-1.5U_{eq}(CH_3)$. The hydrogen atoms on the hydroxyl groups with O1 and O2 were found and refined with $U_{iso}(H) = 1.5U_{eq}(O)$. The data set for this light atom (C, H and O only) structure was measured with Mo-Kα radiation. Hence only the relative and not the absolute configuration could be determined in the absence of anomalous dispersion. The determined Flack or absolute structure parameter for the non-centrosymmetric space group has no meaning.[5]

Crystal data and details on the structure refinement are given in Table S1. Graphics were drawn with DIAMOND.[6] The structural data has been deposited with the Cambridge Crystallographic Data Center (CCDC 1512431).

Table S1. Crystal data and structure refinement for **6**.

CCDC number	1512431
Empirical formula	$C_{15}H_{26}O_3$
M/g mol^{-1}	254.36
Crystal size/mm^3	0.30 × 0.20 × 0.01
Temperature/K	173
θ range/°	2.8–26.6°
h; k; l range	-7/7 ,17/17, -10,/10
Crystal system	Monoclinic
Space group	$P2_1$
a/Å	6.2908 (7)
b/Å	14.4437 (19)
c/Å	8.4505 (11)
α/°	90
β/°	111.852 (2)
γ/°	90
V/Å^3	712.66 (15)
Z	2
D_{calc}/g cm^{-3}	1.185
μ (Mo Kα)/mm^{-1}	0.08
F(000)	280
Max./min. transmission	0.746, 0.393
Reflections collected	3732
Independent reflect. (R_{int})	1926 (0.0671)
Data/restraints/parameters	1926/1/172
Max./min. Δρ/e Å^{-3} [a]	0.19 /-0.19
R_1/wR_2 [I>2σ(I)] [b]	0.0473/0.0919
R_1/wR_2 (all data) [b]	0.0634/0.0957
Goodness-of-fit on F^2 [c]	0.926
Flack parameter [d]	n.a. [e]

[a] Largest difference peak and hole; [b] $R_1 = [\sum(||F_o| - |F_c||)/\sum|F_o|]$; $wR_2 = [\sum[w(F_o^2 - F_c^2)^2]/\sum[w(F_o^2)^2]]^{1/2}$; [c] Goodness-of-fit = $[\sum[w(F_o^2 - F_c^2)^2]/(n - p)]^{1/2}$; [d] Absolute structure parameter **Error! Bookmark not defined.** [e] n.a. = not applicable; for a light-atom structure the Flack parameter from Mo-Ka radiation is meaningless in the absence of anomalous dispersion.

References

25. Kjer, J; Debbab, A; Aly, AH; Proksch, P. *Nat. Protoc.* **2010**, *5*, 479−490.

26. Apex2, Data Collection Program for the CCD Area-Detector System; SAINT, Data Reduction and Frame Integration Program for the CCD Area-Detector System. Bruker Analytical X-ray Systems, Madison, Wisconsin, USA, 1997-2006.

27. Sheldrick, G. M. Program SADABS: Area-detector absorption correction, University of Göttingen, Germany, **1996**.

28. Sheldrick, G. M. *Acta Crystallogr. Sect. A* **2008**, *64*, 112−122.

29. (a) Flack, H. D.; Sadki, M.; Thompson, A. L.; Watkin, D. J. *Acta Crystallogr., Sect. A: Fundam. Crystallogr.* **2011**, *67*, 21–34. (b) Flack, H. D.; Bernardinelli, G. *Chirality*, **2008**, *20*, 681–690. (c) Flack, H. D.; Bernardinelli, G. *Acta Crystallogr., Sect. A: Fundam. Crystallogr.* **1999**, *55*, 908–915. (d) Flack, H. *Acta Crystallogr., Sect. A: Fundam. Crystallogr.* **1983**, *39*, 876–881.

30. Brandenburg, K. Diamond (Version 3.2), Crystal and Molecular Structure Visualization, Crystal Impact – K. Brandenburg & H. Putz Gbr, Bonn (Germany) **2009**.

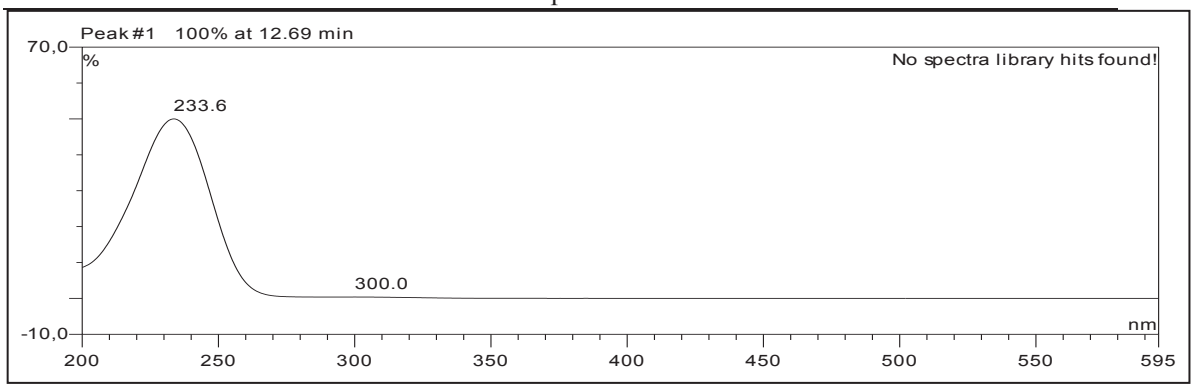

S1. UV spectrum of compound **1**.

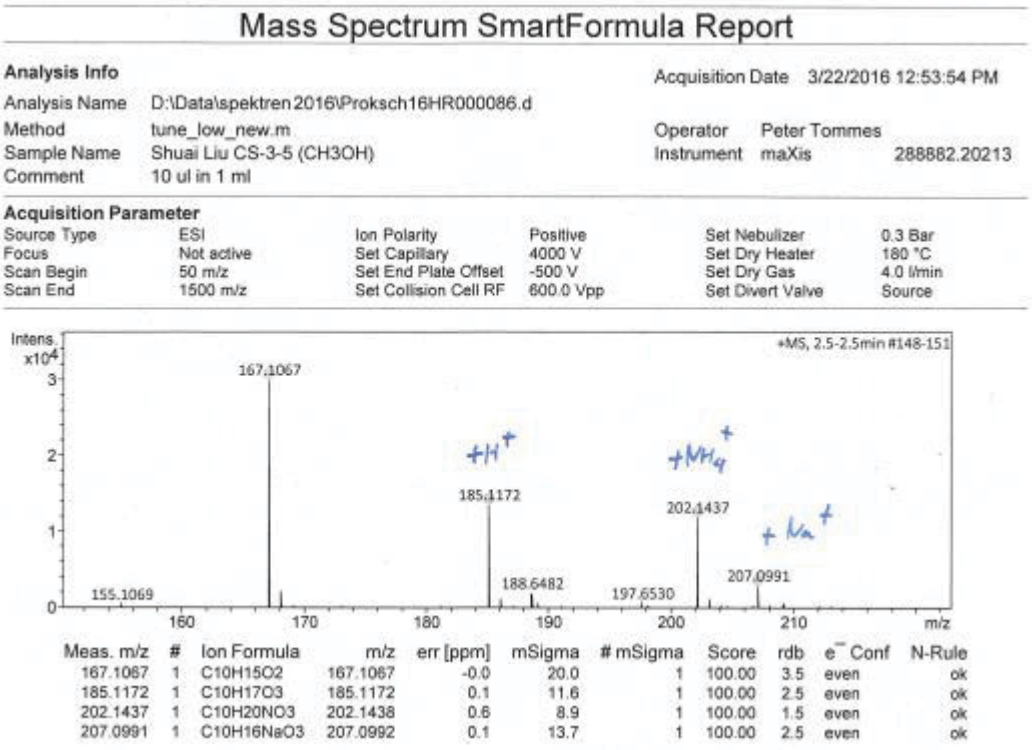

S2. HRESIMS spectrum of compound **1.**

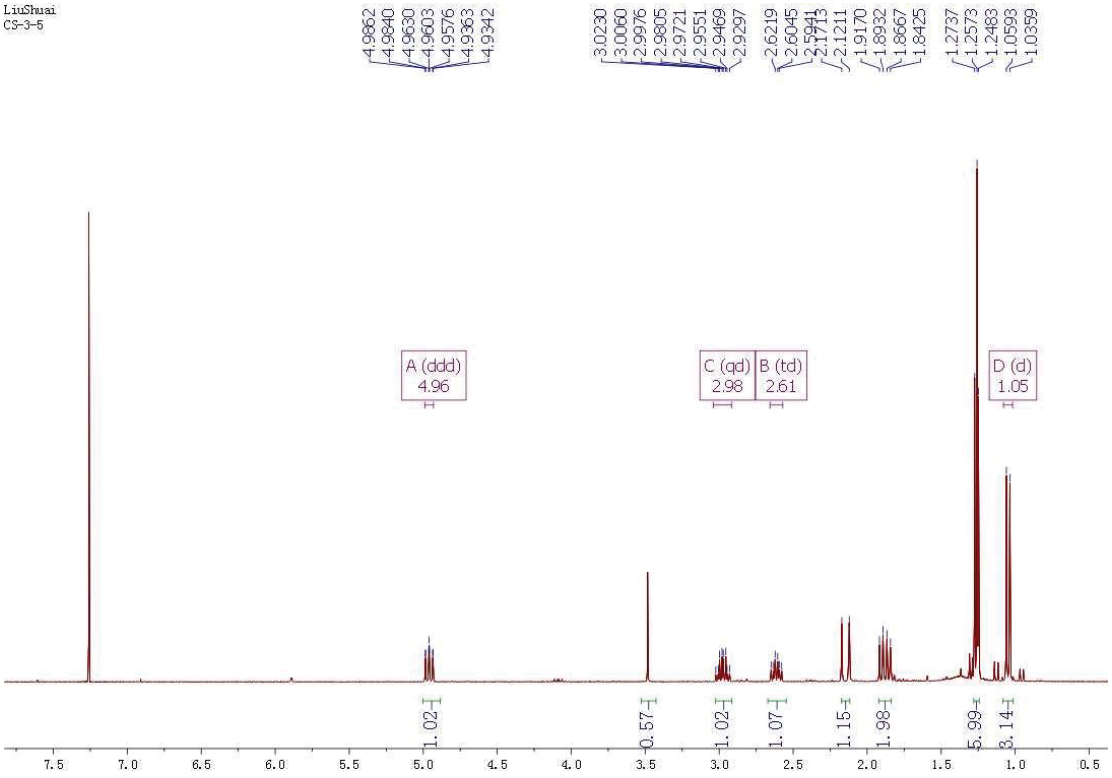

S3. ^{1}H NMR (600 MHz, $CDCl_3$) spectrum of compound **1**.

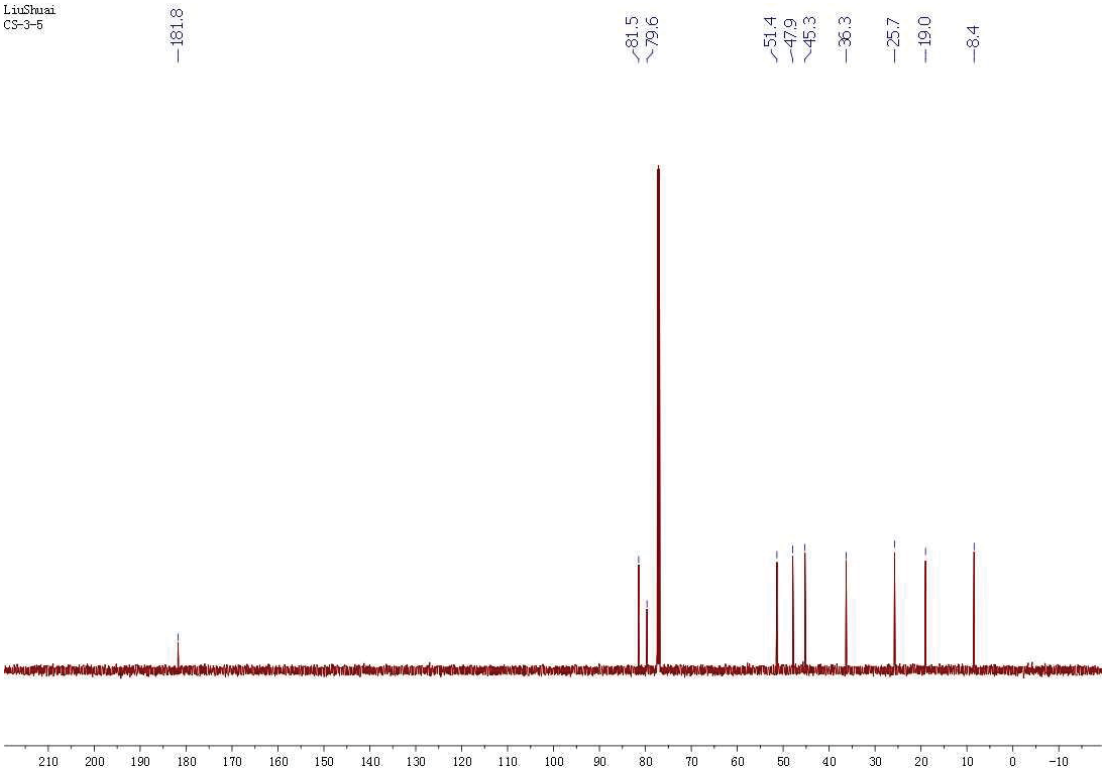

S4. ^{13}C NMR (150 MHz, $CDCl_3$) spectrum of compound **1**.

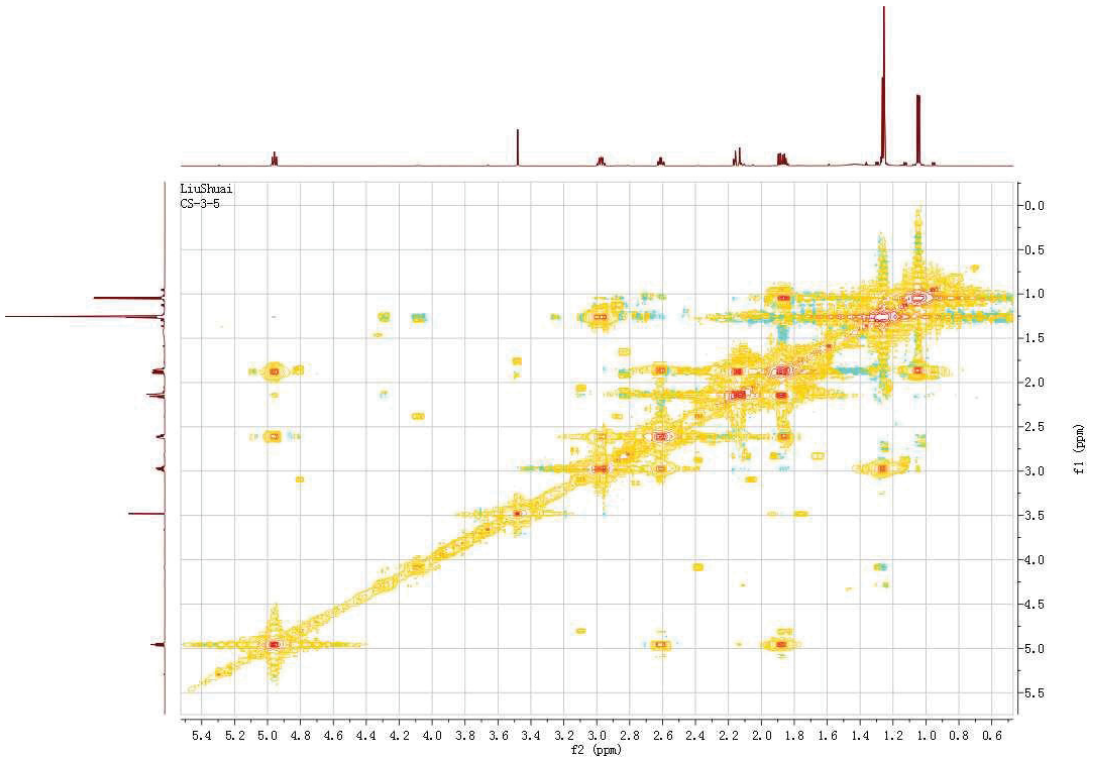

S5. ^{1}H-^{1}H COSY (600 MHz, $CDCl_3$) spectrum of compound **1**.

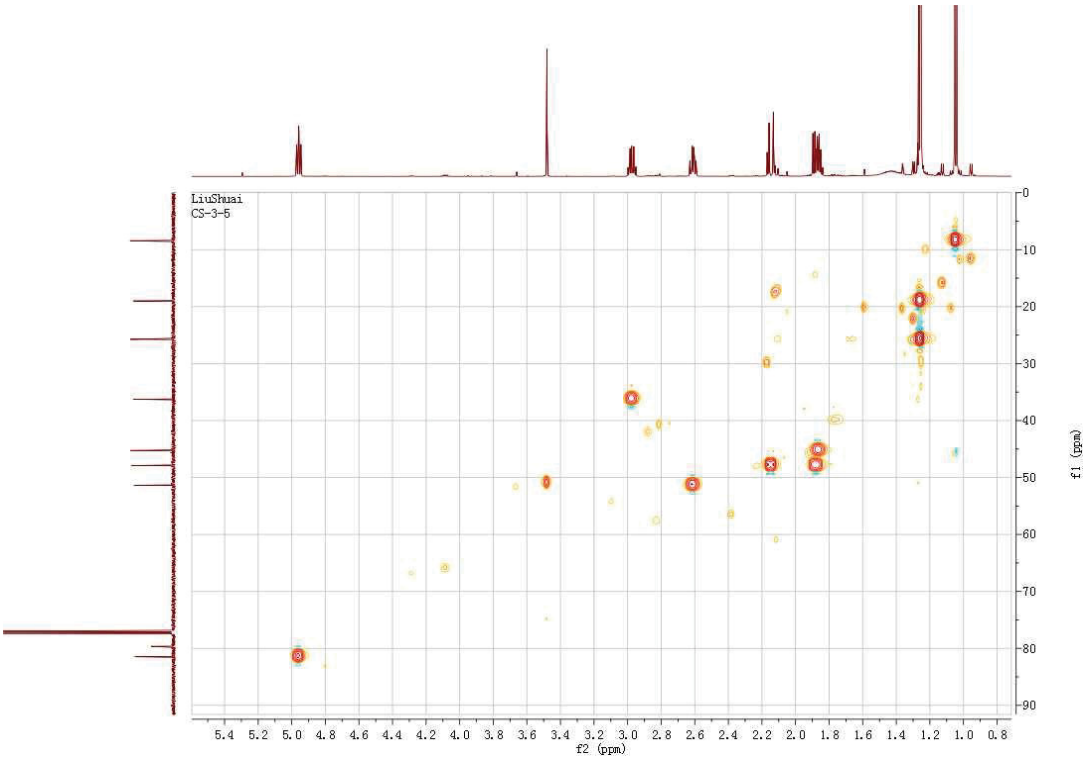

S6. HSQC (600 and 150 MHz, $CDCl_3$) spectrum of compound **1**.

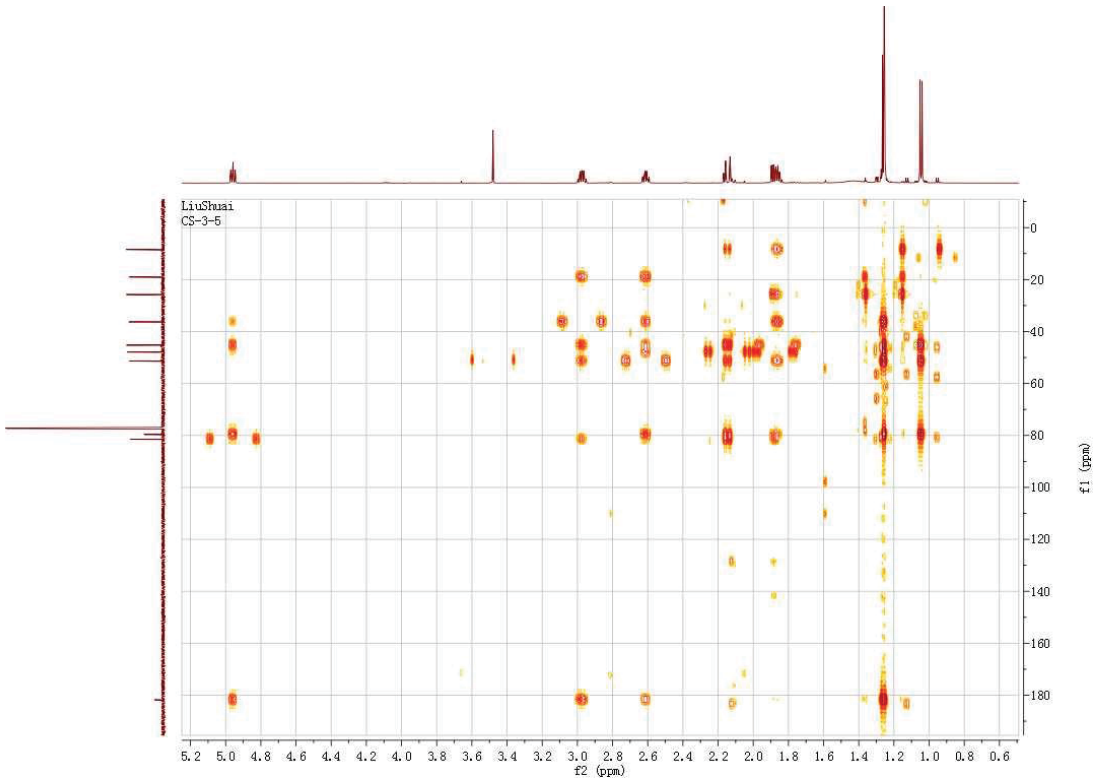

S7. HMBC (600 and 150 MHz, $CDCl_3$) spectrum of compound **1**.

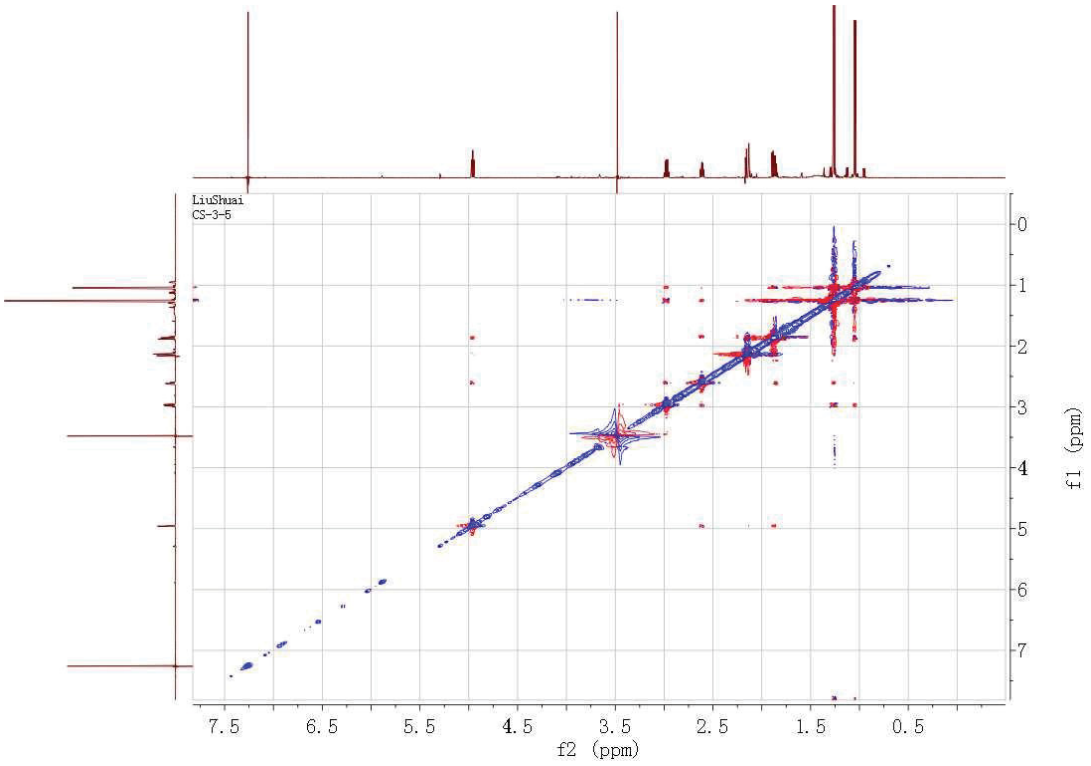

S8. ROESY (600 MHz, $CDCl_3$) spectrum of compound **1**.

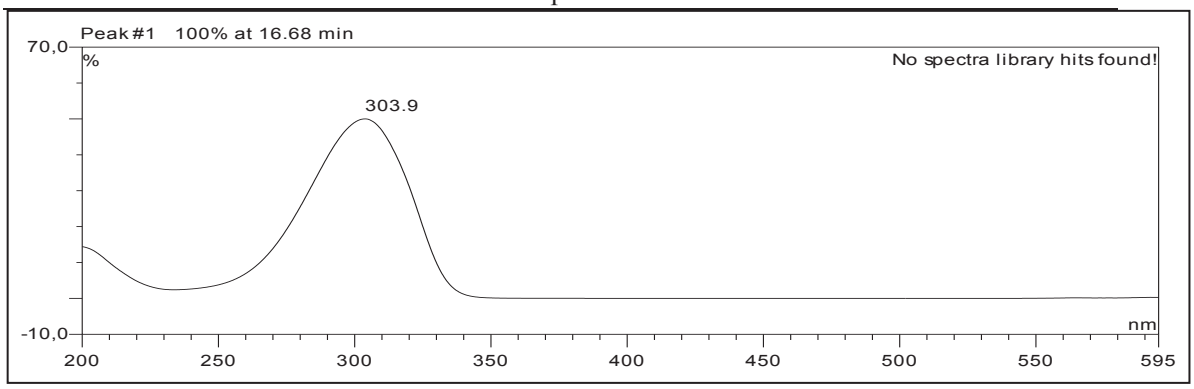

S9. UV spectrum of compound **2**.

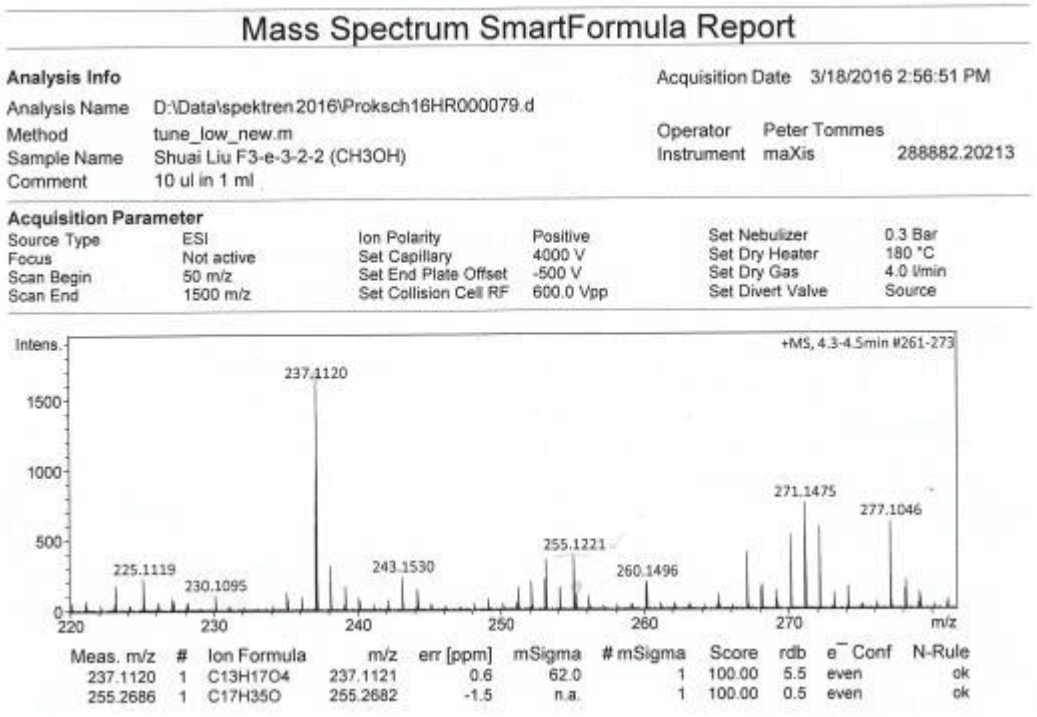

S10. HRESIMS spectrum of compound **2.**

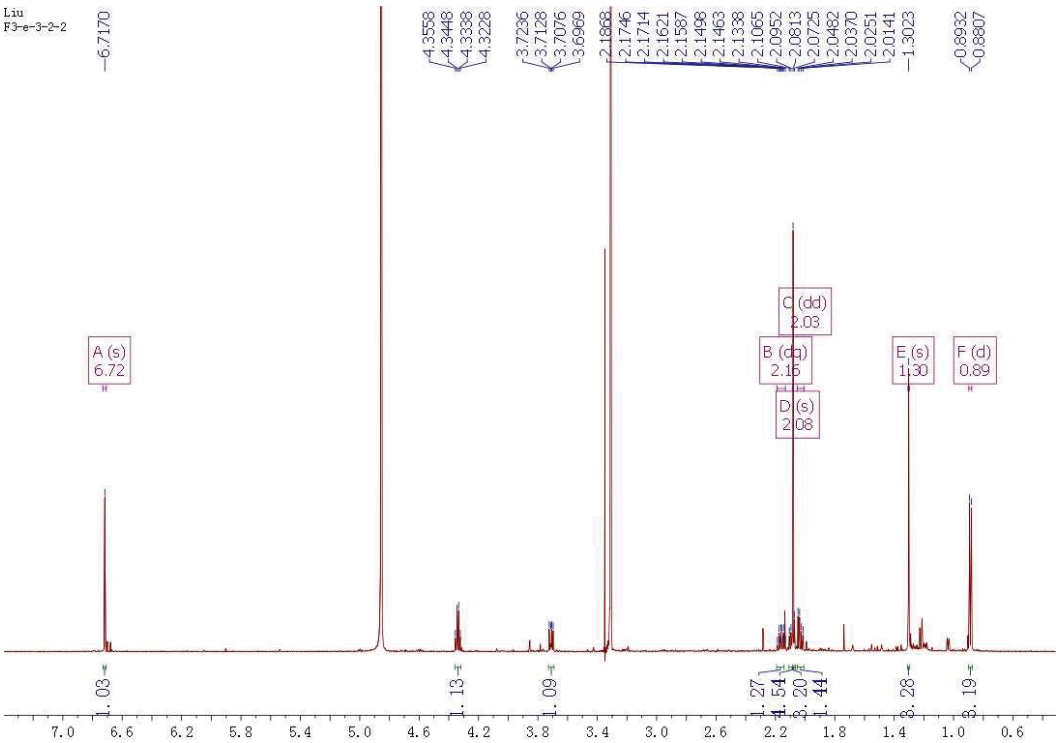

S11. ^{1}H NMR (600 MHz, CD_3OD) spectrum of compound **2**.

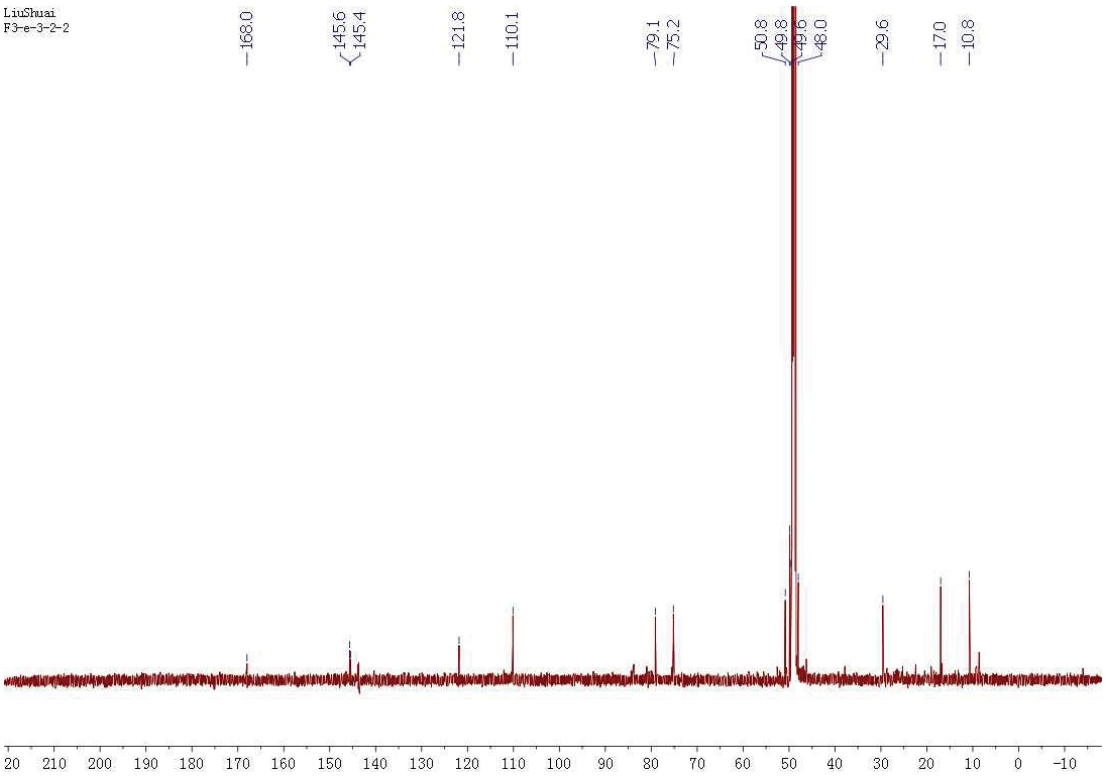

S12. ^{13}C NMR (150 MHz, CD_3OD) spectrum of compound **2**.

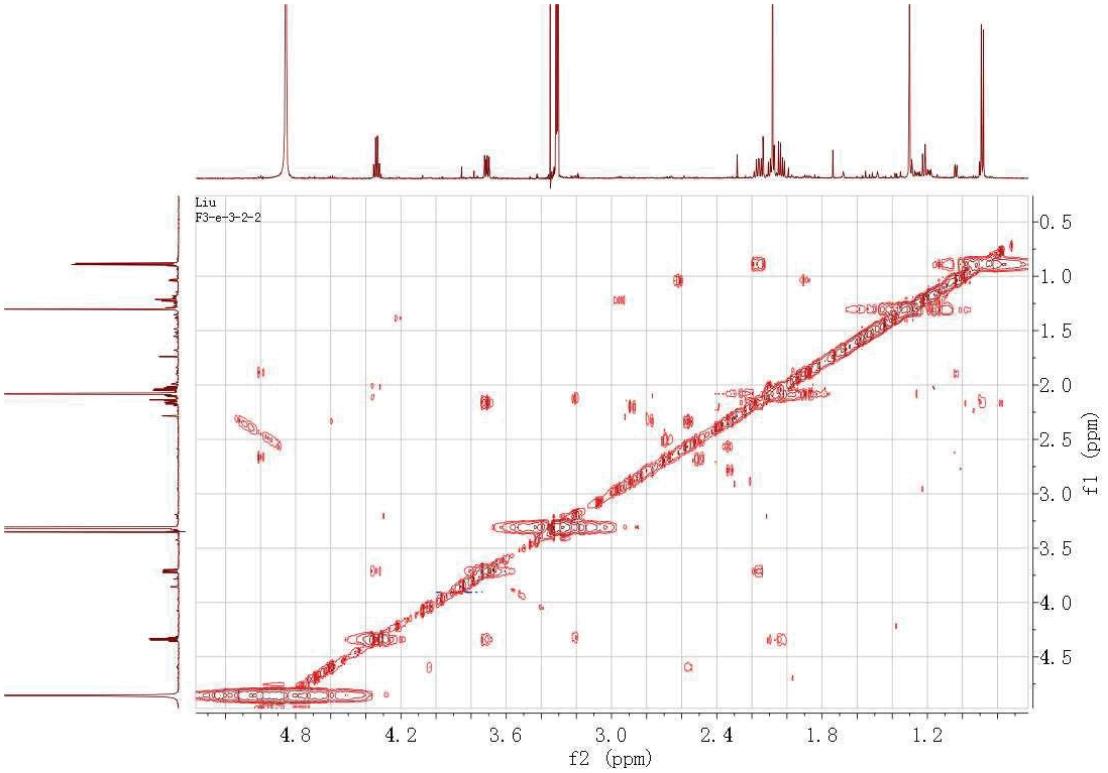

S13. ^{1}H-^{1}H COSY (600 MHz, CD_3OD) spectrum of compound **2**.

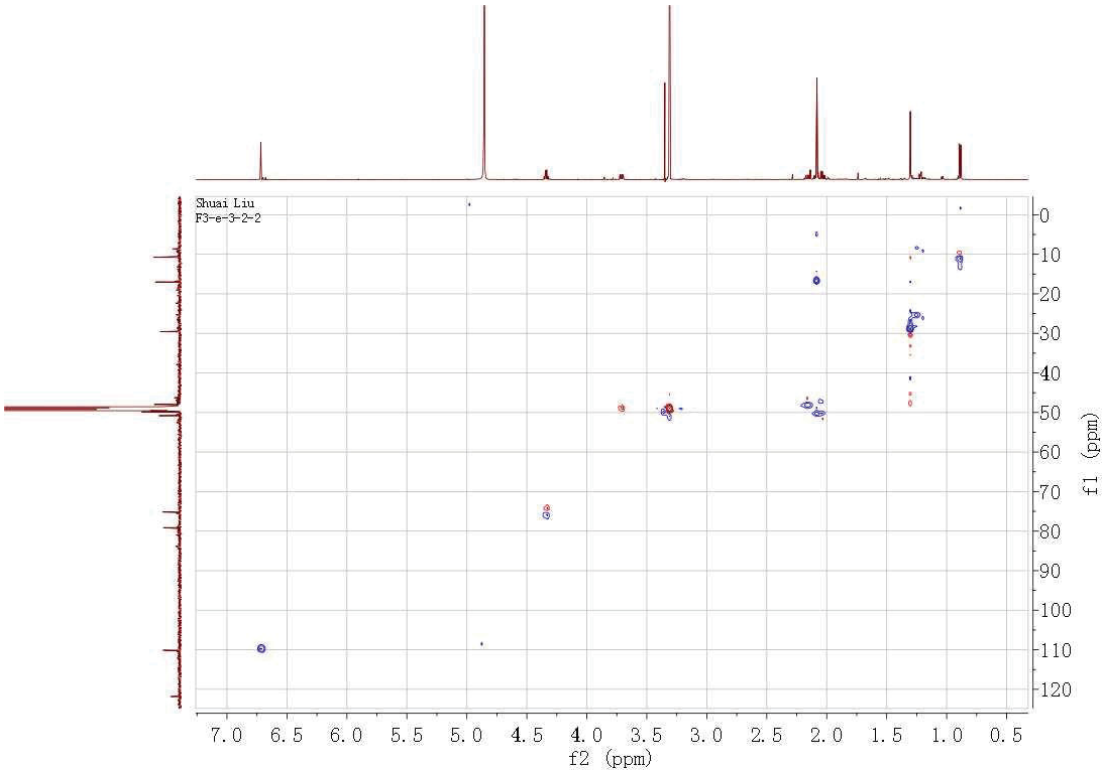

S14. HSQC (600 and 150 MHz, CD_3OD) spectrum of compound **2**.

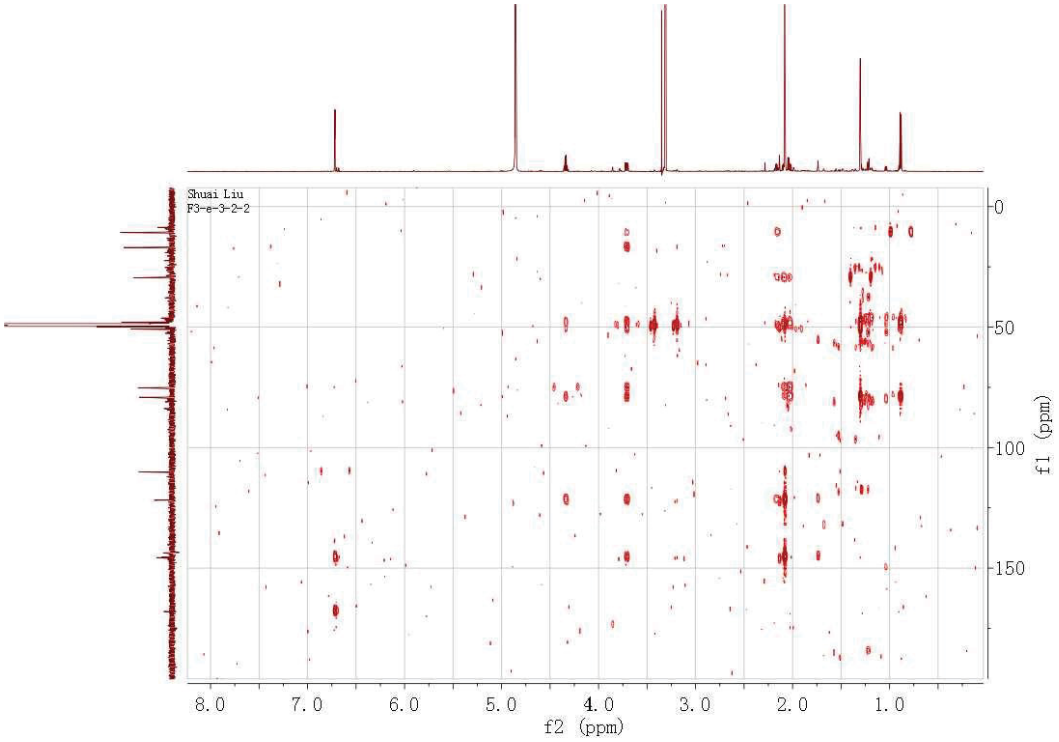

S15. HMBC (600 and 150 MHz, CD_3OD) spectrum of compound **2**.

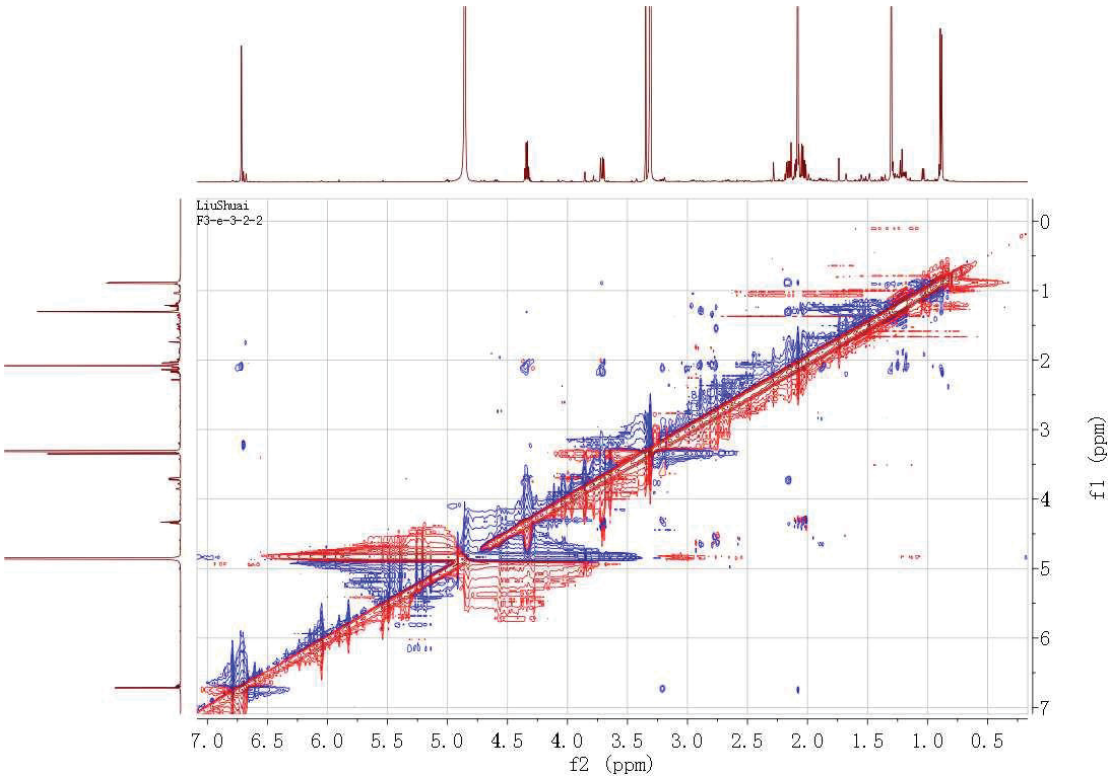

S16. ROESY (600 MHz, CD_3OD) spectrum of compound **2**.

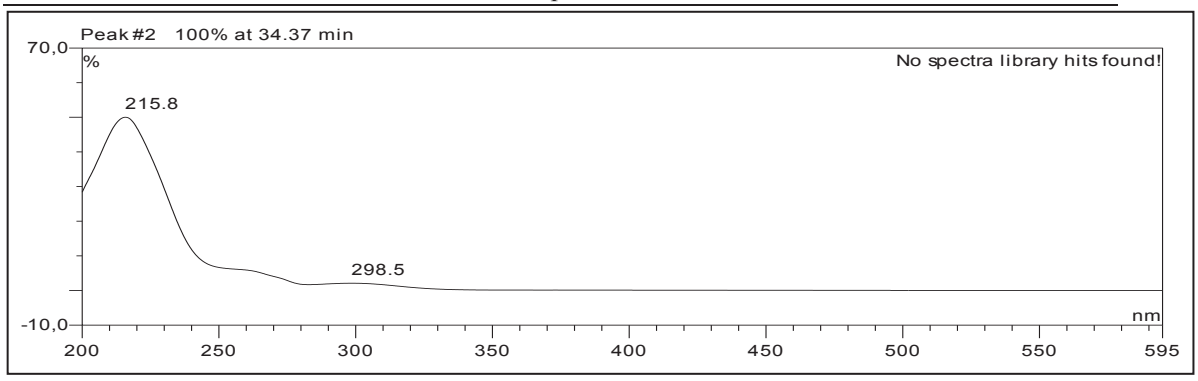

S17. UV spectrum of compound **6**.

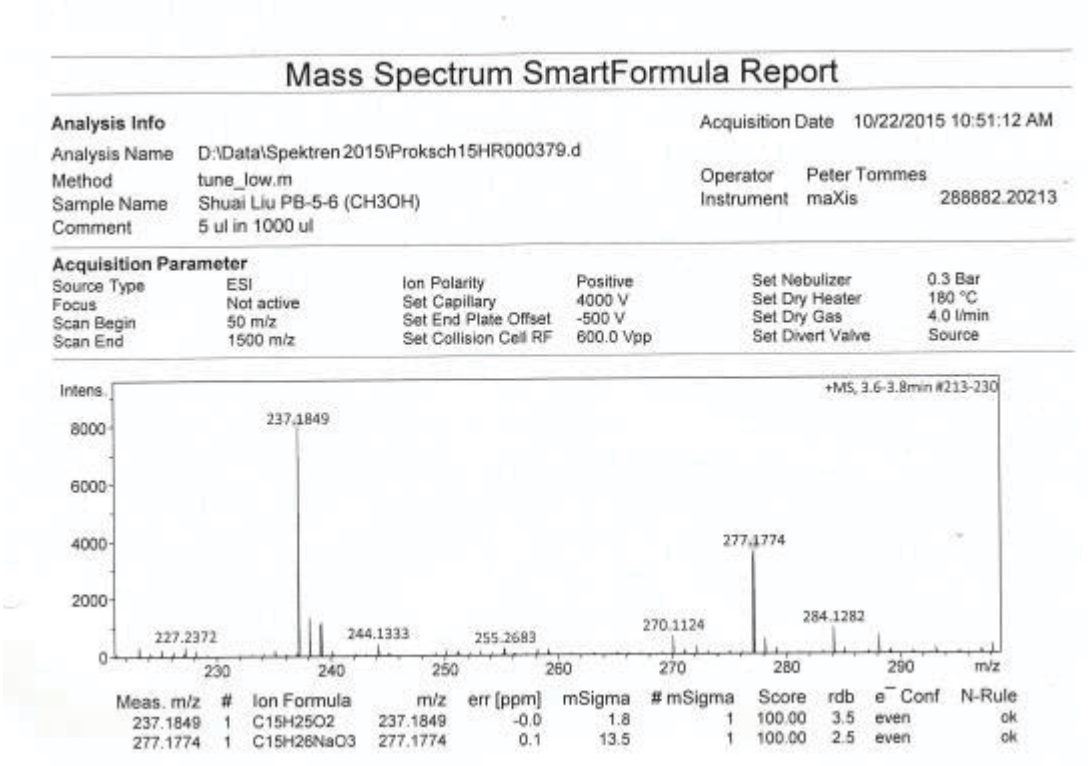

S18. HRESIMS spectrum of compound **6**.

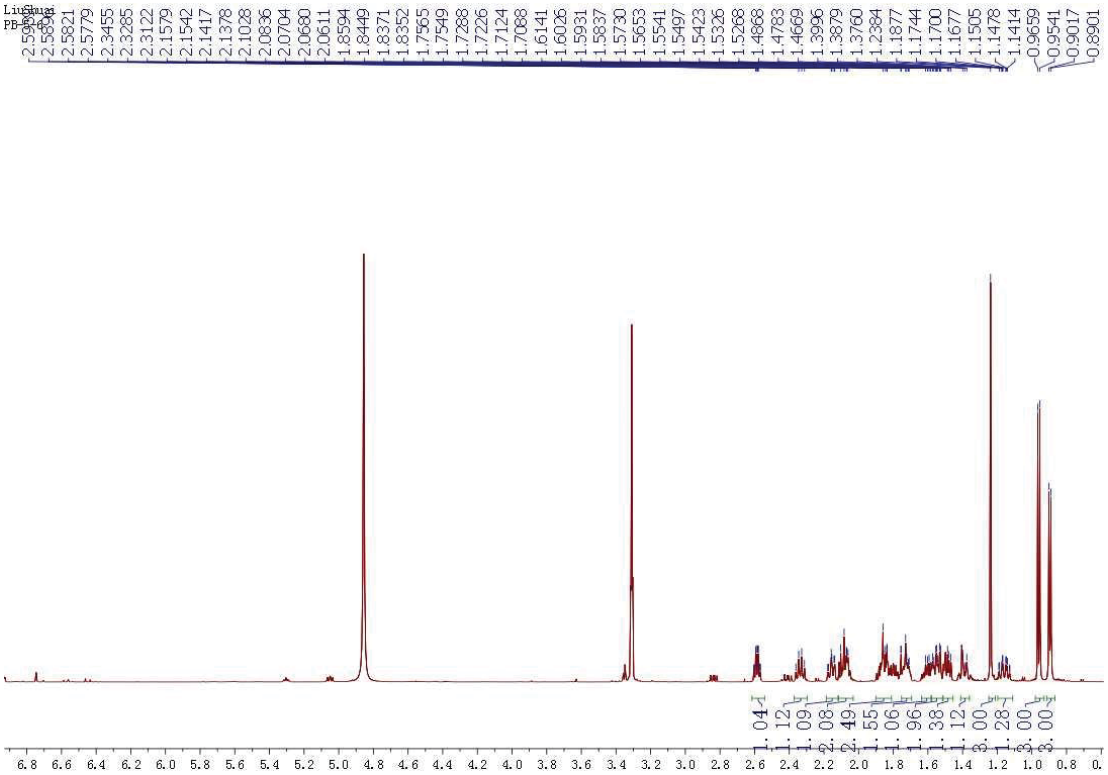

S19. ^{1}H NMR (600 MHz, CD_3OD) spectrum of compound **6**.

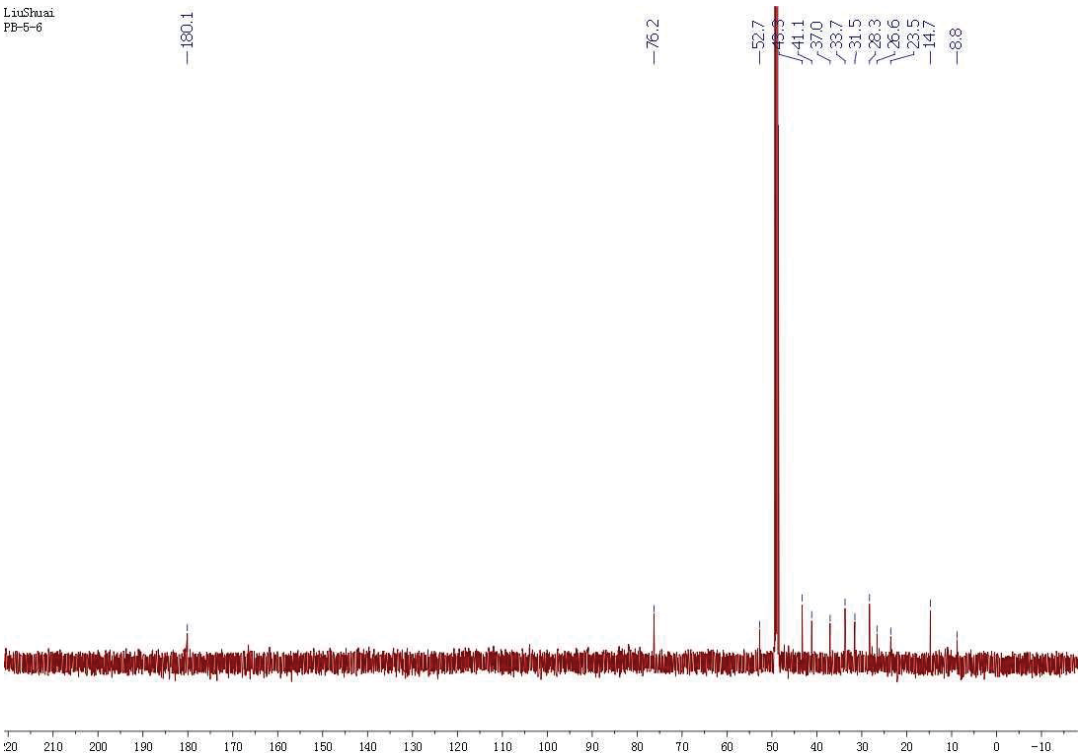

S20. ^{13}C NMR (150 MHz, CD_3OD) spectrum of compound **6**.

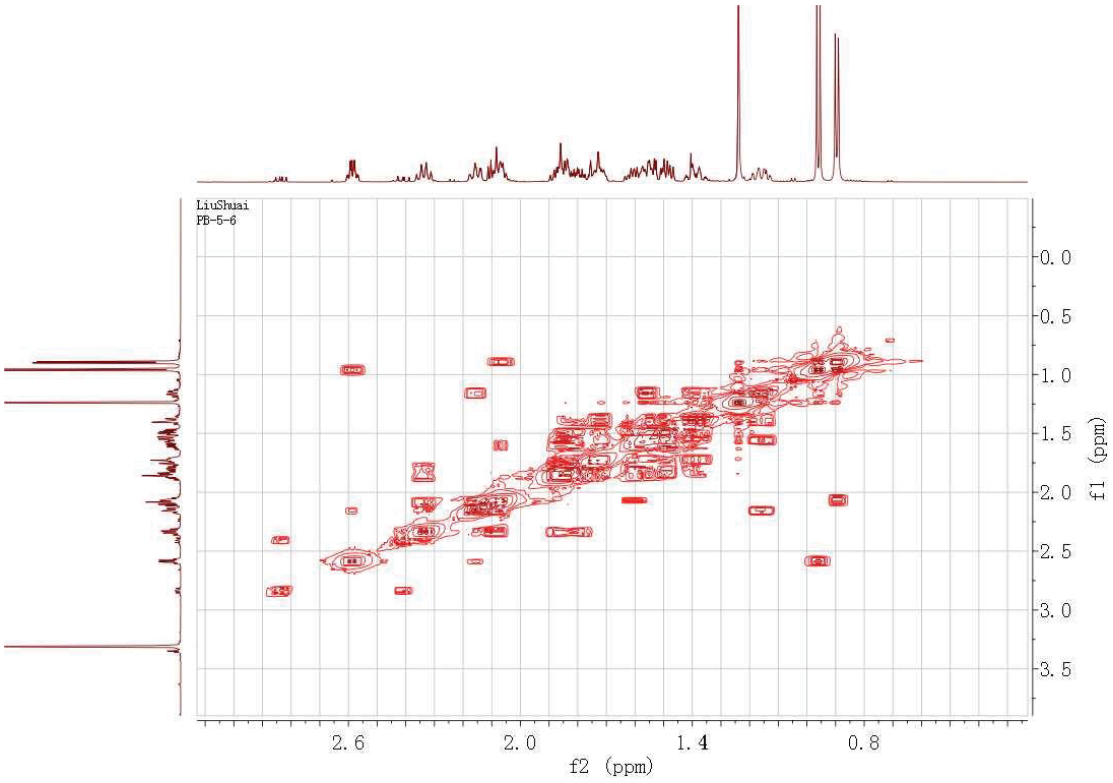

S21. ^{1}H-^{1}H COSY (600 MHz, CD_3OD) spectrum of compound **6**

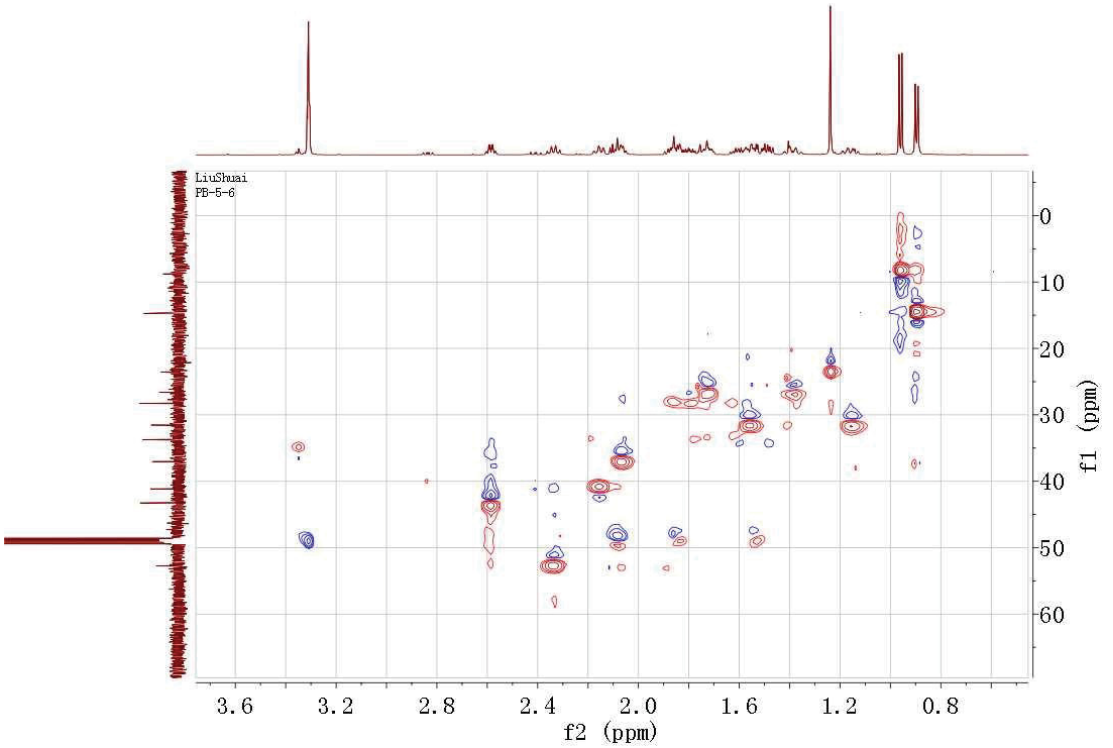

S22. HSQC (600 and 150 MHz, CD_3OD) spectrum of compound **6**.

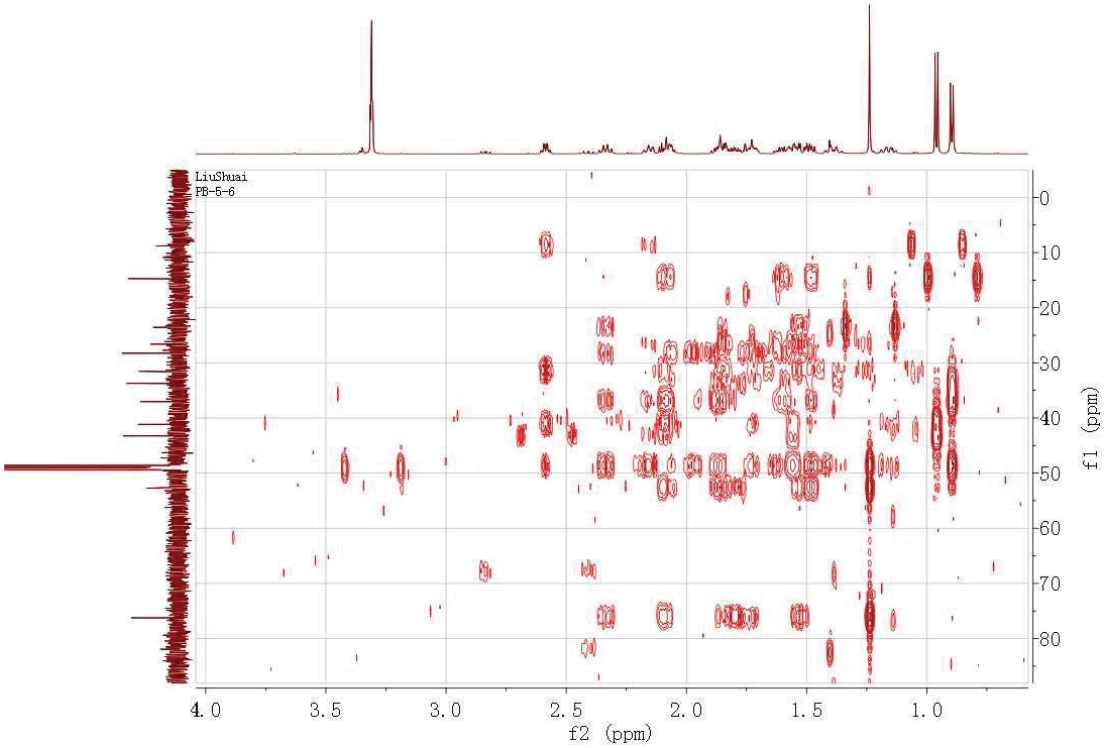

S23. HMBC (600 and 150 MHz, CD_3OD) spectrum of compound **6**.

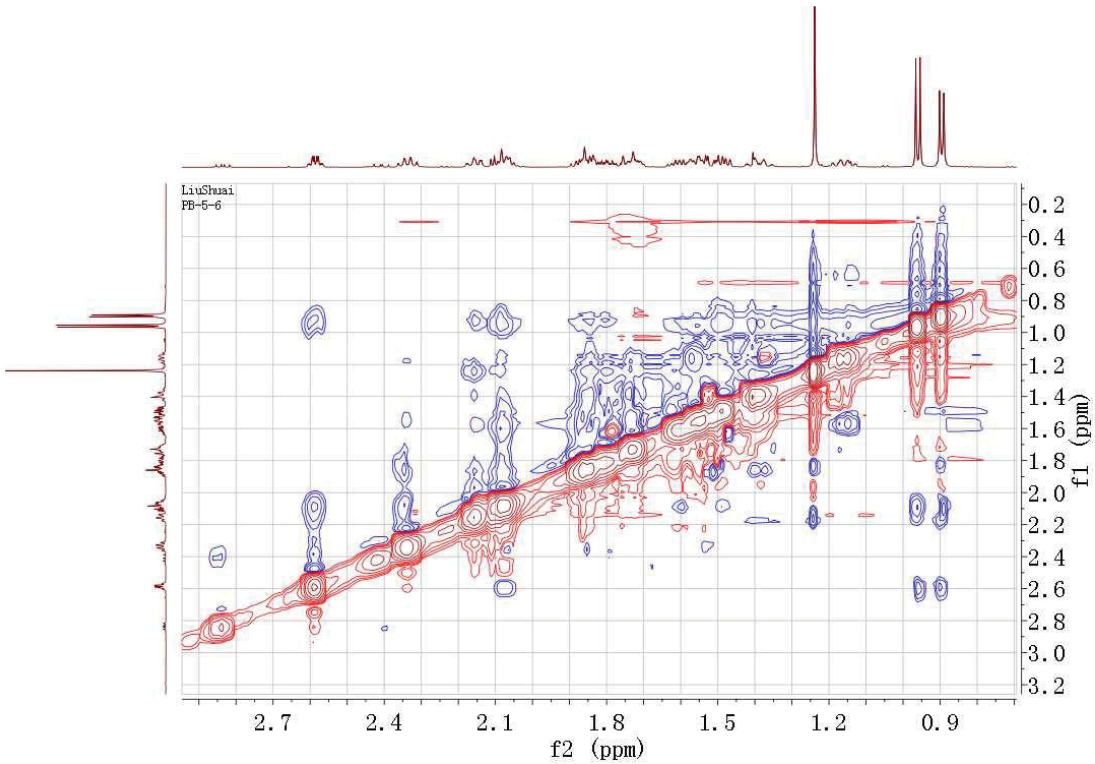

S24. ROESY (600 MHz, CD_3OD) spectrum of compound **6**.

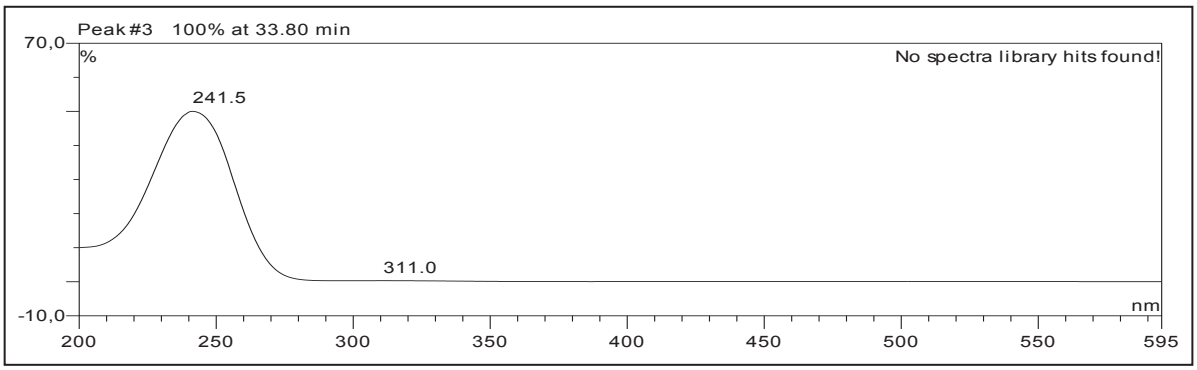

S25. UV spectrum of compound **7**.

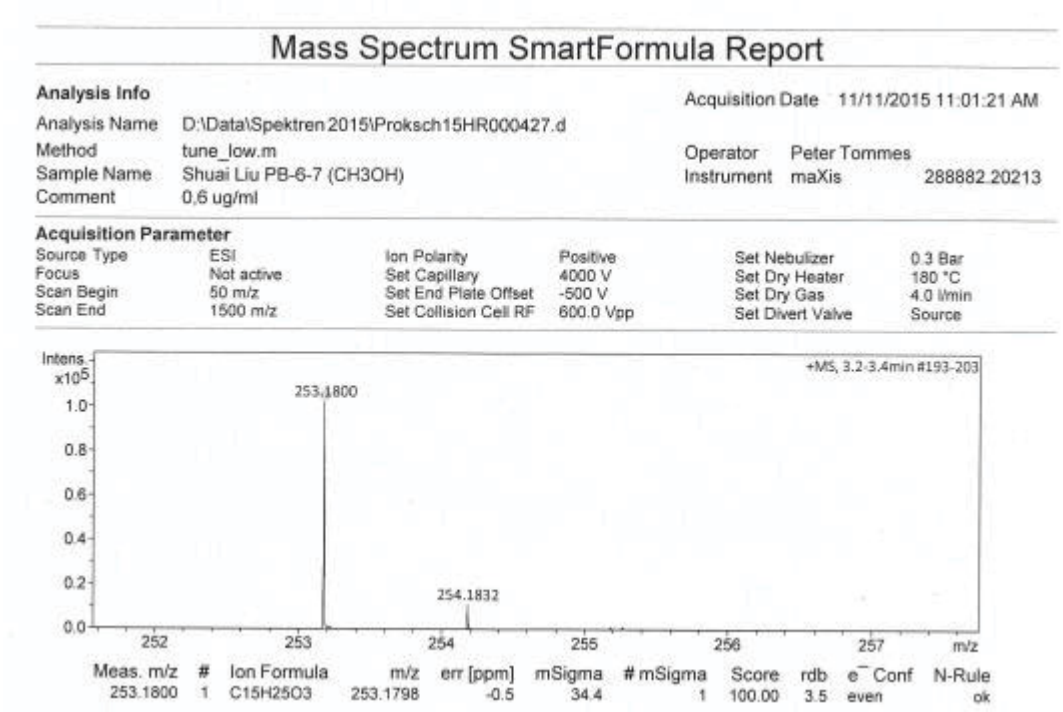

S26. HRESIMS spectrum of compound **7**.

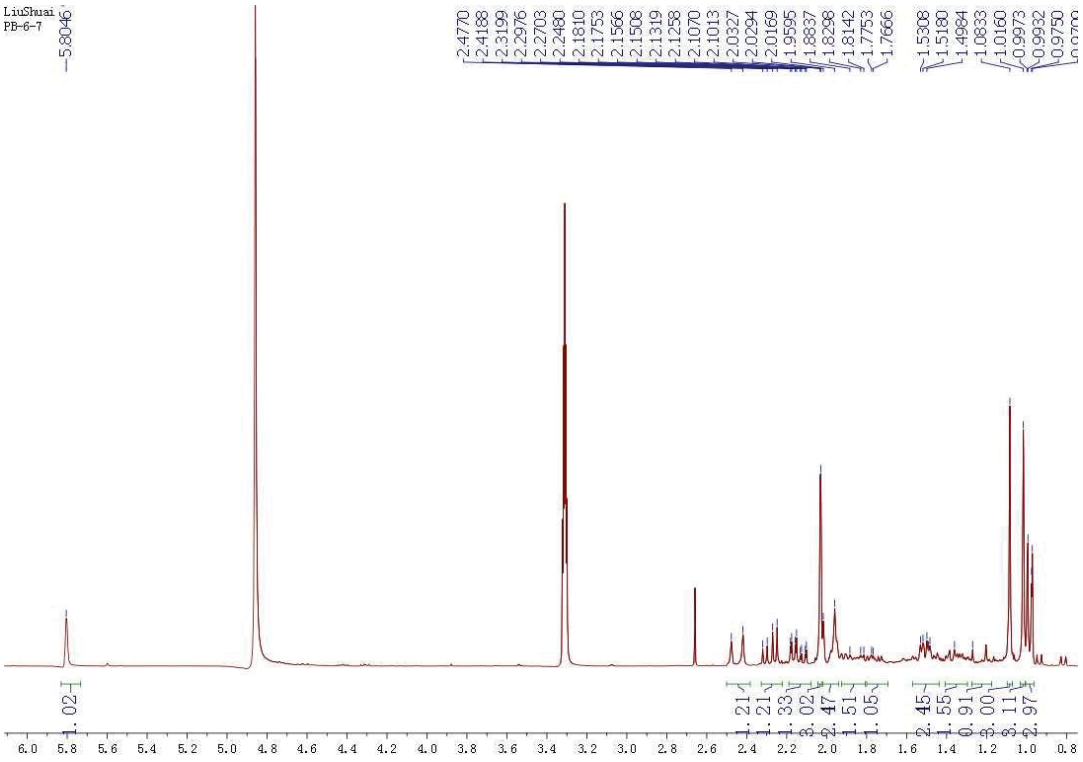

S27. ^{1}H NMR (600 MHz, CD_3OD) spectrum of compound **7**.

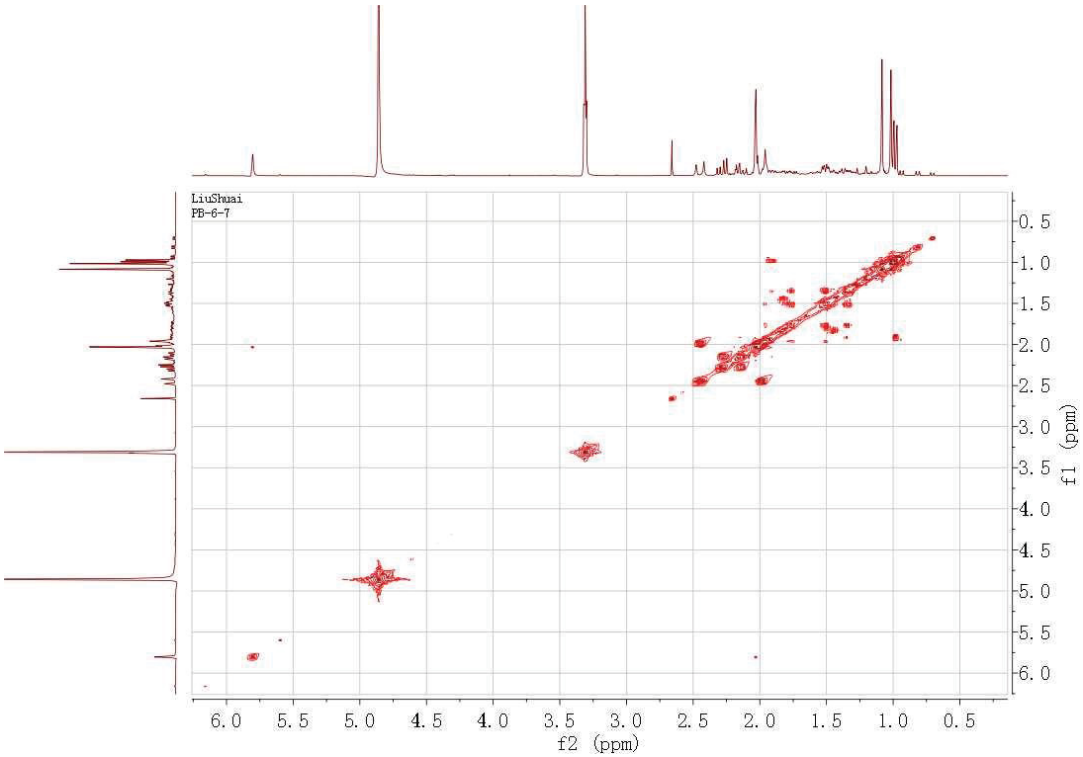

S28. ^{1}H-^{1}H COSY (600 MHz, CD_3OD) spectrum of compound **7**.

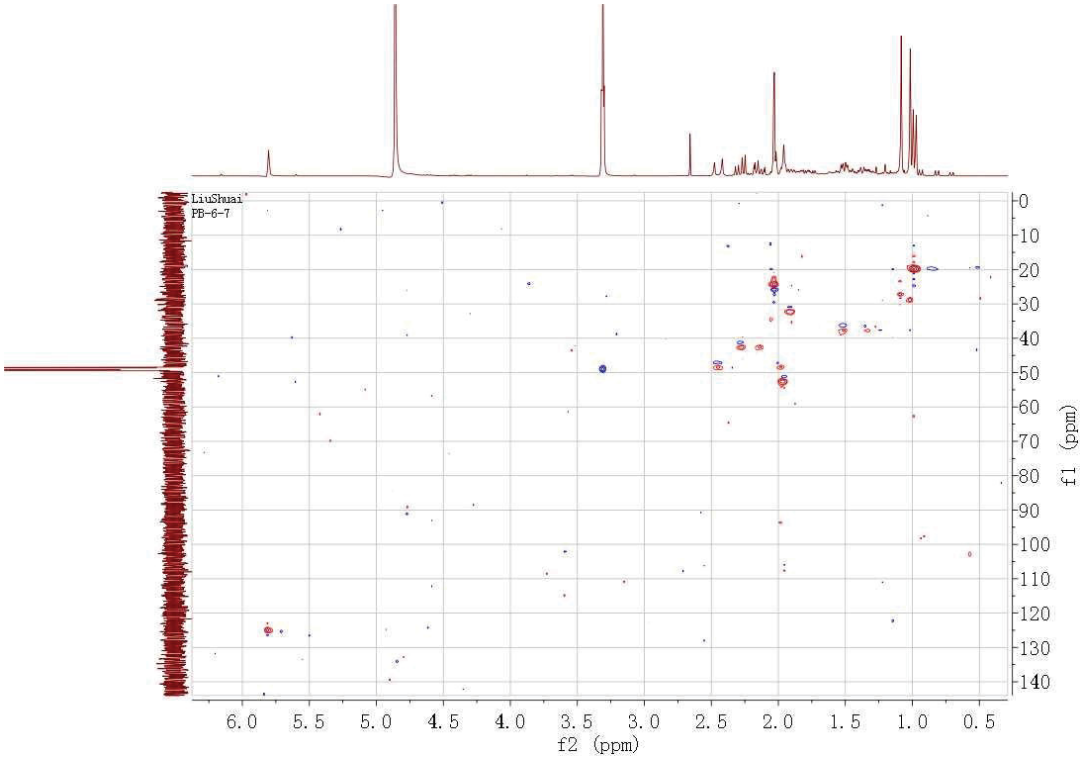

S29. HSQC (600 and 150 MHz, CD_3OD) spectrum of compound **7**.

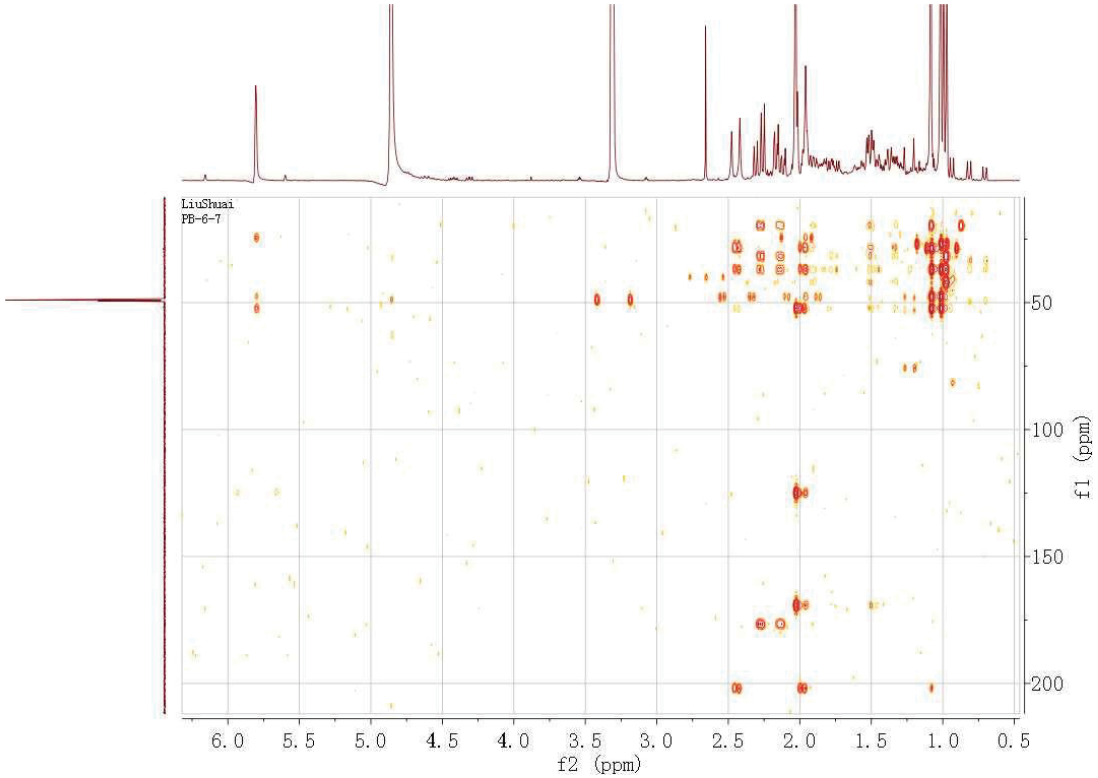

S30. HMBC (600 and 150 MHz, CD_3OD) spectrum of compound **7**.

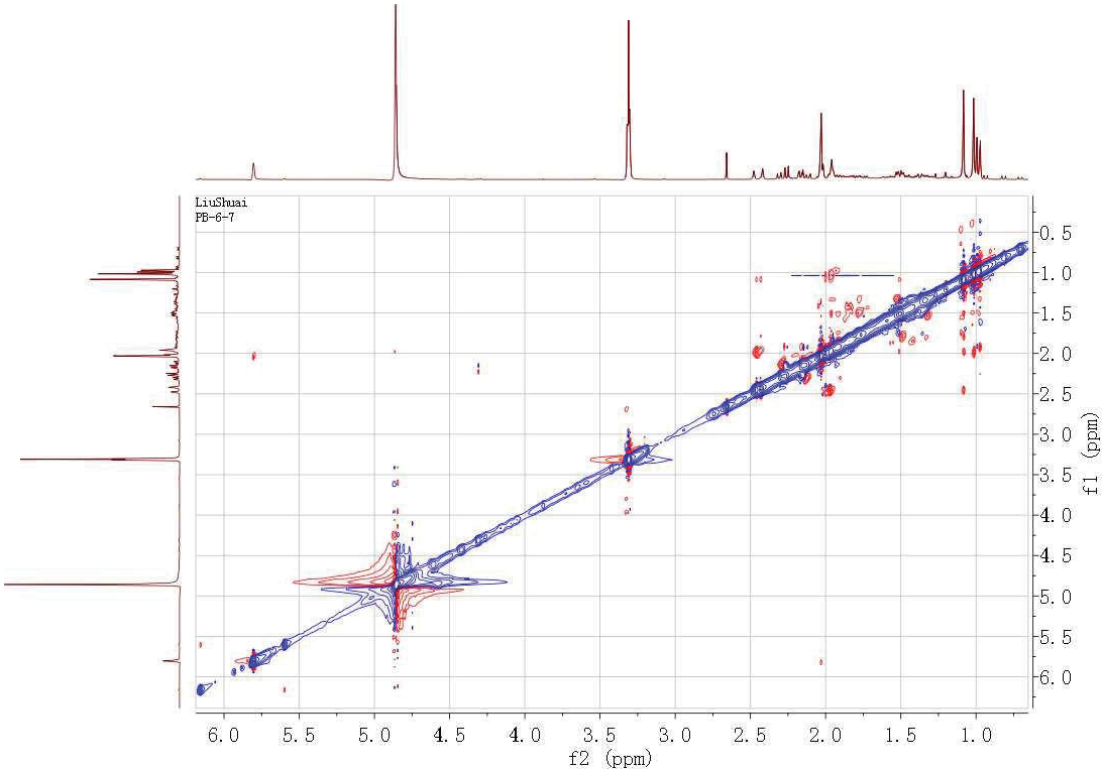

S31. ROESY (600 MHz, CD_3OD) spectrum of compound **7.**

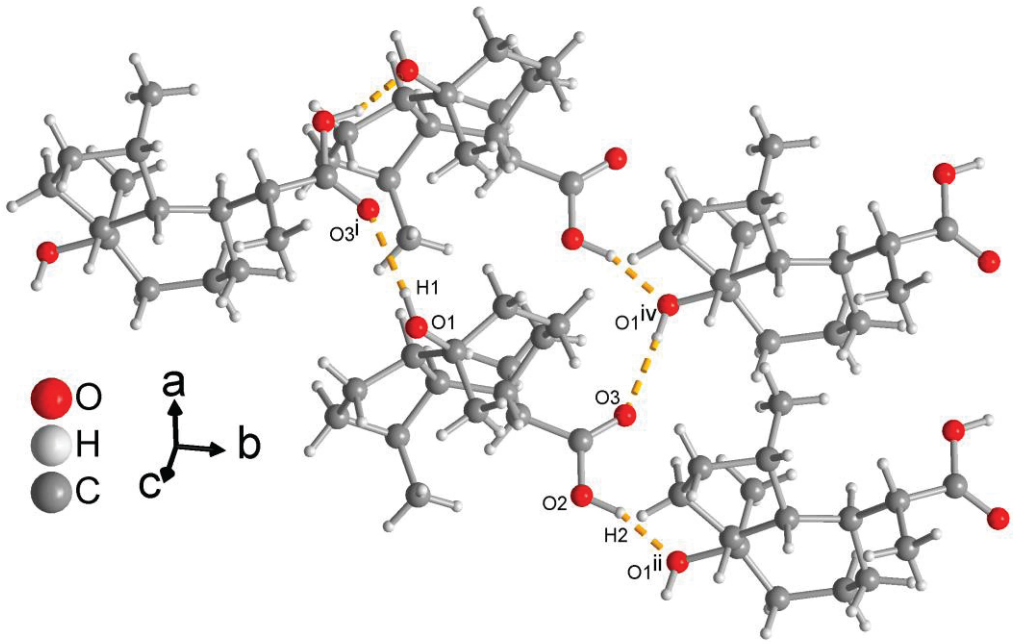

S32. Hydrogen-bonding chains in the crystal structure of **6** between alternating –OH and –COOH groups along the *a* axis.

Table S2. Hydrogen-bond geometry (Å, º) for **6**. [a]

D—H···*A*	*D*—H	H···*A*	*D*···*A*	*D*—H···*A*
O1—H1···O3^{i}	0.83 (5)	2.12 (5)	2.943 (4)	175 (5)
O2—H2···O1^{ii}	0.94 (6)	1.73 (6)	2.633 (4)	161 (5)

[a] Symmetry codes: (i) -*x*+1, *y*-1/2, -*z*+1; (ii) -*x*, *y*+1/2, -*z*+1.

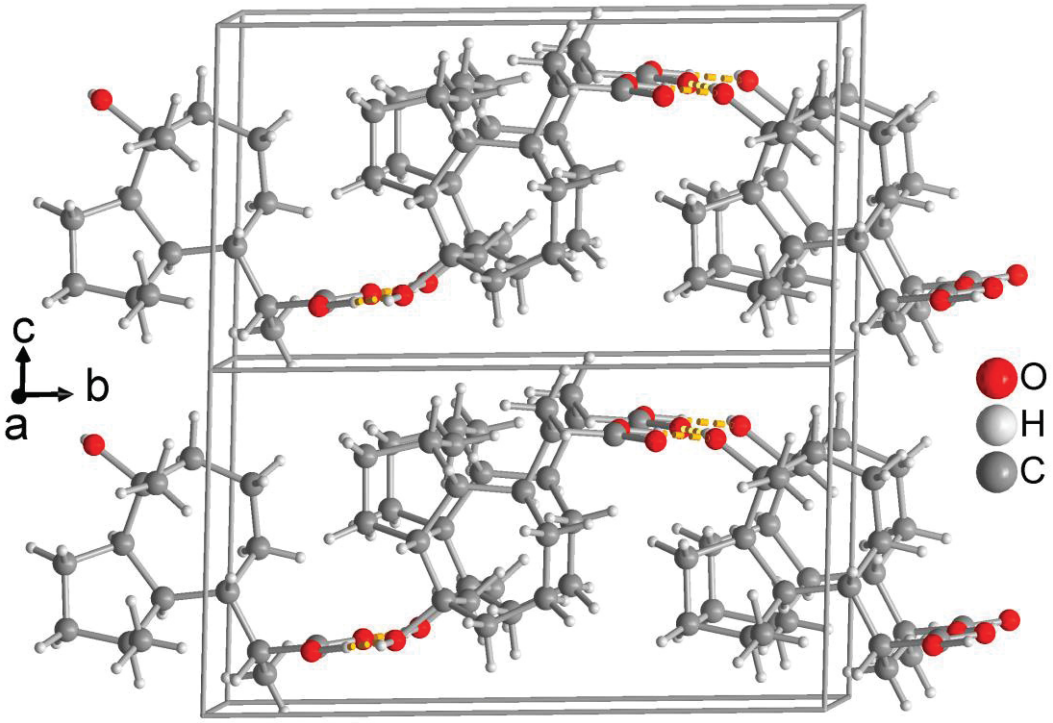

S33. Layer arrangement of the molecules in the crystal structure of **6** parallel to the *ab* plane through the H-bonding interactions with only weak van-der-Waals interactions along the *c* axis which explains the formation of very thin plate-like crystals.

Chapter 6

General Discussion

6.1 Co-Cultivation

The co-cultivation of two or more microorganisms has been shown to be an effective way to enhance the accumulation of known compounds and to induce new secondary metabolites (Marmann *et al*., 2014). Unlike the traditional way of cultivating one single microbial strain on nutrient-rich medium, two or more microorganisms compete in a mixed fermentation to struggle for limited nutrients and space for living. Co-cultivation of multi-microbes is mimicking the natural environment microorganisms live and thrive in. Through diverse and complex communications between fungi and bacteria (Frey-Klett *et al*., 2011), the original silent gene clusters for secondary metabolites could be triggered to be expressed and to produce novel structures. Hence, the fungal-bacterial co-cultivation has been applied to maximize the potential for fungal secondary metabolites. In our co-cultivation work, the mangrove endophyte *P. microspora* and the sponge associated fungus *Aspergillus* sp. were chosen to compete with either of two bacteria, *S. lividans* or *B. subtilis*. The co-cultivation of *Aspergillus* sp. with *B.subtilis* led to increase in the accumulation of two known compounds: 4-methoxycarbonyldiorcinol and cordyol C. When co-cultivated together with *S. lividans* at a starting concentration of 0.2 g per flask, the fungus *P. microspora* could produce larger amounts of known compounds (such as pestalotioprolide E), and also to secrete additional macrolides, which could not be detected in axenic controls. The long-term co-cultivation of *P. microspora* with the bacterium *B. subtilis* afforded two new sesquiterpenes: pestabacillin A and pestabacillin B.

6.1.1 Enhancement of the Accumulation of Natural Products by Co-Cultivation

B. subtilis is a very common and human-safe Gram-positive bacterium, which can be found in different habitats from soil to the human gastrointestinal tract (Pinchuk *et al*., 2002). As a model strain, it has been well studied in numerous scientific areas including cell differentiation, chromosome replication, and genetic studies. Its complete genome sequence was also published in 1997 (Kunst *et al*., 1997). Meanwhile, *B. subtilis* is a common genetic engineering strains for enzyme production in biotechnology companies (Ye *et al*., 1999). Furthermore, *B. subtilis* has been found to be an effective inducer in the fungal-bacterial co-cultivation experiments, and has successfully triggered new fungal natural products or enhanced the production of bioactive

compounds as reported (Ola *et al*., 2013; Ebrahim *et al*., 2016).

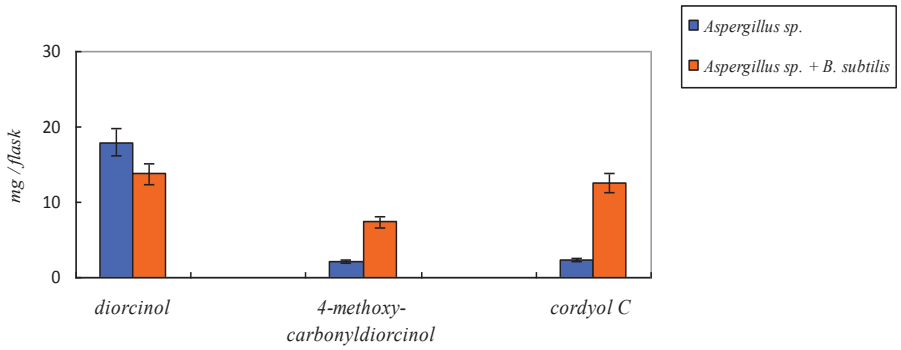

Figure 1. Yields of three compounds per flask of *Aspergillus* sp. and of its co-cultivation with *B. subtilis*.

Based on our experience, fungi usually grow more quickly than bacteria on the stationary rice medium. Thus, to guarantee a fair start of competition, *B. subtilis* was first inoculated to the rice medium and pre-incubated for seven days before the introduction of the marine fungus *Aspergillus* sp.. During the co-cultivation, we observed that *Aspergillus* sp. in all flasks of mixed fermentation grew more slowly than the axenic fungal control, indicating the interaction between *Aspergillus* sp. and *B. subtilis*. The comparison of HPLC chromatograms afterwards suggested that the amount of main compound diorcinol slightly decreased in co-cultivation, whereas 4-methoxy-carbonyldiorcinol and cordyol C increased 3.5 and 5.4 fold, respectively (Figure 1). Since these three compounds were previously isolated from the axenic fermentation of *Aspergillus* sp. and repeatedly detected in the HPLC chromatograms of extracts from fungal controls, they are undoubtedly fungal natural products. The two enhanced compounds 4-methoxy-carbonyldiorcinol and cordyol C in co-cultivation did not show any antimicrobial activities against eight human pathogenic bacteria in chapter 3, but 4-methoxy-carbonyldicorcinol was reported for its significant inhibitory effect against *S. epidermidis* with MIC value of 2.71 μM (Chen *et al*., 2013). In the co-cultivation, the enhanced fungal secondary metabolites are possibly produced as chemical defense, or as precursors of other bioactive compounds, or as signals for defense gene expression.

Another co-cultivation experiment of *P. microspora* with different cell densities of *S. lividans* enhanced the production of bioactive secondary metabolites as well (Figure 2). As a filamentous bacterium, the concentration of *S. lividans* could not be determined by the optical density at 600 nm (OD600), thus a mass-dependent inoculation method was introduced in chapter 3. As shown in

figure 2, a general increasing trend of accumulation of pestalotioprolides E and F could be noticed along with the increase of bacterial cell density. In particular, when the concentration of *S. lividans* was 0.2 g/flask, co-cultivation led to 9.0 fold increase of the production of pestalotioprolide E compared with the axenic fungal control, whereas pestalotioprolide F increased 10.4 fold. Both of these two enhanced fungal natural products exhibited cytotoxicities against murine lymphoma cell line L5178Y and human ovarian cancer cell line A2780 with IC_{50} value in the range of 1.2 – 12 μM.

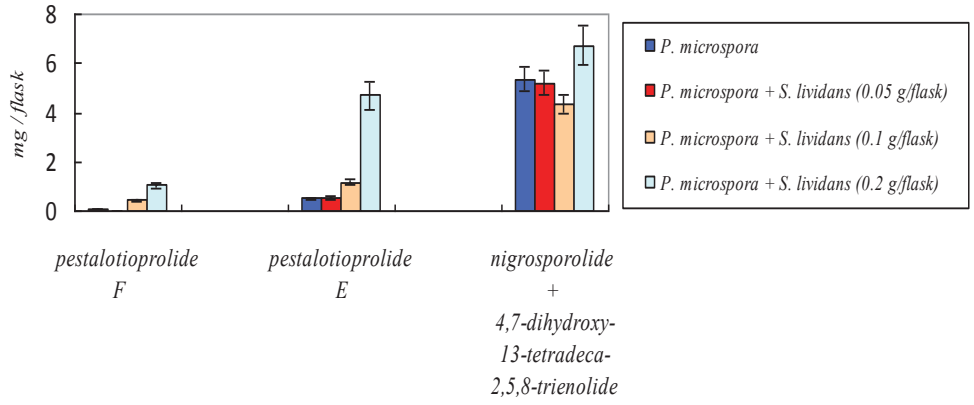

Figure 2. Yields of natural products of *P. microspora* and of its co-cultivation with *S. lividans*.

It's worthwhile to mention that the enhancement by co-cultivation is selective, and not all the secondary metabolites will be increased. For example, the production of two diastereoisomers nigrosporolide and 4,7-dihydroxy-13-tetradeca-2,5,8-trienolide is relatively stable (shifting in the range of 20%) during the co-cultivation of *P. microspora* with three different concentrations of *S. lividans*, and diorcinol suffers a 23% decrease during the co-cultivation of *Aspergillus* sp. with *B. subtilis*.

6.1.2 Inducing New Natural Products Through Co-Cultivation

Since most gene clusters encoding the biosynthesis of natural products in fungi remain silent under standard laboratory conditions, the fungal-bacterial interactions in co-cultivation can trigger the cryptic genes to express new compounds. A number of new natural products have been reported from the mixed fermentations of fungi and bacteria. The novel alkaloid glionitrin A with potent cytotoxic and antibacterial activities was isolated from the co-cultivation of two marine microorganisms *Aspergillus fumigatus* and *Sphingomonas* sp. (Park *et al*., 2009).

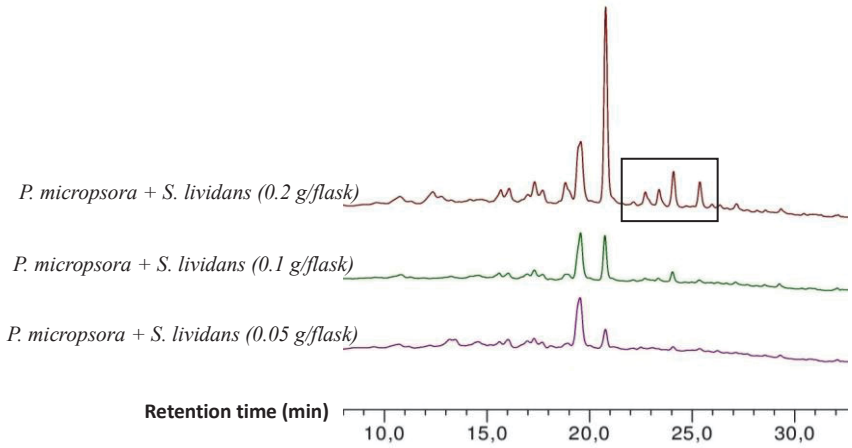

Figure 3. New induced natural products in HPLC chromatograms of co-cultured *P. microspora* and *S. lividans*.

Figure 3 shows the HPLC chromatograms of co-cultures of *P. microspora* with *S. lividans*, and four new peaks at retention times of around 25 min (retention time) were observed only when the bacterium concentration at 0.2 g/flask. These four peaks represent four different macrolides, which share the identical UV spectra with pestalotioprolide E. However, their structures could not be elucidated in the course of this dissertation due to their low amounts.

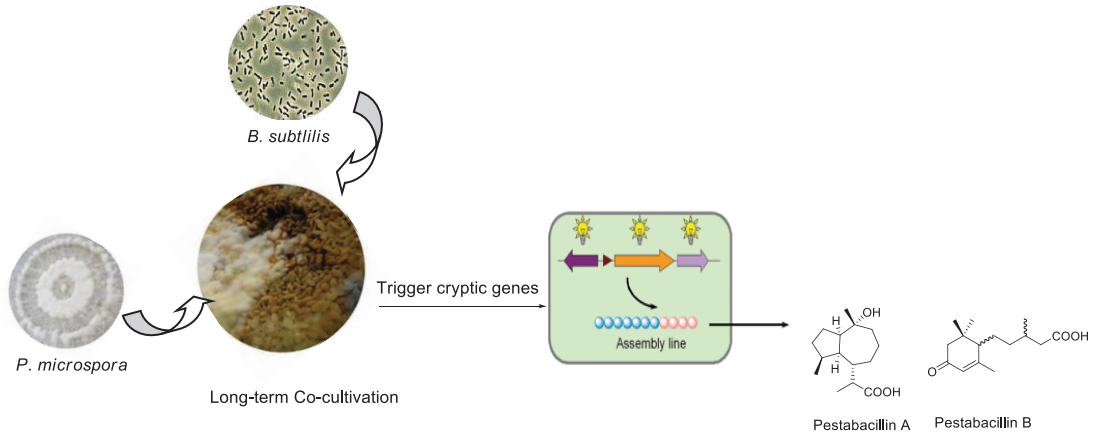

Figure 4. Two new sesquiterpenes induced through co-cultivation of *P. microspora* with *B. subtilis*.

Compared with *Aspergillus* sp., the fungus *P. microspora* is more sensitive to the bacterium *B. subtilis*, and grows extremely slow in the mixed fermentation. One possible reason for that could be that *B. subtilis* can produce a kind of signals or slight-amount of antibiotics specifically inhibiting the growth of *P. microspora*. The long-term co-cultivation of the fungus *P. microspora* with the bacterium *B.subtilis* successfully triggered the expression of cryptic biosynthetic genes in *P. microspora*, and led to the production of two new sesquiterpenes pestabacillins A and B. Since

similar structures have never been reported from *B. subtilis*, the fungus *P. microspora* is more likely to be the real producer.

Interestingly, pestabacillin A has a novel structure with an uncommon isopropyl substituent at the position C-6. The skeleton of pestabacillin A has been rarely reported under the name of zierane type sesquiterpene. Several examples of zierane sesquiterpenes have been isolated from two plants *Melicope denhamii* (Nakashima *et al*., 2012) and *Chandonanthus hirtellus* (Komala *et al*., 2010). It has been suggested that zierane sesquiterpenes are derived from the similar skeleton of aromadenrane sesquiterpenes (Komala *et al*., 2010), which can be produced by fungi (Isaka *et al*., 2015). Under the extreme stress from the over-growing *B. subtilis*, the silent genes for aromaderane sesquiterpenes in the fungus *P. microspora* seemed to have been activated.

By simulating the natural interactions between fungi and bacteria, the co-cultivation has been proven to be a promising method to trigger new natural products, which can not be expressed by cryptic gene clusters under standard laboratory conditions.

6.2 Biosynthesis and SAR of Macrolides

Macrolides are macrocyclic lactones or lactams. The rings of macrolides most commonly consist of 12, 14 or 16 atoms, but sometimes even 26-38 atoms, such as antifungal amphotericins (Omura, 2002). It has been proven that biosynthesis of most macrolides is accomplished by type I polyketide synthases (PKSs) and that is why macrolides belongs to polyketides (Kao *et al*., 1995). The PKS is composed of different functional proteins organized as modules. The 14-membered ring of erythromycin consists of seven propionate units.

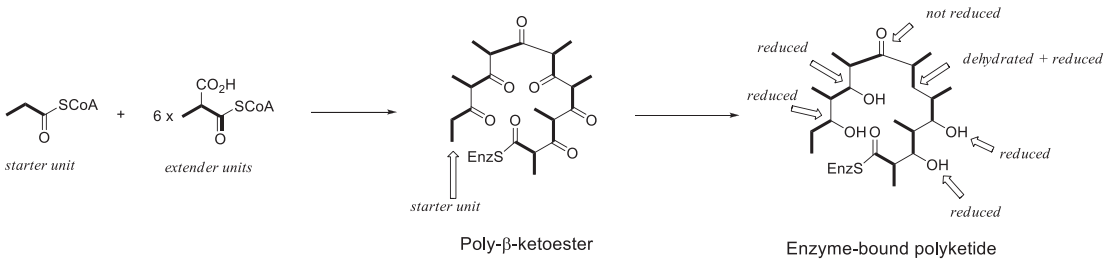

Figure 5. Biosynthetic process of the macrolide ring of erythromycin A.

During each step of chain extension, acyl carrier protein (ACP), acyltransferase (AT) and β-ketoacyl synthase (KS) take part in the condensation of the poly-β-ketoester (Marsden *et al*., 1994). Meantime, different modifications (especially reductions) of the enzyme-bound polyketide are controlled by enzymes like dehydrase (DH), enoyl reductase (ER) and β-ketoacyl reductase (KR) (Donadio *et al*., 1993). Finally, the macrolide ring of erythromycin is released by the PKS

after the cyclization catalysed by thioesterase (TE) (Gokhale *et al*., 1999).

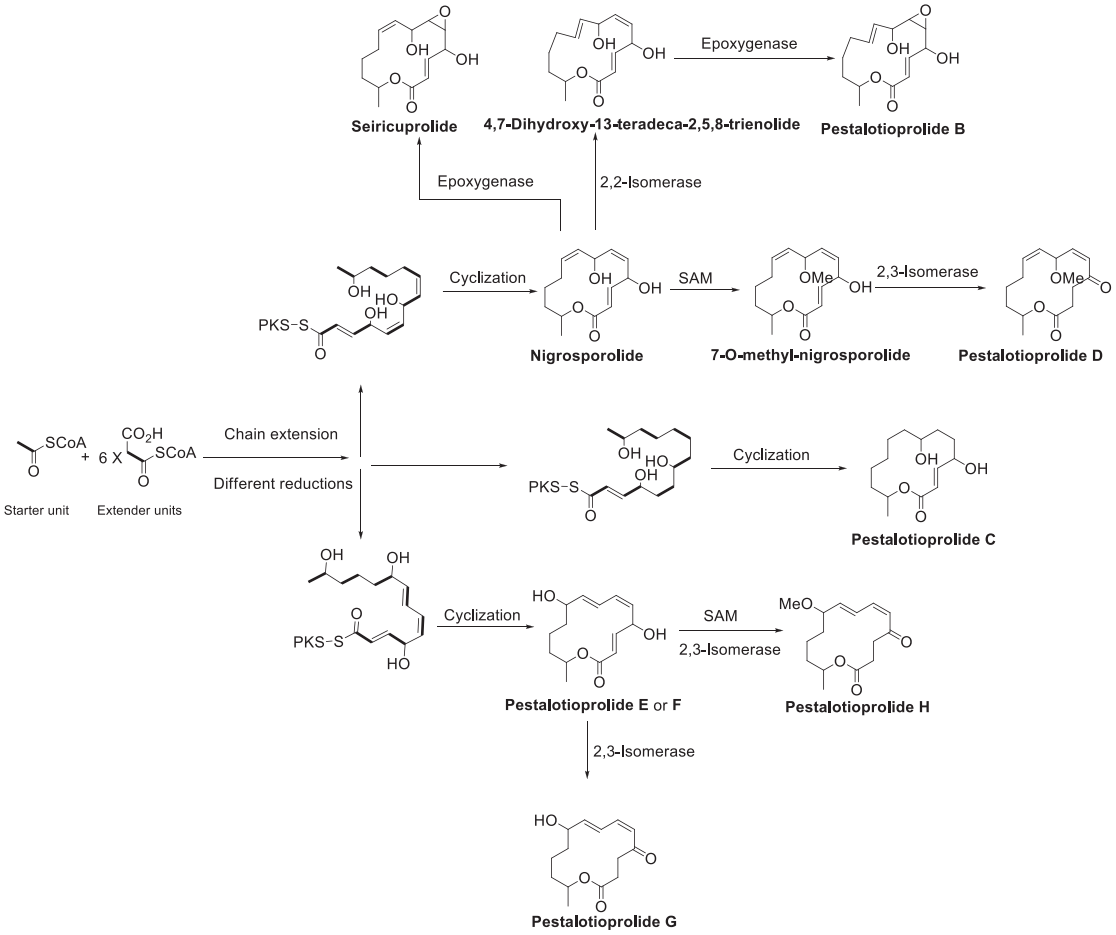

Figure 6. Proposed biosynthetic pathway of natural macrolides from *P. microspora*.

Although all 14-membered macrolides isolated from *P. microspora* (in chapter 3) are composed of entirely acetate units, their biosynthetic pathway should be similar with that of erythromycin. Starting with acetate coenzyme A, the polyketide rings of pestalotioprolides extend by adding two carbons in each condensation with one malonate unit. With different reduction modes, which were likely conducted by different sequence of dehydrations and reductions, three different enzyme-bound polyketides are formed (Figure 6). The cyclization of the three polyketides leads to nigrosporolide, pestalotioprolide C, pestalotioprolide E or F. The *O*-methylation at C-7 of nigrosporolide is likely accomplished by class I methyltransferase with the cosubstrate S-adenosyl methionine (SAM) (Roje, 2006), resulting in 7-O-methyl-nigrosporolide. The transformation from nigrosporolide to the stereoisomer 4,7-dihydroxy-13-teradeca-2,5,8-trienolide could be conducted by 2,2-isomerase (Kaulmann and Hertweck, 2002) before or after the cyclization step of the macrolide ring. The epoxy groups between C-5 and C-6 of seiricuprolide and pestalotioprolide B can be easily formed by the

enzyme epoxygenase (Zeldin, 2001), from nigrosporolide and 4,7-dihydroxy-13-teradeca-2,5,8-trienolide, respectively. Pestalotioprolide E and F are two diastereoisomers with different stereochemistry at C-4. The determination of their absolute configurations by ROESY and ECD calculation methods were discussed in chapter 3. As both of pestalotioprolide E and F are detected repeatedly from the HPLC chromatograms of different cultivations of the strain, they are natural products rather than artificial products. Their 4*R* or 4*S* configuration could result from action of an isomerase or unselective reduction process.

It's worthwhile to mention that the macrolides from *P. microspora* are highly unstable in acidic solvents, based on our experience in the purification work. When exposed to acids, the compounds may suffer double bond rearrangements to form different low-energetic configurations, which were analyzed by HPLC-UV and HPLC-MS chromatograms. Therefore, all purification processes have been conducted carefully to avoid acids, high temperature, over exposure to oxygen, or strong sunlight with the aim to isolate true natural products. However, during absolute configuration determination, both *R*- and *S*- Mosher products suffered a double bond rearrangement due to the acidic environment when Mosher's reaction was conducted. Both of their double bonds at C-2 transferred to C-3, which subsequently formed a more stable configuration with a keto group at C-4 after the keto-enol tautomerism. In this case, the absolute configuration of the chiral center at C-4 can not be determined by the Mosher's method. This unexpected change made the ECD calculations of pestalotioprolide E and F quite important. The similar double bond rearrangement also happened during the Mosher reactions on chloriolide (Jiao *et al*., 2006). It seems that the rearrangement products are more stable than the natural products, but the mechanism of reaction is still unknown. Interestingly, an enzyme named 2,3-isomerase can also finish this doubled bond transfer from C-2 to C-3. This is also helpful to explain the biosynthetic pathway of natural products pestalotioprolide D, G, and H.

All macrolides isolated from *P. microspora* were evaluated for cytotoxic activities against mouse lymphoma cell line L5178Y and human ovarian carcinoma cell line A2780. Compounds 7-O-mehtyl-nigrosporolide and pestalotioprolides D-F, showed pronounced inhibitory activities to both cancer cell lines, while the remaining compounds showed weak activities or no activities (chapter 3). Moreover, the IC_{50} values of a same compound against two cell lines differed considerably, maybe because of the different sensitivity to the two cell lines. Generally, mouse

lymphoma cell line L5178 is more sensitive than human ovarian cell line A2780. From the bioassay result, we can see that the most active macrolide against L5178 cell line is 7-O-methyl-nigrosporolide with IC_{50} value of 0.7 μM, while the most active macrolide against A2780 cell line is pestalotioprolide E with IC_{50} value of 1.2 μM. From nigrosporolide to 7-O-methyl-nigrosporolide, a simple methylation of the hydroxyl group at C-7 can increase the cytotoxic activities against both cell lines, especially against L5178Y cell line. However, the double bond transferring from C-2 to C-3 decreases the cytotoxic effects on both L5178Y and A2780 cell lines (Figure 8).

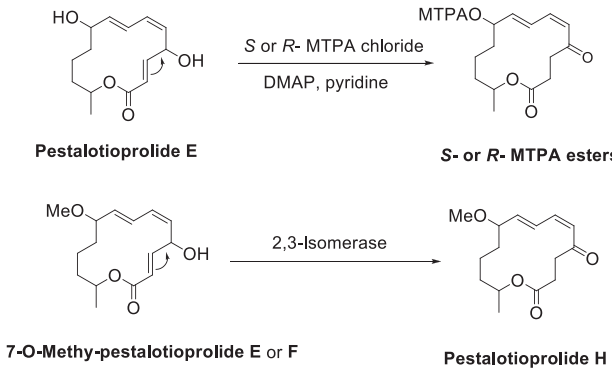

Figure 7. Two possible ways of transferring double bond from C-2 to C-3.

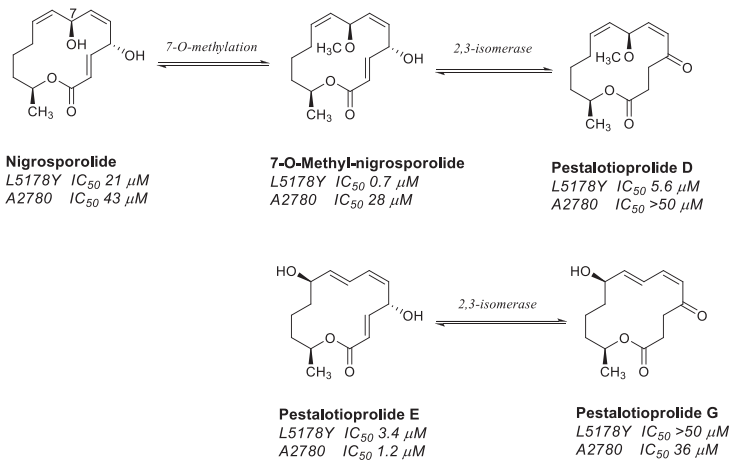

Figure 8. Basic structure-activity relationships of some macrolides from *P. microspora*.

6.3 Relationship between *F. oxysporum* and its Host Plant

F. oxysporum has been described as a plant pathogen in most publications, but in publication 1, it was introduced as an endophytic fungus. The reason is that this fungus was isolated from the healthy fruit of the mangrove plant *Drepanocarpus lunatus* under a strict isolation method for endophytes. As this strain didn't cause any disease symptoms to the host plant, it was described as an endophyte rather than a pathogen. Similar examples can be found in publications, such as *F.*

oxysporum to banana (Vu *et al.*, 2006) and *F. verticillioides* to maize (Bacon and Hinton, 1996).

Sometimes, there is blurring lines to define a fungus as an endophyte or a pathogen. The mutualistic relationship between the endophyte and the host plant depends on a sophisticated balance of their defense responses and nutrient demand (Kogel *et al.*, 2006). If the balance is destroyed by some factors, the endophyte can change its lifestyle to be a pathogen. For example, the endophytic fungus *Epichloe festucae* can support the host plant *Lolium perenne* with growth improvement and tolerance increase in the balanced status. However, *E. festucae* switches to be strongly pathogenic when mutant happened on *NoxA* gene, and can cause the host plant to die (Tanaka *et al*., 2006). The same strain *F. oxysporum* in this study should be pathogenic to barley due to the documented the phytotoxicity of its secondary metabolites, but it failed to show any pathogenic effects to its host, the mangrove plant *Drepanocarpus lunatus*. A possible reason could be that the mangrove plants are highly evolved to tolerate this endophyte.

In chapter 2, the strain *F. oxysporum* showed its genius by producing seven new fusaricates, which are ester products of fusaric acid and sugar alcohols, isolated from the small scale cultivation with only two flasks. Surprisingly, fusaric acid itself was not isolated from the fractions or detected from the crude extract. The different secondary metabolites underline that this strain is quite different from other fusaric acid producing fungi. In this strain, one more esterification step should be contained in the biosynthetic pathway of fusaric acid derivatives. And this esterification could be conducted by a lipase enzyme like Novozyme 435 from *Candida antarctica*, which can catalyze the attachment of alcohols to phenolic acids *in vitro* (Croitoru *et al*., 2012). The additional side chain of sugar alcohol increases the solubility of fusaric acid derivatives in water, which is helpful for the phytotoxin to diffuse in plant tissues.

Fusaric acid is a famous phytotoxin produced by many fungal pathogens. It can cause the plant to necrotize in numerous ways, like inhibition of cellular respiration by blocking oxygen uptake in the mitochondria (Marré *et al*., 1993), chelation with Cu, Fe, Co, and Zn to cause mineral deficiency in the plant (Chakrabarti and Ghosal, 1989), and suppression of the defensive responses of the plants. Fusaricates show similar phytotoxcity on barley leaves compared to the positive control fusaric acid. Based on their chemical and biological similarity, fusaricates should act in the same mode of fusaric acid.

Like other phytotoxins produced by fungi, fusaric acid derivatives can be interpreted as

chemical weapons used to acquire more living space for *F. oxysporum* itself. If this chemical defense from *F. oxysporum* can be avoided, tolerated or overcome by the plant, and can match the non-specific resistance responses from the plant, the interactions will reach a balance beneficial for both sides. In the balanced status, the fungus acts like a friendly intruder to the host plant by promoting plant growth and improving tolerance to environmental stresses (Redecker *et al*., 2000; Redman *et al*., 2002). If the balance fails to be maintained, the fungus will act like a pathogen to cause disease symptoms or the host plant will exclude the fungus.

6.4 Mechanisms of Drug-resistant Bacteria and the Strategies

Antibiotics and antibiotic-resistance are two sides of contradiction in nature, just like swords and shields in the war field. For several billion years microorganisms have evolved to produce antibiotics to inhibit the growth of neighboring microbial strains, with the purpose to protect their scarce food, space, or any other resources. Meantime, with high exposure to antibiotics, some strains have evolved their own resistance mechanisms in order to survive in the toxic environment. In general, both antibiotics and antibiotic-resistance are two parallel steps in evolution, with a relationship of reciprocal causation.

In the past 70 years, diverse antibiotics have been widely introduced in medicine to cure bacteria infections, to increase agriculture harvests, or to improve the production life stock. Undoubtedly, antibiotics have made great contributions to human society development. The only drawback is that the increasingly observed drug-resistant bacteria are emerging under the selective pressure of extensive antibiotic use.

Recently, a group of antibiotic-resistant bacteria named ESKAPE (*Enterococcus faecium*, *Staphylococcus aureus*, *Klebsiella pneumoniae*, *Acinetobacter baumannii*, *Pseudomonas aeruginosa* and *Enterobater* spp.) have been highlighted, since they possess multidrug resistance mechanisms to escape the treatment by antibiotics (Boucher *et al*., 2009). All ESKAPE pathogens are clinically dangerous, because the current antibiotics on market are ineffective or less effective to them. For example, methicillin-resistant *S. aureus* (MRSA) causes almost 100,000 deaths every year in the United States (Balaban, 2005).

There are three main mechanisms in those antibiotic-resistant bacteria: (1) producing special enzymes to inactivate antibiotics by destroy the active center of structure, such as β-lactamases; (2) pumping out the antibiotics from intracellular fluid of bacteria, like tetracycline efflux pumps; (3)

minor modification on the antibiotics' targets, resulting in less affinity of binding without influence on cell function, exemplified by PBP 2a protein in MRSA (Worthington and Melander, 2013). The bacteria can acquire drug-resistance by mutation or by acquiring resistance genes from other bacteria (Tenover, 2006).

With the growing threats of resistant pathogens, new antibiotics with different modes of action are required in the market, and the job of searching new antibiotics shall never end since the endless evolutionary arms race of antibiotic resistance. Meanwhile, the combination therapy of using two or more antibiotics with different mechanisms of action can be applied for the treatment of dangerous bacterial infections. For example, four antibiotics (isoniazid + rifampin + ethambutol + pyrazinamide) are combined to treat tuberculosis, which is one of the most difficult bacterial infections worldwide caused by *Mycobacterium tuberculosis* (Organization, 2013). On the other hand, it is also necessary to reduce the misuse of antibiotics as much as possible.

In chapter 4, nine phenolic bisabolanes including two new natural products and four diphenyl ethers were isolated from a sponge-derived fungus *Aspergillus* sp., and all isolated compounds were evaluated for antibacterial activities against seven ESKAPE strains and *M. tuberculosis*. Some of the compounds showed significant antibacterial activities against *S. aureus* ATCC700699, *E.faecalis* ATCC29212, *E.faecalis* ATCC51299, *E.faecium* ATCC35667, *E. faecium* ATCC700221. All strains mentioned above are gram-positive strains, which have a permeable cell wall consisting of mainly of thick peptidoglycan layers. None of the isolated compounds showed inhibition of the Gram-negative strain *A. baumannii* ATCC 1605, which is resistant to ciprofloxacin, cefepime, getamicin and some other antibiotics. The possible reason for this could be that the additional outer membrane in Gram-negative bacteria, which is comprised of lipopolysaccharide, which can prevent the diffusion of the testing compounds into the cell (Leive, 1974).

By comparing of the antibacterial results on two strains of *S. aureus*, it is found that expansol D (**3**), expansol F (**4**), and diorcinol (**10**) showed even better activity against the MRSA strain *(S. aureus* ACTT700699) with IC_{50} value of 25 μM, than against the reference strain (*S. aureus* ACTT25923) with IC_{50} value of 50 μM. It suggests that unlike methicillin that binds to penicillin-binding proteins, these three compounds may act in a different way by binding different targets. Similar results was observed with the vancomycin-resistant strains of *E. faecalis* ACTT51299 and *E. faecium* ACTT700221, compared with the reference strains *E. faecalis*

ACTT29212 and *E. faecium* ACTT51299, respectively. It implies that the vancomycin-resistant strain *E. faecalis* ACTT51299 is more sensitive to expansol A (**5**), expansol D (**3**) and peniciaculin A (**7**) than the reference strain *E. faecalis* ACTT29212. Similarly, expansol A (**5**) and diorcinol (**10**) showed better activity against the vancomycin-resistant strain *E. faecium* ACTT700221 than against *E. faecium* ACTT51299.

These analyses can conclude that the search for new antibiotics from natural sources is important and also promising to solve the current problems caused by drug-resistant bacteria. After a long evolutionary process, countless natural occurring antibiotics have been produced by microorganisms, and act with various mechanisms. Only limited antibiotics have been transferred to clinical use until now, leaving us with the urgent quest to find new antibiotics to deal with the increasing antibiotic-resistant bacteria.

References (for **Chapter 1** and **6**)

Abbott Laboratories, E. E. S. (2002) (Erythromycin ethylsuccinate) prescribing information, *Physicians' desk reference. 56th ed.*, 450-452.

Aboltins, C., Page, M., Buising, K., Jenney, A., Daffy, J., Choong, P., and Stanley, P. (2007) Treatment of staphylococcal prosthetic joint infections with debridement, prosthesis retention and oral rifampicin and fusidic acid, *Clinical microbiology and infection 13*, 586-591.

Allison, A. C. (2000) Immunosuppressive drugs: the first 50 years and a glance forward, *Immunopharmacology 47*, 63-83.

Allison, A. C., and Eugui, E. M. (2000) Mycophenolate mofetil and its mechanisms of action, *Immunopharmacology 47*, 85-118.

Almeida, C., Kehraus, S., Prudêncio, M., and König, G. M. (2011) Marilones A–C, phthalides from the sponge-derived fungus Stachylidium sp, *Beilstein journal of organic chemistry 7*, 1636-1642.

Al-Suwailem, K., Al-Tamimi, A., Al-Omar, M., and Al-Suhibani, M. (2006) Safety and mechanism of action of orlistat (tetrahydrolipstatin) as the first local antiobesity drug, *Journal of Applied Sciences Research 2*, 205-208.

Aly, A. H., Debbab, A., and Proksch, P. (2011) Fungal endophytes: unique plant inhabitants with great promises, *Applied Microbiology and Biotechnology 90*, 1829-1845.

An, C.-Y., Li, X.-M., Luo, H., Li, C.-S., Wang, M.-H., Xu, G.-M., and Wang, B.-G. (2013) 4-Phenyl-3, 4-dihydroquinolone derivatives from Aspergillus nidulans MA-143, an endophytic fungus isolated from the mangrove plant Rhizophora stylosa, *Journal of natural products 76*, 1896-1901.

Angell, S., Bench, B. J., Williams, H., and Watanabe, C. M. (2006) Pyocyanin isolated from a marine microbial population: synergistic production between two distinct bacterial species and mode of action, *Chemistry & biology 13*, 1349-1359.

Arnold, A. E., Mejía, L. C., Kyllo, D., Rojas, E. I., Maynard, Z., Robbins, N., and Herre, E. A. (2003) Fungal endophytes limit pathogen damage in a tropical tree, *Proceedings of the National Academy of Sciences 100*, 15649-15654.

Anon (2003) Drugs of choice for cancer, *Treatment Guidelines from Medical Letter 1*, 41-52.

Asai, T., Yamamoto, T., and Oshima, Y. (2011) Histone deacetylase inhibitor induced the production of three novel prenylated tryptophan analogs in the entomopathogenic fungus, Torrubiella luteorostrata, *Tetrahedron Letters 52*, 7042-7045.

Bacon, C., and Hinton, D. (1996) Symptomless endophytic colonization of maize by Fusarium moniliforme, *Canadian Journal of Botany 74*, 1195-1202.

Balaban, N. (2005) Barriers on the road to new antibiotics: regulatory obstacles and lack of investment are in the way of innovation, *The Scientist 19*, 42-44.

Barradell, L. B., and Bryson, H. M. (1994) Cefepime, *Drugs 47*, 471-505.

Batchelor, F., Doyle, F., Nayler, J., and Rolinson, G. (1959) Synthesis of penicillin: 6-aminopenicillanic acid in penicillin fermentations, *Nature 183*, 257-258.

Beekman, A. M., and Barrow, R. A. (2014) Fungal metabolites as pharmaceuticals, *Australian Journal of Chemistry 67*, 827-843.

Belofsky, G. N., Gloer, J. B., Wicklow, D. T., and Dowd, P. F. (1995) Antiinsectan alkaloids: shearinines AC and a new paxilline derivative from the ascostromata of Eupenicillium shearii, *Tetrahedron 51*, 3959-3968.

Bent, K., and Moore, R. (1966) The mode of action of griseofulvin, In *Symp. Soc. Gen. Microbiol*, p 1.

Bentley, S. D., Chater, K. F., Cerdeno-Tarraga, A.-M., Challis, G. L., Thomson, N., James, K. D., Harris, D. E., Quail, M. A., Kieser, H., and Harper, D. (2002) Complete genome sequence of the model actinomycete Streptomyces coelicolor A3 (2), *Nature 417*, 141-147.

Bergmann, S., Schümann, J., Scherlach, K., Lange, C., Brakhage, A. A., and Hertweck, C. (2007) Genomics-driven discovery of PKS-NRPS hybrid metabolites from Aspergillus nidulans, *Nature chemical biology 3*, 213-217.

Bernard, W. S., and Christopher, P. (2014) World cancer report 2014, *World Health Organization*.

Bode, H. B., Bethe, B., Höfs, R., and Zeeck, A. (2002) Big effects from small changes: possible ways to explore nature's chemical diversity, *ChemBioChem 3*, 619-627.

Bode, H. B., Walker, M., and Zeeck, A. (2000) Structure and Biosynthesis of Mutolide, a Novel Macrolide from a UV Mutant of the Fungus F‐24′ 707, *European Journal of Organic Chemistry 2000*, 1451-1456.

Boucher, H. W., Talbot, G. H., Bradley, J. S., Edwards, J. E., Gilbert, D., Rice, L. B., Scheld, M.,

Spellberg, B., and Bartlett, J. (2009) Bad bugs, no drugs: no ESKAPE! An update from the Infectious Diseases Society of America, *Clinical Infectious Diseases 48*, 1-12.

Brown, A. G., Smale, T. C., King, T. J., Hasenkamp, R., and Thompson, R. H. (1976) Crystal and molecular structure of compactin, a new antifungal metabolite from Penicillium brevicompactum, *Journal of the Chemical Society, Perkin Transactions 1*, 1165-1170.

Burg, R. W., Miller, B. M., Baker, E. E., Birnbaum, J., Currie, S. A., Hartman, R., Kong, Y.-L., Monaghan, R. L., Olson, G., and Putter, I. (1979) Avermectins, new family of potent anthelmintic agents: producing organism and fermentation, *Antimicrobial agents and Chemotherapy 15*, 361-367.

Canafax D. M., Ascher N. L. (1983) Cyclosporine immunosuppression, *Clinical Pharmacology 2*, 515-524.

Campbell, W. C., Tu, Y., and Ōmura, S. The Nobel Prize in Physiology or Medicine 2015.

Celgene (2013) Abraxane for injectable suspension (paclitaxel protein-bound particles for injectable suspension) (albumin-bound) prescribing information, *Summit, NJ*.

Chakrabarti, D., and Ghosal, S. (1989) The Disease Cycle of Mango Malformation Induced by Fusarium moniliforme var. subglutinans and the Curative Effects of Mangiferin‐Metal Chelates, *Journal of Phytopathology 125*, 238-246.

Challis, G. L. (2014) Exploitation of the Streptomyces coelicolor A3 (2) genome sequence for discovery of new natural products and biosynthetic pathways, *Journal of industrial microbiology & biotechnology 41*, 219-232.

Champney, W. S., and Burdine, R. (1996) 50S ribosomal subunit synthesis and translation are equivalent targets for erythromycin inhibition in Staphylococcus aureus, *Antimicrobial agents and chemotherapy 40*, 1301-1303.

Charity, J. C., Katz, E., and Moss, B. (2007) Amino acid substitutions at multiple sites within the vaccinia virus D13 scaffold protein confer resistance to rifampicin, *Virology 359*, 227-232.

Chen, H., Daletos, G., Abdel-Aziz, M. S., Thomy, D., Dai, H., Brötz-Oesterhelt, H., Lin, W., and Proksch, P. (2015) Inducing secondary metabolite production by the soil-dwelling fungus Aspergillus terreus through bacterial co-culture, *Phytochemistry Letters 12*, 35-41.

Chen, M., Shao, C.-L., Fu, X.-M., Xu, R.-F., Zheng, J.-J., Zhao, D.-L., She, Z.-G., and Wang, C.-Y.

(2013) Bioactive indole alkaloids and phenyl ether derivatives from a marine-derived Aspergillus sp. fungus, *Journal of natural products 76*, 547-553.

Chiang, Y.-M., Szewczyk, E., Nayak, T., Davidson, A. D., Sanchez, J. F., Lo, H.-C., Ho, W.-Y., Simityan, H., Kuo, E., and Praseuth, A. (2008) Molecular genetic mining of the Aspergillus secondary metabolome: discovery of the emericellamide biosynthetic pathway, *Chemistry & biology 15*, 527-532.

Choudhary, C., Kumar, C., Gnad, F., Nielsen, M. L., Rehman, M., Walther, T. C., Olsen, J. V., and Mann, M. (2009) Lysine acetylation targets protein complexes and co-regulates major cellular functions, *Science 325*, 834-840.

Cohen, E., Koch, L., Thu, K. M., Rahamim, Y., Aluma, Y., Ilan, M., Yarden, O., and Carmeli, S. (2011) Novel terpenoids of the fungus Aspergillus insuetus isolated from the Mediterranean sponge Psammocinia sp. collected along the coast of Israel, *Bioorganic & medicinal chemistry 19*, 6587-6593.

Croitoru, R., Fiţigău, F., Van den Broek, L., Frissen, A., Davidescu, C., Boeriu, C., and Peter, F. (2012) Biocatalytic acylation of sugar alcohols by 3-(4-hydroxyphenyl) propionic acid, *Process Biochemistry 47*, 1894-1902.

Cully, D. F., Vassilatis, D. K., Liu, K. K., Paress, P. S., Van der Ploeg, L., Schaeffer, J. M., and Arena, J. P. (1994) Cloning of an avermectin-sensitive glutamate-gated chloride channel from Caenorhabditis elegans, *Nature 371*, 707-711.

Cutler, H. G. (1988) Natural products and their potential in agriculture. A personal overview, In *ACS Symposium series-American Chemical Society (USA)*.

Deepika, V., Murali, T., and Satyamoorthy, K. (2016) Modulation of genetic clusters for synthesis of bioactive molecules in fungal endophytes: A review, *Microbiological research 182*, 125-140.

Demain, A. L. (2014) Importance of microbial natural products and the need to revitalize their discovery, *Journal of industrial microbiology & biotechnology 41*, 185-201.

Demain, A. L., and Sanchez, S. (2009) Microbial drug discovery: 80 years of progress, *The Journal of antibiotics 62*, 5-16.

Donadio, S., McAlpine, J. B., Sheldon, P. J., Jackson, M., and Katz, L. (1993) An erythromycin analog produced by reprogramming of polyketide synthesis, *Proceedings of the National*

Academy of Sciences 90, 7119-7123.

Donlan, R. M., and Costerton, J. W. (2002) Biofilms: survival mechanisms of clinically relevant microorganisms, *Clinical microbiology reviews 15*, 167-193.

Donn, G., Köcher, H.(2012) Inhibitors of glutamine synthetase, chapter 4 in herbicide classes in development: mode of action, targets, genetic engineering, chemistry, *Springer Science & Business Media*.

Duke, S. O., and Dayan, F. E. (2011) Modes of action of microbially-produced phytotoxins, *Toxins 3*, 1038-1064.

Duke, S. O., and Lydon, J. (1987) Herbicides from natural compounds, *Weed Technology*, 122-128.

Dumont, F. J., and Su, Q. (1995) Mechanism of action of the immunosuppressant rapamycin, *Life sciences 58*, 373-395.

Dutcher, J. D. (1968) The discovery and development of amphotericin B, *Dis Chest 54*, 296-298.

Ebrahim, W., El-Neketi, M., Lewald, L.-I., Orfali, R. S., Lin, W., Rehberg, N., Kalscheuer, R., Daletos, G., and Proksch, P. (2016) Metabolites from the Fungal Endophyte Aspergillus austroafricanus in Axenic Culture and in Fungal–Bacterial Mixed Cultures, *Journal of natural products*.

Elander, R. (2003) Industrial production of β-lactam antibiotics, *Applied microbiology and biotechnology 61*, 385-392.

Endo, A. (1979) Monacolin K, a new hypocholesterolemic agent produced by a Monascus species, *The Journal of antibiotics 32*, 852-854.

Endo, A. (1992) The discovery and development of HMG-CoA reductase inhibitors, *Journal of lipid research 33*, 1569-1582.

Endo, A., and Hasumi, K. (1993) HMG-CoA reductase inhibitors, *Natural product reports 10*, 541-550.

Endo, A., Kuroda, M., and Tsujita, Y. (1976) ML-236A, ML-236B, and ML-236C, new inhibitors of cholesterogensis produced by Penicillium citrinum, *The Journal of antibiotics 29*, 1346-1348.

Enright, M. C., Robinson, D. A., Randle, G., Feil, E. J., Grundmann, H., and Spratt, B. G. (2002) The evolutionary history of methicillin-resistant Staphylococcus aureus (MRSA),

Proceedings of the National Academy of Sciences 99, 7687-7692.

Fan, Y., Wang, Y., Liu, P., Fu, P., Zhu, T., Wang, W., and Zhu, W. (2013) Indole-diterpenoids with anti-H1N1 activity from the aciduric fungus Penicillium camemberti OUCMDZ-1492, *Journal of natural products 76*, 1328-1336.

Feller, I. C., Lovelock, C., Berger, U., McKee, K., Joye, S., and Ball, M. (2010) Biocomplexity in mangrove ecosystems, *Annual Review of Marine Science 2*, 395-417.

Fleming, A. (1929) On the antibacterial action of cultures of a penicillium, with special reference to their use in the isolation of B. influenzae, *British journal of experimental pathology 10*, 226.

Florey, H. W. (1946) The use of micro-organisms for therapeutic purposes, *The Yale journal of biology and medicine 19*, 101.

Food, U., and Administration, D. (2010) Risk evaluation and mitigation strategy (REMS) under review for CellCept and Myfortic, 2010.

Fornari, F. A., Randolph, J. K., Yalowich, J. C., Ritke, M. K., and Gewirtz, D. A. (1994) Interference by doxorubicin with DNA unwinding in MCF-7 breast tumor cells, *Molecular pharmacology 45*, 649-656.

Frey-Klett, P., Burlinson, P., Deveau, A., Barret, M., Tarkka, M., and Sarniguet, A. (2011) Bacterial-fungal interactions: hyphens between agricultural, clinical, environmental, and food microbiologists, *Microbiology and Molecular Biology Reviews 75*, 583-609.

Ganis, P., Avitabile, G., Mechlinski, W., and Schaffner, C. P. (1971) Polyene macrolide antibiotic amphotericin B. Crystal structure of the N-iodoacetyl derivative, *Journal of the American Chemical Society 93*, 4560-4564.

Gapillout, I., Milat, M.-L., and Blein, J.-P. (1996) Effects of fusaric acid on cells from tomato cultivars resistant or susceptible toFusarium oxysporum f. sp. Lycopersici, *European journal of plant pathology 102*, 127-132.

Ghuysen, J.-M., Frere, J.-M., Leyh-Bouille, M., Coyette, J., Dusart, J., and Nguyen-Disteche, M. (1979) Use of model enzymes in the determination of the mode of action of penicillins and delta3-cephalosporins, *Annual review of biochemistry 48*, 73-101.

Girgis, N., Kilpatrick, M., Farid, Z., Sultan, Y., and Podgore, J. (1993) Cefixime in the treatment of enteric fever in children, DTIC Document.

Glaxo Smith Kline (2009) GSK receives European Commission approval to market alli (orlistat 60 mg), *Press release*.

Glaxo Smith Kline (2010) Ceftin (cefuroxime axetil) powder for oral suspension and film-coated tablets, prescribing information, *Research Triangle Park*.

Gokhale, R. S., Hunziker, D., Cane, D. E., and Khosla, C. (1999) Mechanism and specificity of the terminal thioesterase domain from the erythromycin polyketide synthase, *Chemistry & biology 6*, 117-125.

Gordee, R. S., Zeckner, D. J., Ellis, L. F., Thakkar, A. L., and Howard, L. C. (1984) In vitro and in vivo anti-Candida activity and toxicology of LY121019, *The Journal of antibiotics 37*, 1054-1065.

Gosio, B. (1896) Ricerche bacteriologiche e chimiche sulle alterazioni del mais, *Rivista di Igiene e Sanità Pubblica 7*, 825-868.

Grond, S., Papastavrou, I., and Zeeck, A. (2002) Novel α‐L‐Rhamnopyranosides from a Single Strain of Streptomyces by Supplement‐Induced Biosynthetic Steps, *European Journal of Organic Chemistry 2002*, 3237-3242.

Grove, J. F., MacMillan, J., Mulholland, T., and Zealley, J. (1952) 761. Griseofulvin. Part III. The structures of the oxidation products C 9 H 9 O 5 Cl and C 14 H 15 O 7 Cl, *Journal of the Chemical Society (Resumed)*, 3967-3977.

Guchelaar, H.-J., Ten Napel, C., De Vries, E., and Mulder, N. (1994) Clinical, toxicological and pharmaceutical aspects of the antineoplastic drug taxol: a review, *Clinical Oncology 6*, 40-48.

Hanifin, J. M., Ling, M. R., Langley, R., Breneman, D., Rafal, E., and Group, T. O. S. (2001) Tacrolimus ointment for the treatment of atopic dermatitis in adult patients: part I, efficacy, *Journal of the American Academy of Dermatology 44*, S28-S38.

Hauptman, J., Jeunet, F. S., and Hartmann, D. (1992) Initial studies in humans with the novel gastrointestinal lipase inhibitor Ro 18-0647 (tetrahydrolipstatin), *The American journal of clinical nutrition 55*, 309S-313S.

Hay, R. J., Johns, N. E., Williams, H. C., Bolliger, I. W., Dellavalle, R. P., Margolis, D. J., Marks, R., Naldi, L., Weinstock, M. A., and Wulf, S. K. (2014) The global burden of skin disease in 2010: an analysis of the prevalence and impact of skin conditions, *Journal of*

Investigative Dermatology 134, 1527-1534.

Hobby, G. L., Meyer, K., and Chaffee, E. (1942) Observations on the Mechanism of Action of Penicillin, *Experimental Biology and Medicine 50*, 281-285.

Hooks, M. A. (1994) Tacrolimus, a new immunosuppressant—a review of the literature, *Annals of Pharmacotherapy 28*, 501-511.

Hyde, K. D., Jones, E. G., Leaño, E., Pointing, S. B., Poonyth, A. D., and Vrijmoed, L. L. (1998) Role of fungi in marine ecosystems, *Biodiversity & Conservation 7*, 1147-1161.

Ikeda, H., Ishikawa, J., Hanamoto, A., Shinose, M., Kikuchi, H., Shiba, T., Sakaki, Y., Hattori, M., and Ōmura, S. (2003) Complete genome sequence and comparative analysis of the industrial microorganism Streptomyces avermitilis, *Nature biotechnology 21*, 526-531.

Kanoh, K., Kohno, S., Asari, T., Harada, T., Katada, J., Muramatsu, M., Kawashima, H., Sekiya, H., and Uno, I. (1997) (−)-Phenylahistin: a new mammalian cell cycle inhibitor produced by Aspergillus ustus, *Bioorganic & Medicinal Chemistry Letters 7*, 2847-2852.

Kao, C. M., Luo, G., Katz, L., Cane, D. E., and Khosla, C. (1995) Manipulation of macrolide ring size by directed mutagenesis of a modular polyketide synthase, *Journal of the American Chemical Society 117*, 9105-9106.

Katz, L., and Baltz, R. H. (2016) Natural product discovery: past, present, and future, *Journal of industrial microbiology & biotechnology 43*, 155-176.

Kaulmann, U., and Hertweck, C. (2002) Biosynthesis of polyunsaturated fatty acids by polyketide synthases, *Angewandte Chemie International Edition 41*, 1866-1869.

Kinch, M. S., Haynesworth, A., Kinch, S. L., and Hoyer, D. (2014) An overview of FDA-approved new molecular entities: 1827–2013, *Drug discovery today 19*, 1033-1039.

Kino, T., Hatanaka, H., Hashimoto, M., Nishiyama, M., Goto, T., Okuhara, M., Kohsaka, M., Aoki, H., and Imanaka, H. (1987) FK-506, a novel immunosuppressant isolated from a Streptomyces. I. Fermentation, isolation, and physico-chemical and biological characteristics, *The Journal of antibiotics 40*, 1249-1255.

Kirst, H. A. (2010) The spinosyn family of insecticides: realizing the potential of natural products research, *The Journal of antibiotics 63*, 101-111.

Kirst, H. A., Creemer, L. C., Naylor, S. A., Pugh, P. T., Snyder, D. E., Winkle, J. R., Lowe, L., Rothwell, J. T., Sparks, T. C., and Worden, T. V. (2002) Evaluation and development of

spinosyns to control ectoparasites on cattle and sheep, *Current topics in medicinal chemistry 2*, 675-699.

Kitchin, J. E. S., Pomeranz, M. K., Pak, G., Washenik, K., and Shupack, J. L. (1997) Rediscovering mycophenolic acid: a review of its mechanism, side effects, and potential uses, *Journal of the American Academy of Dermatology 37*, 445-449.

Knudsen, E., Rolinson, G. N., and Sutherland, R. (1967) Carbenicillin: a new semisynthetic penicillin active against Pseudomonas pyocyanea, *British medical journal 3*, 75.

Kogel, K.-H., Franken, P., and Hückelhoven, R. (2006) Endophyte or parasite–what decides?, *Current opinion in plant biology 9*, 358-363.

Krautter, M. (1998) Ecology of siliceous sponges-Application to the environmental interpretation of the Upper Jurassic sponge facies (Oxfodian) from Spain, *Cuadernos de Geologia ibérica 24*, 223-240.

Kumar, N. (1981) Taxol-induced polymerization of purified tubulin. Mechanism of action, *Journal of Biological Chemistry 256*, 10435-10441.

Lawn, S. D., Zumla, A. I. (2011) Tuberculosis, *Lancet 378*, 57-72.

Lebel, M. H., Hoyt, M. J., and McCracken, G. H. (1989) Comparative efficacy of ceftriaxone and cefuroxime for treatment of bacterial meningitis, *The Journal of pediatrics 114*, 1049-1054.

Leive, L. (1974) The barrier function of the Gram‐negative envelope, *Annals of the New York Academy of Sciences 235*, 109-129.

Levin, M. E., and Hatfull, G. F. (1993) Mycobacterium smegmatis RNA polymerase: DNA supercoiling, action of rifampicin and mechanism of rifampicin resistance, *Molecular microbiology 8*, 277-285.

Li, H., Huang, H., Shao, C., Huang, H., Jiang, J., Zhu, X., Liu, Y., Liu, L., Lu, Y., and Li, M. (2011) Cytotoxic norsesquiterpene peroxides from the endophytic fungus Talaromyces flavus isolated from the mangrove plant Sonneratia apetala, *Journal of natural products 74*, 1230-1235.

Lindsten, J., and Ringertz, N. (2001) The Nobel Prize in physiology or medicine, 1901-2000, *The Nobel prize: the first 100*, 111-137.

MacMillan, J. (1959) 361. Griseofulvin. Part XIV. Some alcoholytic reactions and the absolute

configuration of griseofulvin, *Journal of the Chemical Society (Resumed)*, 1823-1830.

Marmann, A., Aly, A. H., Lin, W., Wang, B., and Proksch, P. (2014) Co-cultivation—A powerful emerging tool for enhancing the chemical diversity of microorganisms, *Marine drugs 12*, 1043-1065.

Marrè, M., Vergani, P., and Albergoni, F. (1993) Relationship between fusaric acid uptake and its binding to cell structures by leaves of Egeria densa and its toxic effects on membrane permeability and respiration, *Physiological and Molecular Plant Pathology 42*, 141-157.

Marsden, A. F., Caffrey, P., Aparicio, J. F., Loughran, M. S., Staunton, J., and Leadlay, P. F. (1994) Stereospecific acyl transfers on the erythromycin-producing polyketide synthase, *Science-AAAS-Weekly Paper Edition-including Guide to Scientific Information 263*, 378-379.

Matsuda, S., and Koyasu, S. (2000) Mechanisms of action of cyclosporine, *Immunopharmacology 47*, 119-125.

McCarthy, C. G., Finland, M., Wilcox, C., and Yarrows, J. H. (1960) Absorption and excretion of four penicillins: Penicillin G, penicillin V, phenethicillin and phenylmercaptomethyl penicillin, *New England Journal of Medicine 263*, 315-326.

McDougal, L. K., and Thornsberry, C. (1986) The role of beta-lactamase in staphylococcal resistance to penicillinase-resistant penicillins and cephalosporins, *Journal of Clinical Microbiology 23*, 832-839.

McGovern, P. E., Zhang, J., Tang, J., Zhang, Z., Hall, G. R., Moreau, R. A., Nuñez, A., Butrym, E. D., Richards, M. P., and Wang, C.-s. (2004) Fermented beverages of pre-and proto-historic China, *Proceedings of the National Academy of Sciences of the United States of America 101*, 17593-17598.

McGrath, N. A., Brichacek, M., and Njardarson, J. T. (2010) A graphical journey of innovative organic architectures that have improved our lives, *Journal of chemical education 87*, 1348-1349.

McGuire, J. M., Bunch, R., Anderson, R., Boaz, H., Flynn, E., Powell, H., and Smith, J. (1952) Ilotycin, a new antibiotic, *Antibiotics & chemotherapy (Northfield, Ill.) 2*, 281-283.

Mertz, F. P., and Yao, R. C. (1990) Saccharopolyspora spinosa sp. nov. isolated from soil collected in a sugar mill rum still, *International Journal of Systematic and Evolutionary*

Microbiology 40, 34-39.

Merck & Co. Inc. (2005) Cosmegen for injection (dactinomycin for injection) prescribing information, *Whitehouse Station, NJ*.

Mesa-Arango, A. C., Scorzoni, L., and Zaragoza, O. (2012) It only takes one to do many jobs: Amphotericin B as antifungal and immunomodulatory drug, *Frontiers in microbiology 3*, 286.

Miller, L. H., and Su, X. (2011) Artemisinin: discovery from the Chinese herbal garden, *Cell 146*, 855-858.

Momparler, R. L., Karon, M., Siegel, S. E., and Avila, F. (1976) Effect of adriamycin on DNA, RNA, and protein synthesis in cell-free systems and intact cells, *Cancer research 36*, 2891-2895.

Morin, R. B., Jackson, B. G., Flynn, E. H., and Roeske, R. (1962) Chemistry of cephalosporin antibiotics. I. 7-aminocephalosporanic acid from cephalosporin C, *Journal of the American Chemical Society 84*, 3400-3401.

Morris, M. I., and Villmann, M. (2006) Echinocandins in the management of invasive fungal infections, part 1, *American journal of health-system pharmacy 63*.

Morris, M. I., and Villmann, M. (2006) Echinocandins in the management of invasive fungal infections, Part 2, *American journal of health-system pharmacy 63*, 1813-1820.

Neu, H. C. (1979) Amoxicillin, *Annals of Internal Medicine 90*, 356-360

Newton, G., and Abraham, E. (1954) Degradation, structure and some derivatives of cephalosporin N, *Biochemical Journal 58*, 103.

Nyfeler, R., and Keller-Schierlein, W. (1974) Echinocandin B, A novel polypeptide-antibiotic from Aspergillus nidulans var. echinulatus: isolation and structural components, *Helv Chim Acta 57*, 2459-2477.

Oh, D.-C., Kauffman, C. A., Jensen, P. R., and Fenical, W. (2007) Induced production of emericellamides A and B from the marine-derived fungus Emericella sp. in competing co-culture, *Journal of natural products 70*, 515-520.

Ola, A. R., Thomy, D., Lai, D., Brötz-Oesterhelt, H., and Proksch, P. (2013) Inducing secondary metabolite production by the endophytic fungus Fusarium tricinctum through coculture with Bacillus subtilis, *Journal of natural products 76*, 2094-2099.

Omura, S. (2002) *Macrolide antibiotics: chemistry, biology, and practice*, Academic press.

Oradell, N. J. (1994) Erythromycin base (E-Mycin, Boots), in *PDR Physicians' desk reference, 48th ed*, 625-626.

Organization, W. H. 19th WHO Model List of Essential Medicines. 2015.

Organization, W. H. (2013) Tuberculosis, *Saudi Medical Journal 34*, 1205-1207.

Ortho Dermatologics (2002) Grifulviv V (griseofulvin) tablets microsize and oral suspension microsize prescribing information, *Physicians' desk reference., 56th ed.*, 2518-2519.

Oxford, A. E., Raistrick, H., and Simonart, P. (1939) Studies in the biochemistry of micro-organisms: Griseofulvin, C17H17O6Cl, a metabolic product of Penicillium griseo-fulvum Dierckx, *Biochemical Journal 33*, 240.

Pahon, E. (2015) FDA approves Rapamune to treat LAM, a very rare lung disease, *U. S. Food and Drug Administration*.

Paracchini, R. (1992) Il signore delle cefalosporine, Ed. Demos, Cagliari, Italia.

Park, J. T., and STROMISTGER, J. (1957) Mode of Action of Penicillin. Biochemical Basis for the Mechanism of Action of Penicillin and for its Selective Toxicity, *American Association for the Advancement of Science. Science 125*, 99-101.

Patel, R. N. (1998) Tour de paclitaxel: biocatalysis for semisynthesis, *Annual Reviews in Microbiology 52*, 361-395.

Payne, A. S., and van Leeuwenhoek, A. (1970) *Discoverer of the Unseen World. The Cleere Observer. A Biography of Antoni Van Leeuwenhoek... Illustrated by Charles Prickard*, Macmillan.

Petcher, T. J., Weber, H. P., and Rüegger, A. (1976) Crystal and molecular structure of an iodo‐derivative of the cyclic undecapeptide cyclosporin A, *Helvetica chimica acta 59*, 1480-1488.

Pinchuk, I. V., Bressollier, P., Sorokulova, I. B., Verneuil, B., and Urdaci, M. C. (2002) Amicoumacin antibiotic production and genetic diversity of Bacillus subtilis strains isolated from different habitats, *Research in Microbiology 153*, 269-276.

Pitterna, T., Cassayre, J., Hüter, O. F., Jung, P. M., Maienfisch, P., Kessabi, F. M., Quaranta, L., and Tobler, H. (2009) New ventures in the chemistry of avermectins, *Bioorganic & medicinal chemistry 17*, 4085-4095.

Proksch, P., Ebel, R., Edrada, R., Riebe, F., Liu, H., Diesel, A., Bayer, M., Li, X., Han Lin, W., and Grebenyuk, V. (2008) Sponge-associated fungi and their bioactive compounds: the Suberites case, *Botanica Marina 51*, 209-218.

Rateb, M. E., and Ebel, R. (2011) Secondary metabolites of fungi from marine habitats, *Natural product reports 28*, 290-344.

Redecker, D., Kodner, R., and Graham, L. E. (2000) Glomalean fungi from the Ordovician, *Science 289*, 1920-1921.

Redman, R. S., Sheehan, K. B., Stout, R. G., Rodriguez, R. J., and Henson, J. M. (2002) Thermotolerance generated by plant/fungal symbiosis, *Science 298*, 1581-1581.

Reen, F. J., Romano, S., Dobson, A. D., and O'Gara, F. (2015) The sound of silence: Activating silent biosynthetic gene clusters in marine microorganisms, *Marine drugs 13*, 4754-4783.

Reinhold-Hurek, B., and Hurek, T. (2011) Living inside plants: bacterial endophytes, *Current opinion in plant biology 14*, 435-443.

Roje, S. (2006) S-Adenosyl-L-methionine: beyond the universal methyl group donor, *Phytochemistry 67*, 1686-1698.

Salgado, V. L. (1998) Studies on the mode of action of spinosad: insect symptoms and physiological correlates, *Pesticide Biochemistry and Physiology 60*, 91-102.

Salque, M., Bogucki, P. I., Pyzel, J., Sobkowiak-Tabaka, I., Grygiel, R., Szmyt, M., and Evershed, R. P. (2013) Earliest evidence for cheese making in the sixth millennium BC in northern Europe, *Nature 493*, 522-525.

Schatz, A., Bugle, E., and Waksman, S. A. (1944) Streptomycin, a Substance Exhibiting Antibiotic Activity Against Gram-Positive and Gram-Negative Bacteria.*†, *Experimental Biology and Medicine 55*, 66-69.

Scherlach, K., and Hertweck, C. (2009) Triggering cryptic natural product biosynthesis in microorganisms, *Organic & biomolecular chemistry 7*, 1753-1760.

Sensi, P., Margalith, P., and Timbal, M. (1959) Rifomycin, a new antibiotic; preliminary report, *Il Farmaco; edizione scientifica 14*, 146.

Sharma, D., Cukras, A. R., Rogers, E. J., Southworth, D. R., and Green, R. (2007) Mutational analysis of S12 protein and implications for the accuracy of decoding by the ribosome, *Journal of molecular biology 374*, 1065-1076.

Singh, A. V., Bandi, M., Raje, N., Richardson, P., Palladino, M. A., Chauhan, D., and Anderson, K. C. (2011) A novel vascular disrupting agent plinabulin triggers JNK-mediated apoptosis and inhibits angiogenesis in multiple myeloma cells, *Blood 117*, 5692-5700.

Smith, D., Burnham, M., Bull, J., Hodgson, J., Ward, J., Browne, P., Brown, J., Barton, B., Earl, A., and Turner, G. (1990) Beta-lactam antibiotic biosynthetic genes have been conserved in clusters in prokaryotes and eukaryotes, *The EMBO journal 9*, 741.

Sobell, H. M. (1985) Actinomycin and DNA transcription, *Proceedings of the National Academy of Sciences 82*, 5328-5331.

Solieri, L., and Giudici, P. (2009) *Vinegars of the World*, Springer.

Stierle, A., Strobel, G., and Stierle, D. (1993) Taxol and taxane production by Taxomyces andreanae, an endophytic fungus of Pacific yew, *SCIENCE-NEW YORK THEN WASHINGTON- 260*, 214-214.

Stockwell, V., and Duffy, B. (2012) Use of antibiotics in plant agriculture.

Svarstad, H., Bugge, H. C., and Dhillion, S. S. (2000) From Norway to Novartis: cyclosporin from Tolypocladium inflatum in an open access bioprospecting regime, *Biodiversity & Conservation 9*, 1521-1541.

Syed, Y. Y. (2014) Ceftobiprole medocaril: A review of its use in patients with hospital-or community-acquired pneumonia, *Drugs 74*, 1523-1542.

Sykes, R., and Matthew, M. (1976) The β-lactamases of gram-negative bacteria and their role in resistance to β-lactam antibiotics, *Journal of Antimicrobial Chemotherapy 2*, 115-157.

Tabata, H. (2004) Paclitaxel production by plant-cell-culture technology, In *Biomanufacturing*, pp 1-23, Springer.

Tager, M. (1946) Penicillin, Its Practical Application, *The Yale journal of biology and medicine 19*, 138.

Tanaka, A., Christensen, M. J., Takemoto, D., Park, P., and Scott, B. (2006) Reactive oxygen species play a role in regulating a fungus–perennial ryegrass mutualistic interaction, *The Plant Cell 18*, 1052-1066.

Tenover, F. C. (2006) Mechanisms of antimicrobial resistance in bacteria, *The American journal of medicine 119*, S3-S10.

Thomson, A., Bonham, C., and Zeevi, A. (1995) Mode of action of tacrolimus (FK506): molecular

and cellular mechanisms, *Therapeutic drug monitoring 17*, 584-591.

Tomlinson, P. B., and Tomlinson, P. B. (1994) *The botany of mangroves*, Cambridge University Press.

Tsujita, Y., Kuroda, M., Shimada, Y., Tanzawa, K., Arai, M., Kaneko, I., Tanaka, M., Masuda, H., Tarumi, C., and Watanabe, Y. (1986) CS-514, a competitive inhibitor of 3-hydroxy-3-methylglutaryl coenzyme A reductase: tissue-selective inhibition of sterol synthesis and hypolipidemic effect on various animal species, *Biochimica et Biophysica Acta (BBA)-Lipids and Lipid Metabolism 877*, 50-60.

Twilley, R. R., and Day, J. W. (2012) *Mangrove wetlands*, Wiley Online Library.

Vezina, C., Kudelski, A., and Sehgal, S. (1975) Rapamycin (AY-22,989), a new antifungal antibiotic. I. Taxonomy of the producing streptomycete and isolation of the active principle, *The Journal of antibiotics 28*, 721-726.

Vu, T., Hauschild, R., and Sikora, R. A. (2006) Fusarium oxysporum endophytes induced systemic resistance against Radopholus similis on banana, *Nematology 8*, 847-852.

Waksman, S. A., and Woodruff, H. B. (1940) Bacteriostatic and Bactericidal Substances Produced by a Soil Actinomyces, *Experimental Biology and Medicine 45*, 609-614.

Wall, M. E., and Wani, M. C. (1995) Camptothecin and taxol: discovery to clinic—thirteenth Bruce F. Cain Memorial Award Lecture, *Cancer research 55*, 753-760.

Walsh, G. E. (1974) Mangroves: a review, *Ecology of halophytes*, 51-174.

Wang, Q.-X., Bao, L., Yang, X.-L., Guo, H., Ren, B., Guo, L.-D., Song, F.-H., Wang, W.-Z., Liu, H.-W., and Zhang, L.-X. (2013) Tricycloalternarenes F–H: Three new mixed terpenoids produced by an endolichenic fungus Ulocladium sp. using OSMAC method, *Fitoterapia 85*, 8-13.

Wang, Q.-X., Bao, L., Yang, X.-L., Guo, H., Yang, R.-N., Ren, B., Zhang, L.-X., Dai, H.-Q., Guo, L.-D., and Liu, H.-W. (2012) Polyketides with antimicrobial activity from the solid culture of an endolichenic fungus Ulocladium sp, *Fitoterapia 83*, 209-214.

Weibel, E., Hadvary, P., Hochuli, E., Kupfer, E., and Lengsfeld, H. (1987) Lipstatin, an inhibitor of pancreatic lipase, produced by Streptomyces toxytricini. I. Producing organism, fermentation, isolation and biological activity, *The Journal of antibiotics 40*, 1081-1085.

Weiss, R. B. (1992) The anthracyclines: will we ever find a better doxorubicin?, In *Seminars in*

oncology, pp 670-686.

Welling, P., Huang, H., Koch, P., Craig, W., and Madsen, P. (1977) Bioavailability of ampicillin and amoxicillin in fasted and nonfasted subjects, *Journal of pharmaceutical sciences 66*, 549-552.

White, N. (1997) Assessment of the pharmacodynamic properties of antimalarial drugs in vivo, *Antimicrobial agents and chemotherapy 41*, 1413.

Willard, A. K., and Smith, R. L. (1982) Incorporation of 2 (S) - methylbutanoic acid - 1 - 14C into the structure of mevinolin, *Journal of Labelled Compounds and Radiopharmaceuticals 19*, 337-344.

Winston, D. J., Murphy, W., Young, L. S., and Hewitt, W. L. (1980) Piperacillin therapy for serious bacterial infections, *The American journal of medicine 69*, 255-261.

Woodward, B. (2009) Howard Florey - over 6 million lives saved. Scientists Greater Than Einstein, *Fresno: Quill Diver Books*.

Worthington, R. J., and Melander, C. (2013) Combination approaches to combat multidrug-resistant bacteria, *Trends in biotechnology 31*, 177-184.

Wyeth Laboratories (2010) Rapamune (sirolimus) oral solution and tablets prescribing information, *Philadelphia, PA*.

Yamazaki, Y., Sumikura, M., Hidaka, K., Yasui, H., Kiso, Y., Yakushiji, F., and Hayashi, Y. (2010) Anti-microtubule 'plinabulin'chemical probe KPU-244-B3 labeled both α-and β-tubulin, *Bioorganic & medicinal chemistry 18*, 3169-3174.

Yang, J., Xu, F., Huang, C., Li, J., She, Z., Pei, Z., and Lin, Y. (2010) Metabolites from the mangrove endophytic fungus Phomopsis sp.(# zsu - H76), *European Journal of Organic Chemistry 2010*, 3692-3695.

Ye, R., Kim, J. H., Kim, B. G., Szarka, S., Sihota, E., and Wong, S. L. (1999) High - level secretory production of intact, biologically active staphylokinase from Bacillus subtilis, *Biotechnology and bioengineering 62*, 87-96.

Zeldin, D. C. (2001) Epoxygenase pathways of arachidonic acid metabolism, *Journal of Biological Chemistry 276*, 36059-36062.

Zhao, K., Zhou, D., Ping, W., and Ge, J. (2004) Study on the preparation and regeneration of protoplast from taxol-producing fungus Nodulisporium sylviforme, *Nature and science 2*,

52-59.

Zhou, Y., Debbab, A., Mándi, A., Wray, V., Schulz, B., Müller, W. E., Kassack, M., Lin, W., Kurtán, T., and Proksch, P. (2013) Alkaloids from the Sponge‐Associated Fungus Aspergillus sp, *European Journal of Organic Chemistry 2013*, 894-906.

List of Abbreviations

7-ACA	7-aminocephalosporanic acid
ACP	acyl carrier protein
6-APA	6-aminopenicillanic acid
AT	acyltransferase
$[\alpha]_D$	specific rotation at the sodium D-line
CD	circular dichroism
CE	cotton effect
CH_2Cl_2	dichloromethane
CD_3OD	deuterated methanol
CLSI	Clinical & Laboratory Standards Institute
COSY	correlation spectroscopy
CRC	colorectal cancer
DCM	dichloromethane
DFT	discrete Fourier transform
DEPT	distortionless enhancement by polarization transfer
DH	dehydrase
DMAP	4-dimethylaminopyridine
DMSO	dimethyl sulfoxide
DNA	deoxyribonucleic acid eq equatorial
ECD	electronic circular dichroism
EMA	European Medicines Agency
ER	enoyl reductase
ESKAPE	*Enterococcus faecium*, *Staphylococcus aureus*, *Klebsiella pneumoniae*, *Acinetobacter baumannii*, *Pseudomonas aeruginosa* and *Enterobater* spp.
EtOAc	ethyl acetate
FDA	Food and Drug Administration
FKBP	FK506 (Tacrolimus) binding protein
GC-MS	gas chromatography–mass spectrometry
HDAC	histone deacetylase
HMBC	heteronuclear multiple bond connectivity
HMG-CoA	3-hydroxy-3-methyl-glutaryl-coenzyme A
HSQC	heteronuclear single quantum coherence
HPLC	high performance liquid chromatography
HPLC-MS	liquid chromatography–mass
HRESIMS	high resolution electrospray ionisation mass
HR-MS	high resolution mass spectrometry
IC_{50}	half maximal inhibitory concentration

IMPDH	inosine-5′-monophosphate dehydrogenase
ITS	internal transcriber spacers
KR	*β*-ketoacyl reductase
KS	*β*-ketoacyl synthase
LAM	lymphangioleiomyomatosis
LC/MS	liquid chromatography-mass spectrometery
LD_{50}	lethal dose, 50%
MeOH	methanol
MHz	mega Herz
MIC	minimum inhibitory concentration
MMFF	Merck molecular force field
MRSA	methicillin-resistant *Staphylococcus aureus*
MS	mass spectrometry
mTOR	mechanistic target of rapamycin
MTPA	*α*-methoxy-*α*-trifluoromethylphenylacetic acid
MTT	3-(4,5-dimethylthiazol-2-yl)-2,5-diphenyltetrazolium bromide
m/z	mass per charge
NMR	nuclear magnetic resonance
OSMAC	one strain many compounds
PBP	penicillin-binding proteins
PKS	polyketide synthase
ppm	parts per million
RNA	ribonucleic acid
ROESY	rotating frame overhauser effect spectroscopy
RP 18	reversed phase C18
SAM	*S*-adenosyl methionine
SAR	structure and activity relationship
SAHA	suberanilohydroxamic acid
SBHA	suberoyl bis-hydroxamic acid
TDDFT	time-dependent density functional theory
TE	thioesterase
TFA	trifluoroacetic acid
TLC	thin layer chromatography
UV	ultraviolet
VLC	vacuum liquid chromatography
WHO	World Health Organization

Research Contributions

Publications

(1) **Shuai Liu**, Haofu Dai, Raha S. Orfali, Wenhan Lin, Zhen Liu, and Peter Proksch. (**2016**) New fusaric acid derivatives from the endophytic fungus *Fusarium oxysporum* and their phytotoxicity to barley leaves. *J. Agric. Food Chem.*64, 3127-3132.

The first author contributed 70% to this publication. The first author's work involves all laboratory works including the bioassay and GC-MS experiments, as well as the manuscript preparation.

(2) **Shuai Liu**, Haofu Dai, Gamall Makhloufi, Christian Heering, Christoph Janiak, Rudolf Hartmann, Attila Mándi, Tibor Kurtán, Werner E. G. Müller, Matthias U. Kassack, Wenhan Lin, Zhen Liu, and Peter Proksch. (**2016**) Cytotoxic 14-membered macrolides from a mangrove-derived endophytic fungus, *Pestalotiopsis microspora*. *J. Nat. Prod.* 79, 2332-2340.

The first author contributed 50% to this publication. The first author's work involved all laboratory works including compound isolation, structure elucidation and Mosher's reaction, as well as the manuscript preparation.

(3) **Shuai Liu**, Haofu Dai, Belma Konuklugil, Raha S. Orfali, Wenhan Lin, Rainer Kalscheuer, Zhen Liu, Peter Proksch. (**2016**) Phenolic bisabolanes from the sponge-derived fungus *Aspergillus* sp. *Phytochem. Lett.* 18, 187-191.

The first author contributed 60% to this publication. The first author's work involved all laboratory works including compound isolation, structure elucidation, as well as the manuscript preparation.

(4) **Shuai Liu**, Haofu Dai, Christian Heering, Christoph Janiak, Wenhan Lin, Zhen Liu, Peter Proksch. (**2016**) Inducing new secondary metabolites through co-cultivation of the fungus *Pestalotiopsis microspora* with the bacterium *Bacillus subtilis*. *Tetrahedron Lett*. (accepted).

The first author contributed 60% to this publication. The first author's work involved all laboratory works including compound isolation, structure elucidation, as well as the manuscript preparation.

Declaration of Academic Honesty/Erklärung

Hiermit erkläre ich ehrenwörtlich, dass ich die vorliegende Dissertation mit dem Titel „Bioaktive Sekundärmetabolite aus marinen Pilzen und Untersuchungen zur Co-Kultivierung zwischen Pilzen und Bakterien“ selbst angefertigt habe. Außer den angegebenen Quellen und Hilfsmitteln wurden keine weiteren verwendet. Diese Dissertation wurde weder in gleicher noch in abgewandelter Form in einem anderen Prüfungsverfahren vorgelegt.

Düsseldorf, den 21.10.2016

Shuai Liu

Acknowledgments

First of all, I would like to express my deepest gratitude and sincere thanks to Prof. Dr. Peter Proksch for offering me this precious opportunity to pursue my doctoral degree at the Institut für Pharmazeutische Biologie und Biotechnologie, Heinrich-Heine-Universität, Düsseldorf. I will never forget his excellent guidance, helpful discussions, and continuous supports to my work. Moreover, his rigorous scientific spirit, high work efficiency, as well as his kind and generous attitude towards students will be inspiring me in all my life.

Great thanks to Prof. Dr. Haofu Dai (Chinese Academy of Tropical Agricultural Sciences) for his good supervision during my postgraduate research and introducing me to Prof. Proksch.

My appreciation goes to Dr. Zhen Liu's help on improving manuscripts, NMR data recheck and valuable suggestions on my experiments.

My appreciation goes to Prof. Dr. Rainer Kalscheuer (Institut für Pharmazeutische Biologie und Biotechnologie, Heinrich-Heine-Universität) for officiating as my second referee and his collaboration on antibacterial tests.

My deep thanks to Prof. Dr. Wenhan Lin (Peking University) for his helpful suggestions on structure elucidation.

I am deeply indepted to Prof. Dr. Bingui Wang (Institute of Oceanology, Chinese Acedemy of Science) for his kind assistance with my manuscripts.

I would like to thank Prof. Dr. Claus Paßreiter (Institut für Pharmazeutische Biologie und Biotechnologie, Heinrich-Heine-Universität) for his support, help and safety instructions during the study.

My deep thanks to Dr. Tibor Kurtán (Department of Organic Chemistry, University of Debrecen, Hungary) for ECD calculation.

I would like to express my cordial thanks My Prof. Dr. Werner E. G. Müller (Institut für Physiologische Chemie und Pathobiochemie, University of Mainz), and Prof. Dr. Matthias U. Kassack (Institut für Pharmazeutische und Medizinische Chemie, Heinrich Heine University Duesseldorf) for their collaboration on cytotoxicity tests.

I am grateful to Prof. Dr. Heike Brötz-Oesterhelt (Interfakultäres Institut für Mikrobiologie und Infektionsmedizin, Mikrobielle Wirkstoffe, Tübingen, Germany) and Mrs Heike Goldbach-Gecke (Institut für Pharmazeutische Biologie und Biotechnologie, Heinrich-Heine-Universität) for their

support and help of co-cultivation experimentss and antibiotic assays.

I would like to thank Prof. Dr. Christoph Janiak, Dr. Christian Heering, Dr. Gamall Makhloufi (Institut für Bioanorganische Chemie, MOFs, Nanos und Katalyse, Heinrich Heine University Duesseldorf) for their collaboration on single-crystal X-ray testing and analysis.

I would like to thank Prof. Dr. Vlada B. Urlacher and Mr. Ansgar Rühlmann (Institut für Biochemie II, Heinrich Heine University Duesseldorf) for their support on my GC-MS experiment.

Great thanks to Dr. Rudolf Hartmann from Institute of Complex Systems: Strukturbiochemie (ICS-6), Forschungszentrum Julich, for the skillful 700 MHz NMR measurements on slight amount compounds.

I would like to especially thank our postdoctoral researchers Dr. Yang Liu, Dr. Ramsay Kamdem, Dr. Georgios Daletos, Dr. Weaam Ebrahim, and Dr. Elena Ancheeva for their assistance, guidance, and discussions during my entire Ph.D.

I also appreciate the kind support from Mrs. Claudia Eckelskemper and all the technicians Mrs. Waltraud Schlag, Mrs. Simone Miljanovic, Mrs. Katja Friedrich, Mrs Eva Müller, Ms. Linda Wiegand, Mrs. Simone Monninghoff-Putzer and Mr. Dieter Jansen.

During my PhD study, I received help, support, and happiness from time to time, so I would like to take this opportunity to express my profound gratitude to all of these group members:

- The former colleagues Dr. Andreas Marmann for the guidances regarding the work on fungi, Dr. A. R. B. Ola for the initiation on co-cultivation experiments, and Dr. Cong-Dat Pham, Dr. Hendrick Niemann, Dr. Sherif Elsayed, Dr. Lena Hammerschmidt and Dr. Mousa. Al Tarabeen for their kind help and nice discussions.
- Ms. Imke Form for her fungal identification instruction and translation of abstract, Ms. Mi-Yong Chung for her help on my new apartment contract, Mr. Nam Michael Tran-Cong for his kind help for me on applying the scholarship from Hera Office, Ms. Mariam Moussa for the telephone callings for me, Mr. Marian Frank and Ms. Catalina Perez Hemphill for their great efforts and help in public responsibilities.
- I really enjoyed the happy time with Dr. Yanbo Zeng, Dr. Fang Lv, my dear sisters Dr. Huiqin Chen, Ms. Chenyin Wang and my brothers Mr. Hao Wang and Mr. Haiqian Yu.
- I really appreciate the time with my international friends: Mr. Amin Mokhlesi, Dr.

Sergi Akone, Dr. Rini Muharini, and Dr. Rudi Rudiyansyah, Dr. Mohamed Elnaggar, Mr. Ferhat Oezkaya, Dr. Kenneth G Ngwoke.

- Nice time spent with all of you: Dr. Linghong Meng, Dr. Xin Li, Ms. Xiaoqin Yu, Mr. Feng Pan, Ms. Arta Kuci, Mrs Blessing Umeokoli, Mr. Peter Eze, Mr. Tino Seidemann, Ms. Julia Werner, Dr. Odontuya, Ms. Pamela Nangmo Kemda, Dr. Festus Okoye, Ms. Lisa Kuppers, Mrs. Catherine Bogner, Ms. Ni Putu Ariantari, Mr. Harwoko, Ms. Nada Mohamed, Ms. Miada Fouad, Ms. Miada Fouad, Dr. Masriani, Dr. Andi Haeril Alimuddin.

In the end, I would like to thank China Scholarship Council, Ministry of Education of China for the financial support during my study in Germany.